ABSTRACT

ALISON C. SOUTHGATE Ph.D. Thesis, 1989

MOORLAND AND BRACKEN CHANGE IN THE NORTH YORK MOORS: AN INVESTIGATION USING REMOTE SENSING.

The semi-natural vegetation of the North York Moors is dominated by Calluna vulgaris (common heather), and it is the concern of the National Park Moorland Management Programme to preserve and protect it for landscape amenity, hill farming, grouse rearing and recreational use. There are several important pressures related to the management of the moorland, including the invasion of moorland and agriculture by Pteridium aquilinum (bracken); the over-aging of Calluna vulgaris; the conversion of moorland to forestry and agriculture; and severe erosion. Information about the exact extent and distribution of these problems is incomplete and out of date, hindering conservation attempts. This thesis investigates the feasibility of using remote sensing techniques to develop a system for the routine monitoring of the vegetation of the North York Moors, especially Calluna vulgaris and Pteridium aquilinum, in order to produce vegetation maps, which may be used as a direct input to the Management Programme.

Field spectral, Airborne Thematic Mapper and Landsat Thematic Mapper data are used to investigate the temporal, spectral and spatial resolutions important to the remote sensing of a moorland environment. Detailed field maps of a 40km^2 study area along Blakey Ridge are used to train for image interpretation, as a basis for supervised classifications, and to test the accuracy of results. Summary statistics, scatter plots and discriminant analysis are used to investigate thoroughly the temporal and spectral characteristics of the data. A degradation experiment performed on a 512 x 512 pixel subscene of the Airborne Thematic Mapper image, is used to examine the effects of changes in spatial resolution on cluster classification accuracy, and the location and character of class boundaries. The optimum temporal, spectral and spatial resolution for the mapping of moorland vegetation are identified. These initial investigations form a basis for the development of an operational system using satellite data for large-scale moorland monitoring. Visual interpretation of single band and false colour composite images, together with the supervised maximum likelihood classification and filtering of Landsat Thematic Mapper images, results in the production of vegetation distribution maps of Calluna vulgaris and Pteridium aquilinum in the North York Moors, comparable in quality and detail to those used at present by the National Park Committee.

MOORLAND AND BRACKEN CHANGE IN THE NORTH YORK MOORS: AN INVESTIGATION USING REMOTE SENSING.

By

Alison Clare Southgate

Thesis presented for the degree of
Doctor of Philosophy

University of Durham
Department of Geography

1989

CONTENTS

LIST OF TABLES

CHAPTER 3

CHAPTER 5

CHAPTER 6

page

CHAPTER 7

APPENDIX 2

APPENDIX 4

LIST OF FIGURES

LIST OF PLATES

DECLARATION

I, Alison Clare Southgate, hereby declare that this thesis has been composed by myself, that it is a record of my own work, and that it has not been submitted in partial or complete fulfilment of any other degree or professional qualification.

Signed.....A.C. Southgate.....Date.22nd June 1989

COPYRIGHT

ACKNOWLEDGMENTS

Financial support for this research project was provided by a Natural Environment Research Council Studentship (1986-1988). Additional funding for fieldwork was provided by the North York Moors National Park Committee. The work was undertaken at the Department of Geography, The University of Durham.

I would like to thank Dr. Ray Harris for initial help, Dr. Roy Brown for valuable advice and discussion, and my supervisor, Dr. Ian Shennan, for encouragement and advice, and for helpful comments on drafts of the thesis.

I would also like to thank all those who helped with computing and image analysis, including Sinclair Sutherland, Dr. Danny Donoghue, Simon Hook and Dr. Ray Harris at the Geography Department, Durham; Vanya Gordon, David Ritchie, and Andrew McDonald at The British Geological Survey, Keyworth; and the duty advisors and computer operators at the Durham Computer Centre.

I am grateful to Dr. William Reed and Susan Southgate for help with fieldwork.

Thanks must also go to the technical staff of the Geography Department at Durham, including Mr D. Hudspeth, Mrs L. Scott and Mr A. Hudspeth in the photographic unit; Mrs M. Crichton for photocopying; Mr W. Corner, Mr D. Cowton, Mr P. Hume and Mr S. Allan in the drawing office; and all the secretaries.

I am grateful to all those people who have provided me with advice, support and encouragement throughout the research, including Susan Southgate, Rosemary Stone, Chris McBean, Saleh Schueb, and the other postgrads. Finally, I would like to thank Bill, for numerous discussions, for his comments on early drafts of the thesis, and most of all, for keeping me sane!

For Bill

CHAPTER 1. INTRODUCTION

1.1 Aims and objectives

The main aim of the research presented in this thesis is to evaluate remote sensing techniques for the routine mapping and monitoring of the distribution of moorland vegetation, particularly Calluna vulgaris and Pteridium aquilinum, in order to provide a regular input to management decisions.

The motivation for this work is derived from previous attempts at the management of conflicting landuse within the moorland area. It has been recognised that there are insufficient or obsolete data available to assess fully the extent and exact distribution of serious moorland problems. It is the intention of this research to establish an operational system utilising remote sensing techniques to generate vegetation maps, based on a detailed investigation of the temporal, spectral and spatial characteristics of the data. The main input of data is information acquired from satellite, airborne and ground based remote sensing platforms, in conjunction with traditional field work. The resultant maps may be used to identify areas where problems are acute and might best be alleviated through management intervention.

The North York Moors National Park was designated in 1952 "to preserve and enhance the natural beauty of the area" (North York Moors National Park Committee, 1985). Calluna vulgaris (common heather) is the dominant species in the moorland area, and it is considered crucial to conserve it as an integral part of the natural beauty of the landscape. No other area in England and Wales has such extensive areas of this vegetation and it is the primary aim of the management programme to help in its conservation. The present landuses on the Calluna moorland include extensive sheep grazing; the rearing of grouse for shooting; and recreation. Management problems arise as there is often conflict between these, and a balance between

the competing landuses must be reached (Simmons, 1975; Simmons, 1981a).

The spread of Pteridium aquilinum (bracken) into areas previously occupied by Calluna vulgaris or agriculture, is provoking considerable interest at present on a national scale. Pteridium expansion is a problem not only in the North York Moors, but in many other areas, for example, the uplands of Scotland (Birnie, 1985) and Wales (Williams et al, 1987), where it is increasing rapidly. The main reasons for concern are that it infests agricultural fields, mainly improved pasture in the North York Moors, and makes them less productive; it is tall and impedes access to walkers and stock; when it senesces the dry fronds are a fire risk; it causes stomach and rectal cancers if consumed by stock; and it harbours ticks (Ioxodes micinus) which can kill sheep and grouse, by tick pyaemia (Smith, 1977).

Pteridium aquilinum has the competitive edge over Calluna vulgaris and other species, and this has led to its spread, so that now 12,000 of the 50,000 hectares of moorland within the North York Moors National Park are infested, and it is spreading by about 120 hectares a year (North York Moors National Park Committee, 1982; plates 1.1 and 1.2).

Its spread has been enhanced by a reduction in its commercial use (for potash, fuel, thatch, compost and soap), so that it is no longer harvested. Its spread is also exacerbated by the depopulation of rural areas, and increases in labour costs, so that clearing is not carried out (Rymer, 1976). Traditional methods of control, such as mowing, crushing and ploughing, have generally been superseded by the use of chemical herbicides or mychoherbicides, such as fungi (Norton, 1982). However, this is expensive and target areas which would most benefit from spraying must be identified for effective control.

Plate 1.1 An example of the invasion of Calluna moorland by Pteridium aquilinum; Hutton Beck, Blakey Ridge (May 1987)

Plate 1.2 An example of the invasion of agricultural areas by Pteridium aquilinum; the western slope of Blakey Ridge, from Farndale (July 1987)

There are several concerns related to the conservation of Calluna moorland, in addition to the expansion of Pteridium, including the over-aging of Calluna, resulting from a lack of regular burning; the loss of moorland to agriculture and forestry; and erosion, often caused by overuse of footpaths for recreational purposes.

The objective of the research reported in this thesis is to develop and evaluate a routine methodology for the production of detailed vegetation distribution maps of Calluna vulgaris and Pteridium aquilinum, together with other important moorland species, in the North York Moors. Remote sensing has a valuable role to play in the preservation of a unique landscape, so that management can be made less time-consuming, less expensive, and more efficient.

1.2 Structure of the thesis

This thesis is organised into three main sections: in the first section relevant background information concerning the study area and data sources are discussed; in the second section the temporal, spectral and spatial aspects of remote sensing are examined; and in the third section the potential for the use of satellite data to map the vegetation of a moorland environment is assessed. The final chapter draws together the conclusions of the thesis.

Chapter two introduces the main physical features of the study area, in order to provide a framework in which to assess the management pressures within the North York Moors National Park. The geographical location, topography, geology, soils, climate and vegetation are all outlined. The effect of management policies on the environment and landuse is also considered.

Chapter three introduces the data which are used in the research. The roles of ground mapping, field spectroscopy, aerial photography, airborne multispectral scanner data and Landsat Thematic Mapper data, within the remote sensing of vegetation, are assessed. In each case the characteristics of the actual data used in the project are

detailed, and any required preprocessing performed on the data is described.

Chapter four considers the temporal factors affecting the spectral response of moorland surfaces. Such factors can change the contrast between surfaces, so that it is vital to select imagery at a time when the spectral discrimination is optimum. Temporal resolution is defined, and the general effect of change through time on spectral response is considered. The chapter concludes with the identification of the optimum temporal resolution for the remote sensing of a moorland environment, based on a careful examination of the temporal characteristics of important moorland species.

Chapter five investigates the spectral characteristics of moorland surfaces. Spectral resolution is defined, and the main factors influencing the response of vegetated surfaces in general are described. Spectral data sets extracted from the field spectral, Airborne Thematic Mapper and Landsat Thematic Mapper data, are statistically analysed in order to characterise important moorland species, and to identify the optimum spectral resolution for moorland mapping. This is completed with careful consideration of the temporal context outlined in the previous chapter.

Chapter six is concerned with the spatial aspect of remote sensing. Spatial resolution is defined, and the complex effects of a change in pixel size upon the accuracy of an image are specified. A case study experiment, using an Airborne Thematic Mapper scene degraded to successively coarse resolutions, is used to assess the importance of spatial resolution, and its affect on classification accuracy, and the location and characteristics of boundaries.

Chapter seven draws on the conclusions of the previous three chapters in order to assess the potential of satellite data for the development of an operational moorland mapping and monitoring system. Single band, false colour composite and maximum likelihood classification images are investigated in detail, leading to the

production of maps of key vegetation types. The accuracy of these maps is assessed with reference to published National Park maps. Finally the effect of spatial filtering on a mapping accuracy and scene noise is briefly evaluated.

In chapter eight, the principal findings of the thesis are presented, and possible directions for future research are suggested.

CHAPTER 2. THE STUDY AREA

2.1 Introduction

The aim of this chapter is to introduce the study area and to provide a physical context for the relevant management pressures within the National Park. The first section describes the geographical location and topography of the area, and subsequent sections discuss the solid geology, soils, climate, vegetation and the effect of management policies upon the landuse and vegetation.

2.2 Location and topography

The North York Moors form a dissected upland plateau in the north-east of England (figure 2.1), rising in sharp contrast to the surrounding lowlands to a height of over 400m. The main moorland area, termed the Central Watershed by Elgee (1930), trends from west to east, falling from a highpoint of 454m on Urra Moor, to the lowlands at the North Sea coast (183m). The boundary between the moorland and the valleys below follows the 183m contour quite closely. The area extends for approximately 54km from west to east, and 24km from north to south.

To the west, the Hambleton Hills end in a steep escarpment which overlooks the Vale of Mowbray, while the more gentle northern limit is marked by the Cleveland Hills, which separate the moorland from the Tees basin. The Tabular Hills form the southern boundary into the Vale of Pickering, and the eastern margin is delimited by steep cliffs at the coast (figure 2.1).

The main topographical variations in the North York Moors massif are caused by stream erosion (Palmer, 1973). The dome-shaped plateau was formed by uplifts during the Tertiary (Kent, 1980), and today it is dissected by river valleys which radiate from the Central Watershed, mainly to the north and south.

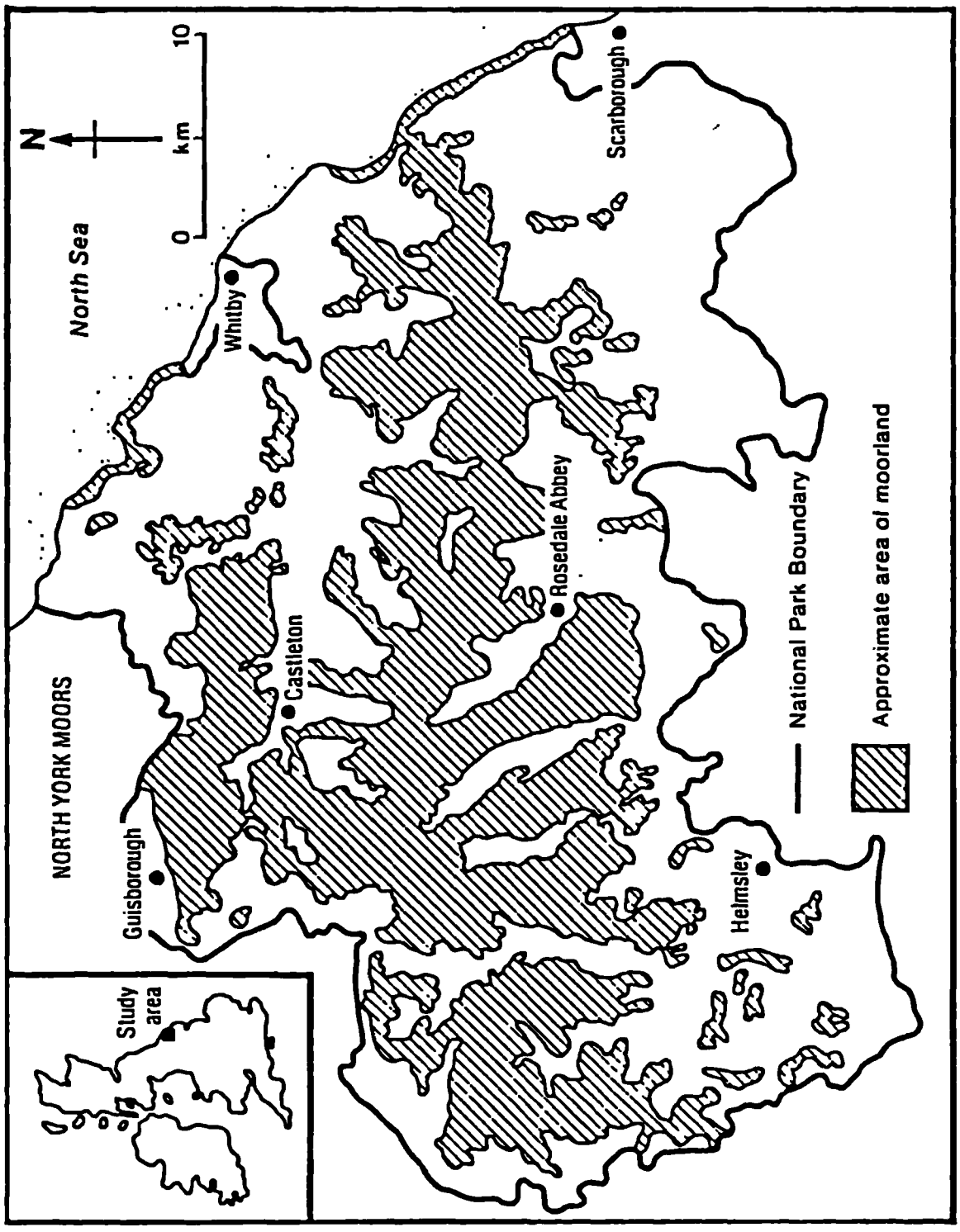

Figure 2.1 The location of the North York Moors

In the north the moors are bisected by the River Esk, which carries the waters from the deeply incised north-running valleys, such as Glaisdale and Danby Dale, to the coast at Whitby. The south-flowing streams generally have broader valleys, such as Rosedale and Farndale, and these drain through the River Derwent to the Humber. The high land is broken by the valleys of the Murk Esk and Newton Dale, which separates the lower moors to the east from the Central Watershed (figure 2.1).

In contrast to the valleys with fairly steep slopes, the moorland of the Central Watershed has a relatively flat and featureless surface, and gentle gradients with minor undulations are characteristic.

2.3 Geology

The solid geology of the North York Moors is illustrated in figure 2.2. The rocks which underlie the region are mainly Jurassic in age. The geological structure is relatively simple since there has been little disturbance to the almost horizontal sedimentary strata (Fox-Strangeways et al, 1885). Middle Jurassic rocks are evident in the highest areas, and where these have been removed, predominantly by stream erosion, the older Lower Jurassic rocks have been progressively revealed. As a result, a close relationship between topography and geology is evident.

The Lower Jurassic valley rocks are composed mainly of the Lias Group, which are easily eroded shales, limestones and sandstones. The Dogger, an ironstone deposited at the end of the Lias, has been extensively worked, causing surface disturbance. This is particularly evident in Rosedale (North York Moors National Park Committee, 1979a).

Most of the moorland is composed of more resistant Middle Jurassic rocks, the most extensive being the Deltaic Series of clays, clay shales, sandstones, coals and ironstones, sometimes capped by Moor Grit, a hard quartzitic sandstone (Carrol and Bendelow, 1981).

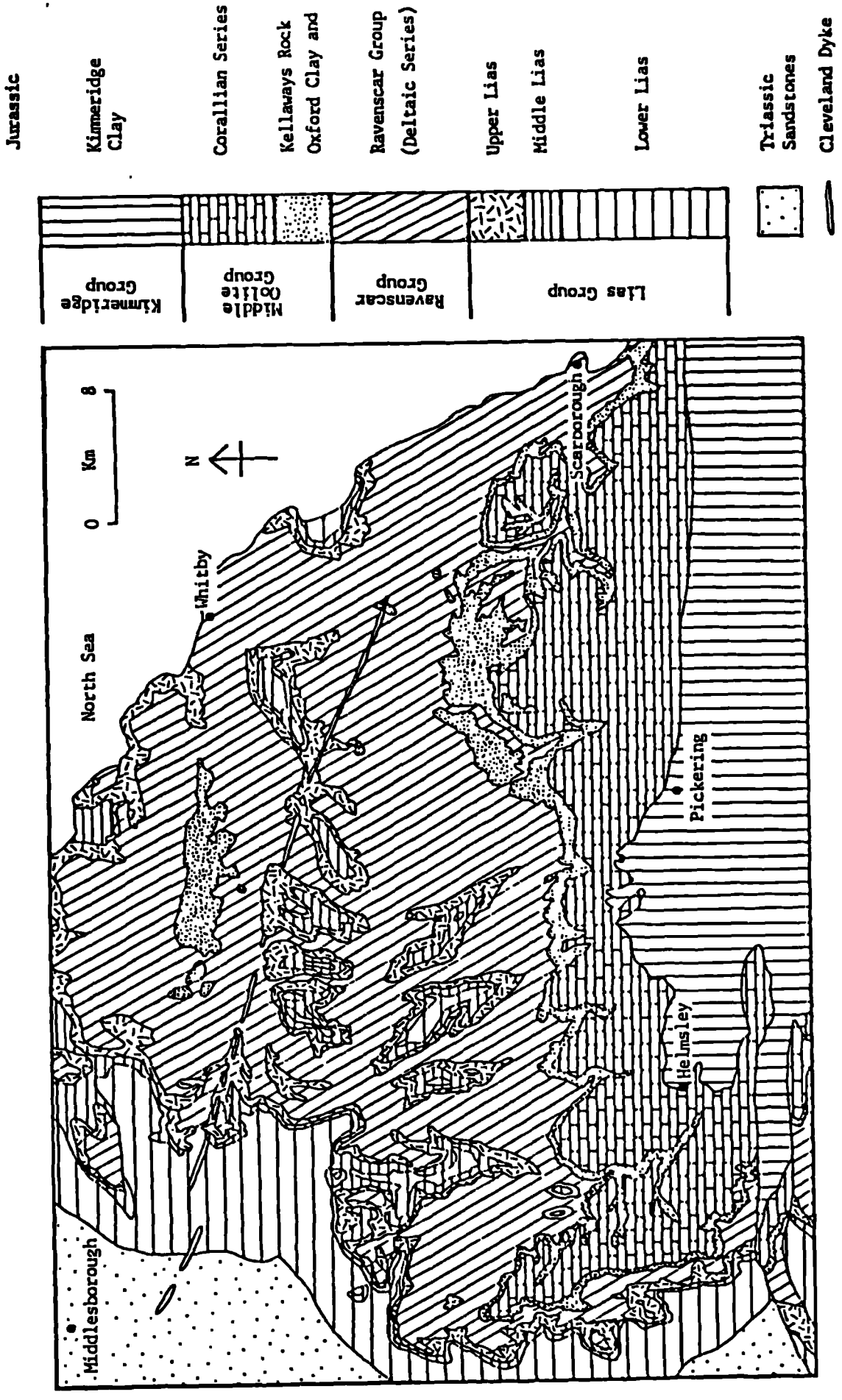

Figure 2.2 The geology of the North York Moors
(North York Moors National Park Committee, 1979a)

The Upper Jurassic rocks may be split into two main types, Oxford Clay and the Corallian Series. Oxford Clay is a soft silty clay or clay shale, which is at the base of the Tabular Hills. The Corallian Series consist of more resistant calcareous grits and oolites, which outcrop in the south on the moors and in the Cleveland Hills.

It is thought that the North York Moors were not glaciated by the last (Devensian) ice sheet (Maltby, 1980; North York Moors National Park Committee, 1979a). Consequently, glacial deposits, such as boulder clay or glacial gravels, which are present at the fringes of the moorland, are not evident on the Central Watershed (North York Moors National Park Committee, 1979a).

2.4 Soils and peat cover

The soils of the North York Moors are generally acid and low in nutrients. The Soil Survey identifies six major soil groups; Lithomorphic soils, such as rendzinas and rankers; Pelosols which are slowly pervious clay soils; Brown earths; Podzolic soils, including gley-podzols and stagnopodzols; Gley soils, including stagnogleys and stagnohumic gleys; and Organic or peat soils (Carrol and Bendelow, 1981).

A strong relationship has been identified between the soils and the solid geology of the moorland area (Anderson, 1958). The sandstone rocks are associated with free drainage and rapid leaching, leading to the formation of podzols, which are acidic and low in nutrients. In contrast the valley soils are more fertile, where the softer Liassic rocks result in heavy clay pelosols and more free-draining brown earths.

However, within these generally homogeneous soil areas, local differences occur. These may be accounted for by topography and the resultant differences in drainage. For instance, local gleying may occur in valley soils where drainage is poor, resulting in the formation of stagnogleyic brown earths; and where drainage is impeded

in upland areas, peaty gleys may develop. This is especially so where iron is present and a hard pan develops in the 'B' horizon. In such locations the downward movement or organic material is hindered, waterlogging occurs causing gleying, and peat deposits may subsequently become established (Innes, 1981).

There are two main types of organic soil on the Watershed; basin peat and blanket peat. Basin peats develop in natural depressions and on flat land where drainage is restricted. These form some of the deepest peat areas. For example, more than 3m of peat have been recorded at Bluewath Beck on Glaisdale Moor (Gundill, 1971), and 6m of peat have been found in a filled-in channel, on Egton High Moor (Simmons, 1969). Blanket peat has spread from the basin centres onto surrounding gently sloping land, to cover much of the Watershed with a shallow layer of organic material (Maltby, 1980; Innes, 1981).

The close and apparently simple relationship between soils and geology has led past authors to argue that podzol soils were natural to the Watershed (e.g. Elgee, 1912). However, more recent work suggests that brown earth soils under deciduous woodland were once dominant. Fossil brown earths have been found to exist below Bronze Age barrows in areas that are now podzolised (Dimbleby, 1962). It is now thought that the change to podzol soils was indirectly induced by man, as a consequence of a direct effect upon the vegetation. In deforesting the area, Bronze Age man enabled the establishment of the present vegetation (section 2.6; Tinsley, 1981). Heath vegetation breaks down to form a mor humus which further acidifies the soils, and the removal of trees exposes the soil and increases the likelihood of leaching.

2.5 Climate

The climate of the North York Moors is influenced by three main factors; relief, location in the rain-shadow to the east of the Pennines, and proximity to the coast (Atherden, 1972). The influence of relief may clearly be seen when the rainfall isohyets are

considered, as they follow the contour lines quite closely. Surrounding lowland areas have an average of 725mm per annum, while the Central Watershed receives over 1000mm (King, 1965; Cundill, 1971). However, the rainfall is relatively low, considering the height of the area, and this is mainly due to the location in the rain-shadow of the Pennines, so that the rain-bearing potential of westerly winds is reduced.

Temperature is considerably affected by the maritime location, as the North Sea has a moderating influence preventing climatic extremes. Consequently, the mean monthly temperature rarely falls below zero, and in the summer the average is seldom over 15° C (Maltby, 1980; Atherden, 1972). Temperature is also related to relief. The lower temperatures on the higher land are exacerbated by exposure to strong winds which are maximised by the flat and treeless nature of the Watershed. Just below the break in slope on the sides of the valleys, conditions are more sheltered. The winds are predominantly from the south-west (Carrol and Bendelow, 1981).

Relief is also an important factor when snow cover is considered. The high moorland in snow-covered for approximately 40 days per year, while lower areas characteristically have snow cover for a shorter period and a lower incidence of frost (Carrol and Bendelow, 1981).

2.6 Vegetation

One of the most striking features of the vegetation is the sharp contrast between the moorland communities on the higher land, and the agriculture of the valleys. In this section the moorland communities are considered in greater detail. The cover types which predominate on lower land are discussed in more detail in section 2.7.

The upland areas, including most of the Central Watershed, are dominated by Calluna vulgaris (common heather). Variations within the vegetation associated with the Calluna have been closely related to peat depth and associated levels of moisture (Elgee, 1914; Cundill,

1971). The National Park Committee divides the plateau vegetation into four main categories: flushes; damper areas; drier areas; and dry moorland slopes (North York Moors National Park Committee, 1979b).

Flushes, or spring areas, lie mainly on mineral or thin peat soils, or on small, deep peat accumulations at valley heads. They usually arise where water is moving across the surface (North York Moors National Park Committee, 1984a). These are boggy areas dominated by pools of Sphagnum (bog moss) and expanses of Juncus squarrosus (heath rush). Other common species include Carex echinata (star sedge) and Agrostis canina (brown bent grass) (North York Moors National Park Committee, 1979b).

The damper areas occur in some of the highest parts of the Watershed where the surface is flat or depressed, and rainfall is high, leading to the build-up of the deepest basin peats. Calluna vulgaris is present but it is often dominated by Erica tetralix (cross-leaved heath), Eriophorum vaginatum (hare's tail) and Molinia caerulea (purple moor grass). Juncus squarrosus and Sphagnum occur in the wettest areas. (North York Moors National Park Committee, 1979b).

The drier areas, which are mainly on the Deltaic rocks in parts of the Watershed surrounding the damper areas, have the most luxuriant and vigorous heather growth. In very dry parts, the vegetation is more varied, and Vaccinium myrtillus (bilberry), Erica cinerea (bell heather), Empetrum nigrum (crowberry) and Potentilla tormentilla (tomentil) become more common. In slightly wetter areas Calluna is often co-dominant with Nardus stricta (mat grass) (Carrol and Bendelow, 1981). However, according to Cundill (1971), the variety which was noted in 1914 by Elgee in drier areas has been reduced as a result of interference by man, especially the burning heather areas (section 2.7 below). This has led to a lowering of species diversity on these drier moors.

The final category is dry moorland slope vegetation. This coincides with the Upper Lias clays and is dominated by Pteridium aquilinum (bracken) and Vaccinium myrtillus. In these areas there is little peat development and drainage is relatively free, the soils change from podzols to brown earths and there are generally more sheltered conditions. Pteridium cannot tolerate waterlogging (Jeffreys, 1917) and is sensitive to frost and wind exposure (Haffey, 1978) and therefore it flourishes on these sheltered well-drained slopes. It often extends unbroken for miles along the sides of valleys. In increasing areas the Pteridium has spread upwards into the Calluna (North York Moors National Park Committee, 1984a; section 1.1). Pteridium often occurs in almost pure stands but it can be mixed with Calluna, Vaccinium and grasses such as Deschampsia flexuosa (wavy hair grass) (North York Moors National Park Committee, 1979b). On more exposed slopes Vaccinium tends to dominate (Carrol and Bendelow, 1981).

At the beginning of this century authors suggested that the heather moorland was the natural climax vegetation (e.g. Elgee, 1912; Tansley, 1939). This is no longer thought to be the case, and it is considered to be a cultural, semi-natural vegetation community (Simmons, 1981a). More recent work with pollen analysis (e.g. Simmons, 1969; Cundill, 1971; Simmons and Innes, 1987) and soil analysis (e.g. Dimbleby, 1952) suggest that the moors were previously forested, and that manipulation by man has led to the development of an artificial landscape. Large-scale felling by Bronze Age people after 1500 B.C. led to the deforestation of the area, the podzolisation of the soil (section 2.4; Tinsley, 1981; Simmons, 1981b), and the establishment of the present vegetation. In more recent times the domination by Calluna has been maintained and increased, especially by the burning regime associated with grouse-rearing (section 2.7).

2.7 Landuse and management

The North York Moors National Park Plan Review (1984b) identifies

four basic landuse categories within the boundaries of the park. Farmland is the largest category, covering approximately 40% of the area; moorland covers approximately 36%; coniferous forest, which has recently increased markedly, accounts for 20% of the park, and deciduous woodland covers the smallest extent at 5%. In addition to these categories there are minor amounts of settlement and industrial land use.

Agriculture is the biggest single employer (and landuse) in the Park (North York Moors National Park Committee, 1984b). Arable and mixed farming are important close to the coast and to the south of the moors, but stock rearing is the dominant agricultural practice in the Central Watershed. Sheep farming is traditional, but as this has become less lucrative, dairying and hay production have become more important (Carrol and Bendelow, 1981). It is the policy of the National Park Authority to discourage the conversion of moorland into agricultural land. However, since 1950 almost 50km^2 (7.3% of the 1950 moor) has been changed to agriculture (North York Moors National Park Committee, 1984b).

The moorland category covers 494km^2 (North York Moors National Park Committee, 1984b). This area is used for two main activities: extensive sheep grazing and the rearing of grouse. Management associated with these two landuse practices has led to a virtual monoculture, dominated by Calluna. Calluna seeds require the high temperatures associated with fire in order to germinate, and the sheep and grouse need young shoots to feed on. This necessitates a phased burning of the moor, which results in a patchwork of Calluna at different growth stages. If burning is not completed at regular intervals, older areas become less productive, and the woody nature of the material creates a fire hazard. If accidentally ignited the uncontrolled fires can burn too deeply and destroy the seeds, which hinders regeneration. As the Calluna ages, the stems spread and flatten, causing bare patches to appear in the centre of plants where other species may invade. It was estimated that in 1983, 59.2% of the heather was over-aged (North York Moors National Park Committee,

1985). It is National Park policy to encourage regular burning in order to avoid dangerous fires and lowering productivity. Ninety-five percent of the open moorland could theoretically be converted to other uses and it is the aim of the National Park Committee to prevent this occurring in order to preserve the unique landscape for both conservation and recreation. Sixty-one percent of the moorland is protected to some degree, and landuse cannot be changed without formal proceedings. These areas include common land, Sites of Special Scientific Interest and land owned by the National Park Committee and the National Trust (North York Moors National Park Committee, 1984b). The pressures on the moorland which have been outlined above are seen as major management concerns alongside the problems of Pteridium invasion (North York Moors National Park Committee, 1984a; section 1.1).

Conifer plantations are a relatively recent phenomena in the National Park. Most are in large blocks owned by the Forestry Commission and have been planted within the last century. The major species is Pinus sylvestris (Scots pine). There are also large areas of Picea sitchensis (sitka spruce) and Larix kaempferi (Japanese larch), and smaller areas of Pinus contorta (lodgepole pine), Picea abies (Norway spruce) and Larix decidua (European larch) (Polunin, 1976; Carrol and Bendelow, 1981). Over 18% of the 1950 moorland has been converted to forestry, and the National Park Committee is attempting to prevent further loss of moor and to reduce the detrimental impact of any future felling and replanting upon the landscape (North York Moors National Park Committee, 1984b).

Deciduous and mixed woodland is the smallest of the four basic landuses, occupying approximately 7200 hectares of the Park. Broadleaved woodland tends to occur in fairly small blocks, with 60% of sites less than 4 hectares (North York Moors National Park Committee, 1984b). The main species are Quercus petraea (sessile oak), Fraxinus excelsior (ash) and Betula pubescens (birch). The ground flora tends to be rich and diverse, providing valuable bird and animal habitats where stock are excluded. But where grazing and

trampling are permitted, ground cover is sparse and regeneration of trees is a problem. Some areas of deciduous woodland have been felled and replaced with more commercially attractive conifers. The National Park Committee recognises the importance of broadleaved woodlands, as both a wildlife habitat and as a part of the landscape, and encourages as much regeneration as possible (North York Moors National Park Committee, 1984b).

Tourism is becoming increasingly more important within the National Park. The open spaces and solitude, together with the attractions of the villages and the facilities provided by the Park Committee, bring in a large number of visitors, especially from the nearby urban areas of Cleveland and West Yorkshire. Over 11 million people visit the Park each year, mostly for informal recreation such as walking, picnicking and sightseeing (North York Moors National Park Committee, 1984b).

2.8 Conclusion

The outline of the characteristics of the area is intended as a framework, to understand better the physical context in which the management pressures related to the remote sensing of moorland and bracken operate.

CHAPTER 3. DATA AND PREPROCESSING

3.1 Introduction

The purpose of this chapter is to outline the experimental design of the project and to introduce the data sources which are to be used, describing the position each occupies within the general structure of the research.

The linkages between the data types are considered, and subsequently the individual sources and any preprocessing are briefly described. The data sections progress from ground level, including mapping and field spectroscopy, through the intermediary airborne level, including aerial photographs and Airborne Multi-spectral Scanner data, to the satellite level with Landsat Thematic Mapper data.

3.2 Experimental design

The ultimate aim of this research is to develop a methodology for the routine monitoring of changes in moorland vegetation using remote sensing data. The most obvious data source for such a task is a sensor on board a satellite, in order that regular and large area coverage are guaranteed. However, to attempt to understand fully the relationships between the digital number (DN) on a satellite scene and the vegetation on the ground, and to select the optimum sensor, in temporal, spectral and spatial terms, an experimental design including the study of data from other sources is required. A firm scientific base to an operational management system is vital, and therefore the modelling of the relationship between surface biophysical characteristics and their spectral characteristics at ground and airborne levels is essential.

It was decided to analyse field spectroscopy data in order to assess the amount and nature of spectral information required for the task of moorland mapping. It was also intended to model the spectral

response of various species and assess the feasibility of separating vegetation to the sub-species level using spectral data alone.

Air Photographs were included in the experimental design for two basic reasons: Firstly, as a representation of traditional methods of vegetation mapping, for both comparison with, and an assessment of, the more complex digital analyses of modern remote sensing. And secondly, to assist in field mapping. The decision to use airborne data was taken for similar reasons to the field spectroscopy, with the added feature that the path of the reflectance through the atmosphere more closely represented the satellite data. In addition, the spatial dimension could be investigated using airborne data. The degradation of airborne data enables both the modelling of the effect of spatial resolution on the ability of the data to discriminate between different species, and the identification of the optimum pixel size.

Finally, the satellite data, in the form of Landsat Thematic Mapper data, should be considered in the light of the conclusions derived from the ground and air data, in order to assess the feasibility of using such data for monitoring and mapping the vegetation.

It was decided that throughout the research the analysis should concentrate on three aspects of remote sensing: the temporal, spectral and spatial resolution most suitable for the task. It was within this broad structure that the more detailed design of the project was formulated.

In each case it was decided to investigate the data statistically using point samples extracted from the data, and then, with the air and satellite multi-spectral data, to perform any necessary preprocessing before attempting image processing on the I^2S.

At every stage the need for data from remote sensing sources to be firmly rooted in a thorough knowledge of ground conditions was

considered essential. This led to the inclusion of detailed field mapping as an important part of the research.

3.3 Fieldmapping

3.3.1 The role of fieldmapping in remote sensing

Although it has often been suggested, remote sensing should not be considered as a replacement for the more traditional field survey, but as complementary to it (Steven, 1987). It is still essential to incorporate ground data within remote sensing applications and research (Justice and Townshend, 1981).

Field data are commonly used for three main purposes within remote sensing: for the delimiting of training sites of known characteristics; for the identification of key classes in unsupervised classifications; and for the assessment of the accuracy of a classification (Short, 1982). It was for these three basic reasons that detailed field maps were completed.

3.3.2 The field area

The fieldmapping was undertaken in a 40km^2 study area along Blakey Ridge. This sub-area extends for 10 km from north to south and for 4 km from west to east, and it covers parts of Farndale, Rosedale and Spaunton Moor (figure 3.1).

The area was selected for both scientific and practical reasons. The area has a diverse vegetation cover, with Pteridium aquilinum and Calluna vulgaris at all growth stages, together with a wide range of other species, the most dominant being Erica tetralix, Vaccinium myrtillus and bog vegetation such as Sphagnum and Juncus. The higher moorland areas are typical of the 'patchwork' appearance of the landscape, due to the burning regime which is carried out.

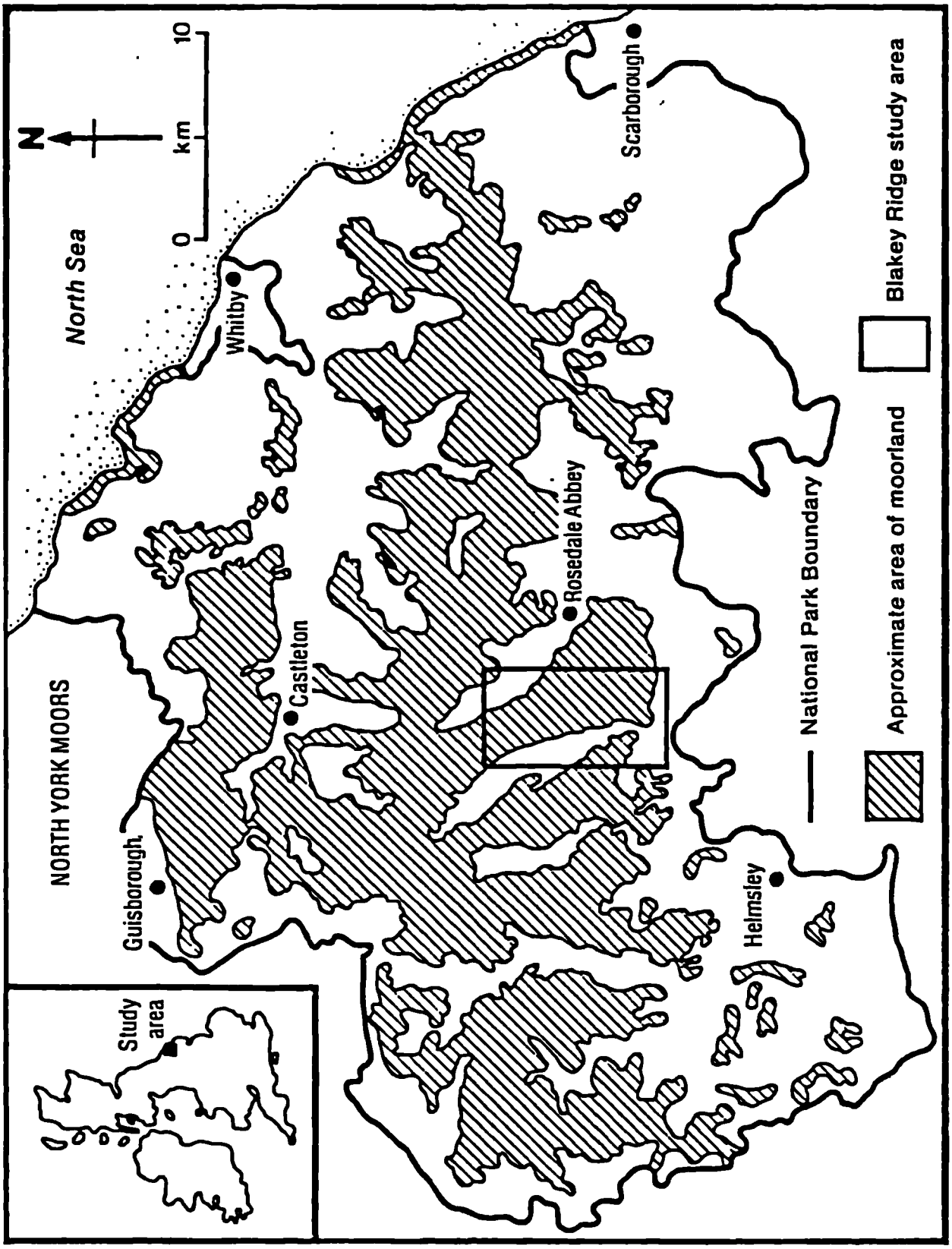

Figure 3.1 The location of the Blakey Ridge study area

There is also a full range of topographic variation, from the gently undulating moorland plateau to the steep sided valley slopes, with their associated variation in geology and soils (sections 2.3 and 2.4).

The practical motivation for the choice of area was mainly the ease of access, since there is a road bisecting the area, a vital requirement when using a radiometer and stand without assistance. The area is also mainly owned by two estates, both of which agreed to allow access to the grouse moors.

3.3.3 Methodology

Prior to fieldwork, aerial photographs were interpreted, and boundaries were drawn onto 1:10,000 Ordnance Survey maps of the area (section 3.5.5), as a basis for field mapping. The whole study area was visited, mapping the dominant species occuring within each boundary. The maturity of the Pteridium aquilinum and the Calluna vulgaris was also noted. In many cases the boundaries between vegetation types were extremely sharp, and could therefore be mapped accurately. This was especially the case at the edges of areas of Calluna vulgaris which had previously been burnt. However, other boundaries, where a gradual transition took place, could not be so objectively determined. These included areas where Pteridium aquilinum was encroaching into the moorland. In such cases the decision of where to locate the boundary on the field map was made after consideration of the evidence of subtle textural and tonal changes in the aerial photography, and a close investigation in the field. Areas where the dominant species covered over eighty per cent of the ground surface were classed as a pure stand of that species. Boundaries were located as accurately as possible on the margins of transitional zones where non-dominant species exceeded twenty per cent of the cover. Such zones were termed mixed vegetation, and the plant types present were recorded and their proportions estimated. Although great care was taken in this exercise it is impossible to place accurately a line on a map where in reality there is no exact

boundary, but rather a transition. However, after investigation in the field it was considered that this methodology was both consistent and a fair representation of the limit between areas dominated by one species alone, and areas with a mixed or transitional vegetation cover. The mapping was completed during the summers of 1986 and 1987. Copies of the original fieldmaps may be found in Appendix 1.

3.4 Field spectroscopy

3.4.1 Introduction

Field spectroscopy, a term introduced by Longshaw (1974), is the study of the relationship between the near-surface spectral response of objects and their biophysical characteristics in the field environment (Milton, 1987). The spectral response may be measured with a spectrometer, which can sense over a wide range of the spectrum in a continuous manner, or, as in this research, with a radiometer, which senses a limited number of preset wavebands (Milton, 1987). The radiometer receives radiation reflected from the objects in its Field Of View (FOV), and this falls onto a detector and produces a measurable voltage. The data may be calibrated to give the reflectance of the surface (Jackson et al, 1980). This reflectance is known as the Bi-directional Reflectance Factor (Milton, 1987), or the Hemispherical-Directional Reflectance Factor (Duggin, 1980), and is the ratio between the radiance reflected from the surface in a certain direction, and the total incoming radiance (irradiance) (Duggin, 1980).

The technique of field spectroscopy has been considerably refined since its early use at the beginning of the century. The increase in the use of airborne sensors in the U.S.A. during the 1960's, led to the development of ground instruments to calibrate the new wavebands (Milton, 1987). One of the earliest descriptions of a radiometer specifically designed for use within remote sensing was given by Silva et al (1971). Since the development of satellite remote sensing

the number and type of radiometers has proliferated, so that now many different designs are used within remote sensing.

3.4.2 The role of field spectroscopy in remote sensing

Field spectroscopy has an important role in three main areas of remote sensing: calibration; modelling; and prediction (Milton, 1987).

Although in-flight calibration is common, it may be more effectively achieved for air- and satellite-borne sensors by using ground sites where reflectivity is known. Field spectroscopy, using instruments with identical wavebands to the more remote sensors, may be used to determine the spectral response of chosen dark and light surfaces on the ground, which may be used to calibrate the air and satellite data (Marsh and Lyon, 1980).

Field spectroscopy may also provide data for the development and testing of models describing the relationships between biophysical and radiometric attributes (Milton, 1987). Well-established models based on field spectral data include: the relationship between Green Leaf Area Index (GLAI) and the infrared/red ratio (e.g. Budd and Milton, 1982); and various canopy reflectance models (e.g. Suits, 1972).

The third use of field spectroscopy is for prediction. Field radiometer data may be used to spectrally characterise various cover types which are of interest, so that their response on satellite or airborne data may be predicted. Radiometer data may be used to predict the optimum bands, the optimum geometric configuration of sensor and source, and the optimum season, for a particular task (Milton, 1987). They may also be used to assess the general separability of certain cover types, in order to predict the likely degree of success for classification techniques carried out on air or satellite data.

The present research is mainly concerned with the predictive use of field spectroscopy, and several factors must be considered before fully evaluating its potential in this role.

The distortions in reflectance detected by air and satellite sensors, due to its path through the atmosphere, mean that ground spectral data are more of an approximation of what is to be expected than an exact prediction. Among the causes of these distortions are atmospheric attenuation and forward scattering (Duggin and Phillipson, 1985).

The response of a radiometer also differs from that of more remote sensors in both spatial and spectral resolution. The spatial resolution of an airborne sensor is commonly above 2m, and satellite sensors range from 10m for the SPOT panchromatic mode (Chevrel et al, 1981), to over a kilometre for the AVHRR (Mather, 1987). A radiometer with just under 15° FOV has an approximate resolution of a circle of 45cm diameter if positioned 2m above the surface (Milton and Rollin, 1987).

The precise spectral resolution may also differ. For example, the Milton Multi-band Radiometer used in this research, has four bands which roughly correspond with the Landsat Thematic Mapper bands 2, 3, 4 and 5. The first three are very close, but the fourth band differs quite markedly from the TM band (section 3.4.4, table 3.1) (Short, 1982; Milton, 1987).

However, despite these problems, ground spectral data have a valuable predictive role in estimating the likely responses from other sensors.

3.4.3 Previous work

Field spectroscopy is now a well-established technique within remote sensing, especially within geological and geomorphological studies (e.g. Gladwell et al, 1983; Rothery and Lefebvre, 1985), soil studies

(e.g. Stoner et al, 1980), and agricultural studies (e.g. Curran and Williamson, 1985). It is only recently that ground spectral data have been collected on a wide scale for natural or semi-natural vegetation. Nevertheless, there have been several recent near-surface spectral studies of heath and moorland communities, including work in the New Forest on Calluna vulgaris by Milton and Rollin (1987), and Wardley et al (1987), and in the North York Moors by Weaver (1984, 1986), Alam (1987) and Alam and Harris (1987).

3.4.4 The Milton Multiband Radiometer

This research was carried out using a Geodata Unit Milton Multiband Radiometer (MMR). A brief description will be presented here, but a fuller account may be found in Milton (1986). The specifications are given in table 3.1.

The first three band widths are close approximations to the Thematic mapper bands 2, 3 and 4 but the fourth is significantly different, being 0.80-1.70μm compared to TM5, which is 1.55-1.75μm (table 3.1) (Milton and Rollin, 1987). The angular field of view is approximately 15° (Milton, 1986), giving a spatial resolution of 45cm at ground level, if used at the recommended height of 2m.

CHANNEL	WAVELENGTH (μm)	TM BAND	TM WAVELENGTH	REGION
1	0.54 - 0.57	2	0.52 - 0.60	green
2	0.62 - 0.64	3	0.63 - 0.69	red
3	0.78 - 0.96	4	0.76 - 0.90	near IR
4	0.80 - 1.70	5	1.55 - 1.75	short wave IR

FOV = 15° 45cm diameter circle at 2m

(after Milton and Rollin, 1987)

Table 3.1 MMR radiometer specifications (compared with TM)

3.4.5 Methodology

The sequential method of calibration was used. In this mode a single sensor head measures the surface reflectance, immediately followed by the reflectance of a Kodak grey card. Despite the very small delay between the two sets of data (one or two seconds), short-term fluctuations in irradiance may occur, causing slight errors in the data. The alternative method of simultaneous calibration removes these variations by employing two sensor heads at the same time; one viewing the surface, and a second viewing a Kodak grey card (Milton, 1986). The two sensors must be carefully inter-calibrated prior to use. However, financial considerations and availability of equipment prevented this slightly more accurate method being used.

The radiometer was bolted to a mast to ensure that the geometry between sensor, grey card and surface was fixed, and the head of the sensor was consistently orientated directly towards the sun, in order to maintain the same solar azimuth angle, and to avoid shadowing the surface and grey card targets. All measurements were taken between 10am and 3pm to avoid low sun angles, and cloudy or windy days were avoided.

Ten vegetation sites were selected within the Blakey Ridge study area (figure 3.1), with the assistance of Dr Roy Brown of the National Park. The classes are listed in table 3.2, and their locations are shown in figure 3.2.

The classes were chosen to cover the major vegetation species present in the study area. The Pteridium aquilinum class was subdivided in order to assess the separability between the different growth stages. Ten representative sites were selected, and within each one, ten sample points were randomly located. At each of these, three sets of radiometer measurements were taken, of both surface grey card. In addition the dark level voltage was recorded at the beginning and end of measurements at each site, by blocking all light from entering the sensor.

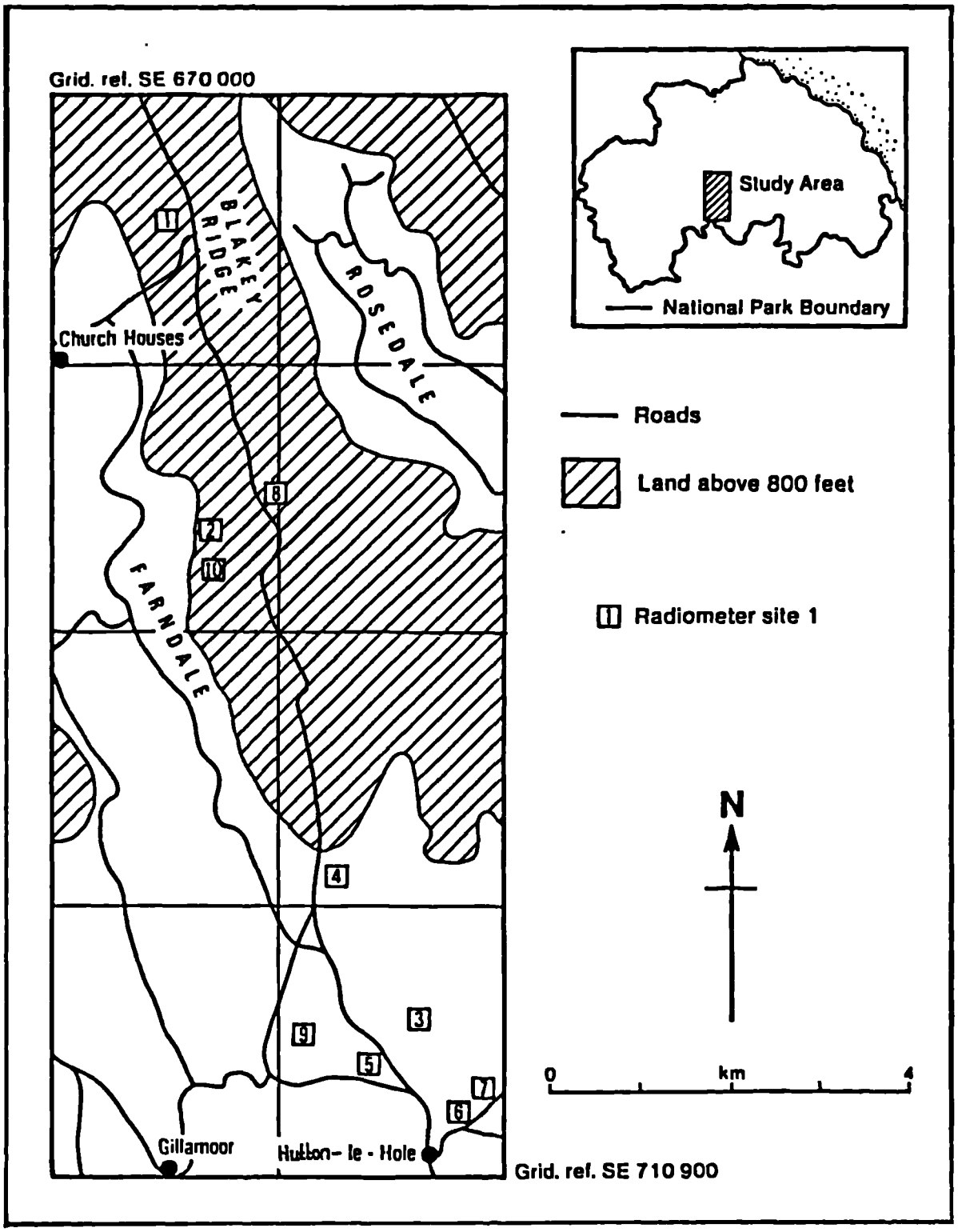

Figure 3.2 The location of the field spectroscopy sites

An environmental survey was also completed at each point, recording the species, percentage cover, presence of litter, soil moisture and slope. Two full sets of data were collected; the first between 17th and 20th June, and the second between 9th and 20th August 1986. It was originaly intended to collect another set of field spectral data during the flowering of Calluna vulgaris (late September; section 4.4.2), but weather conditions did not permit this. It was also intended to record the reflectance of Calluna vulgaris growth and management stages in the following year (1987), but adequate atmospheric conditions did not remain stable for a long enough period to collect sufficient data.

1. Mature Pteridium aquilinum (with unvegetated litter understorey)

2. Mature Pteridium aquilinum (with Vaccinium myrtillus understorey)

3. Pioneer Pteridium aquilinum (advancing into Calluna vulgaris)

4. Pioneer Pteridium aquilinum (advancing into Erica tetralix)

5. Treated Pteridium aquilinum (with unvegetated litter understorey)

6. Treated Pteridium aquilinum (with Vaccinium myrtillus understorey)

7. Degenerate Pteridium aquilinum (with unvegetated litter understorey)

8. Calluna vulgaris (full canopy)

9. Erica tetralix (full canopy)

10. Vaccinium myrtillus (full canopy)

Table 3.2 Field spectroscopy sample classes

3.4.6 Preprocessing

The means of the three sets of measurements taken at each sample point were used in all further analysis. This was done to help reduce any short-term fluctuations caused by atmospheric variation, or slight wind disturbance of the vegetation. The dark level voltage offsets were subtracted from the Digital Number (DN) values, and the calibration of the data was completed by converting the data to the Bi-directional Reflectance Factor (Milton, 1987), using the data from the grey card (equation 3.1).

Equation 3.1 Bi-directional Reflectance Factor

$$BDRF = \frac{es}{ec} \times K\lambda$$

where;
BDRF = Bidirectional Reflectance Factor
es = reflectance of surface
ec = reflectance of grey card
$K\lambda$ = wavelength dependent constant;
Channel 1 = 20.953
Channel 2 = 22.007
Channel 3 = 26.151
Channel 4 = 31.986

(after Milton, 1987)

3.5 Aerial photography

3.5.1 Introduction

Photographic systems use cameras and film to record information in the visible and parts of the Near Infrared (IR) (Hardy, 1981), and they are considered to be the precursors of modern remote sensing techniques. The first photographs were taken in 1839, and the first aerial photograph was taken from a balloon over Paris in 1858 (Short, 1982). The development of aerial photography was boosted by the First and Second World Wars, and today it is the best known and most commonly used remote sensing system (Hardy, 1981).

3.5.2 The role of aerial photography in remote sensing

Aerial photography has two major roles within remote sensing; cartography and reconnaissance (Slater, 1983). Topographic maps have been produced from air photographs since the end of the last century, and the techniques of photogrammetry are well-established, and considered as a science in their own right. Such techniques are well documented (e.g. Thompson, 1966; Wolf 1974). However, aerial photographs have a considerable role to play within airborne and satellite remote sensing. They have been used as "ground truth" where fieldwork is not possible, or as reconnaissance or mapping tools complementary to fieldwork (e.g. Adomeit et al, 1981). They have also been compared to the results of multi-spectral analyses in order to assess the accuracy or usefulness of modern techniques compared with traditional ones (e.g. Birnie, 1983).

In this research, air photographs were used for reconnaissance in the pre-fieldwork stage, and for comparison to traditional methods.

Air photographs have several key advantages over multi-spectral data, the main one being a superior spatial resolution. Many tasks require a detailed resolution, and in such cases multi-spectral data may only have a supplementary role (Short, 1982). Additional advantages of

aerial photography are the use of stereo pairs which adds another dimension to the coverage (Lo, 1986), and a greater geometric fidelity (Hardy, 1981).

However, air photographs suffer from several disadvantages compared with multi-spectral scanner data. They cannot record information outside the visible region and parts of the near IR, they require film which must be recovered and replaced, absolute calibration is not possible, and the results are not in digital form, and are therefore not amenable to computer processing, without first being digitised (Hardy, 1981).

3.5.3 Previous work

Aerial photography has been routinely used for decades in such areas as geology (e.g. Howard, 1965), geomorphology (e.g. Conway and Holz, 1973), and crop identification and condition assessment (e.g. Philipson and Liang, 1975; Curran, 1981, 1985a). More recently air photographs have been incorporated into remote sensing studies of moorland surfaces, for example, work on Pteridium aquilinum in Scotland by Birnie (1983), and moorland erosion in The North York Moors by Alam and Harris (1987).

3.5.4 The data

Two sets of imagery were recorded at the same time as the Airborne Thematic Mapper data (section 3.6) on 26th May and 22nd July 1986, over the Blakey Ridge study area (figure 3.3). A Wild RC8 wide angled lens (focal length 6 inches, 0.1524m), and Kodak black and white film were used. The nominal height of the camera was 1000m, but this was later more accurately determined (section 3.5.5).

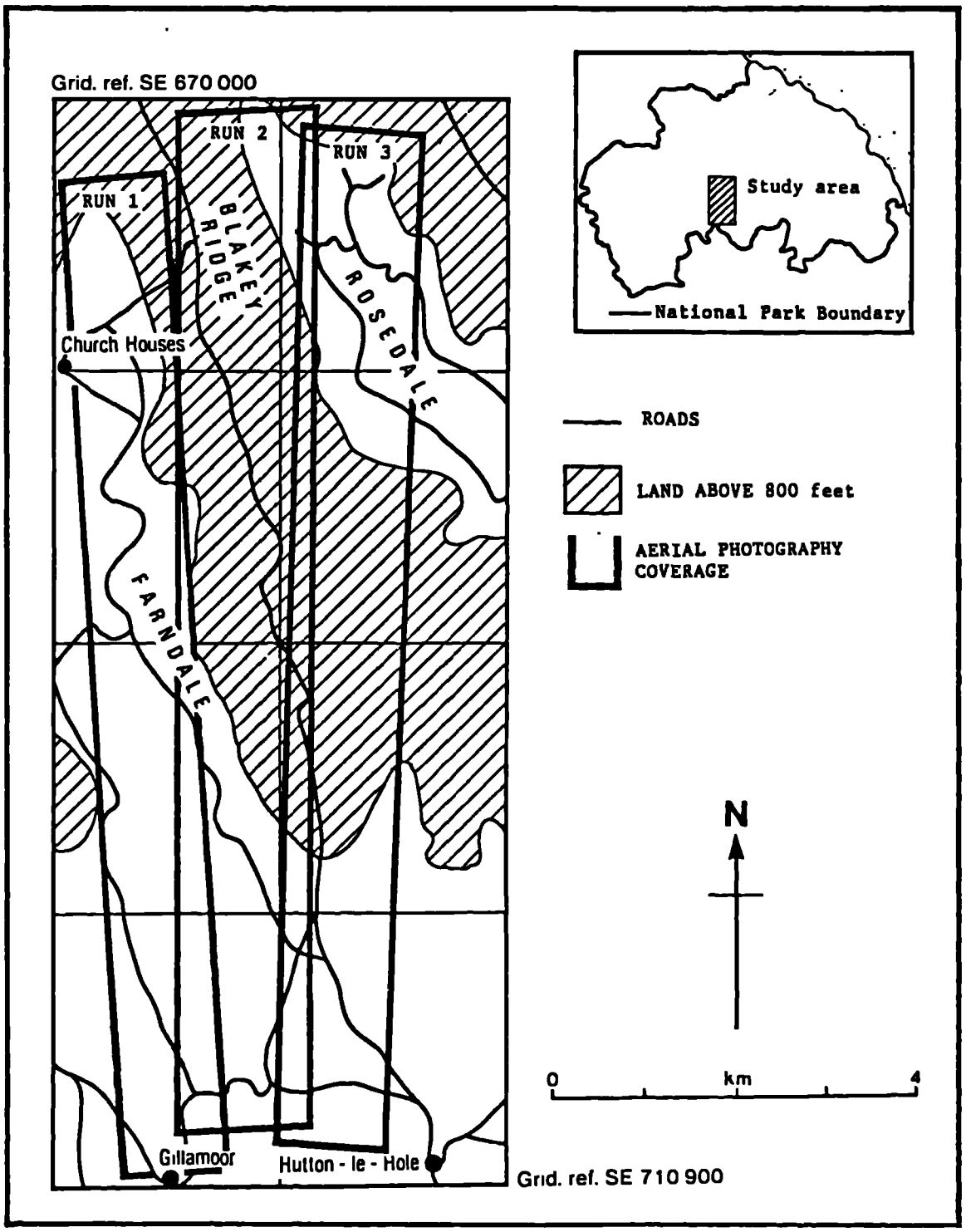

Figure 3.3a The extent of the aerial photography coverage: May 1986

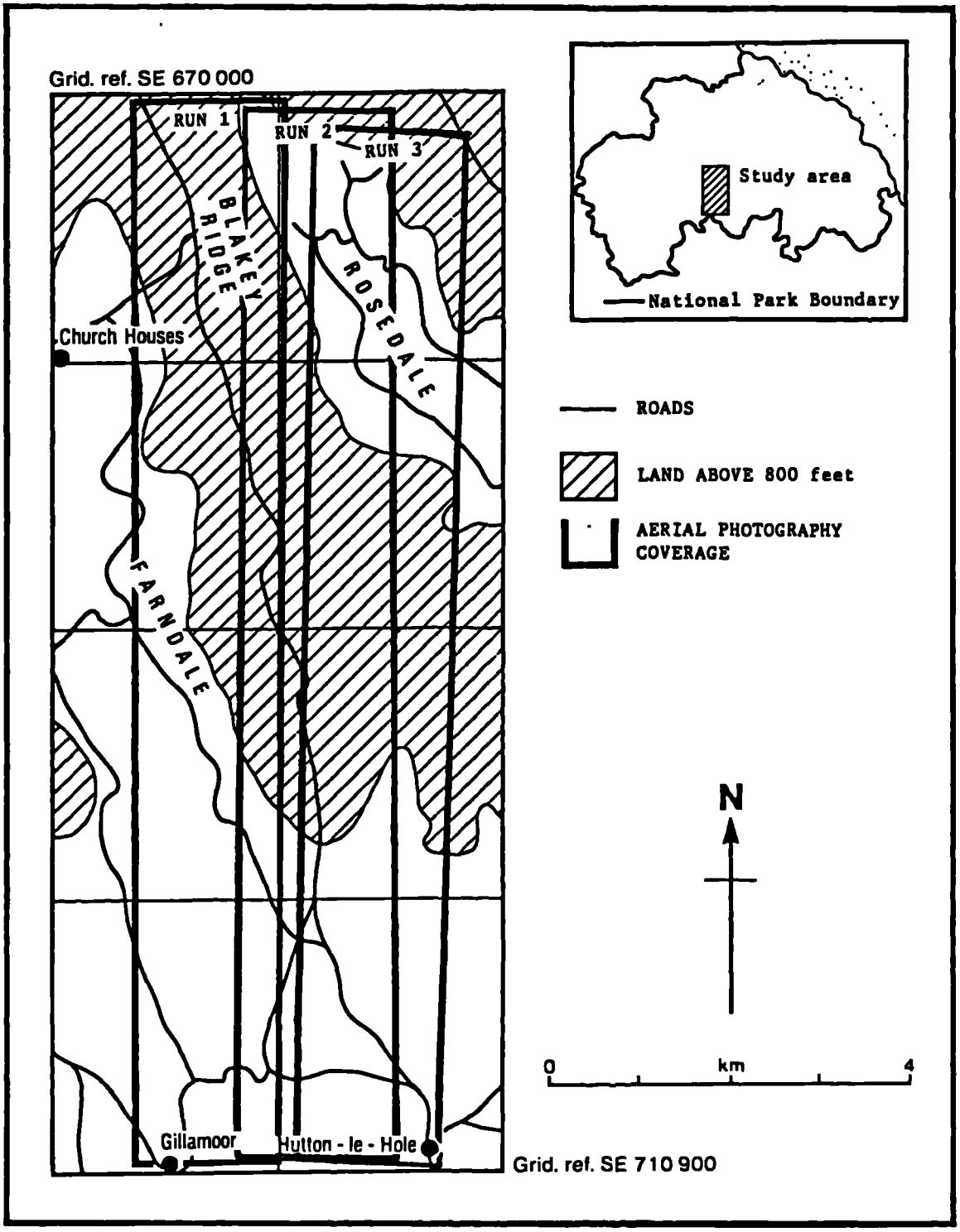

Figure 3.3b The extent of the aerial photography coverage: July 1986

3.5.5 Methodology

The height of the camera above ground was determined by measuring a distance on the image (keeping to the central portion of the photograph to avoid distortions), and then measuring the same distance on an Ordnance Survey map. The following formula was used to calculate the height;

Equation 3.2 Height above ground

$$HAG = \frac{0.1524 \times \text{known distance on ground}}{\text{measured distance on image}}$$

where;
HAG = Height above ground

The calculated heights were 1002.63m for May, and 849.92m for July. The photographs were used as a tool prior to fieldmapping. After a reconnaissance field visit, the photographs were interpreted using the basic characteristics of objects, which are; shape, size, pattern, shadows, tone, texture, and context (Lillesand and Kiefer, 1979). Boundaries were drawn onto 1:10,000 Ordnance Survey maps of the area. The problems associated with delimiting boundaries between vegetation types where a transitional zone exists have been outlined above (section 3.3.3). Where changes in species domination were not abrupt, initial boundaries were positioned on the basis of changes in texture and tone, and these were later refined in the field (section 3.3.3). These preliminary maps proved invaluable, since the complex nature of the species distribution and the flat and featureless

surface of the moorland, created difficulties of exact location whilst in the field.

3.6 Airborne Multi-spectral Scanner data

3.6.1 Introduction

Airborne Multi-spectral scanners (AMSS), such as the Daedalus Airborne Thematic Mapper (ATM) used in this research, are passive systems designed to collect and record radiation from the earth s surface in a number of narrow spectral bands simultaneously, using an airborne platform (Lillesand and Kiefer, 1979). In such systems a mirror reflects radiation onto a detector. The mirror is oscillated about an axis parallel to the flight direction, and this produces data along a scanline which is perpendicular to the path of the aircraft. The forward movement of the plane enables successive scanlines to be recorded. With suitable detectors AMSS systems may be used to collect data for any wavelength up to the microwave (Hardy, 1981).

The potential of AMSS was first appreciated in the 1960s, particularly in the U.S.A. (Milton, 1987). Their development has moved hand-in-hand with the development of satellite sensors, in order to test the design specifications (Hunting Geology and Geophysics Ltd., 1986).

3.6.2 The role of Airborne Multi-spectral Scanner data in remote sensing

The earliest role for AMSS was, as mentioned above, in the development and testing of satellite sensors. But AMSS data now have a prominant role in their own right (Hunting Geology and Geophysics Ltd., 1986).

Aircraft data are often used in experimental work for both modelling and prediction, in similar ways to field spectral data, and in

addition they are routinely used in operational surveys, particularly thermal surveys of heat loss over buildings, and in geological applications, such as mineral exploration (Daedalus Enterprises Inc., 1986).

AMSS data have several advantages over traditional air photographs. Photographic systems are limited to the 0.3 to 0.9 μm spectral region, whereas AMSS can image into the microwave (Hardy, 1981). Data from AMSS systems are more easy to calibrate and can be analysed by computer as they are recorded digitally (Lillesand and Kiefer, 1979).

AMSS offer a more flexible source of multi-spectral data than satellite sources. An aircraft is more directly under the control of users in terms of the timing and location of flights, and the data are also less rigid where spatial resolution is concerned, as an alteration in altitude and speed of the plane alters the pixel size. AMSS also tend to have a greater number of spectral channels, with a greater potential for modification than satellite sensors (Hunting Geology and Geophysics Ltd., 1986). Thus airborne data have a more comprehensive and flexible selection of temporal, spectral and spatial resolutions than photographic or space-borne detectors.

However, there are problems associated with AMSS data. The most common problems are the geometric distortions to the data caused by the unstable platform. Correction for roll can often be achieved as the sensor is usually fitted with a vertical gyro. However, pitch and yaw variations cannot usually be corrected for by the electronics of the scanner (Hunting Geology and Geophysics Ltd., 1986). This may result in data which are distorted and difficult to relate to a map projection.

AMSS have a relatively narrow swath width compared to satellite data, and several independent swaths are needed to cover any significant area. This causes problems which are exacerbated by the geometric distortions.

Problems may also be caused by a systematic brightening of pixel values towards the edges of swaths, especially if the sensor is viewing into and away from the sun. But these may be corrected for by several normalisation techniques (Hook and Donoghue, 1988).

3.6.3 Previous work

AMSS are now a well-established technique within remote sensing especially in geology and heat loss studies (section 3.6.2), and agricultural studies (e.g. Pearson et al, 1976, Curran and Williamson, 1985). However, more recently AMSS have been used to study semi-natural vegetation, including work by Curran in Berkshire (1981, 1983), by Milton et al (1986) and Wardley et al (1987) in The New Forest, and by Weaver (1986, 1987) in the North York Moors.

3.6.4 The Daedalus AADS-1268 Airborne Thematic Mapper

A brief description of the Daedalus scanner will be presented here, but a fuller account is given by Hunting Geology and Geophysics Ltd. (1986). The sensor specifications may be found in table 3.3. The Daedalus AADS-1268 ATM is the most advanced AMSS system available. It is an eleven channel system (table 3.3) which may be used to simulate Landsat Thematic Mapper and Multi-spectral scanner, and SPOT bands. (Hunting Geology and Geophysics Ltd., 1986).

The N.E.R.C. (Huntings) Daedalus scanner was flown on two occasions over the Blakey Ridge area, on 26th May and 22nd July, 1986. The flight paths were erratic due to low flying (c. 1000m) to avoid cloud, and the imagery subsequently has problems with cloud and cloud shadow.

3.6.5 Preprocessing

3.6.5.1 Byte-swapping

The ATM data are packed by two bytes per 16 bit computer word, numbered in the standard Hewlett Packard form, such that the most significant byte is first and the least significant is second (Hunting Geology and Geophysics Ltd., 1986). This standard is the reverse of that used by many computer manufacturers, including I^2S, where the least significant bit is first. Therefore, a byte-swapping programme was applied to the data before any further analysis.

CHANNEL	WAVELENGTH (μm)	TM BAND	SPECTRAL REGION
1	0.420 - 0.450		blue
2	0.450 - 0.520	1	blue
3	0.520 - 0.600	2	green
4	0.605 - 0.625		
5	0.630 - 0.690	3	red
6	0.695 - 0.750		
7	0.760 - 0.900	4	near IR
8	0.910 - 1.050		
9	1.550 - 1.750	5	short wave IR
10	2.080 - 2.350	7	short wave IR
11	8.500 - 13.00	* 6	thermal IR

* not exact equivalent (c.f. table 3.5)

IFOV= 2.5mrad
pixel size = 2.5m at 1000m, 25m at 10,000m
swathwidth = 1.5km at 1000m, 15km at 10,000m

(after Hunting Geology and Geophysics Ltd., 1986)

Table 3.3 Daedalus AADS-1268 ATM specifications

3.6.5.2 Radiometric calibration

In order to exploit the full 0 to 255 DN intensity range, the gain of the Daedalus AADS-1268 scanner may be preset before each run, to one of five gainsettings; 0.5, 1, 2, 4, and 8. This may be set independently on each channel. In addition, there is a dark level voltage offset, so that a value greater than zero may be recorded when all light is blocked from entering the sensor. This is regularly checked and recorded by Huntings in the laboratory (Wilson, 1986). The use of data uncorrected for gainsetting can lead to erroneous interpretations, and accurate quantitative comparison between swaths is not possible (Hook and Donoghue, 1988). Errors may also occur if uncalibrated data are used to examine inter-band relationships, for example ratioing two bands (Wilson, 1986). Therefore calibration was applied to the data. Calibration is the determination of the quantitative relationship between an instrument's response and the input values it is intended to measure (Norwood and Lansing, 1983). The linear conversion from DN to radiance is given in equation 3.3. The gainsettings may be extracted from the header information on the magnetic tape, and the gain and offset values (derived from laboratory tests) may be found in Wilson (1986). It must be stressed that this is not calibration to a ground target in order to calculate actual reflectance of the surfaces, but interband calibration to account for gainsettings and offsets.

The programme used to calibrate the data was written by S.J. Hook. ATM data often have problems caused by a systematic brightening of pixel values towards the edges of swaths (c.f. section 3.6.2). However, when collecting the Blakey Ridge data, the flight path of the plane was from north to south, and so the sensor did not alternately view into and away from the sun on each east-west scan-line, which is the main cause of the problem. In addition, as only 512 x 512 pixels were selected, the edges of swaths could be avoided. Investigation of the data did not show any obvious brightening across the images, and so no atmospheric or shade correction was performed on the data.

Equation 3.3 Calibration equation

$$Gain_g = \frac{gain}{gainsetting}$$

$$Offset_g = offset \times gainsetting$$

$$Radiance = Gain_g \times (DN - Offset_g)$$

where;
g = corrected for gainsetting
(after Hook and Donoghue, 1988)

3.6.5.3 Subscening and co-registration

Due to the problems of cloud and cloud shadow and a desire for a manageable area, one 512 x 512 subscene which was relatively clear on both the May and July data was selected (figure 3.4). This was used in all further analysis. Geometric distortions were large on both images, although slightly less on the July image, and so the July data were corrected to the British National Grid to enable overlay with field maps. 17 control points were used in the warping procedure, which was performed on an I^2S image processor. A nearest neighbour resampling technique was used to retain as much spectral information as possible. This method ensures that "real" values are copied directly from the input image, they are not interpolated or fabricated (Mather, 1987). The root mean square (RMS) error was 13.221 pixels. The May data were then co-registered with the corrected July image, using the same control points and resampling method. The RMS error was 5.007 pixels.

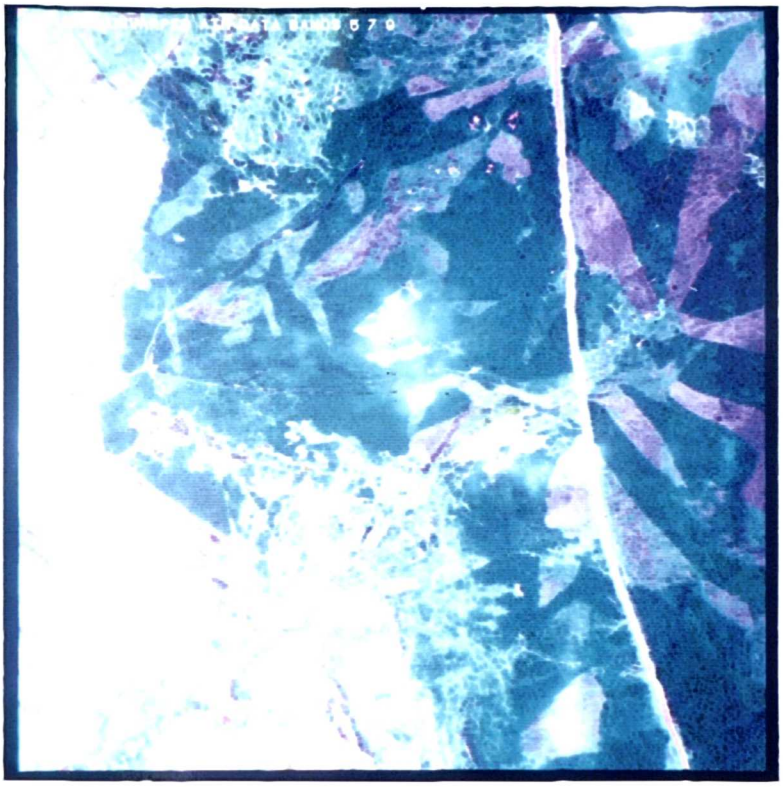

Plate 3.1 Unwarped ATM subscene showing part of Blakey Ridge: May 1986

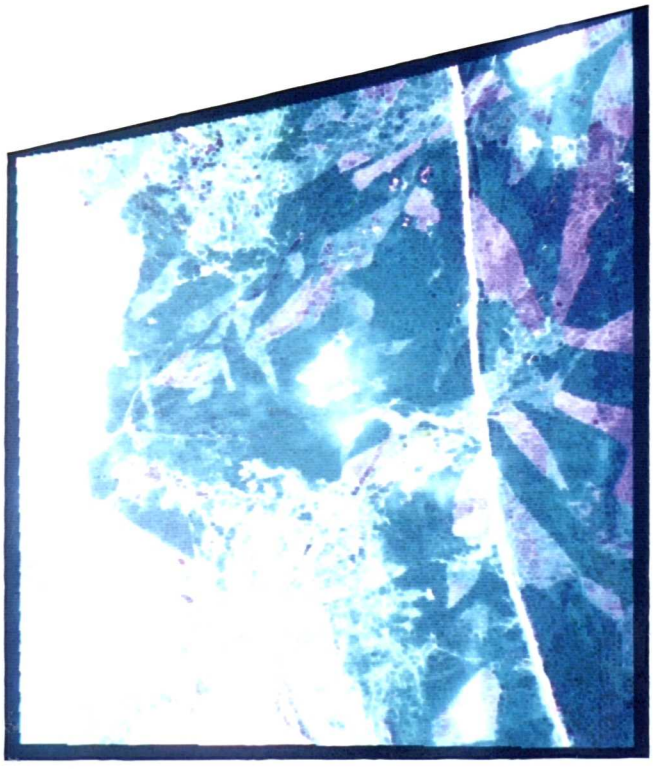

Plate 3.2 Geometrically corrected ATM subscene showing part of Blakey Ridge: May 1986

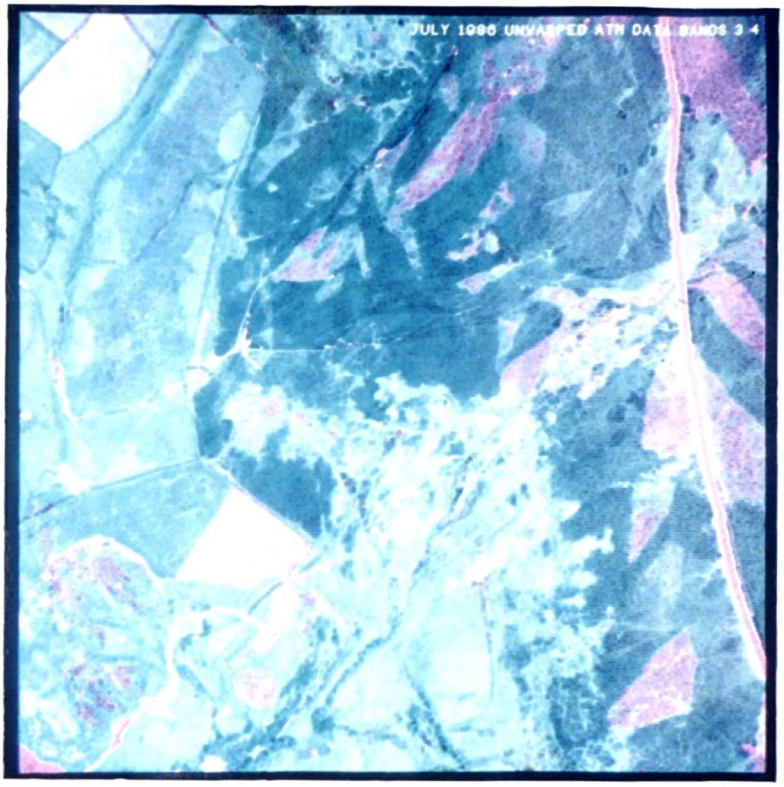

Plate 3.3 Unwarped ATM subscene showing part of Blakey Ridge: July 1986

Plate 3.4 Geometrically corrected ATM subscene showing part of Blakey Ridge: July 1986

These RMS errors are relatively large, as is to be expected when using a standard geometric correction algorithm, which does not take account of the sudden and unpredictable changes in attitude that are common in AMSS data (Fuller et al, 1988). However, a more complex algorithm, attempting to take into account such fluctuations, was not available. The selection of ground control points was refined as carefully as possible to obtain the best fit in the circumstances, and the correspondence, both between the two dates and with the British National Grid, was considerably improved. The original and corrected data are shown in plates 3.1 to 3.4.

3.6.5.4 Degradation and replication

The two 512 x 512 subscenes covering part of Blakey Ridge (figure 3.4), were spatially degraded from a 2.5m pixel size to a series of scenes, each with a successively coarser ground resolution. The aim of this experiment was to simulate the spatial resolutions of airborne data flown at higher altitudes (5m and 10m), and those of satellite sensors, SPOT at 20m, and Landsat Thematic Mapper (TM) at 30m. Aircraft data cannot provide an exact simulation of satellite performance (Townshend, 1984), and so comparison is not direct between the degraded scenes and the data from other sensors, because of atmospheric alterations and differences in sensor configuration and characteristics. Nevertheless, this work allows a general assessment of the relative usefulness of data at various resolutions, for the remote sensing of moorland vegetation.

Several authors have used similar experiments in the past to assess the effect of spatial resolution. These often use an algorithm with a weighted filter, to allow for the point spread function of the sensor they are simulating, followed by a filter which selects every other pixel on every other line, in order to degrade the image. (e.g. Sadowski et al, 1976; Markham and Townshend, 1981; Cushnie, 1987). However, in the present study, two sensors were simulated, TM and SPOT, and therefore a constant weighting could not be used.

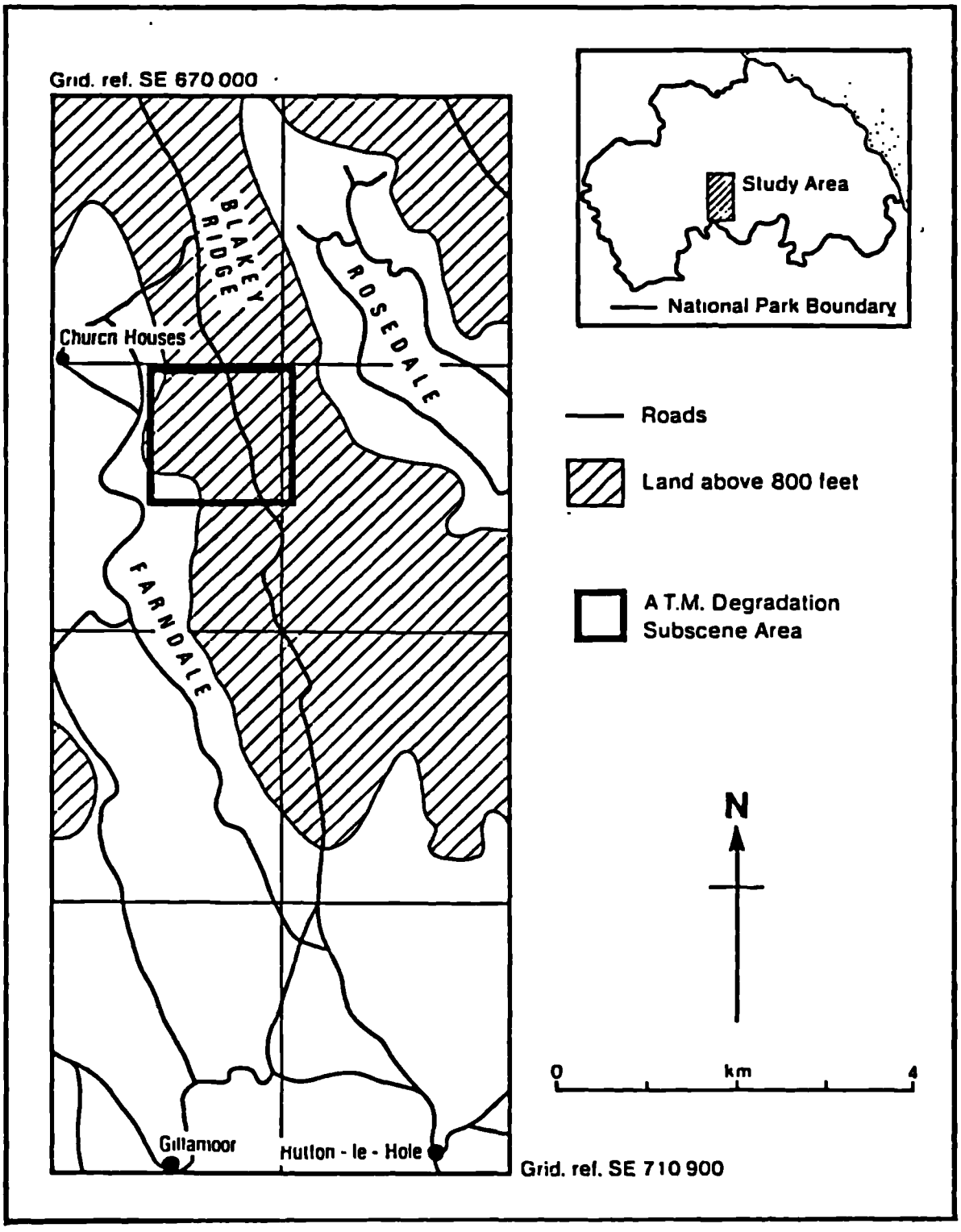

Figure 3.4 The location of the Airborne Thematic Mapper data degradation subscene

There are also problems associated with adding such noise to the data, and some authors have recognised anomalies in scene noise which were probably caused by adding a greater than necessary amount of simulated sensor noise (e.g. Markham and Townshend, 1981). Therefore, in this study, no scene noise was added, and pixel values were simply averaged, using a method suggested by previous authors (e.g. Clark and Bryant, 1976; Woodcock and Strahler, 1987). This approach assumes that the value recorded by the sensor is derived only from the area on the ground within the pixel (Woodcock and Strahler, 1987). This assumption is, however, unrealistic, but it does avoid the problems of determining exactly how much noise to add, and also the controversy over the precise definition of the measurement of spatial resolution (section 6.2; Townshend, 1980). In addition, it was the intention of this research to study the general relationships and impact of spatial resolution, rather than to mimic exactly the response of any particular sensor.

The ATM data flown on 26th May were collected at an altitude of 1002.63m. The 22nd July data were collected at an altitude of 849.92m (section 3.5.5). The nadir pixel resolution (NPR) was calculated using the following formula;

Equation 3.4 Nadir pixel resolution

$$NPR = 2 \times \tan\left(\frac{\theta}{2}\right) \times HAG$$

$$= 2 \times (0.00125 \times HAG)$$

where;
NPR = nadir pixel resolution
θ = 2.5 mrad (IFOV of sensor)
HAG = height above ground

The NPR was 2.5005m for the May data, and 2.1248m for the July data. In this study, only the bands equivalent to six TM bands (excluding the thermal band 6) were considered. However, the dynamic range in band 10 (TM 7) was so small that this data could not be used in any analysis. Thus only bands 2, 3, 5, 7 and 9 were used.

The original data were resampled using a scale factor of 1.0026 for May, and 0.84992 for July to achieve an exact 2.5m pixel size, using a nearest neighbour resampling method, in order to retain as much spectral information as possible. These 2.5m resolution scenes were subsequently resampled to resolutions of 5m, 10m, 20m and 30m (table 3.4).

	May	July
HAG	1002.63m	849.92m
NPR	2.5065	2.1248
scale factor from NPR to 2.5m	1.0026	0.84992
scale factor from 2.5m to 5m	0.5	0.5
scale factor from 2.5m to 10m	0.25	0.25
scale factor from 2.5m to 20m	0.125	0.125
scale factor from 2.5m to 30m	0.08333	0.08333

Table 3.4 Values used in degradation process

In this case the resampling method used was bilinear interpolation, in order to average the four nearest pixels to try to simulate the averaging effect of a coarser resolution.

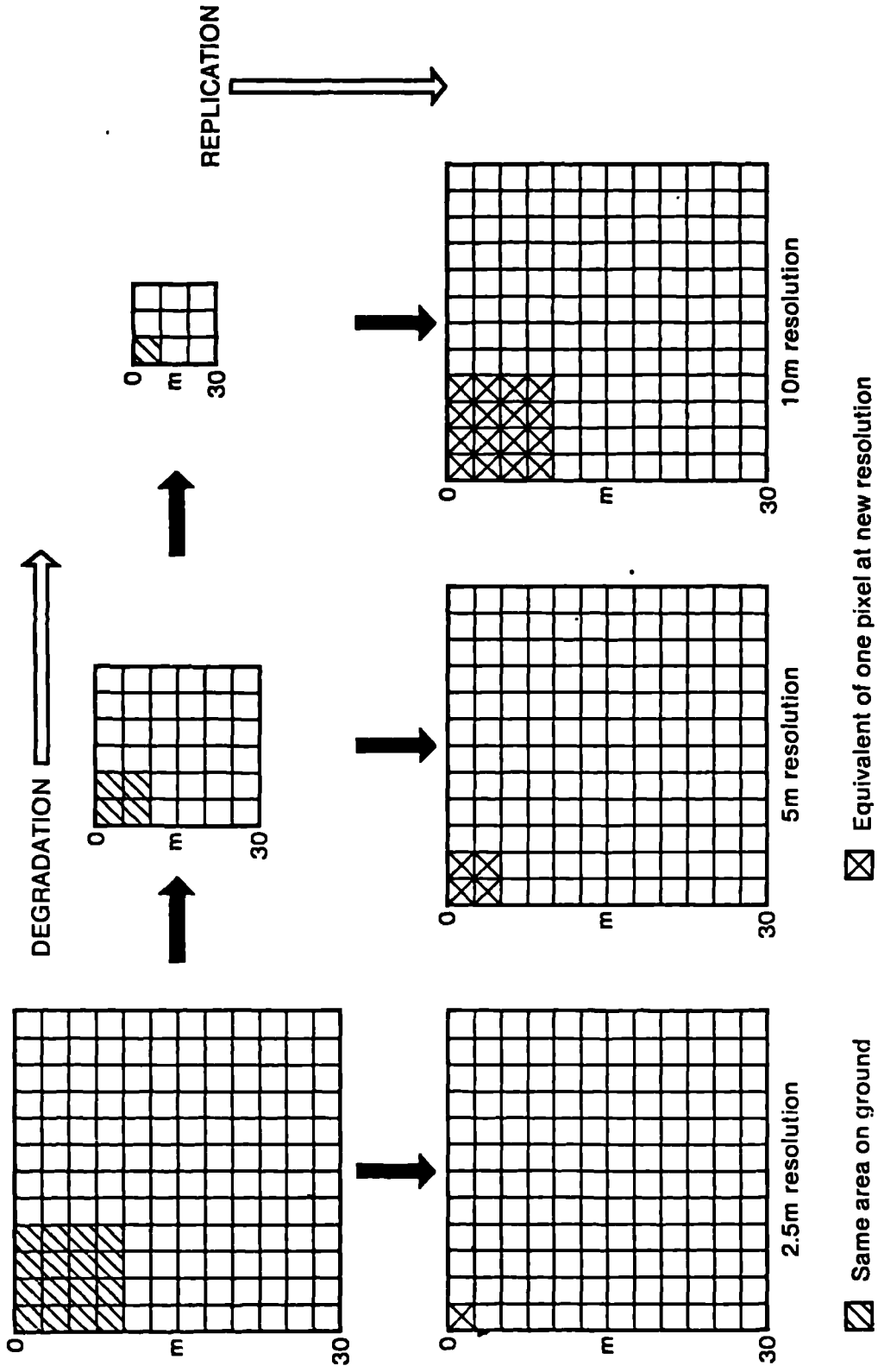

Figure 3.5 The Airborne Thematic Mapper degradation and replication methodology

A nearest neighbour method was not used, although this is computationally less complex, since it can cause mislocation of boundaries and does not account for averaging over the larger pixel size. A cubic convolution was not used as this method tends to over-average, which can blur boundaries and does not maintain the original spectral information (Mather, 1987). Due to resampling, every time the resolution was doubled (e.g. from 2.5m to 5m), the number of pixels was quartered (Woodcock and Strahler, 1987), i.e. from 512 x 512, to 256 x 256 (figure 3.5 top half). Therefore, in the above case, each pixel had to be replicated by four, to bring the total number back to 512 x 512, so that the same area on the ground was represented by the same area on the display image. On the new image, each block of four pixels represents one pixel at the new resolution, since all four have the same Digital Number (DN) value. This replication method has been used by several authors, including Markham and Townshend (1981), Cushnie (1987), Townshend and Justice, (1988). This was repeated for all the resampled images. As the resolution became more coarse, the pixels had to be replicated by a greater scale factor. For example, by eight to get a 10m resolution, where eight pixels of identical DN represent one pixel at the new resolution (figure 3.5 bottom half). The results of this process were five images for each date, covering the same area on both the ground and the screen, but of varying spatial resolution.

3.6.5.5 Extraction of training samples

DN values for the 5 bands equivalent to TM bands TM1 to TM5 (ATM2, ATM3, ATM5, ATM7 and ATM9) were extracted from each of the two 2.5m resolution images for use in statistical analysis. Reasonably homogenous areas of seven dominant vegetation types were selected on each image, with reference to field maps (section 3.3.3; appendix 1). Training areas were then delimited using the tracker-ball cursor on the I^2S image processing system, for each of the seven classes. The pixel values within each region were extracted and entered for analysis on the MTS mainframe computer at Durham. The classes and pixel counts are shown in table 3.5.

Class	No. of pixels
Mature Calluna vulgaris	100
Pioneer Calluna vulgaris	100
Burnt Calluna vulgaris	100
Degenerate Calluna vulgaris	100
Pteridium aquilinum	100
Grassland	100
Agriculture	100

Table 3.5 Extracted training samples - ATM data

3.7 Landsat Thematic Mapper

3.7.1 Introduction

Satellite remote sensing began in July 1972 with the launch of ERTS-1, the first in the series of Landsat sensors. Landsat evolved from early photographic missions from Mercury and Gemini flights, to become the first earth resources satellite dedicated to recording radiance from the visible into the thermal IR (Simonett, 1983).

3.7.2 The role of satellite sensors in remote sensing

Satellite sensors now have a dominant role in remote sensing. The data are used in many disciplines and analysis techniques are well-developed. The initial role for satellite data was to collect synoptic views of large areas, which were interpreted as aerial photographs. Today, as a result of the development and availability of more complex image processors, such data are also used for

classification of surface cover, estimating characteristics of the earth's surface, and monitoring change (Curran, 1985b). The synoptic coverage which satellites offer enable large areas to be studied relatively cheaply and easily. Such data also allow access to areas which are inaccessible on the ground.

The orbit of satellites mean that repeat scenes may be recorded which facilitates the monitoring of change. One of the most important roles of satellite sensors is that they broaden our knowledge of the earth's surface beyond the visible range. The extension into the near, short wave and thermal IR gives a new insight to the study of the environment (Townshend, 1981a).

However, there are some important drawbacks to satellite remote sensing. Non-radar sensors cannot penetrate clouds, and the signals are often distorted because of their path through the atmosphere (Duggin and Phillipson, 1985). The relationship between a DN recorded by the detector and the biophysical characteristics at the surface is not a simple one, and needs careful attention if it is to be understood fully. Also, the capital outlay required to buy image processing equipment is large compared with the costs of traditional air photograph interpretation, although recently, personal computer based systems have become more widely available, and this has lowered the costs.

3.7.3 Previous work

Landsat data have been used for many different applications. It has commonly been used in geological studies (e.g. Raines and Wynne, 1982) and in landuse mapping (e.g. Lo, 1981). More recently, attention has turned, as with other sensors, to the monitoring of semi-natural vegetation. For example, work in the New Forest by Townshend and Justice (1980), in Wales by Williams *et al* (1987), and in the North York Moors by Weaver (1986).

3.7.4 The Landsat Thematic Mapper

A brief description of the Landsat Thematic Mapper (TM) will be presented here, but a fuller account may be found in Short (1982) and Freden and Gordon (1983). The sensor specifications may be found in table 3.6.

The Landsat TM has seven spectral bands ranging from the blue to the thermal IR. The nominal resolution of the sensor is 30m, and it images the same area every 16 days (Freden and Gordon, 1983).

Two scenes of Northern England were used in this research (scene number 203/22). The first was recorded on 26th April 1984, and the second on 31st May, 1985. Uncalibrated DN values were used in all analysis. This means that quantitative comparison between the DN values on seperate scenes is not possible, as differences in the recorded values, mainly due to changed atmospheric and illumination conditions, are not taken into account.

CHANNEL	WAVELENGTH (μm)	SPECTRAL REGION
1	0.45 - 0.52	blue
2	0.52 - 0.60	green
3	0.63 - 0.69	red
4	0.76 - 0.90	near IR
5	1.55 - 1.75	short wave IR
6	10.4 - 12.5	thermal IR
7	2.08 - 2.35	short wave IR

IFOV = 11.56° pixel size = 30m Swathwidth = 185km

(after Short, 1982)

Table 3.6 Thematic Mapper specifications

3.7.5 Preprocessing

3.7.5.1 Subscening

Data from both dates were subscened to show just the North York Moors National Park area. Both subscenes were 1300 x 2200 pixels in size (figure 3.6).

3.7.5.2 Geometric correction and co-registration

The 1984 data were geometrically corrected to the British National Grid on an I^2S system, using 17 ground control points and a nearest neighbour resampling method. The RMS error was 3.4. The 1985 data were then co-registered with the 1984 data, using the same control points and resampling method. The RMS error was 0.675.

3.7.5.3 Extraction of training samples

Pixel DN values for eight classes were extracted from both the 1984 and 1985 scenes, in six bands, using the same method outlined for the ATM data (section 3.6.5.5). The classes and pixel counts are shown in table 3.7. The small size of some of the training areas is because larger contiguous pure areas of these classes could not be found within the study area.

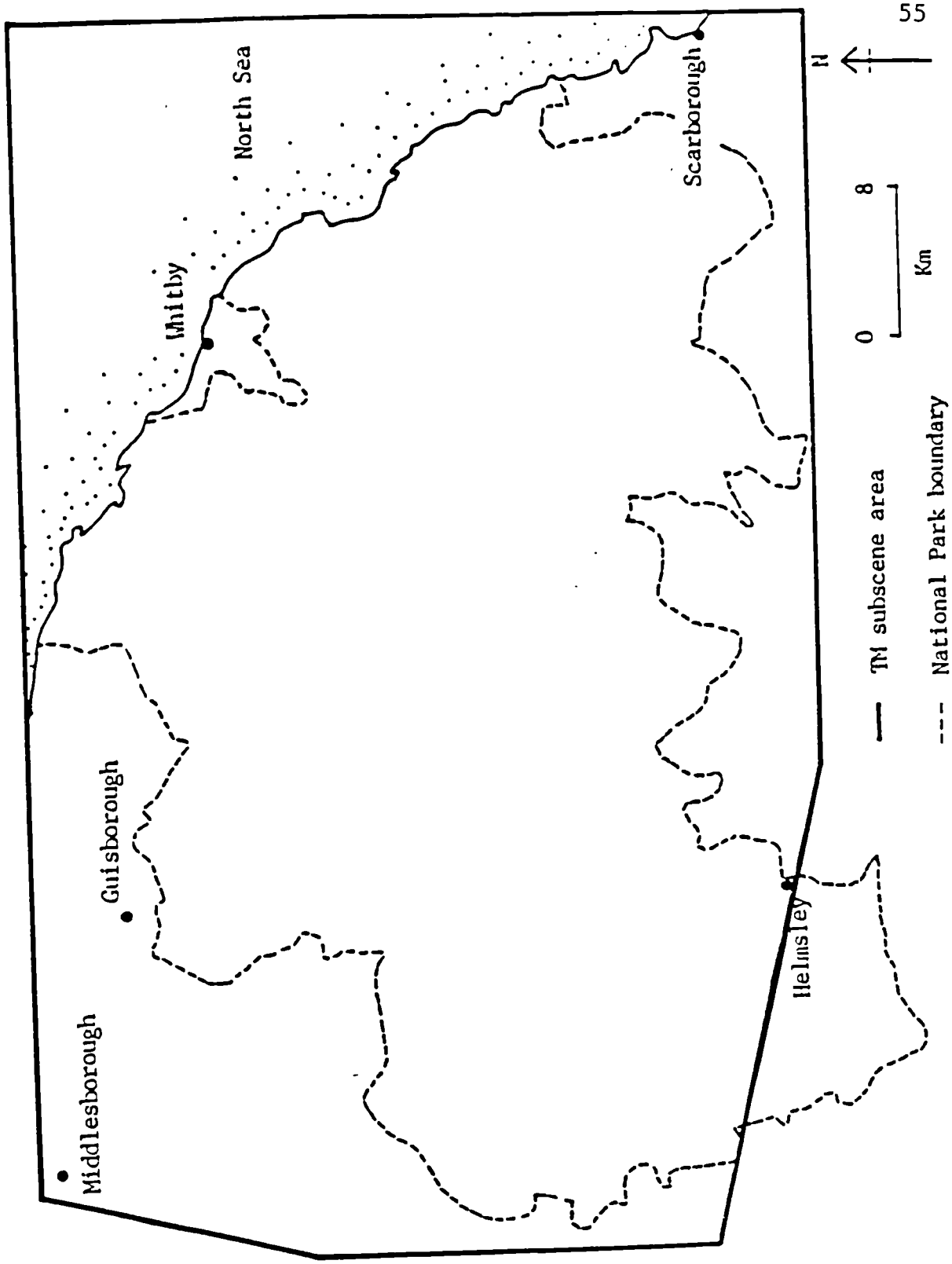

Figure 3.6 The location of the Landsat Thematic Mapper data subscenes

Class	No. of pixels
Mature Calluna vulgaris	30
Pioneer Calluna vulgaris	20
Burnt Calluna vulgaris	20
Degenerate Calluna vulgaris	20
Pteridium aquilinum	30
Grassland	50
Agriculture	100
Conifers	100

Table 3.7 Extracted training samples - TM data

3.7.6 The operational use of Landsat Thematic Mapper data

A satellite sensor is perhaps the most obvious data source for the regular monitoring of a moorland environment covering such a large area as the North York Moors. Landsat data are experimental in nature, but they have the potential to be used operationally, at least in the forseeable future. However, a constant data supply cannot be guaranteed, since the sensor could malfunction in orbit before it has reached its design life expectancy. In addition, although the satellite overpasses the same ground area once every 16 days a successful cloud-free scene may not be imaged on every occasion. In northern Britain it is unusual to obtain more than one or two images of acceptable quality in a year. Neverthless, despite these problems, at the onset of this research satellite data appears to offer the most potential for use as a tool to monitor and map moorland vegatation.

3.8 Summary

This chapter has described the data sources and any preprocessing techniques which were employed. The data have been set within the framework of the experimental design which will be implemented in further chapters.

CHAPTER 4. TEMPORAL RESOLUTION

4.1 Introduction

Temporal factors can greatly alter the spectral characteristics of a surface. These factors may be natural, such as seasonal changes in vegetation, or man-made changes, especially in agriculture, when farmers plough fields and plant and harvest crops. Such changes mean that it is important to select imagery at the correct time of year to optimise both differences in spectral response between classes, and homogeneity within classes. It can be an expensive waste of resources to acquire data at times when the spectral discrimination between cover classes is sub-optimal. The impact of changes through time on the spectral response of features of interest should be identified and understood before selecting the data for a project, or developing effective analysis techniques.

The aim of this chapter is to create a temporal context for the identification of moorland vegetation types, specifically Pteridium aquilinum (bracken) and Calluna vulgaris (heather). This chapter falls into four sections. In the first, the term temporal resolution is defined. Section two examines the influence of changes through time on the spectral response of moorland cover types. The third section identifies the fundamental temporal changes in Pteridium aquilinum, Calluna vulgaris and several other important moorland cover types. In the final section, hypotheses for the selection of the optimum date for mapping moorland vegetation types from remotely sensed data are determined.

4.2 Definition of temporal resolution

Reaching a definition of temporal resolution is not a simple or unique matter, because the phrase may be interpreted with both technical and broad, application-based, meanings. In the technical sense it may be defined as the frequency at which a system senses any

one area (Townshend, 1981b). Thus the technical resolution of TM data is 16 days, since the Landsat orbit has a repeat cycle imaging the same ground area once every 16 days (Freden and Gordon, 1983). However, the term temporal resolution has a broader definition: for many land surface types there are optimum time periods when they may be observed, and contrasted with the surrounding confusion (Simonett, 1983). The latter definition is used in this research.

Optimum periods may occur on a daily basis (the best time of day), or a seasonal basis (the best time of year). With vegetation studies it is likely that the spectral characteristics of a vegetated surface will change through the year as different growth stages are reached (section 4.3.1), and that a particular time of year will provide the optimum separation between classes. There may be as much difference in the spectral response pattern between two stages of growth in one species , as there is between two different species (Myers, 1983). It is therefore necessary to identify the best time, or temporal resolution, for separating cover types. However, there are considerable problems with this approach. In practice it is difficult to optimise, because images are comprised of a complex mix of temporally-varying spectral surfaces, and it is unlikely that it would be possible to optimise all cover types at one point in time. Nevertheless, if certain features are of greater importance in a scene, a compromise can often be reached which emphasises those features.

This problem has been overcome in some cases by the use of multi-date, or multi-temporal, imagery. Such studies use time as an additional discriminant to the spectral data, by combining data sets from different dates, in order to increase the dimensionality of the data (Landgrebe, 1978; Simonett, 1983). For instance, winter wheat may be confused with bare soil in an autumn scene, and with alfalfa in a spring scene. But if both scenes were combined it would be more easy to identify the wheat, because the changes between the dates could be exploited (Lillesand and Kiefer, 1979).

4.3 The influence of temporal changes on spectral response

The spectral response of cover types is strongly influenced by changes over time in vegetation, the illumination source, and the atmospheric and hydrological conditions (Estes et al, 1983). The status of these factors at the time of imaging may influence the recorded values for the whole scene, or for just selective parts. A detailed examination of the effect these factors have on the spectral response of a surface will be presented in chapter 5 (sections 5.3 and 5.4). The general temporal variations that occur are outlined in this section.

4.3.1 The vegetation

One of the most important temporal changes affecting vegetation is the phenology, or the seasonal growth changes of plants. The spectral response of many species are in an almost constant state of change through the year (Hoffer, 1978), as plants pass through the stages of leaf growth, budding, flowering, fruiting, senescence and dormancy. These stages have associated changes in plant morphology, internal structure and pigmentation which affect the spectral response pattern (section 5.4; Senger, 1971; Sinclair et al, 1971). The spectral response of a plant is related to the structural properties of individual leaves, and also to the canopy form as a whole (section 5.4; Milton and Wardley, 1987). As plants grow through the year, the canopy geometry is altered, and as different stages in canopy development are reached, the spectral character of a species may change.

Many crop species have very rapid changes in spectral characteristics. For instance, winter wheat may be lush green vegetation in May, golden brown when mature in late June or July, and yellow stubble after harvesting (Hoffer, 1978). The phenological changes in key moorland species are outlined below (section 4.4).

4.3.2 The illumination source

The temporal variations in illumination are considerable, especially the angle of illumination. Sun angles vary on two scales; on a daily basis as the sun rises and falls in the sky, and on a seasonal basis, especially in higher latitudes, when the sun reaches higher zenith angles in the sky in the summer. Such temporal changes can cause large differences in the spectral response of a surface, in part due to differing penetration into plant canopies (Raines and Canney, 1980) and changing proportions of shadowed and illuminated areas (Curran, 1985b).

4.3.3 The atmosphere

The atmosphere can change rapidly, and the response of a feature is heavily dependent on the atmospheric conditions at the time of imaging. Particulate matter such as dust, haze and clouds, can have a considerable effect, at times totally obscuring parts of the surface (Chahine, 1983). However, a less visually obvious temporal variation is caused by absorption by atmospheric gases, such as water vapour, which fluctuate in concentration over time (Fraser and Curran, 1976).

4.3.4 The hydrological conditions

Hydrological conditions can alter quite considerably through time, and the main factors are the amount of soil and vegetation moisture. The seasonal nature of rainfall in many regions can cause quite different responses at different times of the year, since an increase in soil or plant moisture can cause a reduction in the reflectance, especially in the water absorption bands (Hoffer, 1978).

4.4 Temporal changes in moorland vegetation

There are two major types of temporal change in the moorland species considered in this study: the phenology of the plants; and the stage of development. The seasonal variations and growth phases of the two

important moorland species identified in chapter one, Pteridium aquilinum and Calluna vulgaris, are presented in detail below. The phenology and growth stages of other important moorland cover types, most of which were selected for statistical and image analysis, are also briefly considered.

4.4.1 Temporal changes in Pteridium aquilinum

Pteridium aquilinum has a marked seasonal growth pattern, with three main phases; growth, senescence and decay (figure 4.1; Nicholson and Paterson, 1976). The exact timing of the start of the growth stage is dependent on temperature, frosts, water supply and aspect, but most fronds emerge from the ground in May or early June. During June and July the fronds become gradually unfurled from the curled-up condition of the emergent fronds (the crozier stage; plate 4.1), by which time a mature plant is about 30cm high. The plant continues to grow until there are about five pairs of fully extended pinnae (Williams and Foley, 1976). The peak of growth is in late July and August when the plant may be well over one metre in height (plate 4.2). The first signs of senescence become apparent in September, and this stage is hastened by the incidence of frost. By October the fronds are brown and may be snapped-off by wind, and fall to the ground around the plant (Clark, 1983). The litter layer is gradually compressed by rain and snow during the winter, and begins to decay in the spring (Nicholson and Paterson, 1976).

In addition to seasonal growth, individual plants change in form and growth characteristics as they pass through different stages of development. Pteridium has five main stages of growth (Watt, 1947; Clark, 1983). The ages quoted are approximations, and are dependent on local conditions.

1. Grass heath

No fronds are evident above the surface, but the plant's rhizomes grow underground.

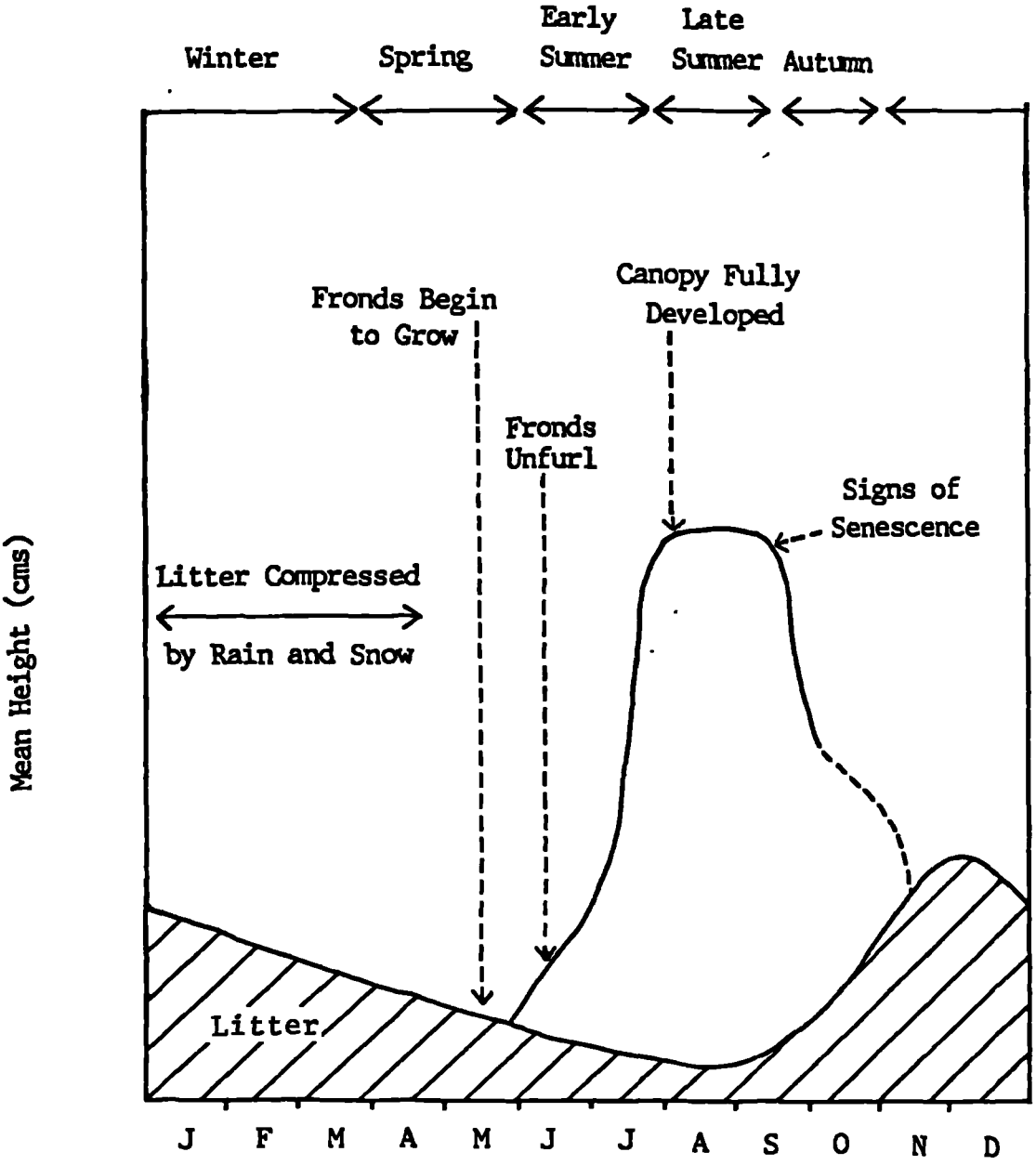

Figure 4.1 The growth cycle of Pteridium aquilinum, showing the five time periods referred to in the text (section 4.5) (after Nicholson and Paterson, 1976)

Plate 4.1 Curled-up Pteridium aquilinum fronds (the crozier stage) emerging from the previous year's litter: Blakey Ridge, May 1987

Plate 4.2 Mature Pteridium aquilinum fronds, close to peak canopy growth: Blakey Ridge, late July 1987

2. Pioneer (0-10 years)

In this stage the fronds are generally small (less than 40cm tall) and sparse. The litter decays quickly in the spring.

3. Building (10-25 years)

The fronds become much more dense and are taller, between 50cm and 1m. More litter is consequently produced and decays more slowly.

4. Mature (25-65 years)

This stage has the most dense fronds, over 70 per 10 square feet (0.93 square metres) according to Watt (1947). The tallest plants can grow to over 1.5m and the canopy cover is complete. So much litter is produced that it cannot decompose before new litter is produced the next year, and so a continuous layer is established.

5. Degenerate (65-80 years)

In this stage fewer fronds are produced and they tend to be smaller in height (less than 1m). The litter becomes more scanty, and the remaining, partly decomposed, layer becomes smoothed and discoloured. Eventually the plant dies, and the litter gradually disappears, although it may remain for some time.

4.4.2 Temporal changes in Calluna vulgaris

In contrast to Pteridium, which is seasonally green, Calluna vulgaris does not die back each year but has minute evergreen leaves (Watt, 1955). Calluna shoots are divided into long and short types. Long shoots have widely spaced leaves of 3-4mm length, and short shoots, which grow from the long shoots, have smaller, more closely-spaced leaves (figure 4.2; Gimmingham, 1960). The annual growth phase begins in April or May when selected over-wintered short shoots grow into long shoots, and from these, new short shoots appear. The current year's growth is bright green, while the previous year's are darker in colour. Throughout July, August and September the short shoots which are two or three years old turn brown and fall to form a litter layer (Cormack and Gimmingham, 1964).

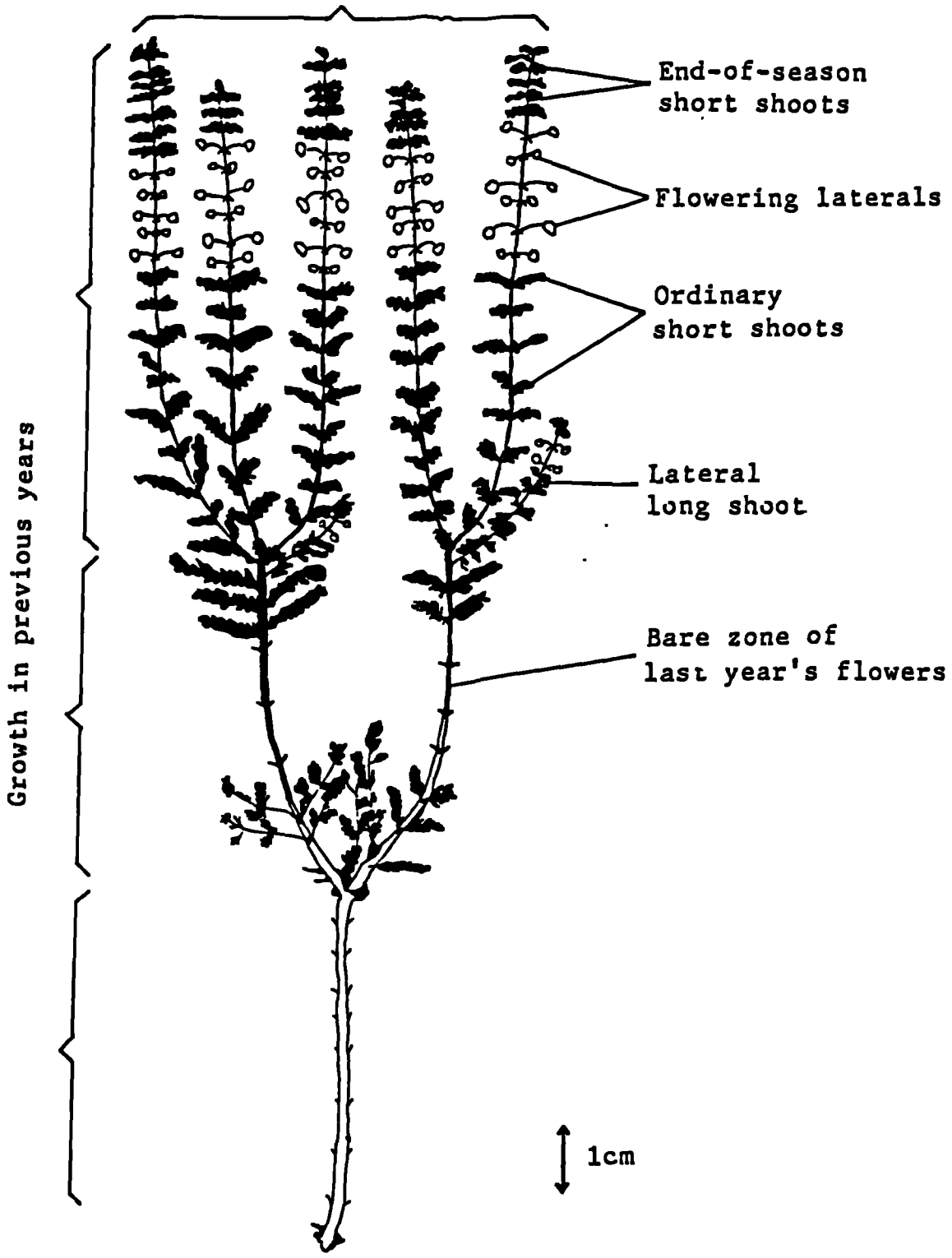

Figure 4.2 Diagram showing the form and growth zones of Calluna vulgaris (after Milton and Rollin, 1987)

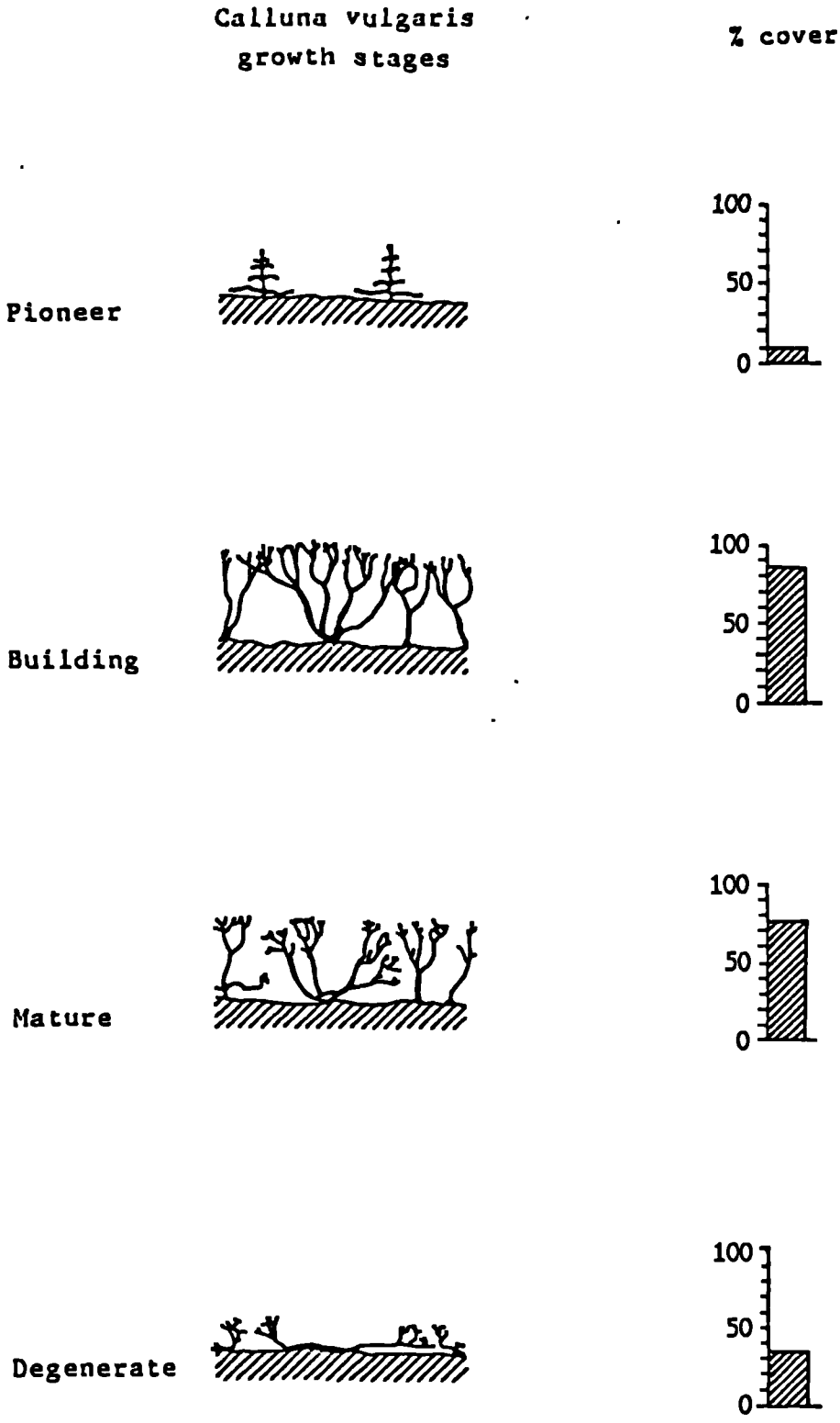

Figure 4.3 The growth stages of Calluna vulgaris (after Milton and Rollin, 1987)

During the end of August and September purple flowers are produced on short stalks, and, after flowering, an end of season growth period of short shoots occurs. These lie dormant through the winter and two or three are activated in the spring to become new long shoots (Milton and Rollin, 1987).

Calluna has four main stages of growth in its 30-40 year life-span (figure 4.3; Watt, 1955; Milton and Rollin, 1987). Again ages are approximate.

1. Pioneer (0-6 years)

The original leading long shoot is replaced after two years by two or more shoots arising just below the tip. Other lateral shoots also bifurcate, producing a pyramid-shaped plant. A fully developed bush is formed by the end of this phase.

2. Building (6-15 years)

In this stage the bushes lose the pyramid shape and become more hemispherical. Productivity is high and the bushes are between 30 and 40cm tall, with a network of woody stems.

3. Mature (15-20 years)

Growth continues as in the building stage, but gradually becomes less vigorous, especially in the short shoots, which become darker and smaller. The bush grows to about 60cm in height. Towards the end of this stage the centre of the bush begins to open and the central frame branches are gradually exposed (plate 4.3).

4. Degenerate (20+ years)

Growth of the leading shoot declines and the canopy opens further. The plant dies from the centre outwards, leaving large areas of bare ground in the middle of each plant (plate 4.4).

Plate 4.3 Mature Calluna vulgaris: Blakey Ridge, August 1987

Plate 4.4 Degenerate Calluna vulgaris: Blakey Ridge, June 1987

In addition to these four, there is a burnt stage in well-managed Calluna stands. Small areas are burnt in a roughly fifteen year rotation in order to regenerate the growth of short shoots for grouse and sheep to graze (section 2.7).

4.4.3 Temporal changes in other important moorland vegetation cover types

1. Erica tetralix (cross-leaved heath) is a an evergreen shrub, which is found mainly in bogs and wet moors. It is usually confined to relatively small areas, although it may occur mixed with Calluna over quite large stretches. The main growth season begins slightly before the Calluna, in late March or April, and clusters of flask-shaped, rose-pink flowers are produced between June and October (Milton and Rollin, 1987).

2. Erica cinerea (bell heather) is an evergreen shrub and is often associated with Calluna, although it is usually only found in drier areas. The main growing season is similar to that of Erica tetralix, and clusters of crimson-purple flowers grow between June and September (Darlington, 1978).

3. Vaccinium myrtillus (bilberry) is a deciduous shrub which can become dominant on deep peat, and is often present beneath Calluna or Pteridium. During the spring and summer months, bright green, oval leaves are produced, and greenish-pink flowers grow between May and July. Fruiting occurs in August and the berries are black with a bluish bloom. The stems of Vaccinium myrtillus are green, and during the winter it becomes a 'switch-plant', so that when there are no leaves, the assimilatory processes are carried out by the stems (Darlington, 1978).

4.4.4 Temporal changes in wetland vegetation

Wetland vegetation, which consists predominantly of grasses, mosses and rushes, generally occurs in small areas: in depressions; at

valley heads; and in areas of very deep, wet peat (North York Moors National Park Committee, 1984a).

1. Eriophorum vaginatum (cottongrass) is a perennial grass which flowers in a rounded spike, and develops white cotton-like bristles between April and June.

2. Sphagnum (bog-moss) is one of the most common mosses, occurring in crimson-red (Sphagnum rubellum) and green (Sphagnum papillosum) hummocks. It produces spherical chestnut-brown spores during the summer, which ripen in July and August.

3. Juncus squarrosus (heath rush) is a rosette-forming perennial herb. It has grass-like leaves, and produces dark chestnut-brown flowers from June to September (Darlington, 1978).

4.4.5 Temporal changes in natural grassland

Rough grasses generally occur in small areas, especially over disturbed ground, although they may be widespread in some locations, especially where conditions are damp. These are mainly perennial grasses, and the predominant types are Nardus stricta (mat grass) which produces small flowers from May to August; Molinia caerulea (purple grass moor) which is a deciduous grass and grows purple flowers between June and September; Agrostis canina (brown bent grass) which has small flowers in June and July; and Eriophorum vaginatum (cottongrass) (mentioned above, section 4.4.4; Darlington, 1978).

4.4.6 Temporal changes in coniferous woodland

Most of the coniferous woodland in the North York Moors has been planted in large regular blocks by the Forestry Commission. The main species is Pinus sylvestris (Scots pine), but there are also areas of Picea sitchensis (Sitka spruce), Pinus contorta (lodgepole pine) and Picea abies (Norway spruce). These are evergreen trees, and so they

retain a green foliage all through the year. An exception to the evergreen nature of conifers is Larix kaempferi (Japanese larch), which is deciduous, and so looses its leaves in the autumn (section 4.4.7 below). Conifers flower between May and June and produce yellow-brown cones in the late summer (Polunin, 1976; Darlington, 1978).

4.4.7 Temporal changes in deciduous woodland

In the North York Moors, deciduous and mixed woodlands tend to occur in small blocks, mainly along valley sides. Such woodland is dominated by Quercus petraea (sessile oak), Fraxinus excelsior (ash) and Betula pubescens (downy birch). In addition, there are areas of the deciduous conifer Larix kaempferi (Japanese larch), which is grown in plantations (section 4.4.6 above). As deciduous trees, they show signs of senescence in the autumn, as their leaves change colour from green, through yellow and red, to brown, and eventually fall to the ground. Through the winter, only the woody branches are left, and any undergrowth is revealed. These trees may also flower in May and June, and produce fruits, such as acorns in the case of Quercus petraea, in the late summer (Polunin, 1976; Darlington, 1978).

4.4.8 Temporal changes in urban areas

Most surfaces in towns and villages remain constant over time, although urban areas do have vegetated regions which vary through the year. Open areas such as parks, gardens and allotments may change through the year, often having large areas of bare soil in the winter. Wooded areas within urban developments will change through the year in the same way as woodland in rural situations (sections 4.4.6 and 4.4.7).

4.5 The optimum temporal resolution: hypotheses for moorland mapping

The selection of the best time of year for the imaging of moorland

vegetation is not an easy matter, since the land cover is made-up of many vegetation types which have different cycles of growth, all of which have an optimum time to be sensed (c.f. section 4.2). Thus it is difficult to determine a single date for general moorland mapping over such a large area as the North York Moors. Nevertheless, by considering individual cover types and the way in which they relate and interact with one another temporally, general periods offering the optimum separation between classes may be identified. In such cases a compromise has to be reached, so that the best overall separation may be achieved, with emphasis on distinguishing between features of special interest.

An alternative to a single compromised date would be the acquisition of more than one data set from different seasons during the year. However, this would introduce considerable technical difficulties and additional expense. It would entail a complex geometrical rectification procedure to allow exact overlay between dates, and complicated inter-calibration to ground reference targets to facilitate quantitative comparison between the reflectance values on the different scenes.

The principal aim of this research is to to identify Pteridium aquilinum and Calluna vulgaris, and to isolate them from other cover types present in the North York Moors, using remotely sensed data. An additional aim is to attempt differentiation between the growth phases of these two important moorland species. The remainder of this chapter therefore presents hypotheses for the selection of the optimum temporal resolution for achieving both of these aims.

The following sections assess the advantages and disadvantages of remotely sensing a moorland environment at certain time periods during the year. Pteridium aquilinum has a seasonal pattern of growth, and so the year has been divided into general seasons, based on its growth cycle (figure 4.1). Periods of stable growth, or rapid transition between growth stages, were identified, resulting in the selection of five general time intervals; winter (from November to

the end of March), spring (from April to the end of May), early summer (from June to mid-July), late summer (from late July to mid-September), and Autumn (from late September to the end of October). The suitability of each season is considered individually, with special reference to the discrimination of Pteridium aquilinum and Calluna vulgaris. Finally an overall optimum period for the regional mapping of a moorland environment is defined.

4.5.1 Winter (November to the end of March)

The moorland vegetation in this season is characterised by dead Pteridium aquilinum fronds, in the form of brown litter, and the dormancy of the heather species (section 4.4).

In winter the contrast between certain vegetation types, especially Pteridium aquilinum and other moorland species, may be optimum (the plant conditions are very similar to those in the spring; section 4.5.2 below). However, the meteorological conditions at this time of year effectively rule out the choice of winter as an optimum temporal resolution. For example, atmospheric conditions may interfere with the recording of data during the winter, since extensive cloud cover and hill fog which develops at this time of year is likely to be a problem. In addition, snow may be lying on the ground, obscuring the surface. On the high moors, snow lies for an average of 40 days per year (Carrol and Bendelow, 1981), which will prevent the vegetation being imaged for lengthy and unpredictable periods during the winter.

4.5.2 Spring (April to the end of May)

The moorland vegetation conditions in this season are generally the same as in the winter (section 4.5.1). Pteridium aquilinum has a very distinctive annual growth cycle, with a complete die-back in the autumn, leaving only a litter layer (section 4.4.1; figure 4.1). Therefore, data acquired after the Pteridium has died in November, but prior to the new year's growth in May, would be likely to enable good discrimination from other moorland vegetation, which remains

green. The likelihood of obtaining good quality data through the winter is slim (section 4.5.1), therefore the period after the spring snow-melt (with better weather conditions for remote sensing), but before the Pteridium begins to grow in May, would offer good separation between Pteridium aquilinum and other moorland species. This is because the contrast between the evergreen heather species, such as Calluna vulgaris, Erica tetralix and Erica cinerea, and the brown Pteridium litter, would be greater than at any other time of year. In addition, Vaccinium myrtillus, would be contrasted with Pteridium litter, because, although it is a deciduous plant, the stems remain green throughout the winter and spring.

Despite the probable success in distinguishing Pteridium from heather types in the spring, there are several major drawbacks to the selection of data from this time of year.

First, during the spring months, there is no green vegetation apparent at the surface of Pteridium aquilinum litter, and therefore it may be subject to confusion with bare ground. There are three common types of bare ground in the North York Moors National Park; bare soil in ploughed agricultural fields, deciduous grasses before the new season's growth, and bare ground in urban areas, such as large gardens, allotments, waste ground, roads and carparks. In the spring, when Pteridium is effectively an unvegetated surface, it is possible that it may be misinterpreted as a bare land-cover class (plate 4.5).

Second, there may be errors in the identification of Pteridium aquilinum and grasses in the spring. During the pioneer and building phases, there is often a grass understorey to Pteridium. This is most common if the Pteridium has invaded agricultural grazing land, or a burnt heather area that had been colonised by grasses prior to Pteridium growth. Where there is such an understorey, confusion between Pteridium aquilinum and grasses may occur in the spring, when there are no fronds to obscure the undergrowth.

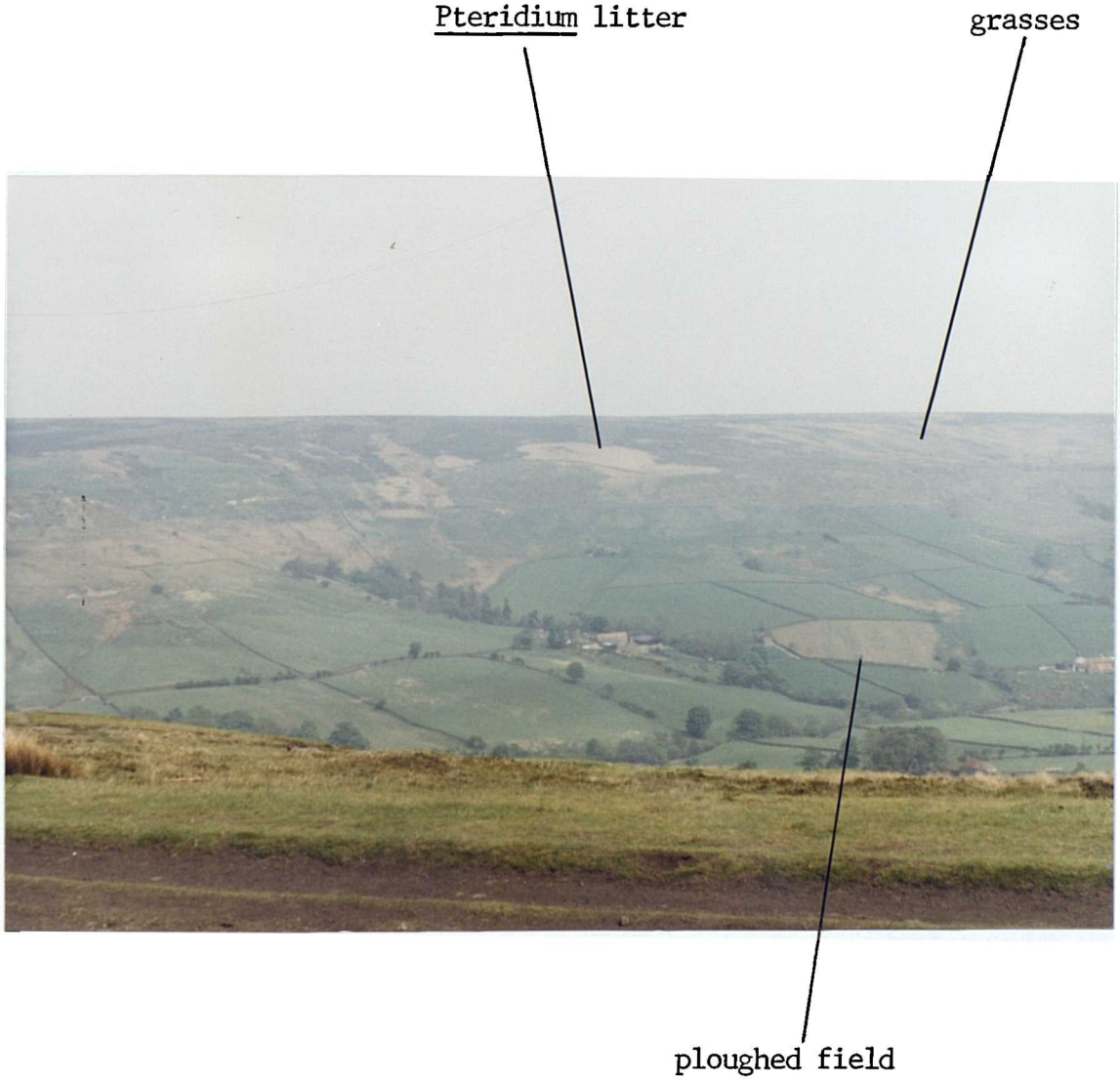

Plate 4.5 Photograph to illustrate the possibility of confusion between cover types with no green vegetation apparent at the surface in the spring; northern Rosedale from Blakey Ridge, May 1987

Third, similar mix-ups may occur in the spring where there is a Vaccinium myrtillus understorey to the Pteridium. Such an understorey is quite common, especially in the transitional zone between Pteridium aquilinum and moorland.

Fourth, there are likely to be problems discriminating between the growth stages of Pteridium aquilinum in the spring. There are few differences between the stages, although there may be different amounts of litter. It decays completely in the pioneer stage, and partially in the building and degenerate stages, while mature plants will have a continuous litter layer. However, these differences are fairly subtle, and the most obvious contrasts are likely to be when there are fronds above the surface.

Fifth, there may be sub-optimal separation between Calluna vulgaris growth stages in the spring. Although Calluna does not die back in the autumn like Pteridium, the differences between growth stages may be subdued in the winter and spring months, as there is very little active growth, and the plants lie dormant.

Finally, there may be problems identifying Calluna vulgaris in the spring. Calluna develops woody branches in the building phase, and these become progressively revealed as the plant matures and degenerates (section 4.4.2). Thus the possibility exists that in the spring older Calluna vulgaris may be confused with deciduous woodland. This is because there are few leaves on the trees at this time of year, causing the woody elements to be exposed.

4.5.3 Early summer (June to mid-July)

During this period the moorland vegetation is characterised by rapid growth of Pteridium aquilinum fronds, from bare litter at the beginning of the season to full canopy cover at the end. There is also active growth of bright green Calluna vulgaris short shoots (section 4.4).

Although data collected at the beginning of this season will be similar to those of the spring, and will therefore be sub-optimal in many cases, data obtained towards the end of this period will probably offer good discrimination between moorland cover types. The full-grown Pteridium fronds will contrast well with bare surfaces. In addition, the understoreys of grasses and Vaccinium myrtillus will be obscured by Pteridium fronds, so there is likely to be less inaccuracy discriminating between these species and Pteridium.

Calluna vulgaris is also less likely to be mistaken for deciduous woodland. This is because the leaves will be covering the woody parts of the trees, but the woody stems and branches of the mature and degenerate Calluna will still be exposed.

The end of the early summer may also be a suitable time to distinguish between the growth stages of both Pteridium aquilinum and Calluna vulgaris, since growth is very vigorous during this period. At this time the differences in plant density and size, which are related to the growth stage, are likely to stand out strongly.

However, there is one major drawback to selecting data from the early summer. The usefulness of the data is highly dependent on the vigour of vegetation growth. The exact timing of the beginning of the growth season is highly unpredictable, and therefore it is difficult to judge when the plants are mature enough to avoid the ambiguities apparent in the spring. The exact timing will vary from year to year, and is mainly dependent on weather conditions.

In addition, there may be misinterpretation between Calluna vulgaris and the other heather types, Erica tetralix and Erica cinerea, in the early summer. All three species are similar in many ways; they are evergreen shrubs, attaining similar heights when mature, with small leaves and branching structures. Thus, confusion between the three heather types may occur at this time of year, when there are no striking differences between them.

4.5.4 Late summer (late July to mid-September)

The moorland vegetation during this time is characterised by the peak growth of a full Pteridium aquilinum canopy, and the maximum vigour of the heather types, including the production of flowers in August and September (section 4.4).

In this season the separation between Pteridium aquilinum and bare ground, grasses and Vaccinium myrtillus is likely to be high, as is the contrast between Calluna vulgaris and deciduous woodland (for the same reasons as in the early summer; section 4.5.3).

The late summer is also likely to be a good time to discriminate between the growth stages of both Pteridium aquilinum and Calluna vulgaris. The variations in frond density and vigour, related to development stage of Pteridium, are greatest at this time of year. The canopy is at its maximum coverage and the complete canopy cover of the mature phase will contrast with the less dense fronds of the other phases.

Differences between the Calluna growth stages are mainly related to the amount of green matter, compared with bare ground between and within plants, the vigour of growth, and changes in canopy form. Therefore, the optimum time for discriminating among the phases is the same as with Pteridium, when growth and productivity is at a peak, in the late summer. The production of flowers is also related to the development stage, and more flowers are produced in the building/mature phase than in the pioneer and degenerate phases.

In addition, the flowers produced by the heather species during this period, will increase the separation between Pteridium aquilinum and other moorland species, and between the heather types.

Pteridium may become confused with other moorland species in the summer, since most of the vegetation types are green at this time, and are growing vigorously. However, during the end of August and the

whole of September the three major heather types will be flowering, and the Vaccinium myrtillus will be fruiting, and these non-green features will contribute to the spectral response of the canopy, and increase the contrast between these species and Pteridium.

Calluna vulgaris and the other heather species may be mixed-up in the early summer (section 4.5.3), but there is likely to be a contrast between them during flowering, because the flowers are different colours and shapes (sections 4.4.2 and 4.4.3).

In addition to the flowers, there is also a difference in the moisture conditions that the plants favour. Erica tetralix thrives in wet and boggy locations, Erica cinerea prefers dry areas, and Calluna vulgaris occupies areas with intermediate moisture conditions. The soil moisture conditions can significantly contribute to the spectral response of a surface (sections 4.3.4 and 5.3.3). The moisture differences between the species are likely to be greatest in the late summer, since the soil moisture deficit is greatest in this season, and only permanently wet areas will still be moist (Carrol and Bendelow, 1981).

4.5.5 Autumn (late September to the end of October)

The vegetation in the final time period is characterised by progressive signs of senescence in Pteridium aquilinum and deciduous trees and plants, and by the onset of dormancy in evergreen species, such as the heather varieties (section 4.4).

The beginning of this season has similar vegetation conditions to the late summer, and may therefore offer a promising opportunity for discriminating moorland cover types. However, as senescence progresses, inaccuracies similar to those in the early spring may occur (section 4.5.2); Pteridium aquilinum may be confused with bare ground, grasses and Vaccinium myrtillus, as the fronds turn brown, break off and fall to the ground around the plant. Calluna vulgaris may be mistaken for deciduous trees and other heather plants, after

flowering ceases. In addition, the distinctions between the growth stages of both Pteridium and Calluna may be sub-optimal.

The early autumn may be a successful time to remotely sense moorland vegetation, since the peak of flower production in the heather plants extends well into September. However, the exact timing of the end of flowering, and the onset of senescence in other plants, cannot be predicted accurately, and varies from year to year. This is likely to make the choice of an acquisition date in the autumn less reliable than one in the late summer.

4.5.6 The optimum temporal resolution for general moorland mapping

The previous discussion highlights the problems of identifying an optimum temporal resolution for moorland remote sensing. There is not a single time period which is optimal for all moorland cover types. Nevertheless, a date in the late summer appears to be most promising. At this time Pteridium aquilinum is at its peak growth, before any signs of senescence have appeared, which will allow differentiation between the growth stages, and maximum discrimination from bare surfaces, grasses and Vaccinium myrtillus. In addition, the moorland species are flowering or fruiting, which will increase their separation from the fully grown fronds of the Pteridium, and enhance the distinctions between the heather types. This time of year would also allow differentiation between the growth stages of Calluna vulgaris, and maximise the separation of Calluna from deciduous woodland.

Other times of year, notably the early summer and autumn, are possible alternatives worth investigation, although the unpredictability of the exact time of the beginning and end of the growing season is problematic. The winter period may be may be discounted because of adverse weather conditions, and spring data is unlikely to be successful, because confusion between moorland surfaces is great during this period.

4.6 Conclusion

The selection of an optimum temporal resolution in remote sensing is not a simple task, and compromises must be reached which take into account the complex mix of temporally-varying surfaces within a scene. In this chapter, the seasonal characteristics of the various cover types present in the study area have been examined. It has been hypothesised, with regard to the temporal inter-relationships between these surfaces, that a date in late summer will be optimum for moorland monitoring and mapping using remote sensing.

CHAPTER 5. SPECTRAL RESOLUTION

5.1 Introduction

Within remote sensing one of the most difficult tasks is the production of floristic maps for natural or semi-natural vegetation. High spatial resolution photography is often inadequate to differentiate species, as classification frequently requires the use of a microscope (Morain, 1974). However, remote sensors can supply data for multicategory vegetation maps, provided the typical spectral response of each class of interest is known and can be identified, usually with the aid of supporting field data. The underlying assumption of multispectral analysis is that the surface features of interest are spectrally distinct, and therefore can be individually identified and mapped. In many cases this assumption is valid, but in others, objects of interest cannot be separated on spectral grounds alone, with currently available sensing systems. Therefore, any successful attempt at a multispectral analysis must be based on a thorough investigation and understanding of the spectral characteristics of features of interest, and the factors which can influence their response (Hoffer, 1978). The purpose of this chapter is first to reach a definition of spectral resolution and to identify the factors which affect the spectral response, and then to investigate the spectral characteristics of vegetated surfaces within the study area, to assess the pairwise and multi-class spectral separability between species and vegetation communities, and to identify the optimum combination of spectral wavebands for moorland mapping, with careful consideration of the temporal context outlined in the previous chapter.

5.2 Definition of spectral resolution

As with temporal resolution there is not a simple, single definition of spectral resolution, as there is both a technical and a broarder

interpretation (Simonett, 1983). In attempting a definition these two distinct but related notions must be considered, as each one characterises the concept at a different level.

The first concerns the specifications of the sensors used to record remotely sensed data. This instrument-oriented definition maintains that the spectral resolution is the width of the Electromagnetic Spectrum (EM) over which the data are collected in each waveband, the total number of individual wavebands, and their distribution over the spectrum (Everett and Simonett, 1976).

The second notion is the broader interpretation that certain spectral regions and/or wavebands are more useful than others for a particular task (Everett and Simonett, 1983). It is the broader sense which is investigated in the research reported in this chapter, although any analysis is constrained by the technical spectral resolution of the sensors involved. If the most effective channels for separating the classes of interest can be identified this can markedly reduce the use of computer storage and processing resources, and the cost of future data purchases for this task (Thomas et al, 1987).

In addition to spectral resolution, the radiometric resolution is also important. Although this property is a distinct one, it is related to, and has a bearing on, the spectral resolution. Defined simply, it is the sensitivity of the sensor to differences in signal strength (Everett and Simonett, 1976), and it is determined by the number of discrete grey levels into which the signal may be divided. The Landsat Multi-Spectral Scanner (MSS) has 64 levels (6 bits of data) and the Thematic Mapper (TM) has 256 (8 bits) (Lo, 1981). The greater radiometric resolution of TM allows an increase in the detection of smaller magnitude changes in radiation within each spectral band (Freden and Gordon, 1983). It is possible to achieve a greater discrimination between objects by using a sensor with identical spectral wavebands but with improved radiometric sensitivity (Everett and Simonett, 1976). Thus two objects which may be discriminated by a sensor with high radiometric resolution, may

have such subtle differences in radiance that they are not distinct on a sensor with identical spectral resolution, but a poorer radiometric sensitivity.

5.3 Factors affecting the spectral response of surfaces

Many factors may cause a variation in the multi-spectral signals received at a sensor from a surface. These may be separated into five main categories: the reflective and emissive properties of the surface; the illumination conditions; the site environmental conditions; the atmospheric conditions; and the sensor parameters (Barrett and Curtis, 1976). These factors are considered below, with special reference to vegetation. In addition to these factors, the temporal and spatial characteristics of the data have a great influence on the spectral response, and these are considered in detail in separate chapters (chapters 4 and 6 respectively).

5.3.1. The reflective and emissive properties of the surface

This includes the spectral properties of the particular object (its colour, or temperature in thermal remote sensing), its internal structure, and the reflective conditions this structure creates, as well as spatial properties, such as the the geometric form, density and pattern of distribution of objects (Barrett and Curtis, 1976). The reflective properties of vegetation are considered in greater detail in section 5.4.

5.3.2. The illumination conditions

This includes the spectral distribution of solar radiation and the illumination geometry of the imaged surface (Barrett and Curtis, 1976). Passive remote sensing systems, such as the ones used in this research, detect radiation reflected or emitted from targets that have been illuminated by an external source; usually the sun (Lowe, 1976). Solar energy is spectrally distributed over the shortwave region of the EM spectrum, ranging from 0.1μm to 5μm, with a peak at

0.5μm (Sabins, 1987). The wavelengths in the region between 0.3μm and 1.5μm are of most interest in remote sensing. These are called the optical wavelengths as it is within present technological capabilities to record them optically. The optical wavelengths may be further divided into the reflective and thermal regions (figure 5.1; Silva, 1978). Solar radiation is not greatly altered during its passage to the earth (Silva, 1978), therefore the solar illumination reaching the atmosphere remains effectively constant. However, the characteristics of solar radiation are considerably altered by the complex structure of the atmosphere. This is dealt with in greater detail below in a section on atmospheric conditions (section 5.3.4).

The illumination geometry of the imaged surface, especially the angle of the sun, is also an important factor affecting the spectral response. All surfaces are not perfect diffuse, or Lambertian, reflectors in all wavelengths; that is they do not reflect incident radiation uniformly in all directions irrespective of illumination angles (Slater, 1980). In some cases, especially with a rough surface, a dependence on the angle of illumination is to be expected. For instance, with vegetation, where the undulating surfaces of leaves and surface features such as hairs, cause changes in reflectance at different sun angles (Milton and Wardley, 1987).

Solar zenith angles may also affect the spectral response of a surface. When the sun is low in the sky, in the mornings or evenings, areas of shadow are increased, and therefore the spectral reflectance, especially in the visible wavelengths, in these areas is decreased (Curran, 1985b). As the day progresses different parts of the canopy sides and top will be illuminated, creating a constantly changing spectral environment (Raines and Canney, 1980).

It is extremely important to consider these illumination effects, especially when recording ground or air-borne spectral data. With Landsat satellite data the scenes are always recorded at around the same time of day (the equatorial crossing time is 9.45am) (Slater, 1980), and with the same look angles, so these conditions remain

fairly constant for data collected at the same time of year. However, the illumination geometry varies considerably through the year, especially in higher latitudes, such as northern Britain.

5.3.3. Site environmental conditions

These include hydrologic, edaphic and geomorphologic factors, as well as atmospheric and plant conditions, which are dealt with in detail below (sections 5.3.4 and 5.4 respectively).

Hydrological conditions have a major impact on spectral response. An increase in moisture in soil or vegetation causes a distinct reduction in reflectance, particularly in the water absorption bands at approximately 1.4μm, 1.7μm and 2.7μm (Hoffer, 1978). If plants are stressed by a lack of water, the character of their response may also change (section 5.4; Bauer, 1985). The presence of snow causes obvious changes in the spectral character of cover types; surface features become obscured and reflectance values are increased, especially in the visible region (Harris, 1987).

Edaphic, or soil, conditions can have a significant affect on the spectral response of a surface, as the response of objects is often complicated by the background soil (Curran, 1985b). The degree of reflectance of soils in the visible and near infrared has been negatively related to four physical characteristics: particle size; moisture content (see above); organic matter content; and iron oxide content. An increase in each of these causes a decrease in the reflectance (Hoffer, 1978).

The geomorphological factors affecting spectral response are mainly related to elevation and aspect. In areas of high relief large areas are likely to be in shadow while others are directly illuminated by the sun. These differences are also dependent upon the solar altitude (section 5.3.2).

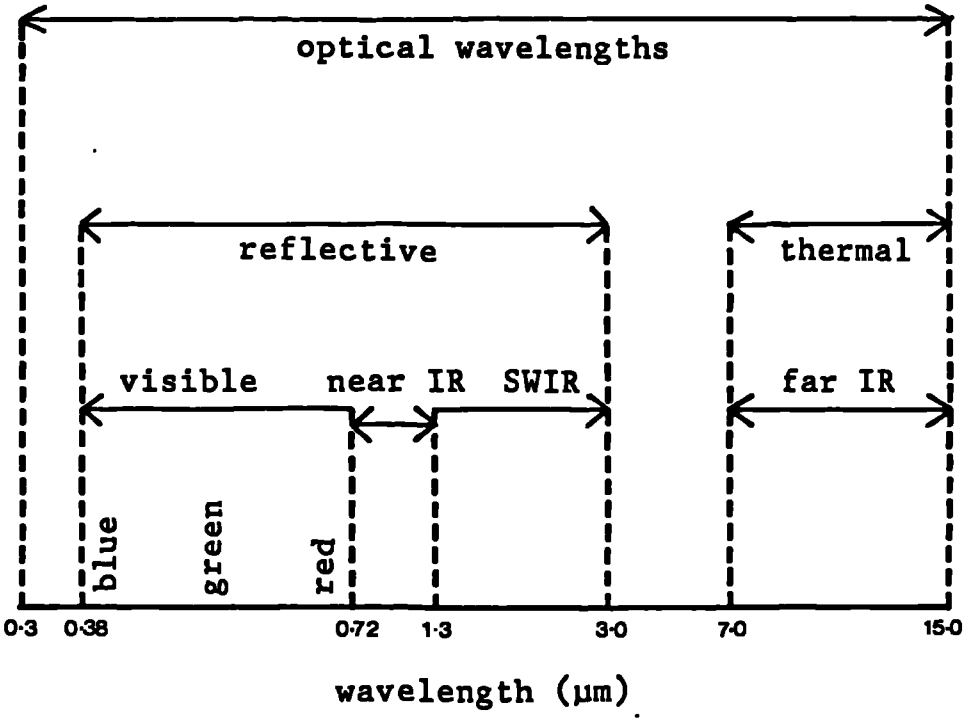

Figure 5.1 The electro-magnetic radiation spectrum (after Silva, 1978)

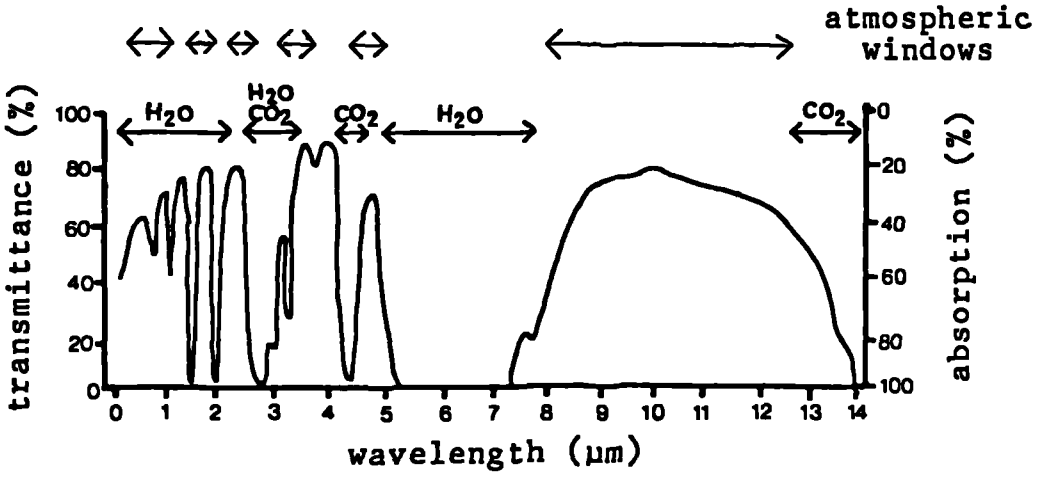

Figure 5.2 Atmospheric windows and absorption bands (after Barrett and Curtis, 1976)

5.3.4 Atmospheric conditions

As electromagnetic radiation passes through the atmosphere to the earth's surface, and then back to the sensor, it is considerably attenuated by scattering and absorption caused by the gas molecules and aerosol particles which are present (Lo, 1986).

Absorption in the ultraviolet wavelengths (less than 0.3μm) is so intense in the upper atmosphere, mainly by oxygen and ozone, that such EM radiation cannot be used for remote sensing (figure 5.2; Slater, 1980).

Other areas of the spectrum are less attenuated and are therefore exploited for remote sensing purposes. These more transparent regions are known as atmospheric windows, but atmospheric effects are still considerable (figure 5.2; Fraser and Curran, 1976).

The visible spectrum is not affected greatly by absorption, but there is some scattering, especially in the blue portion (Estes, 1974). In the near infrared there are various absorption bands, principally caused by water vapour (figure 5.2; Fraser and Curran, 1976).

Further into the infrared, the absorptions are more pronounced with water vapour bands at 2.66μm, 2.74μm, 6.25μm, and from 20μm into the microwave region, and carbon dioxide bands at 4.3μm and 15μm (figure 5.2; Chahine, 1983).

In addition to this clear sky absorption, the presence of cloud and fog below the level of the sensor obscures the ground by absorbing all wavelengths between 0.3μm and 3μm (Chahine, 1983).

Particulate matter in the atmosphere causes a scattering of EM radiation (Fraser and Curran, 1976). Particulates may be natural, such as soil, sea salt or volcanic debris, or man-made, such as emissions from industry, smoke from domestic fires and car exhausts (Chahine, 1983). Such particles remain in the atmosphere for some

time and the distribution is dependent on source areas (mainly urban) and wind strength and direction.

The exact atmospheric conditions at the time of sensing are rarely known, and therefore the complex interactions cannot be fully accounted for, and can add considerable complication to the interpretation of the spectral signal received at the sensor from ground surface targets (Fraser and Curran, 1976). This causes problems when scenes from more than one date are overlain. Calibration to a known ground target is necessary if absolute quantitative comparisn of the DN values is required. The differential presence of cloud is an additional problem.

5.3.5 Sensor parameters

There are many sensor parameters which can influence the spectral response from a surface. Perhaps the most important are the distribution and width of spectral wavebands, or the technical spectral resolution (Everett and Simonett, 1976), and the radiometric sensitivity, or number of grey levels, of the sensor (section 5.1; Freden and Gordon, 1983). However, other less obvious sensor parameters are also important; these include the amount of electronic noise present in the signal, drift and gain changes, and the accuracy and precision of measurements on calibration references (Barrett and Curtis, 1976). These parameters are difficult to determine, especially in a satellite sensor which cannot be periodically checked against a standard in the laboratory. Although, there is usually some form of on-board claibration, when the detectors are directed out into dark space, or at a standard lamp within the satellite.

5.4 The characteristic spectral response of vegetated surfaces in general

Thus, the spectral signal received at a sensor is influenced by many different factors, and is not simply a function of the spectral characteristics of the surface. Nevertheless, the reflective and

emissive properties of the target are extremely important in determining the signal, and characteristic responses may be identified for classes of interest.

Vegetation has a distinctive response which varies with wavelength, and in remote sensing this is often referred to as its "spectral signature" (Lillesand and Kiefer, 1979; Short, 1982). This tends to imply a unique and absolute reflectance curve. However, such a well-defined and single-valued representation does not occur in reality, as it is influenced by the factors discussed above (section 5.3), any of which may slightly alter the spectral characteristics of a surface (Slater, 1980). Therefore it is more appropriate to refer to the response as a pattern, rather than as a signature (Hoffer, 1978; Lillesand and Kiefer, 1979). The typical vegetation response pattern has relatively low visible reflectance, and relatively high near infrared reflectance (figure 5.3; Tucker, 1979). This pattern is dependent on leaf pigmentation, physiological structure and moisture content (Gausman, 1977).

The visible region is dominated by the absorption of EM energy by the pigments present in the epidermis of the leaves (figure 5.4; Bauer, 1985). Chlorophyll is the most important pigment, absorbing light at 0.43μm, 0.45μm, 0.65μm and 0.66μm (the blue and red wavelengths) (Curran, 1985b; Schanda, 1986). Other pigments, such as carotenes and xanthophylls also absorb visible light (Bauer, 1985). Absorption is slightly lower in the green wavelengths, so there is a peak of visible reflectance at 0.5μm, which causes healthy vegetation to appear predominantly green (figure 5.3; Harris, 1987).

The near infrared region is marked by a large increase in reflectance, from about 10% of incoming radiation in the visible wavelengths, to about 55% (Smith, 1983).

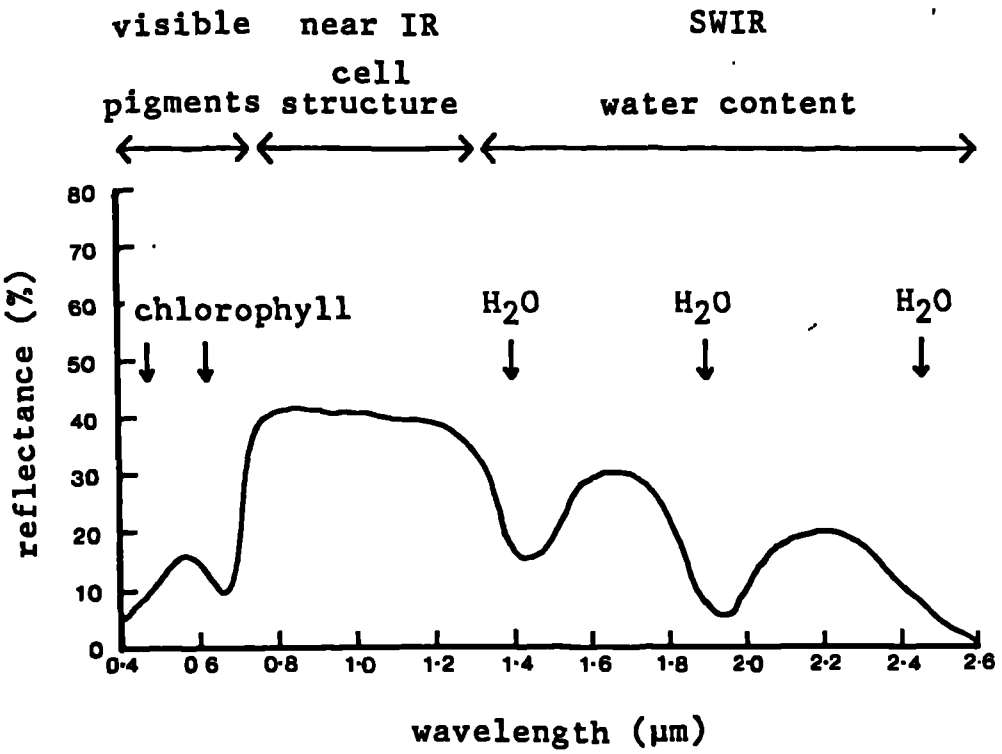

Figure 5.3 The characteristic spectral response pattern of green vegetation (after Hoffer, 1978)

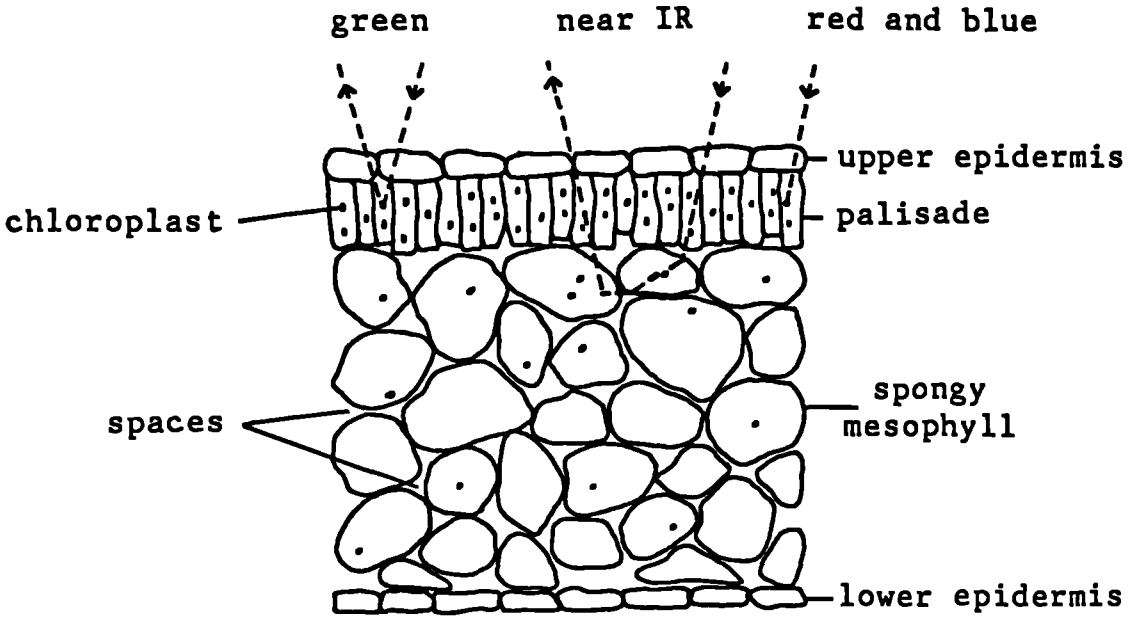

Figure 5.4 Cross-section of a pinule of a Pteridium aquilinum frond (after Parihar, 1962), showing the reflectance characteristics of visible and near infrared light (adapted from Boodle, 1984)

Spectral response in this part of the spectrum is thought to be predominantly affected by the physiological structure of the leaf, in particular by the discontinuities in the refractive index between membranes and cytoplasm, and between individual cells and the separating air spaces, in the spongy mesophyll (figure 5.4; Wooley, 1971).

The spectral response in the middle infrared portion of the spectrum is dominated by strong water absorption bands near 1.4μm, 1.9μm and especially 2.7μm (figure 5.3; Hoffer, 1978). So the response in the middle infrared is strongly related to the amount of moisture present in the leaves, and to the thickness of the leaf (Wooley, 1971; Lillesand and Kiefer, 1979).

Thus a characteristic spectral response pattern may be identified for vegetation, and the form is generally the same for all healthy green plants (Landgrebe, 1978). However, there are many factors which are unrelated to the spectral properties of the plant which may slightly alter the response pattern. These include: the illumination conditions; moisture content; background soil; slope and aspect; atmospheric conditions; and sensor parameters (section 5.3). In addition there are specific plant conditions which have a profound affect on the response, causing variation in the spectral response pattern both within and between vegetation types. Different species have different amounts and distribution of pigments in the leaves, which results in slight differences in the visible reflectance, and different species also have diverse internal structure, which can cause a change in the amount of refraction between cells, which results in alteration of the near infrared response. These variations are what makes it possible to distinguish between the different species of plants (Landgrebe, 1978).

The canopy geometry is also important. The response is not only related to the structural properties of individual leaves, but the canopy as a whole (Milton and Wardley, 1987). Differences in the canopy determine the amount of shadow contributing to the recorded

pattern (Smith, 1983), and canopy features (especially roughness) can influence variations in spectral response caused by changes due to sun and sensor angles (section 5.3.2; Milton and Wardley, 1987). Thus, two species with similar leaves but dissimilar canopy structures may have different spectral patterns, and the same species may appear spectrally distinct at different stages in canopy development.

Vegetation senescence is an important factor. As plants age the pigments which absorb visible light begin to break down, and this results in an increase in visible reflectance, especially in the blue and red wavelengths (Curran, 1985b).

Related to canopy development and senescence is the effect of phenology, or seasonal change. Different growth stages have associated changes in the pigments, plant internal structure and canopy geometry, which causes differences in the spectral pattern (section 4.3.1; Senger, 1971; Sinclair et al, 1971).

If a plant is stressed in a way that causes a disruption to its normal growth, it may cease the production of chlorophyll, which can alter the visible response (Lillesand and Kiefer, 1979). Such stress may be caused by an excess concentration of metal ions (Raines and Canney, 1980), or disease (Bauer, 1985). Moisture stress is an important factor, and it can also increase the reflectance in the water absorption bands (section 5.3.3; Bauer, 1985; Curran, 1985b).

5.5 The spectral characteristics and separability of moorland surfaces

5.5.1 Methodology

The previous discussion has highlighted the importance of the need for a thorough understanding of the spectral characteristics of features of interest before successful multispectral analysis may proceed. This section outlines the spectral response patterns and

general separability of important moorland species. The spectral characteristics are assessed in the context of the temporal resolution established in chapter 4.

Field spectral data, Airborne Thematic Mapper data (ATM) and Landsat Thematic Mapper data (TM), were statistically analysed to determine the spectral response patterns and separability of moorland vegetation types on data from ground, airborne and satellite levels (section 3.2). Descriptive statistics were calculated using the MINITAB package on the Durham MTS mainframe computer (Ryan et al, 1982). Mean and standard deviation values for each vegetation class, for all three data types, may be found in appendix 2.

It must be stressed that only the field spectral data have been inter-calibrated, by conversion to bidirectional reflectance (section 3.4.6). The ATM and TM were not calibrated to ground reference targets in order to calculate the actual reflectance of the surface. DN values were extracted direct from the images (sections 3.6.5.5 and 3.7.5.3), and therefore values from data recorded at different times are not directly comparable in quantitative terms, mainly as a result of the differences, however subtle, in atmospheric and illumination conditions.

The methodology adopted for the analysis of each spectral data set consisted a series of well-defined stages (figure 5.5). In each case any necessary preprocessing was carried-out first (sections 3.4.6, 3.6.5 and 3.7.5). Spectral response patterns were then considered for the species and sub-species classes. Spectral response patterns, often referred to as "spectral signatures", are a concise and visually informative way of displaying the spectral characteristics of individual classes. Examples showing the growth and management stages of Pteridium aquilinum and Calluna vulgaris are presented in Appendix 3 (figures App3.1 to App3.3).

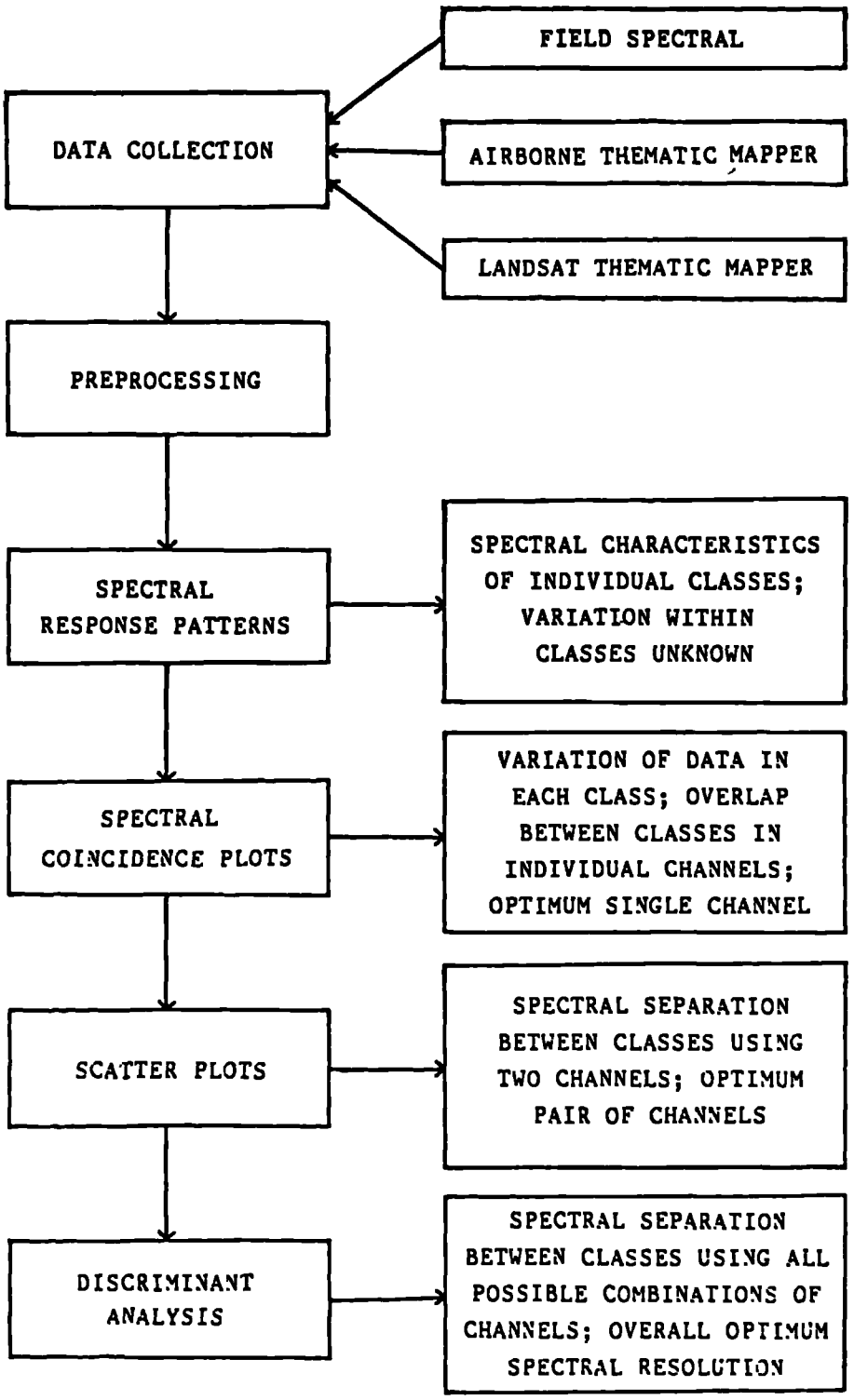

Figure 5.5 Flow diagram to show the stages in the analysis of spectral data, and the information made available at each stage

However, there are several drawbacks to using spectral response pattern diagrams. Such 'signatures' give a misleading impression of a continuous spectrum of measurements. This is because the waveband values are joined by a solid line, whereas in reality they are a set of discrete reflectance or radiance measurements. Signatures also tend to imply a unique and absolute reflectance curve, when in the real world such well-defined and single-valued patterns do not occur (section 5.4; Slater, 1980).

An alternative presentation method which overcomes these drawbacks is the spectral coincidence plot. Individual waveband means are left disconnected to express the discrete nature of recordings, and bars representing the standard deviation around each mean are drawn, in order to indicate the variability within each class. The additional data on the standard deviations of each class, and the compilation of all vegetation classes onto one diagram, without losing clarity, enables a good visual interpretation of class separability and overlap within each band.

Scatter graphs were then plotted. Such plots allow the visual interpretation of the distribution of classes using the data from two wavebands simultaneously. This facilitates an assessment of the class segregation in two-dimensional feature space, and the likely effectiveness of restricting the analysis to the information contained in only two channels. All possible combinations of channels were plotted for each data set, and the most useful graphs were selected for detailed analysis. The inclusion of a scatter plot in the analysis was determined subjectively. For each data set all the plots were carefully considered, and consequently ranked on their merits. The main criteria for ranking the graphs was the general apparent success in discriminating between the classes. Although in some cases more than one band combination had similar attributes, it was generally a straightforward procedure to rank the plots, as certain pairs of channels were noticeably superior to all others.

The final step in the analysis of spectral data was discriminant analysis. This is a statistical technique that defines linear discriminant functions which best separate pre-defined strata or classes (Dixon, 1975). The canonical discriminant method is a dimension-reducing technique, in many ways similar to Principal Component Analysis. It derives combinations of variables (wavebands) which have the greatest correlations with the chosen cover-type classes. This results in a set of orthogonal axes (functions) which seek to maximise the separation between classes (Asrar et al, 1986). Coefficients are derived for the functions and these are used to classify the data points. Cases are classified on the basis of the distance between the individual case and the class centroids. There are several different selection criteria, and the method chosen for this research is the Mahalanobis Squared Distance (Klecka, 1980; equation 5.1). This method seeks to maximise the distance between the closest classes, and tends to guarantee that all the classes are separated. It is a valuable method where overlap between classes may be a problem, or where classes are close together (SPSS Inc., 1983).

The analysis was completed using the 'discriminant' command in the SPSSx statistical package (SPSS Inc., 1983). The procedure results in a classification confusion matrix, which indicates the percentage of cases which have been correctly classified, and those assigned to the wrong class. It also gives an overall success rate, or accuracy value (SPSS Inc., 1983). The most common, and also the most misleading, method of estimating classification accuracy, is to use the 'apparent error rate' (James, 1985). This is obtained by using all the training data to derive the canonical coefficients, which are in turn used to classify the original training data. The error rate will consequently be biased, and will be lower than the 'true' error rate. There are several more reliable methods of assessing the classification success, including the independent sample technique, which was used in this study (James, 1985). Approximately half of the sample was used to derive the functions, and the remaining cases were used to test the classification.

Equation 5.1 The Mahalanobis Squared Distance

$$D^2(X|G_k) = (n.-g) \sum_{i=1}^{p} \sum_{j=1}^{p} a_{ij}(X_i - X_{ik.}) (X_j - X_{jk.})$$

where;

$D^2(X|G_k)$ = squared distance from point X (a case) to the centroid of class k

$n.$ = total number of cases

g = total number of classes (groups)

p = number of discriminating variables

a_{ij} = an element from the inverse of the within-groups sum of crossproducts matrix

$X_{ik.}$ = mean value of variable i for cases in class k

X_i = mean value of variable i for all cases

(after Klecka, 1980)

5.5.2 The spectral characteristics of selected moorland surfaces

5.5.2.1 Introduction

The spectral characteristics of two important moorland vegetation types, Pteridium aquilinum and Calluna vulgaris, are detailed in the following sections. the spectral response of other surfaces may be seen on the spectral coincidence plots (figures 5.6 to 5.11).

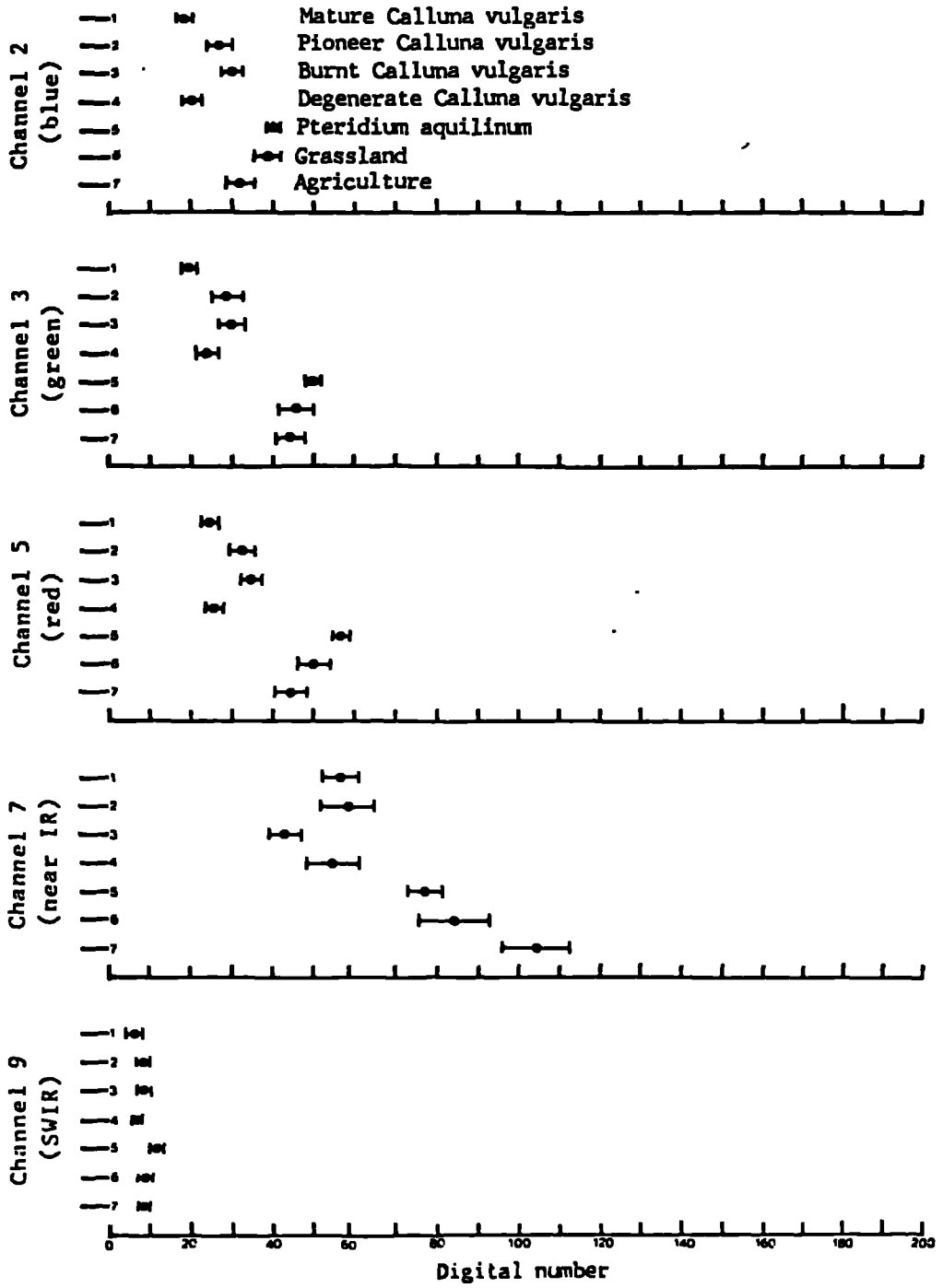

Figure 5.6 Spectral coincidence plot of selected vegetation classes: Airborne Thematic Mapper data, May 1986

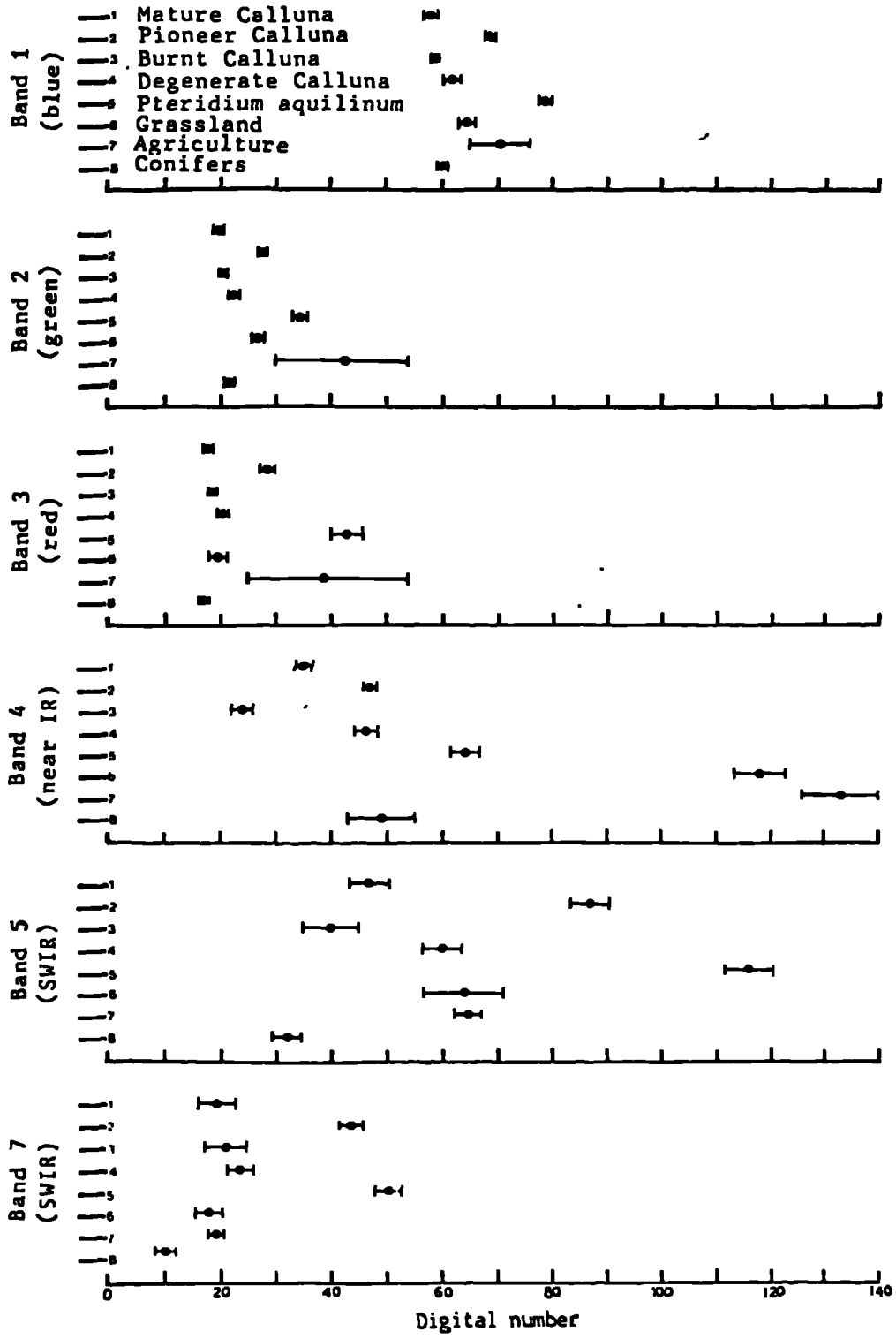

Figure 5.7 Spectral coincidence plot of selected vegetation classes: Landsat Thematic Mapper data, April 1984

5.5.2.2 The spectral characteristics of Pteridium aquilinum

It may be expected that the temporal variations in Pteridium aquilinum, outlined in chapter 4 (section 4.4.1), will have a considerable effect on the spectral response of the plant. Therefore, in this section the response pattern of Pteridium is considered in detail for the three time periods when data are available; spring, early summer and late summer (section 4.5; figure 4.3).

Spring patterns of response, as exemplified by the ATM (June) and TM (April) data, are relatively flat in appearance, and resemble the response of soil more closely than that of green vegetation (figures 5.6 and 5.7). This is due to the Pteridium aquilinum litter, predominant in the spring, with little green vegetation apparent above the surface. The most significant differences between the data sets are in the blue and short wave infrared (SWIR). The ATM blue reflectance is the lowest visible response, while the TM data unexpectedly has the peak visible response in this region (TM1) (figure 5.7). This phenomena occurs in all vegetation types in TM1, and is difficult to explain, unless it is due to disproportionate scattering of blue light by particulates in the atmosphere (Estes, 1974; section 5.3.4 above).

The other relative difference between the May ATM and the April TM data sets is in the SWIR (ATM9 and TM5). The values are very low in ATM9, compared to all other ATM channels, while the TM SWIR has the highest DN value of all TM bands. The low ATM value is probably due to atmospheric conditions. On both ATM overpass dates there was a considerable amount of cloud and haze, and the SWIR has a powerful water absorption band at 1.7μm. This phenomenon has significantly lowered the dynamic range of DN values in ATM9 in both ATM data sets, and greatly reduced the potential usefulness of data from this waveband.

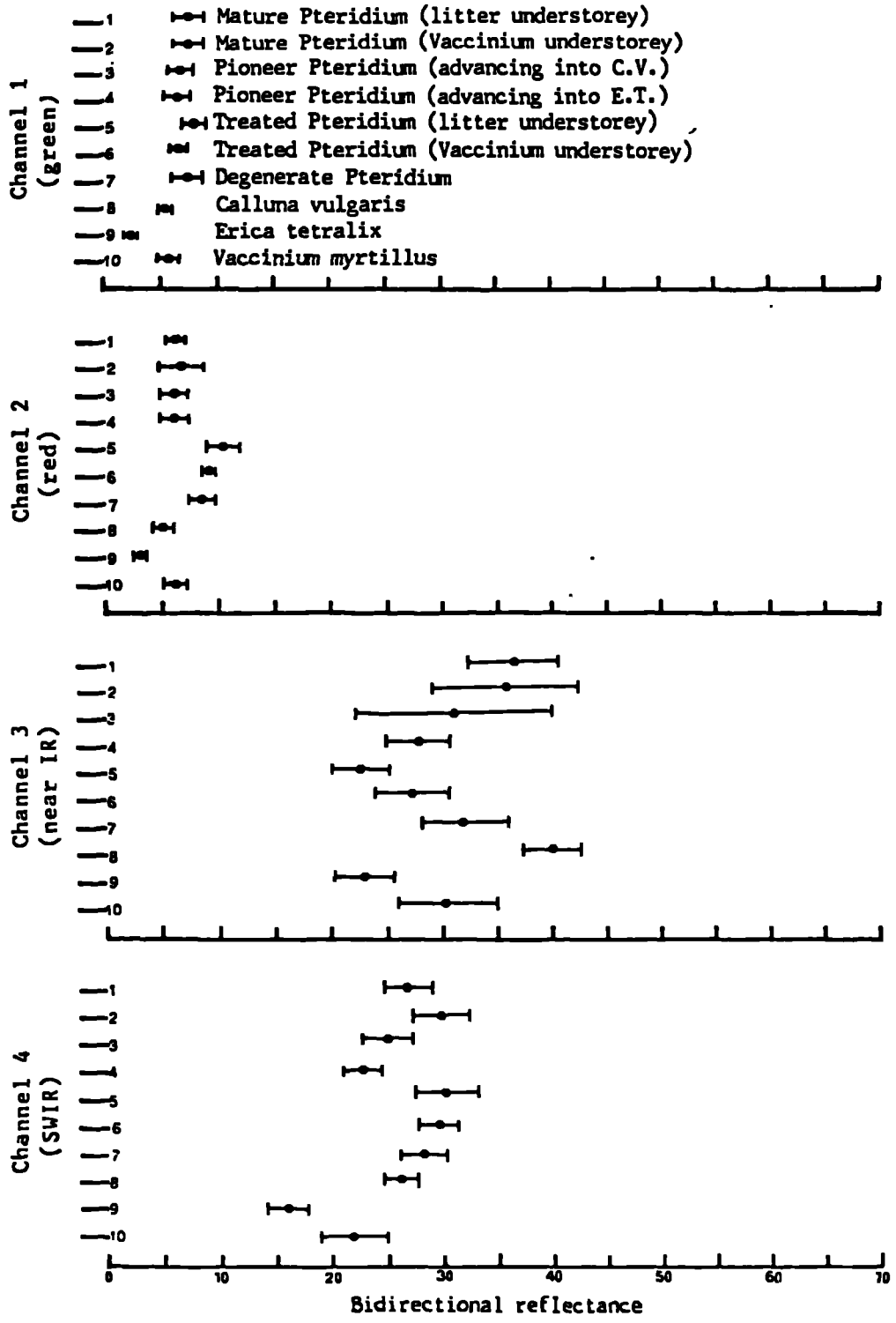

Figure 5.8 Spectral coincidence plot of selected vegetation classes: field spectral data, June 1986

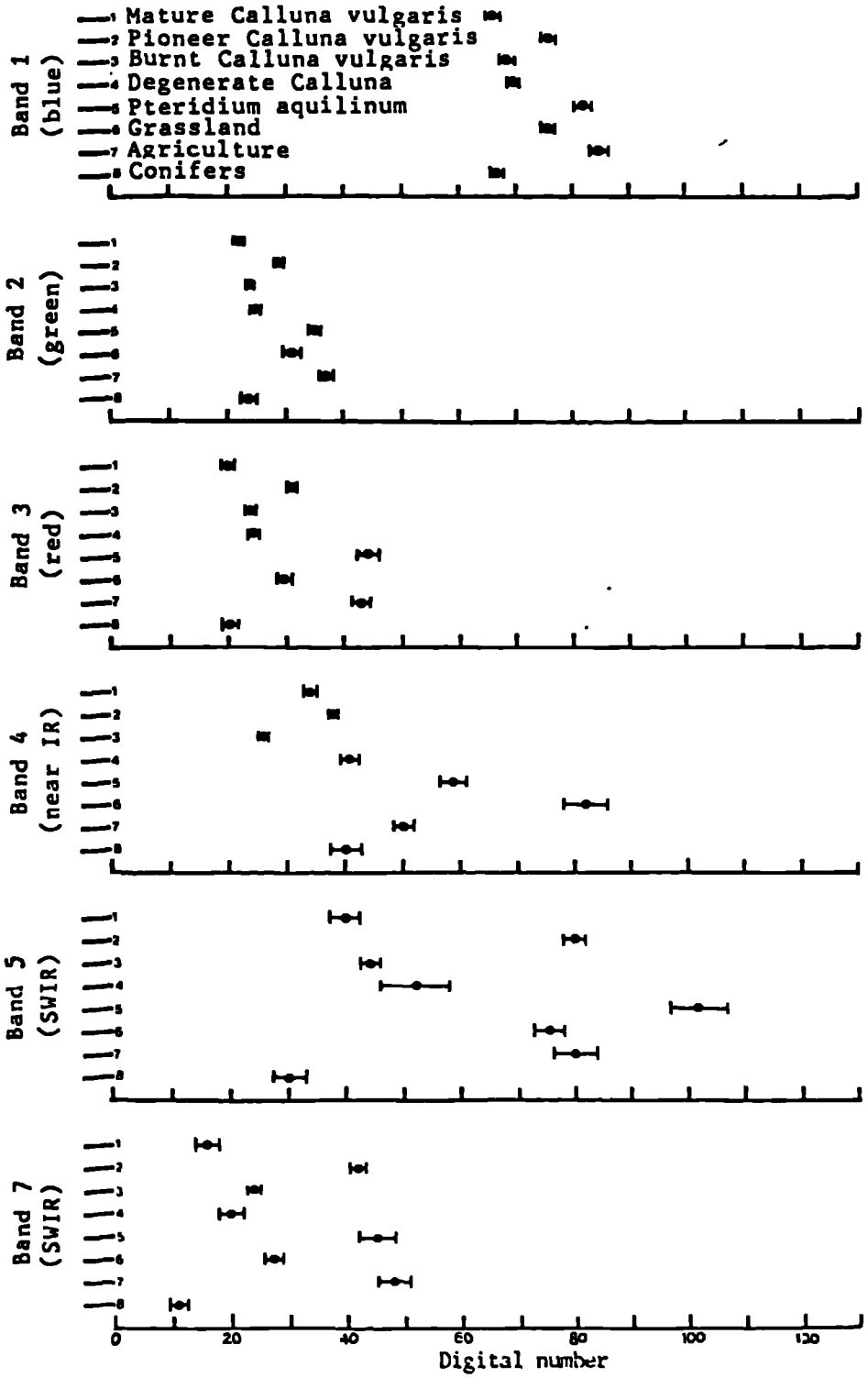

Figure 5.9 Spectral coincidence plot of selected vegetation classes: Landsat Thematic Mapper data, May 1985

The early summer data, field spectral (June) and TM (May), show signs of the appearance of green vegetation, with slightly lower visible and higher infrared (IR) reflectance (figures 5.8 and 5.9). There are quite large differences between the two data sets, the most noticeable of which are in the visible channels, where in the TM data the peak is again in the blue (not available on the radiometer). This high blue reflectance is similar to that outlined above for the April TM data. In addition, the TM red channel has higher mean DN value than the green.This is probably because of the smaller amount of green vegetation apparent above the surface at the time the TM data were recorded (May), than when the field spectral data were collected (June).

In June the growth stages of Pteridium aquilinum all have very similar response patterns, especially in the visible region (figure 5.8; figure App3.1a).

The late summer data, field spectral (August) and ATM (July) (figures 5.10 and 5.11), most closely resemble the characteristic spectral response of green vegetation (section 5.4; figure 5.3). This is primarily due to the greater biomass and vigorous growth at this time of year, causing more efficient absorption of visible light by active chlorophyll pigments, and greater reflectance of IR wavelengths by the increased number of internal discontinuities.

During August there is a greater contrast between Pteridium aquilinum growth stages, especially between the healthy and treated classes. However, there is still considerable confusion between the three healthy types (figure 5.10; figure App3.1b).

5.5.2.3 The spectral characteristics of Calluna vulgaris

It has been established that changes in the annual growth cycle of Calluna vulgaris are less dramatic than those of Pteridium aquilinum (section 4.4.2). Therefore, it is to be expected that the spectral response pattern is less likely to vary through the year.

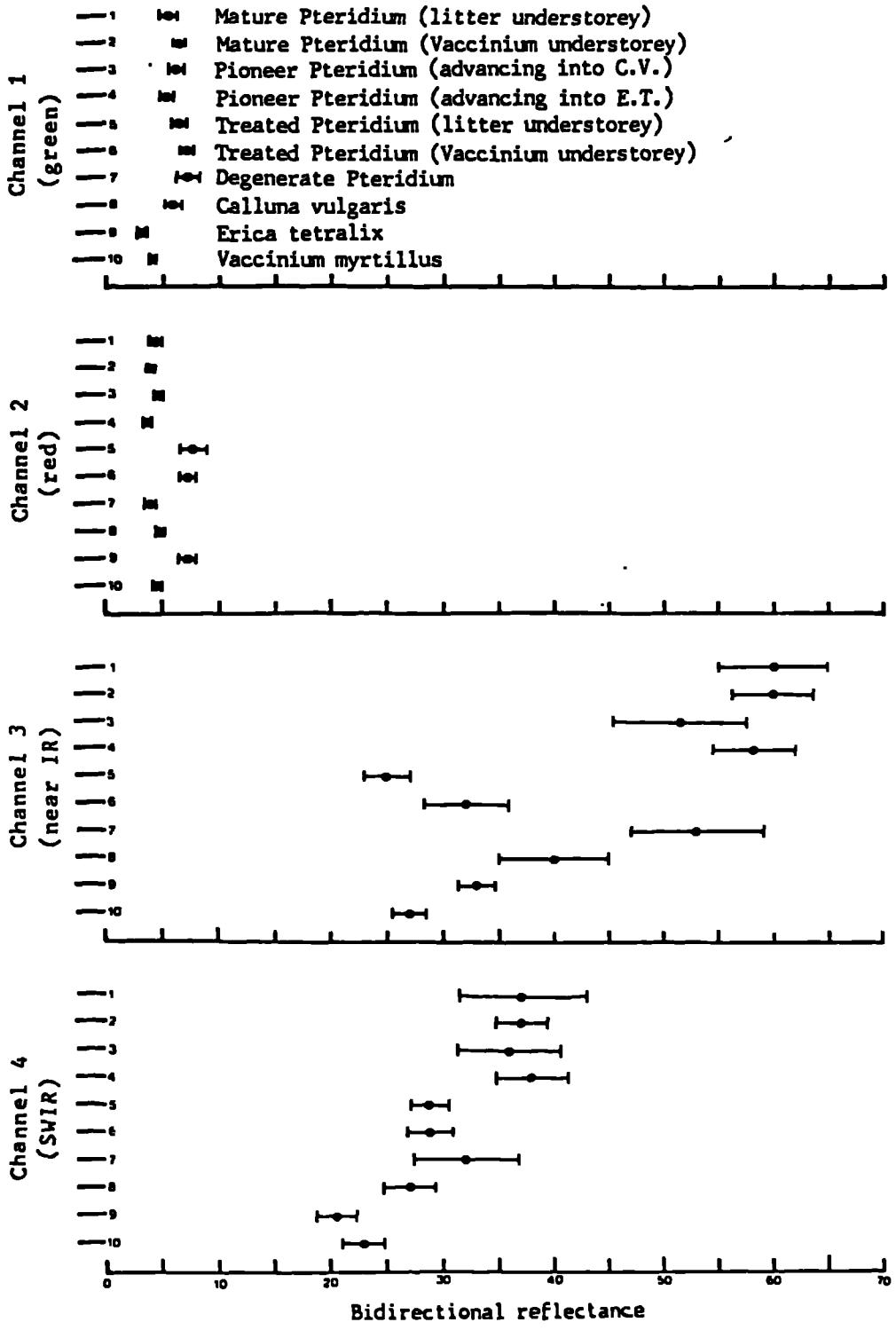

Figure 5.10 Spectral coincidence plot of selected vegetation classes: field spectral data, August 1986

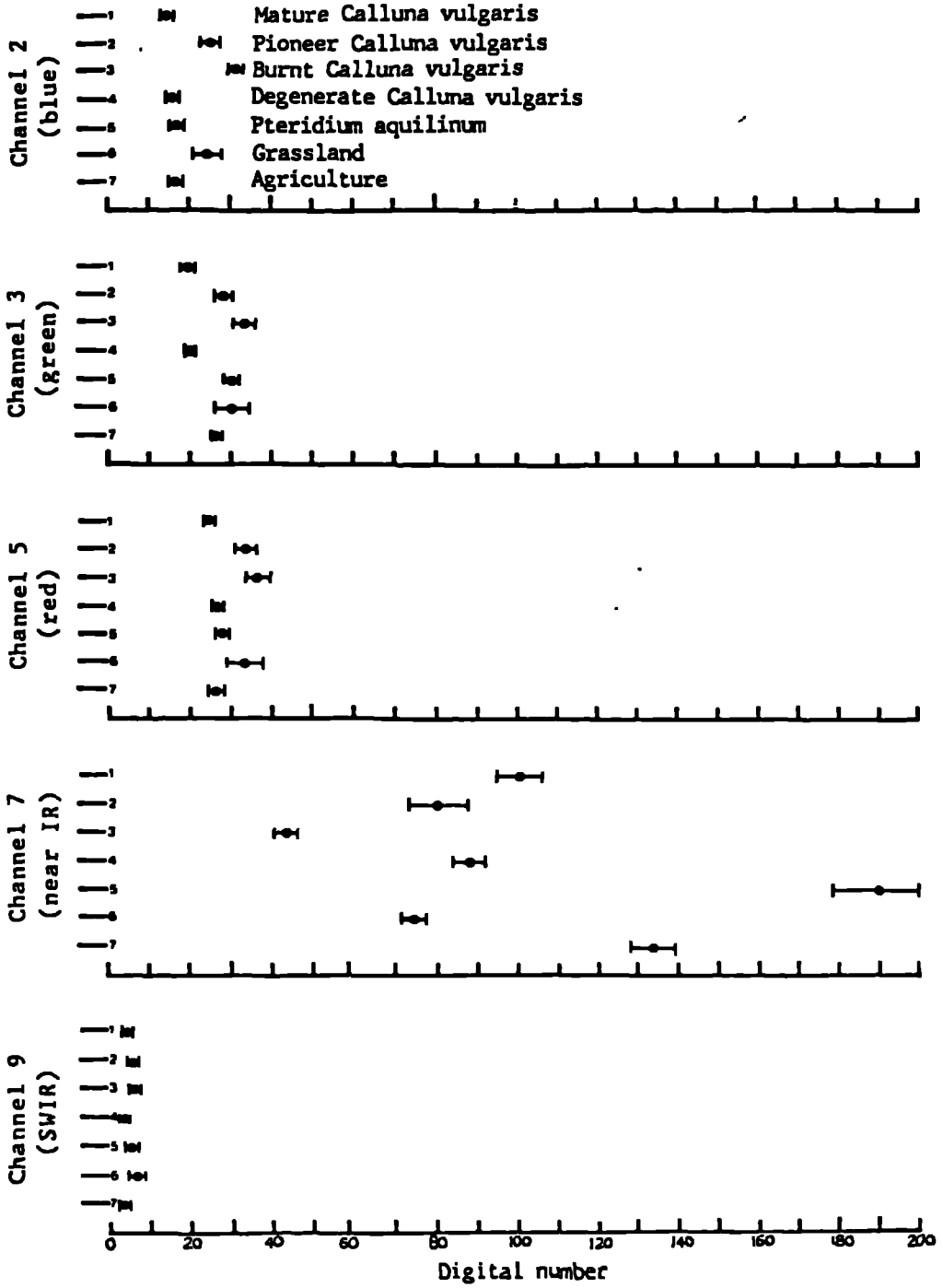

Figure 5.11 Spectral coincidence plot of selected vegetation classes: Airborne Thematic Mapper data, July 1986

In order to test this hypothesis, and for comparison with the Pteridium, the same three periods for which data are available will be considered (section 4.5; figure 4.3). Nevertheless, it has also been established that the most significant differences between growth stages are likely to be apparent in late August or September, during flowering (section 4.5.4). However, no data were available during flowering, so this hypothesis remains untested. It was intended to collect field spectral data during September in either 1986 or 1987, but weather conditions prevented this (section 3.4.5).

It was not possible to record ATM data in September during the period of research for the same reason. At the onset of research there were no cloud-free full TM scenes of the North York Moors in late August or September, although subsequently such a scene has been recorded (20.8.87). In addition, a quarter of a scene was collected on 31.8.86, but the other three quadrants were obscured by cloud.

Spring patterns of spectral response in Calluna vulgaris (May ATM and April TM; figures 5.6 and 5.7) have low visible and high IR reflectance. However, the IR values are not very high because the winter dormancy period of Calluna had not completely ended and vigorous growth had not fully recommenced (section 4.4.2). The blue TM values are again unusually high (figures App3.2a and App3.3a).

There appear to be great similarities within the Calluna vulgaris growth and management stages in the May ATM, especially between the mature and degenerate classes (figure 5.6). There is less of a problem discriminating between them using the TM data (figure 5.7).

The early summer data (June field spectral and May TM; figures 5.8 and 5.9) show a slightly closer resemblance to the characteristic vegetation spectral curve (section 5.4; figure 5.3), due to the further advance into the growing season. However, the TM data exhibit only subtle changes from those recorded in April (figure 5.7). This is because although they are classified into different time periods, they were recorded only one month apart (in successive years). In May

the growth and management stages still show considerable similarities, especially the mature and degenerate classes (figures 5.9 and App3.3b).

There are no dramatic differences in the Calluna vulgaris spectral response when the late summer data are considered; field spectral (August) and ATM (July) (figures 5.10 and 5.11). The differences from the May and June data are only small. The only significant difference is the high relative value of the ATM red channel (ATM5; figure 5.11). This is not to be expected, since red light is absorbed by chlorophyll pigments. However, it may be a result of the browning of older short shoots which then fall to the ground to form a litter layer during July and August (section 4.4.2). The field spectral data were recorded later in the growing season, and therefore most of the brown shoots had fallen to the ground by then, so the red value remains low.

There is more contrast between the Calluna growth and management stages in the July ATM data (figure 5.11). The burnt class spectral response curve is distinct, being relatively flat in appearance, as the surface consists of ash, burnt Calluna stems and background soil and peat, with only small amounts of vegetation. The pioneer Calluna is more distinct from the mature and degenerate, with lower IR and higher visible mean DN values, reflecting the lesser amount and vigour of vegetation in this class. The mature and degenerate Calluna are virtually identical (figure App3.2b).

5.5.3 The spectral separability of moorland surfaces

5.5.3.1 Introduction

The previous section has outlined the detailed spectral characteristics of the two major species, Pteridium aquilinum and Calluna vulgaris, for the three time periods for which data were available. However, the species were considered in isolation, and their general separability from each other, and from other moorland

surfaces, was not assessed. The following sections report the findings of qualitative and quantitative analyses to evaluate such separability, and hence to acquire an estimate of the probable success of computer image processing techniques on data of a moorland environment, and to identify the optimum spectral resolution for the task.

For each data set, tables have been compiled as summaries of the optimum spectral and temporal resolutions for pairwise discrimination between moorland cover types (tables 5.1, 5.3 and 5.5). The information on these matrices was drawn from spectral coincidence plots (figures 5.6 to 5.11), scatter plots (figures 5.12 to 5.15) and discriminant analysis (tables 5.2, 5.4 and 5.6 to 5.9). For each pair of classes the optimum temporal resolution, and the optimum spectral channel at that time, were identified (the top two lines in each box of the matrices). Subsequently, the optimum spectral channel at the sub-optimum time for each pair of classes was established (the bottom line in each box).

In the majority of cases the pairs of cover types were completely separable using only one channel. With several pairs two channels were required in order that no confusion occurred, and in each case these are both stated (determined from scatter plots and discriminant analysis). A few of the cover classes could not be completely separated using all the available spectral channels. These are identified on the matrices with symbols; ## for the optimum time, and *** for the sub-optimum time. For example, in the top left-hand cell of the field spectral data matrix (table 5.1), the pairwise relationship between mature Pteridium (litter understorey) and mature Pteridium (Vaccinium understorey) is shown. The best time for separating these two is August; when the green channel is optimal. The three asterisks (***) below, indicate that the two classes are not separable in June (the sub-optimal date) using all four radiometer channels.

	Pa2	Pa3	Pa4	Pa5	Pa6	Pa7	Cv	Et	Vm
Pa1	Green August ***	NrIr August ***	NrIR June ***	NrIR August *NrIR	NrIR August *NrIR	##green August ***	NrIR August *Green	NrIR August *Green	NrIR August *Green
Pa2		##SWIR June *Red	SWIR June ***	NrIR August *NrIR	NrIR August *Green	SWIR June ***	NrIR August *SWIR	NrIR August *SWIR	NrIR August *SWIR
Pa3			Red August *Red	NrIR August *Red	NrIR August *Red	NrIR August *Red	SWIR August *NrIR	NrIR August *Green	NrIR August *Green
Pa4				NrIR August *SWIR	NrIR August *SWIR	SWIR June *Green	NrIR August *NrIR	NrIR August *Green	NrIR August *Green
Pa5					NrIR June ***	NrIR August *NrIR	NrIR August *R/NrIR	NrIR August *Green	SWIR June *Green
Pa6						NrIR August ***	NrIR June ***	SWIR June *SWIR	Green August *SWIR
Pa7							Red June *NrIR	Red June *NrIR	NrIR August *SWIR
Cv								SWIR June *Gr/NrIR	NrIR August *NrIR
Et									Green June *NrIR

Key: Pa=Pteridium (1=Mature (litter) 2=Mature (Vm) 3=Pioneer (Cv) 4=Pioneer (Et 5=Treated (litter) 6=Treated (Vm) 7=Degenerate) Cv=Calluna Et=Erica Vm=Vaccini

=not completely separable using all bands

* =optimum spectral band, or band combination, at sub-optimal date

***=not completely separable at sub-optimal date using all bands

Table 5.1 Summary of optimum spectral and temporal resolution for pair-wise discrimination between classes; field spectral data (see text for details; section 5.5.3.1)

These matrices were used to establish the number and identity of channels required to separate all combinations of pairs of classes, before moving on to multi-class discrimination. Obviously, different pairs of classes need different channels, and so all the selected wavebands in the pairwise analysis, could be identified, in order to suggest combinations that would achieve the best overall separation between all classes. These combinations of channels were subsequently checked, using scatter plots and discriminant analysis confusion matrices. On these matrices (e.g. table 5.2), the number of cases in each class used to test the classification is stated. The remaining cases were used to calculate the classification function coefficients (section 5.5.1).

5.5.3.2 The pairwise separability of moorland surfaces

When considering the pairwise separation between classes using field spectral data (table 5.1), August is selected as the optimum date in 32 of the 45 pairwise relationships, compared with only 13 examples where June is best. Each of the four radiometer channels is selected in at least three cases, but the near IR is the outstanding individual channel, being selected in 30 of the pairs. Thus, in order to attempt complete discrimination between all pairs of vegetation types, all four channels are needed, although the matrix suggests that either the near IR and green, or the near IR and SWIR, wavebands together can accomplish most of the separation in August.

Nevertheless, even using all four channels certain pairs of classes still remain inseparable (table 5.2). The main confusion is between mature Pteridium (litter understorey) and degenerate Pteridium, and between mature Pteridium (Vaccinium understorey) and pioneer Pteridium (advancing into Calluna). This indicates the sizable overlap between Pteridium aquilinum growth stages, even at the optimum temporal resolution, confirming the confusion that was evident on the coincidence plots (figures 5.8 and 5.10).

real class	No. of cases	predicted class									
		Pa1	Pa2	Pa3	Pa4	Pa5	Pa6	Pa7	Cv	Et	Vm
Pa1	4	25	50	25	0	0	0	0	0	0	0
Pa2	5	0	40	0	0	0	0	20	40	0	0
Pa3	4	20	0	0	80	0	0	0	0	0	0
Pa4	5	0	0	16.7	83.3	0	0	0	0	0	0
Pa5	6	0	0	0	0	83.3	0	16.3	0	0	0
Pa6	6	0	0	0	0	0	80	20	0	0	0
Pa7	5	0	25	0	0	0	25	50	0	0	0
Cv	5	0	0	0	0	0	0	0	100	0	0
Et	5	0	0	0	0	0	0	0	0	100	0
Vm	5	0	0	0	40	0	0	0	0	12.5	47.5

a) June: All four channels Overall Accuracy = 60.38%

real class	No. of cases	predicted class									
		Pa1	Pa2	Pa3	Pa4	Pa5	Pa6	Pa7	Cv	Et	Vm
Pa1	4	75	0	0	0	0	0	25	0	0	0
Pa2	5	0	20	0	20	0	0	60	0	0	0
Pa3	4	20	0	40	40	0	0	0	0	0	0
Pa4	5	33.3	33.3	0	33.4	0	0	0	0	0	0
Pa5	6	0	0	0	0	66.7	33.3	0	0	0	0
Pa6	6	0	0	0	0	20	60	0	20	0	0
Pa7	5	0	25	25	0	0	0	50	0	0	0
Cv	5	0	0	20	0	0	20	0	60	0	0
Et	5	0	0	0	0	0	0	0	0	100	0
Vm	5	0	0	0	0	0	0	0	0	0	100

b) August: All four channels Overall Accuracy = 62.26%

Key: Pa=Pteridium (1=Mature (litter) 2=Mature (Vm) 3=Pioneer (Cv) 4=Pioneer (Et) 5=Treated (litter) 6=Treated (Vm) 7=Degenerate) Cv=Calluna Et=Erica Vm=Vaccinium)

Table 5.2 Discriminant analysis confusion matrices for field spectral data: original ten classes, all four channels (%)

	Cv2	Cv3	Cv4	Pa	Gr	Ag
Cv1	NrIR July *Red	NrIR July *Red	##NrIR July ***	Red May *Bl/NrIR	Red May *NrIR	NrIR May *NrIR
Cv2		##NrIR July ***	##Red July ***	Red May *NrIR	Red May *NrIR	NrIR May *NrIR
Cv3			Red May *Bl/NrIR	Red May *NrIR	Red May *NrIR	#red/NrIR May ***
Cv4				Red May ***	Red May ***	Red May ***
Pa					NrIR July *red/NrIR	NrIR July ***
Gr						NrIR July ***

Key: Cv=Calluna (1=Mature 2=Pioneer 3=Burnt 4=Degenerate)
Pa =Pteridium Gr=Grassland Ag=Agriculture
# =only completely separable using two bands
=not completely separable using all bands
* =optimum spectral band, or band combination, at sub-optimal date
***=not completely separable at sub-optimal date using all bands

Table 5.3 Summary of optimum spectral and temporal resolution for pair-wise discrimination between classes: Airborne Thematic Mapper data (see text for details; section 5.5.3.1)

real class	No.of cases	predicted class						
		Cv2	Cv3	Cv4	Pa	Gr	Ag	
Cv1	53	94.3	0	0	5.7	0	0	0
Cv2	60	0	75.0	18.3	6.7	0	0	0
Cv3	60	0	0	100	0	0	0	0
aCv4	58	34.4	4.9	0	60.7	0	0	0
Pa	60	0	0	0	0	100	0	0
Gr	61	0	0	0	0	0	96.7	3.3
Ag	61	0	0	0	0	1.4	7.1	91.4

Overall Accuracy = 88.18%

a) May: channels ATM5 and ATM7

real class	No.of cases	predicted class						
		Cv1	Cv2	Cv3	Cv4	Pa	Gr	Ag
Cv1	53	100	0	0	0	0	0	0
Cv2	60	0	69.8	1.9	26.4	1.9	0	0
Cv3	60	0	0	95.0	0	0	0	5.0
Cv4	58	1.5	25.8	0	65.2	3.0	4.5	0
Pa	60	0	0	0	0	100	0	0
Gr	61	0	0	0	0	0	100	0
Ag	61	0	0	1.6	0	0	1.6	96.8

Overall Accuracy = 88.97%

b) July: channels ATM5 and ATM7

Key: Cv=Calluna (1=Mature 2=Pioneer 3=Burnt 4=Degenerate)
Pa=Pteridium Gr=Grassland Ag=Agriculture

Table 5.4 Discriminant analysis confusion matrices for Airborne Thematic Mapper data: optimum pair of channels (%)

These results suggest that in practice it might prove impossible to distinguish between the Pteridium stages using operational satellite data, since they are not even adequately separable using high spatial resolution field spectral data.

Using the ATM data (table 5.3), May is selected as the optimal date (13 of the 21 cases), although July is also useful. The choice of May in many pairs, is probably because the analysis is dominated by Calluna vulgaris classes. The optimum time to distinguish Calluna from other moorland cover types is likely to be in the spring, when the other classes are effectively bare surfaces, contrasting with the vegetated Calluna.

Only the red and near IR channels are selected as optimum in the pairwise analysis, and therefore a combination of these two channels appears to offer optimal discrimination between the classes chosen for analysis. However, in three of the Calluna cases (mostly involving degenerate), the pairs are not separable, even when using all of the ATM channels, at the best time. Thus, a two-band combination will not adequately discriminate between all Calluna stages (table 5.4).

When the TM pairwise relationships are considered (table 5.5), the earlier date is selected, as with the ATM, in most cases; April is chosen for 19 of the 28 pairs. However, there is not much to chose between the dates, and the May data is almost as good. This is because the two data sets were recorded only one month apart (but in different years). The SWIR is the most common single band (16 of the 28 pairs), and the near IR is also important, although these two bands cannot individually separate adequately between all the classes (table 5.6). However, on the pairwise summary matrix (table 5.5), all the pairs of cover types may be separated using a maximum of two bands (near IR and SWIR), suggesting that the two in combination may be successful. This is confirmed by excellent discriminant analysis accuracy values (99.48% and 98.5%), when using the near IR and SWIR together (table 5.7).

	Cv2	Cv3	Cv4	Pa	Gr	Ag	Con
Cv1	SWIR May *SWIR	#Nr/SWIR April ***	NrIR May *SWIR	SWIR April *SWIR	SWIR April *NrIR	SWIR April *NrIR	#Nr/SWIR May *Gr/Nr/SWIR
Cv2		NrIR May *Nr/SWIR	#Nr/SWIR April *Nr/SWIR	SWIR April *Nr/SWIR	NrIR May *Nr/SWIR	Red April *NrIR	SWIR May *SWIR
Cv3			NrIR May *Nr/SWIR	SWIR April *SWIR	SWIR April *NrIR	SWIR April *NrIR	SWIR April *NrIR
Cv4				SWIR April *SWIR	NrIR April *NrIR	SWIR April *NrIR	SWIR April *Nr/SWIR
Pa					NrIR May *SWIR	SWIR May *NrIR	Red April *Nr/SWIR
Gr						#Nr/SWIR April ***	SWIR April *NrIR
Ag							SWIR April *NrIR

Key: Cv=Calluna (1=Mature 2=Pioneer 3=Burnt 4=Degenerate)
Pa =Pteridium Gr=Grassland Ag=Agriculture
\# =only completely separable using two bands
* =optimum spectral band, or band combination, at sub-optimal date
*** =not completely separable at sub-optimal date using all bands
SWIR=TM5 (not TM7 which is also SWIR)

Table 5.5 Summary of optimum spectral and temporal resolution for pair-wise discrimination between classes; Landsat Thematic Mapper data (see text for details; section 5.5.3.1)

real class	No. of cases	predicted class							
		Cv1	Cv2	Cv3	Cv4	Pa	Gr	Ag	Con
Cv1	9	81.8	0	18.2	0	0	0	0	0
Cv2	7	0	28.6	18.3	6.7	0	14.3	57.1	0
Cv3	12	0	0	100	0	0	0	0	0
Cv4	12	0	0	50.0	50.0	0	0	0	0
Pa	22	0	0	0	0	100	0	0	0
Gr	32	0	3.1	0	0	0	93.8	3.1	0
Ag	53	0	20.8	0	0	0	17.0	62.3	0
Con	59	3.4	0	0	0	0	0	0	96.6

Overall Accuracy = 81.96%

a) April 1984: channel TM5

real class	No. of cases	predicted class							
		Cv1	Cv2	Cv3	Cv4	Pa	Gr	Ag	Con
Cv1	9	100	0	0	0	0	0	0	0
Cv2	7	0	0	0	60.0	40.0	0	0	0
Cv3	12	4.0	0	96.0	0	0	0	0	0
Cv4	12	0	20	0	30.0	0	0	0	50
Pa	22	0	0	0	0	100	0	0	0
Gr	32	0	0	0	0	0	93.8	6.3	0
Ag	53	0	0	0	0	0	7.3	92.7	0
Con	59	21.4	1.8	0	7.1	10.7	0	0	58.9

Overall Accuracy = 79.5%

b) May 1985: channel TM4

Key: Cv=Calluna (1=Mature 2=Pioneer 3=Burnt 4=Degenerate) Pa=Pteridium Gr=Grassland Ag=Agriculture Con=Conifers

Table 5.6 Discriminant analysis confusion matrices for Landsat Thematic Mapper data: optimum individual channel (%)

real class	No. of cases	predicted class							
		Cv1	Cv2	Cv3	Cv4	Pa	Gr	Ag	Con
Cv1	9	100	0	0	0	0	0	0	0
Cv2	7	0	100	0	0	0	0	0	0
Cv3	12	0	0	100	0	0	0	0	0
Cv4	12	0	0	0	100	0	0	0	0
Pa	22	0	0	0	0	100	0	0	0
Gr	32	0	0	0	0	0	100	0	0
Ag	53	0	0	0	0	0	0	100	0
Con	59	1.7	0	0	0	0	0	0	98.3

Overall Accuracy = 99.48%

a) April 1984: channels TM4 and TM5

real class	No. of cases	predicted class							
		Cv1	Cv2	Cv3	Cv4	Pa	Gr	Ag	Con
Cv1	9	95.5	0	0	4.5	0	0	0	0
Cv2	7	0	100	0	0	0	0	0	0
Cv3	12	4.0	0	96.0	0	0	0	0	0
Cv4	12	0	0	0	100	0	0	0	0
Pa	22	0	0	0	0	100	0	0	0
Gr	32	0	0	0	0	0	100	0	0
Ag	53	0	0	0	0	0	2.4	97.6	0
Con	59	0	0	0	0	0	0	0	100

Overall Accuracy = 98.5%

b) May 1985: channels TM4 and TM5

Key: Cv=Calluna (1=Mature 2=Pioneer 3=Burnt 4=Degenerate) Pa=Pteridium Gr=Grassland Ag=Agriculture Con=Conifers

Table 5.7 Discriminant analysis confusion matrices for Landsat Thematic Mapper data: optimum pair of channels (%)

The great superiority of the TM over the ATM data to discriminate between Calluna growth stages, is possibly due to the poor atmospheric conditions at the time the ATM data were recorded, to different moisture and environmental conditions, and to the slightly different point in the growing season, at the times the data were collected. An additional reason is the difference in spatial scale. The finer spatial resolution of the ATM data, increases the heterogeneity within Calluna classes, which adds to the confusion. These small-scale differences are averaged-out in the coarser TM data (chapter 6).

5.5.3.3 The general multi-class separation of moorland surfaces

Although the pairwise discrimination of moorland surfaces can be achieved in many cases using only one waveband (tables 5.1, 5.3 and 5.5), when more than two cover types are included in the analysis, as explained above, more spectral information is usually required in order to separate all the classes adequately; in other words, a multispectral approach is needed. Discriminant analysis was used to confirm the suggestions from the pairwise analysis, and to determine the overall multi-class optimum spectral and temporal resolutions for the remote sensing of a moorland environment.

It was considered impossible to separate the Pteridium aquilinum growth and management stages successfully (section 5.5.3.2), and so the two mature field spectral data classes were combined to form a new "Pteridium" class. This was used in all further analysis, and the other Pteridium classes were discarded. Thus, subsequent analysis included only 4 cover types, Pteridium, Calluna vulgaris, Erica tetralix and Vaccinium myrtillus.

In the field spectral data, a two-band combination of either the green and the near IR (channels 1 and 3), or the near IR and the SWIR (channels 3 and 4), was suggested by the pairwise analysis (section 5.5.3.2).

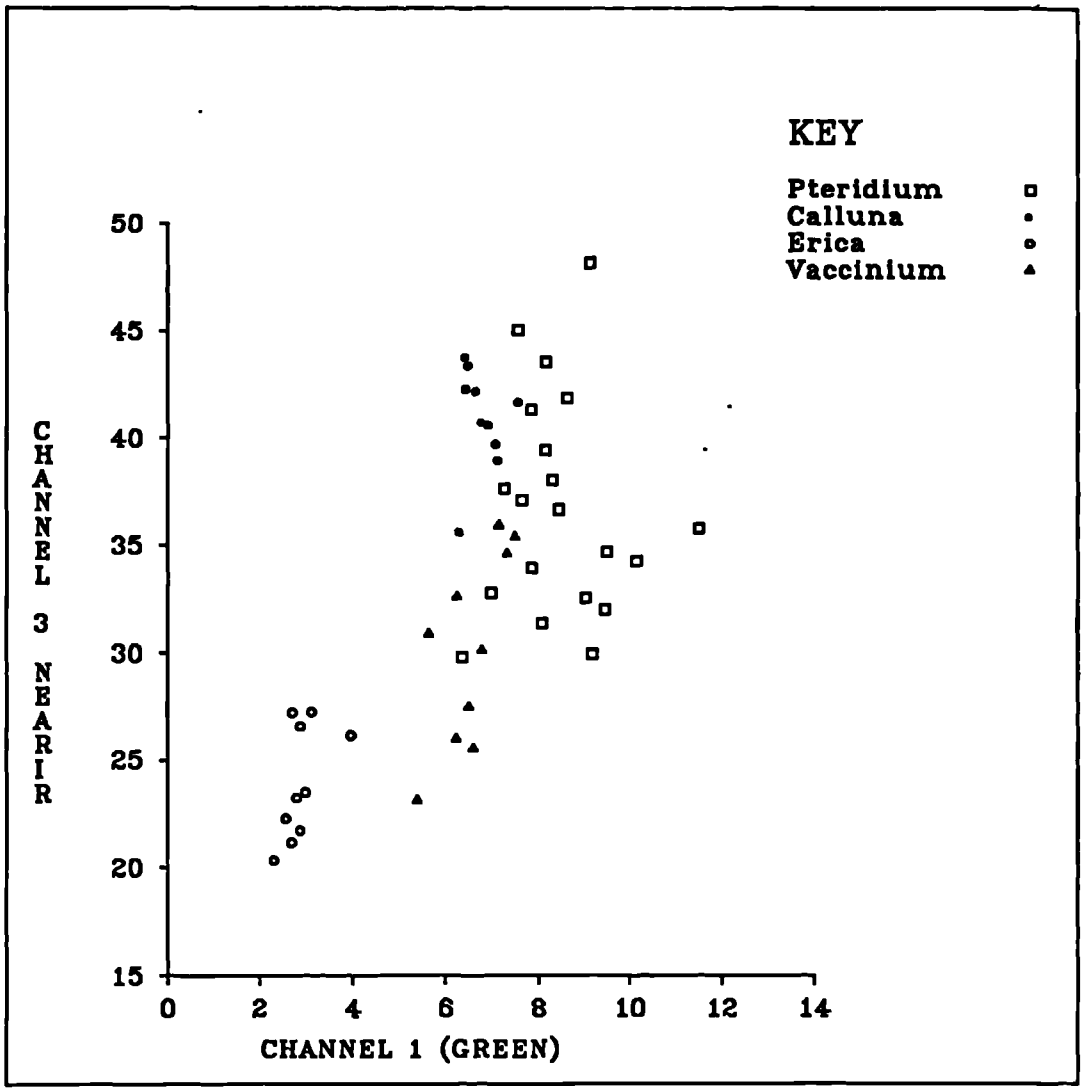

Figure 5.12a Scatter plot to show bidirectional reflectance for field spectral data: channels 1 and 3 (green and near infrared): June 1986

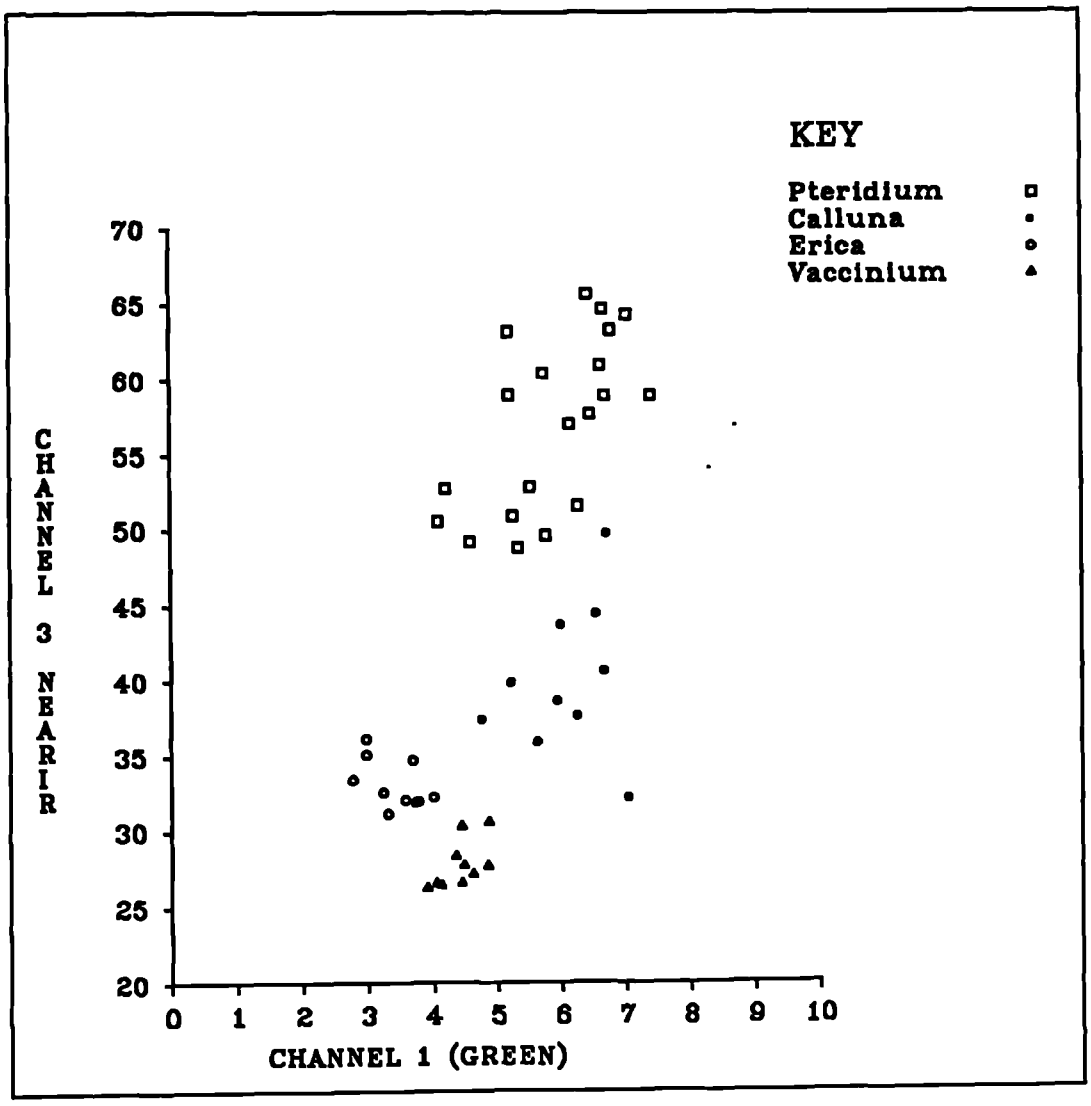

Figure 5.12b Scatter plot to show bidirectional reflectance for field spectral data: channels 1 and 3 (green and near infrared): August 1986

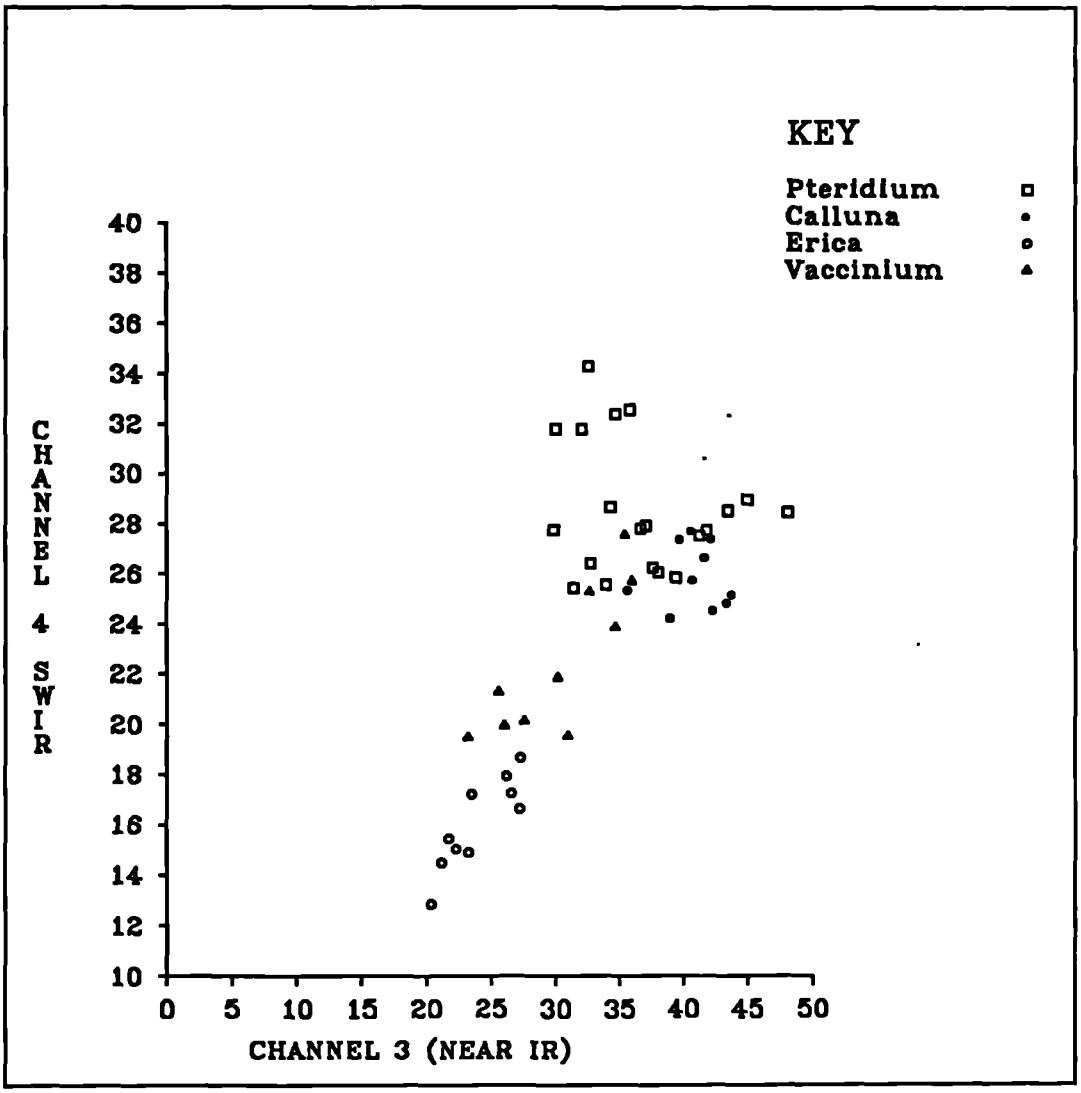

Figure 5.13a Scatter plot to show bidirectional reflectance for field spectral data: channels 3 and 4 (near and short wave infrared): June 1986

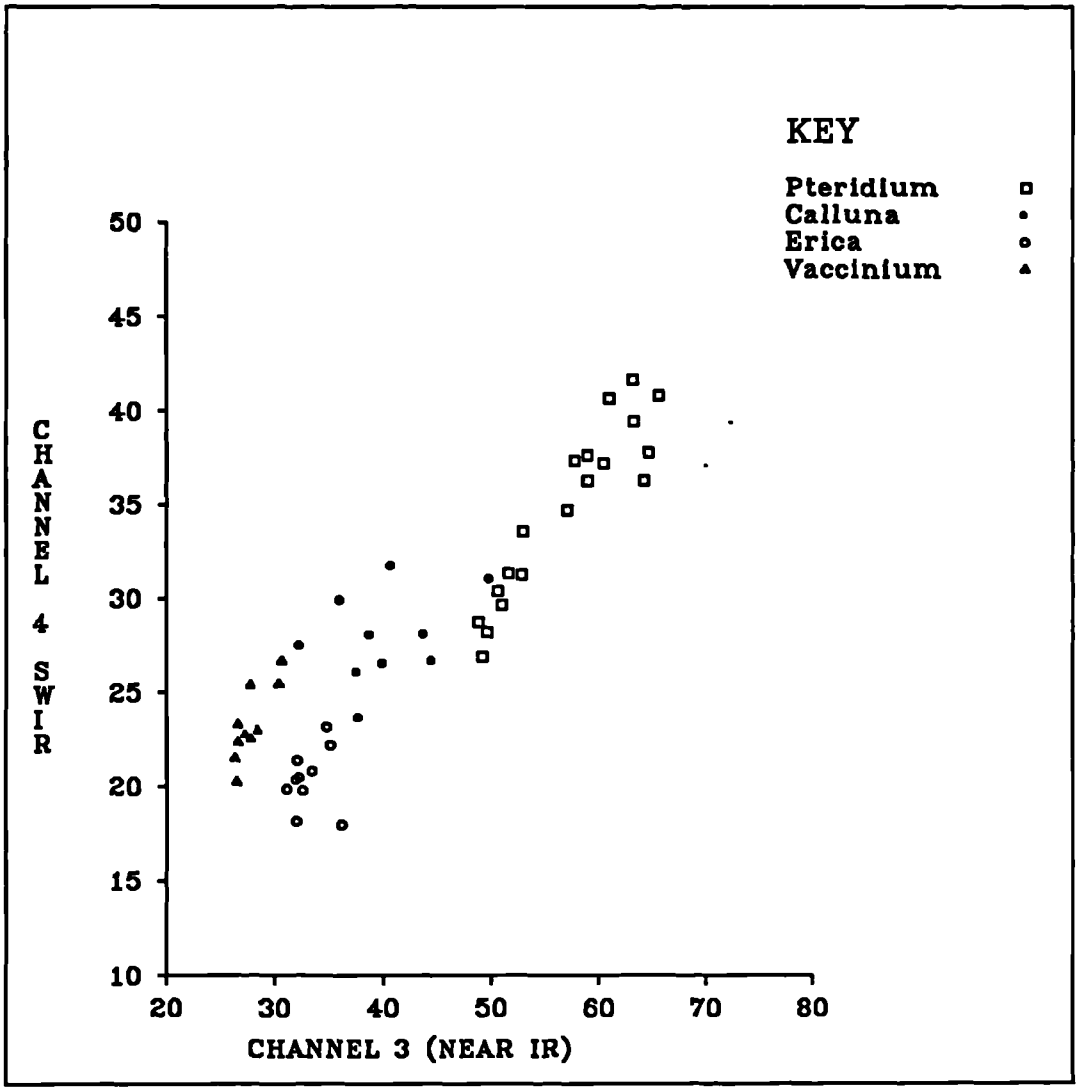

Figure 5.13b Scatter plot to show bidirectional reflectance for field spectral data: channels 3 and 4 (near and short wave infrared): August 1986

Both pairs offer fairly good discrimination (figures 5.12 and 5.13), although there is some confusion between Pteridium aquilinum and Vaccinium myrtillus in the June data of both pairs (figures 5.12a and 5.13a). This is because of the Vaccinium understorey to the Pteridium, which is exposed in June. Using the near IR and SWIR, there is also overlap between Vaccinium and Calluna vulgaris in June. The mix-up is probably because they are both evergreen shrubs of similar vigour and biomass at this time of year.
The two August plots are both more successful, and the green/near IR pairing appears to discriminate completely between the four classes (figure 5.12b). There is one possible mix-up in the near IR/ SWIR plot, where a Calluna case might be misclassified as Pteridium (figure 5.13b). The slightly greater discrimination that is visually apparent on the green and near IR scatter plot, is confirmed when the pair are entered into discriminant analysis. The August data are optimal, achieving a perfect classification, with 100% accuracy (table 5.8b), although the June data is also successfully classified at 95.83% (table 5.8a).

Using the ATM data, the red/near IR combination was suggested as the optimum pair by the pairwise analysis (section 5.5.3.2), although some confusion between the classes was noted on the summary matrix. Scatter plots of these two channels (ATM5 and ATM7) illustrate considerable overlap between the vegetation types, especially among the Calluna vulgaris growth and management stages (figure 5.14). The mature class is completely mixed with the degenerate, and there is also overlap between mature, degenerate and pioneer, and between pioneer and burnt. This reflects the transitional nature of the relatively minor differences in structure, canopy form and biomass between the Calluna stages.

real class	no. of cases	predicted class			
		Pa	Cv	Et	Vm
Pa	9	88.9	11.1	0	0
Cv	4	0	100	0	0
Et	5	0	0	100	0
Vm	6	0	0	0	100

Overall Accuracy = 95.83%

a) June: channels 1 and 3

real class	no. of cases	predicted class			
		Pa	Cv	Et	Vm
Pa	9	100	0	0	0
Cv	4	0	100	0	0
Et	5	0	0	100	0
Vm	6	0	0	0	100

Overall Accuracy = 100%

b) August: channels 1 and 3

Key: Pa=Pteridium Cv=Calluna Et=Erica Vm=Vaccinium

Table 5.8 Discriminant analysis confusion matrices for field spectral data: optimum pair of channels (%)

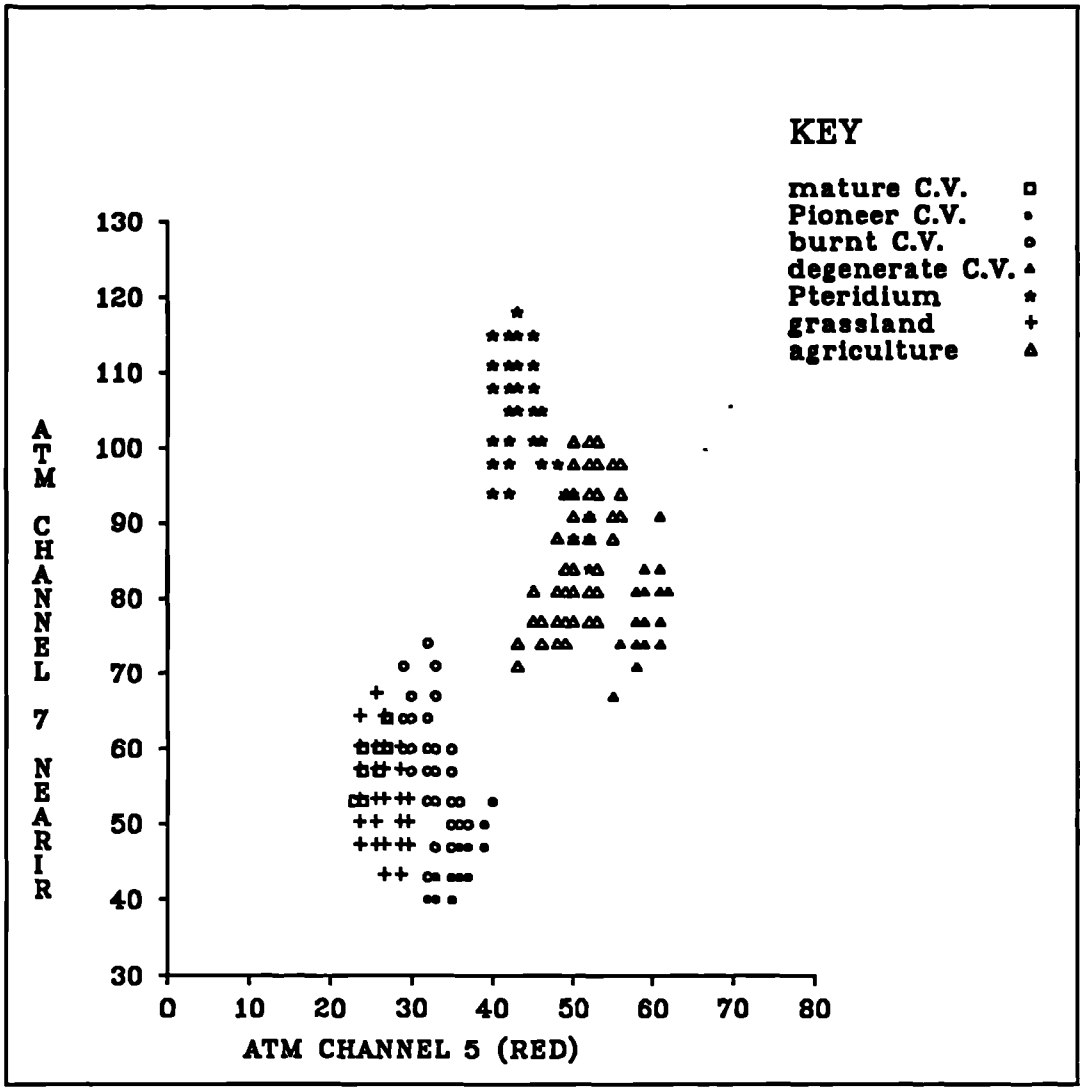

Figure 5.14a Scatter plot to show digital numbers for Airborne Thematic Mapper data: channels 5 and 7 (red and near infrared): May 1986

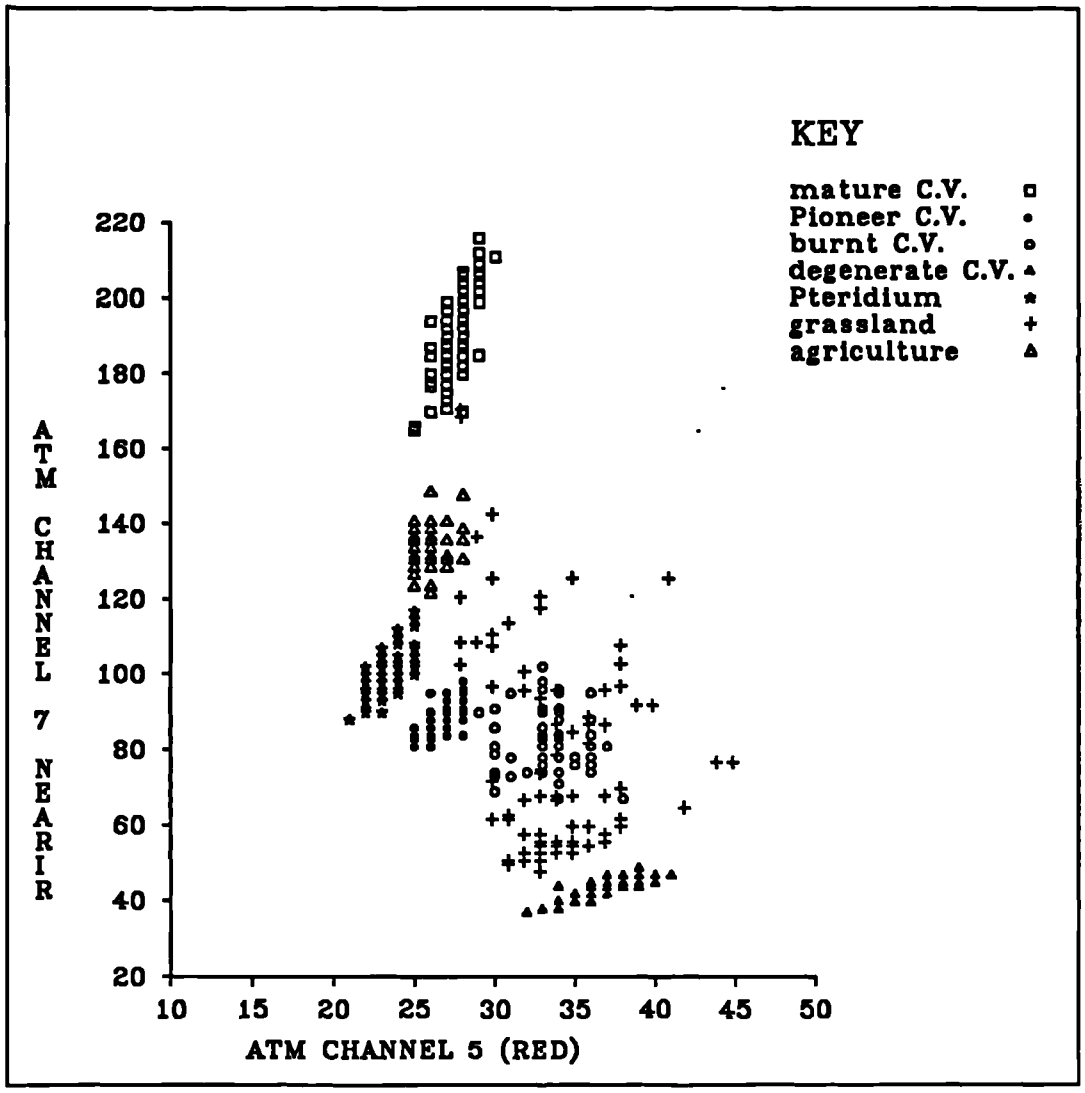

Figure 5.14b Scatter plot to show digital numbers for Airborne Thematic Mapper data: channels 5 and 7 (red and near infrared): July 1986

real class	No. of cases	predicted class						
		Cv1	Cv2	Cv3	Cv4	Pa	Gr	Ag
Cv1	53	84.49	0	0	15.1	0	0	0
Cv2	60	0	76.7	16.6	6.7	0	0	0
Cv3	60	0	0	100	0	0	0	0
Cv4	58	13.1	0	0	86.9	0	0	0
Pa	60	0	0	0	0	100	0	0
Gr	61	0	0	0	0	0	96.7	3.3
Ag	61	0	0	0	0	1.4	7.1	91.4

Overall Accuracy = 91.02%

a) May: channels ATM2, ATM5 and ATM7

real class	No. of cases	predicted class						
		Cv1	Cv2	Cv3	Cv4	Pa	Gr	Ag
Cv1	53	100	0	0	0	0	0	0
Cv2	60	0	88.7	1.9	7.5	1.9	0	0
Cv3	60	0	0	91.7	0	0	0	8.3
Cv4	58	1.5	4.5	0	84.8	4.5	4.5	0
Pa	60	0	0	0	0	100	0	0
Gr	61	0	0	0	0	0	100	0
Ag	61	0	0	15.9	0	0	0	84.1

Overall Accuracy = 92.23%

b) July: channels ATM5, ATM7 and ATM9

Key: Cv=Calluna (1=Mature 2=Pioneer 3=Burnt 4=Degenerate)
Pa=Pteridium Gr=Grassland Ag=Agriculture

Table 5.9 Discriminant analysis confusion matrices for Airborne Thematic Mapper data: optimum three channels (%)

The confusion is confirmed by the discriminant analysis results (table 5.4). Thus, a two-band combination is not adequate to separate the selected vegetation types. Using discriminant analysis, the optimum spectral resolution for distinguishing between these moorland cover types appears to be a three channel combination; blue, red and near IR in May (91.02%; table 5.9a), and red, near IR and SWIR in July (92.23%; 5.9b). The four and five waveband analyses result in slightly higher accuracy, but the improvement is so small that it does not warrant the inclusion of further channels. The optimum temporal resolution is July, although there is not much difference between the two dates.

A near IR and SWIR combination was also suggested by the pairwise summary matrix for both of the TM data sets (section 5.5.3.2). At both dates the discrimination is good (figure 5.15), although it is slightly superior in April, when there is no confusion at all (figure 5.15a). In May, one of the mature Calluna vulgaris cases is closer to the degenerate cluster, which may be problematic, and the grassland and agriculture classes are close in the feature space (figure 5.15b). This is due to their similar characteristics at this time of year. The agricultural fields will have a high proportion of bare ground exposed among the young cereal plants, and the deciduous grassland will be of a similar nature, because the new growth has just begun to obscure the previous year's litter and bare ground.

The near IR/SWIR two-band combination (TM4 and TM5) is selected as optimum using discriminant analysis, in both April (99.48%) and May (98.5%) (table 5.7). The peak accuracy is when five bands are included, in May, but it is only 0.5% higher than the two-band combination. This small increase does not justify their selection as optimum, because of the greater expense of data and processing time involved in using five as opposed to two bands. However, it must be remembered that this analysis was completed using 'pure' training sets, and so when the more heterogeneous vegetation areas on a satellite scene are considered, more than two bands may be necessary to achieve consistently high separability.

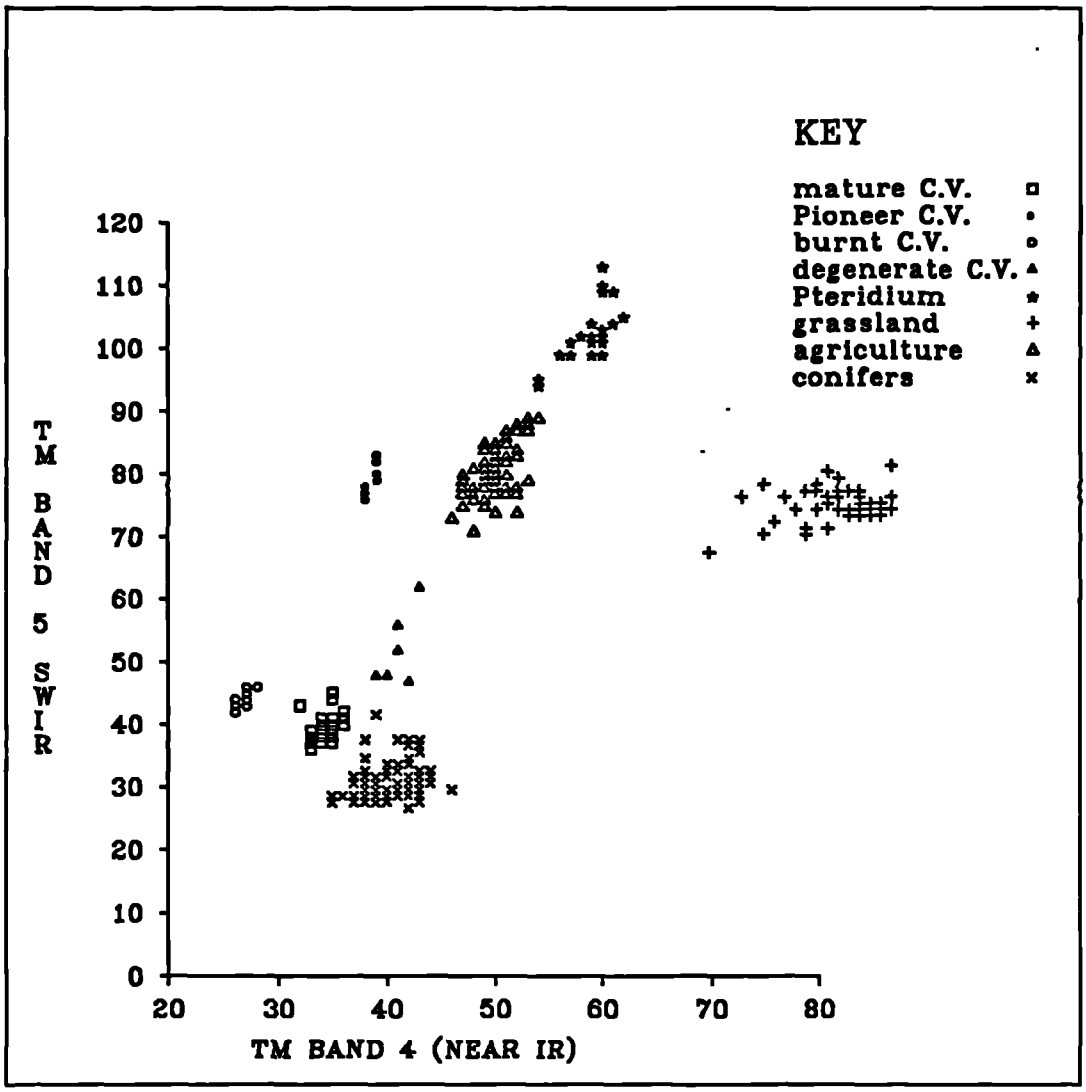

Figure 5.15a Scatter plot to show digital numbers for Landsat Thematic Mapper data: bands 4 and 5 (near and short wave infrared): April 1984

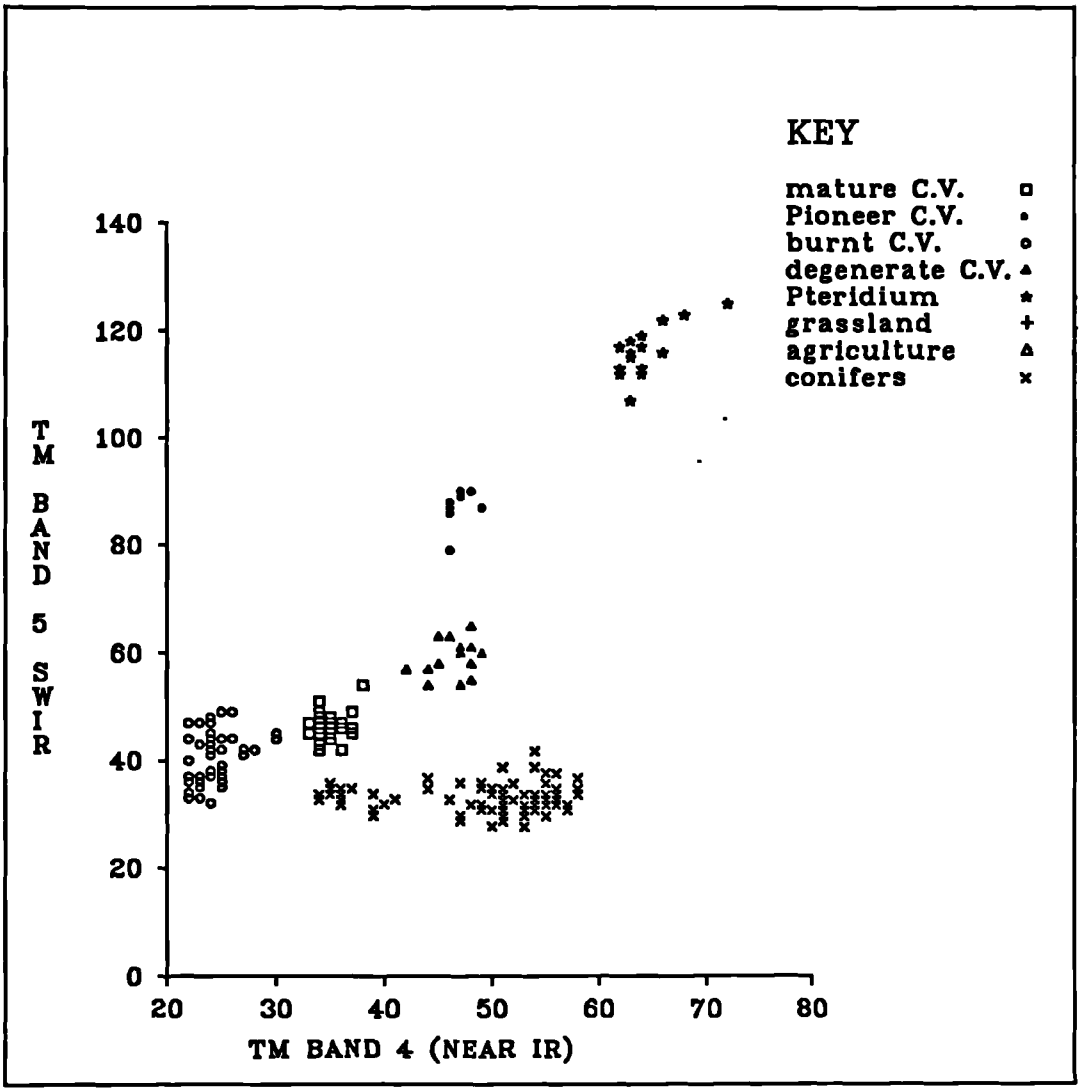

Figure 5.15b Scatter plot to show digital numbers for Landsat Thematic Mapper data: bands 4 and 5 (near and short wave infrared): May 1985

In every combination of bands, the TM discriminant analysis accuracies exceed 79%, being slightly higher in April than in May. This is perhaps not to be expected, but, as was explained above, it is probably due to the closeness of the two image dates, and because of the large number of Calluna vulgaris classes dominating the analysis.

5.6 Conclusion

The selection of an optimum spectral resolution in remote sensing is not a simple task. The spectral response pattern of a surface is complicated by many environmental, illumination and sensor parameters, which affect different surfaces in different ways. Nevertheless, careful analysis of the spectral characteristics of moorland cover types within the study area, and the separation between these surfaces, has enabled an assessment of the best spectral regions for the task, and the likelihood of success using selected waveband combinations.

It was concluded that it is not possible to discriminate between the Pteridium aquilinum growth and management stages with any degree of accuracy using field spectral data. Therefore, it is extremely unlikely that it will be possible on the lower spatial resolution satellite data. There is also considerable confusion between Calluna vulgaris growth and management stages, using airborne data, especially between mature and degenerate, and between pioneer and burnt, in May. Classification is more successful in the July ATM and the TM data, although there is still some intermingling of mature and degenerate Calluna in these data sets. The differences between the May ATM and the TM data may be due to the different atmospheric and environmental conditions, and to the finer spatial resolution of the ATM, which increases the heterogeneity within classes.

No single waveband was found to be optimum in all cases, although the near IR proved to be generally the most successful. There is no consistent optimum spectral resolution for all sensors and dates,

although the likelihood of success is high when only two channels are used in the field spectral and TM data analysis, and when only three ATM wavebands are used.

There is no consistent optimum temporal resolution for all sensors, although July and August are slightly more successful in the ATM and field spectral data respectively. April was found to be optimal in the TM data, although no data were available for later in the growing season, during flowering.

The accuracy values are extremely high in many cases, suggesting it would be possible to achieve a successful classification of air and satellite data using image processing techniques. However, it must be remembered that the analyses reported in this chapter were concerned with the investigation of a limited number of pure training sample classes. This is likely to inflate accuracy values beyond what might reasonably be expected in the classification of a whole scene, since on an image there are a greater variety of classes and transitional zones to add confusion to the procedure. Statistical analysis of transitional classes might give more realistic results, for example, the zone between Pteridium aquilinum and Calluna vulgaris. However, the delimitation of such classes is problematic, as the composition of the vegetation cover can vary dramatically over very short distances, and the heterogeneity within classes would be extremely great, causing large misclassification.

CHAPTER 6. SPATIAL RESOLUTION

6.1 Introduction

Having investigated the temporal and spectral dimensions involved in the remote sensing of moorland surfaces, the contribution of spatial resolution will now be considered. There is much controversy over the exact definition of spatial resolution in remote sensing, and how it should be measured (Townshend, 1980). There is also uncertainty as to the exact effect of the spatial resolving power of the sensor, in particular the pixel size, on the accuracy of results. It is expensive, time-consuming and unnecessary to use data that are more detailed than the level of interpretation demands. However, data that are too coarse to attain the required results are useless (Simonett, 1983). It is therefore imperative to select the optimum available spatial resolution for each application, which in practice is the most degraded resolution that will still adequately perform the task.

Pixel size often has a contradictory effect in different terrain conditions, as its influence is greatly contingent upon the characteristics of the ground surface (Short, 1982). Spatial resolution also has an enormous effect on the information which can be extracted from an image. A poor resolution can lower the separation between classes and restrict the level of aggregation which may be distinguished (Landgrebe, 1978; Simonett, 1983). In addition, linear features may become distorted or lost. Whichever method is used to define spatial resolution, it is of paramount importance to select the resolution appropriate to the particular purpose and environment, or "the resolution germane to the task" (Everett and Simonett, 1976).

The aim of this chapter is first to reach a suitable definition of spatial resolution, and then to assess its importance in one particular case study, using a degradation experiment to simulate resolution changes. The results obtained from the research reported

in this chapter have implications for the effect of pixel size in in remote sensing in general. However, it must be stressed that any results derived from the experiment are inherently scene-dependent.

6.2 Definition of spatial resolution

There is great controversy over the exact definition of spatial resolution within remote sensing (Townshend, 1980). The concept is often oversimplified and definitions are offered that tend to lack an intrinsic quantitative aspect (Short, 1982; Simonett, 1983). The most common explanation is that spatial resolution refers to the fineness of detail apparent in an image (Simonett, 1983), that is, it describes the minimum size of object that can be separately measured or distinguished from others on the data (Townshend, 1980). However, the notion of spatial resolution is far more complex, and four, less qualitative, categories on which to base a definition have been suggested by Forshaw et al (1980):

First, the geometric properties of the imaging system (the Instantaneous Field Of View, or IFOV); second, an ability to distinguish between ground targets (mainly measurements based on the Rayleigh Criterion, e.g. Slater, 1975); third, an ability to measure periodicity of repetitive targets (spatial frequency measures such as the Modulation Transfer Function (MTF), e.g. Steiner and Salerno, 1975); and finally, an ability to measure the spectral properties of targets (for example, the Effective Resolution Element (ERE) of Colvocoresses (1979)).

These alternative definitions often give widely different results for the same sensor (Townshend, 1980), as they are sensitive to different parameters. The selection of a "correct" one is closely related to the individual aims of each study, the characteristics of the surface terrain, and the type of analysis technique (Simonett, 1983). It is impossible to select a single measure of spatial resolution that is applicable to every case, even for the same image. Individual users are concerned with different image properties, and

the criteria for definition vary. For land cover classifications based on spectral separation, a definition accounting for the spectral characteristics of an image would be appropriate. However, a resolution based on the geometry of the optical system of the sensor is often the only available measurement, and so this is the most commonly used (Townshend, 1980). This is either the IFOV, or the Point Spread Function IFOV (PSF IFOV), as it is recognised that a proportion of the response is gained from outside the geometric IFOV, as the value is influenced by neighbouring areas (figure 6.1).

Any image is a representation of a real scene comprising a regular two-dimensional grid or array of picture elements or pixels. The ground area represented by the pixel is related to the effective resolution of the sensor, which is determined by the IFOV (Short, 1982). It is the pixel dimension that is normally regarded as the spatial resolution of the sensor, and in a comparative sense, this is satisfactory, as long as the limitations to its absolute validity are taken into consideration (Townshend, 1980). Some objects that are smaller than the pixel size may be apparent on the image, if the contrast with the surrounding background is sufficient (e.g. a bright road against dark vegetation), and some objects that are several pixels in size may not show up if the contrast is too poor (e.g. an unsurfaced road in a desert) (Simonett, 1983).

Thus the concept and nature of spatial resolution is extremely complex. In this research an "absolute" measure of resolution was not easily available and so a relative geometric resolution, based on the IFOV, or pixel size, of the sensor, was considered acceptable. This may not be the "true" spatial resolution of the data, but it is a suitable comparative label, which is readily available as a sensor parameter, and a tangible measurement on the image.

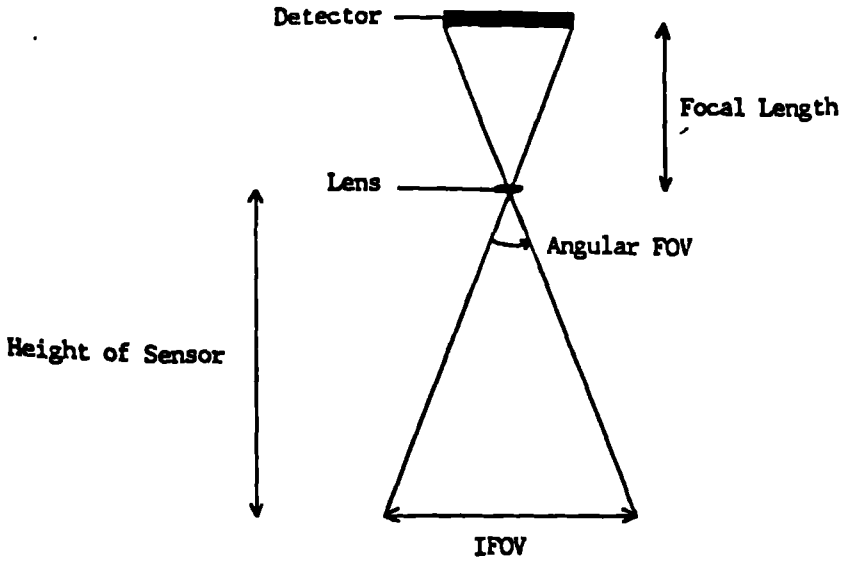

a) Geometric IFOV

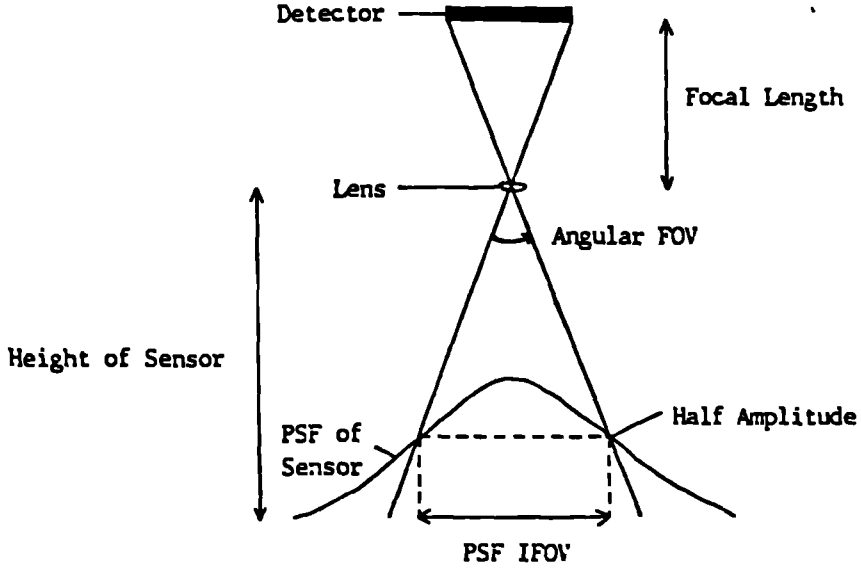

b) Point spread function IFOV

Figure 6.1 Diagrams to show the geometry of the instantaneous field of view (IFOV) of a sensor

6.3 Factors concerning the effect of spatial resolution

It is a common misconception that an increase in spatial resolution automatically brings a corresponding increase in accuracy (Townshend, 1980). The detailed relationship is far more complex than it at first appears. The overriding hypothesis of this chapter is that there is an optimum spatial resolution for monitoring moorland vegetation in Blakey Ridge, and that this resolution may be clearly identified. Encompassed within this general idea, there are more specific hypotheses, concerned with the relationship between mapping accuracies, the IFOV of the sensor and the spatial structure of the environment being imaged. Several authors have attributed changes in accuracy to the balance between two opposing factors; the spatial heterogeneity of a class, and the proportion of mixed or boundary pixels in a class (e.g. Townshend, 1980; Markham and Townshend, 1981; Short, 1982; Cushnie, 1984). Three major hypotheses concerning the expected consequences of the balance of this relationship at successively coarse spatial resolutions may be identified:

i. Fine resolution hypothesis : accuracy will be low

The small size of pixel will increase the internal variation within a class, as small-scale variations will be represented in different pixels, and will therefore be exaggerated. This will only be partially offset by the low proportion of mixed pixels, which lie across the boundary between two classes.

ii. Medium resolution hypothesis : accuracy will be high

The larger pixel size will tend to average-out small-scale variations, resulting in a greater homogeneity within classes. The proportion of boundary pixels will remain fairly low.

iii. Coarse resolution hypothesis : accuracy will be low

In this case the large pixel size will over-average the data, so that although classes are internally homogenous, between-class variation is also lowered, so they may no longer be satisfactorily separated. The resultant errors in classification are exacerbated by the large number of boundary pixels, which may be allocated to one of the two classes, or to a third completely erroneous class.

Thus mapping accuracy should theoretically rise from a low point at fine resolutions, increasing to a peak at medium resolutions, beyond which it will decrease once more as the pixel size becomes too large.

These hypotheses are synthesised from the work of several authors, including Townshend (1980), Short (1982), Cushnie (1984), and Woodcock and Strahler (1987).

The precise dimensions of the optimum pixel size is scene-dependent and is greatly reliant on the spatial structure of the environment, and the level of aggregation of the information to be extracted. If within-class variation is very low, a fine resolution may be optimum. Alternatively, the classification of a scene with heterogeneous classes may be more successful at very coarse resolutions. The size of the objects of interest within a scene (in this case areas of similar vegetation type, and individual plants) will greatly affect accuracy. Woodcock and Strahler (1987) have modelled the affect of spatial structure on accuracy in a forest environment, and conclude that a pixel size slightly smaller than the size of the object (a tree crown) is optimum. But again, this is contingent upon the degree of class homogeneity.

In a complex moorland environment, with quite considerable heterogeneity in selected classes (section 6.6.4.5), it may be hypothesised that the spatial resolution would have to be fairly fine, in order to map the detailed surface reliably. However, the spatial resolution needed for a task is closely related to the

fineness of detail which is required, and the degree of error that is acceptable, in the finished product. The National Park Committee published vegetation maps are of a less detailed nature than the field maps used in this study. The Committee's requirements are to represent generalised areas of species or vegetation associations, ignoring small-scale variations or anomalies. Thus, a coarser resolution may be quite adequate for this task (section 6.6).

Thus, the identification of the optimum resolution is not an easy matter, and is dependent upon the complex interactions between several terrain and sensor parameters. It is the intention of this chapter to assess these parameters within the Blakey Ridge area, and to identify the dominant contributory factors affecting changes in accuracy caused by alterations in resolution, and subsequently to determine the optimum pixel size for moorland mapping.

6.4 Degradation experiment

6.4.1 Methodology

A degradation experiment was performed on a 512 x 512 subscene of ATM data covering part of Blakey Ridge (figure 3.4). Data from both dates were considered for the experiment, and the July data set was chosen as it appeared to offer more visual information than the May data. In addition, the late summer date was selected as the optimum temporal resolution in chapter 4 (section 4.5.6), and this was later confirmed by discriminant analysis, which identified the optimum ATM spectral resolution as a three-band combination in July (92.23% accuracy) (section 5.5.3.3; table 5.9b).

A single ATM scene was degraded in order to keep all the other parameters constant. The use of data from different sensors, collected at different times or heights, to judge the effects of a change in pixel size, is complicated by the contribution of other independent parameters, which may distort the signal. These include the the number and exact placement of spectral bands, signal-to-noise

ratios, and the interference of the atmosphere, and therefore make direct comparison difficult (Sadowski et al, 1976).

The exact degradation and replication methodology is outlined in chapter three (section 3.6.5.4), and the resultant five images were of 2.5m, 5m, 10m, 20m and 30m pixel size. As well as evaluating the effect of spatial resolution upon the accuracy of class separation, its influence on boundary location and characteristics was also examined. Most previous degradation studies have considered the changes in class separation, but few have looked specifically at the effect on the location and nature of boundaries between the classes. This is an extremely important factor in the present research, for it is the location of boundaries and transitional zones between the moorland and the invading bracken which is a major concern.

The first step in the analysis was the visual interpretation of the data using the I^2S image processor. The best three spectral channels were displayed as scaled false colour composites. The channels were ATM5 (red), ATM7 (near IR) and ATM9 (SWIR) (table 3.3). Their selection was based on visual and statistical criteria; the three channels appeared to give more visual information than any other three-band composite, and they were also the channels selected as the optimum ATM spectral resolution using discriminant analysis (section 5.5.3.3; table 5.9b).

The second step was the analysis of photographic prints of the false colour composites, taken from the screen of the I^2S. These prints have been enlarged to facilitate interpretation (plates 6.1 to 6.5). The field map showing the area covered by the ATM degradation subscene has also been enlarged so that it is the same scale as the photographs (figure 6.2). A visual comparison between the images of different resolutions and the field vegetation map was made, in order to evaluate the effect of different scales on the ability to map the surface cover types. At each resolution, the distinction between vegetation species, the size and shape of areal blocks, and the representation of linear features, were considered. In addition, one

vegetation class was chosen for detailed analysis, and maps of the boundaries were drawn from each of the five images. There is bound to be some subjectivity in the interpretation of false colour composite images, as there are no fixed boundaries, and numerous tones and colours. Nevertheless, in order to reduce bias, the 30m image was analysed first, followed by successively finer resolutions. This ensured that information not clearly discernible in the coarser images, but apparent on the most detailed resolutions, was not mistakenly attributed to the coarse images. Pteridium aquilinum was selected because of its importance to the research, and both a "pure" and a mixed category were represented (figures 6.3 to 6.7). The mixed category consisted of Pteridium, together with Calluna vulgaris and Vaccinium myrtillus. The resultant class maps were overlaid on a Pteridium aquilinum boundary map extracted from the field map (figure 6.8).

The accuracy of the Pteridium class map, compared to the field data reference map, was calculated at each resolution. A systematic grid of sample points was used in order to give even and comprehensive coverage of the full extent of the class. This grid had a 40m cell size and it was overlaid on the field map. All intersection points which occurred within the Pteridium area were recorded (98 sample points). In addition, all those within the mixed Pteridium category were marked (52 points). The grid was then placed over each of the image maps, and the number of original Pteridium sample points still falling within the Pteridium boundary were counted. The accuracy of each image (for Pteridium) was then calculated; the number of correct observations as a percentage of the total number of Pteridium points (150). However, stating one value as an accuracy gives an overestimate of the precision of the measure. It is extremely unlikely that any one sample, however unbiased or large, will yield an accuracy value precisely corresponding to the total population accuracy (Congalton et al, 1983; Hay, 1979). A sampling distribution may be used to estimate the limits of the accuracy value at a given confidence level. In the case of a sample count, when an observation is recorded as correct or incorrect, the binomial distribution is

used to establish the limits (Hord and Brooner, 1976; Hammond and McCullagh, 1978; Van Genderen et al, 1978). The binomial standard error was first calculated using the following formula (equation 6.1);

Equation 6.1 The binomial standard error of the mean accuracy value

$$S.E._x = \Theta / \sqrt{n}$$

where; $S.E._x$ = standard error of the mean accuracy value
Θ = standard deviation of the population
n = number of cases

(after Hammond and McCullagh, 1978)

The accuracy limits were then calculated using the 'z-score' for the 95% confidence level. This is the probability, at selected confidence levels, associated with a normal distribution, which may be read from a table (equation 6.2).

Equation 6.2 Binomial confidence limits

$$\text{limit} = \bar{x} \pm (z \times S.E.)$$

where; $\bar{x}$ = mean accuracy value
z = z-score at 95% confidence level
S.E. = standard error of the mean accuracy value

(after Hammond and McCullagh, 1978)

This Pteridium aquilinum example enables the amount of information available about an individual vegetation type at each resolution, to be represented clearly and graphically, so that the accuracy of data at each pixel size can be more easily evaluated, enabling the optimum spatial resolution to be determined.

One block of Pteridium aquilinum and mixed Pteridium was selected in the south east of the subscene area for detailed analysis. The area covered by the species was calculated, and the boundaries from each resolution were enlarged and drawn on individual maps. These are overlaid by the equivalent field boundaries for comparison (shown in a dashed line) (figures 6.12, 6.13 and 6.15 to 6.17), in order to assess the effect of spatial resolution on boundary location and characteristics.

The final part of the analysis was the unsupervised classification of the five subscenes, to ascertain the effect of spatial resolution on automatic classification accuracy. An unsupervised cluster technique was chosen in order to test whether the proposed vegetation classes are in fact discriminable spectral classes on the images, and whether they are pure or mixed in nature (Mather, 1987). It was also chosen to avoid the problems and bias associated with the delimiting of training areas, required for supervised classification, especially with mixed categories.

The I^2S 'cluster' command was used on each of the five three-band composite images. This algorithm first makes an arbitrary estimate of cluster 'seed' location, based on the number of classes. It then divides up the feature space according to the variance of each band. Pixels are then repositioned between classes iteratively, using a minimum distance function, by means of a classification, evaluation and modification sequence. This is repeated until they are optimally located in a class, and a stable classification emerges (I^2S Inc., 1987; Lillesand and Kiefer, 1979).

The cluster analysis simply provides for the extraction of discrete spectral groups, and it is left to the analyst to identify 'information classes' (cover types) existing on the ground which correspond to the spectral classes (Mather, 1976 and 1987; Lillesand and Kiefer, 1979).

The cluster maps were investigated in detail on the I^2S screen and labels were allocated to the classes, with reference to the field map. Not all the cover types recorded in the field were represented in the classification, and some were combined, for example, the bare and burnt classes were merged by the algorithm. Nevertheless, most spectral classes could be relatively easily associated with a cover class.

The accuracy of the resultant cluster images at each resolution (plates 6.6 to 6.10) was calculated using the same method as for the Pteridium aquilinum class maps taken from the false colour composite images (see above). In this case a stratified random sample technique was used to obtain the accuracy check points, in order to locate sufficient sample points within classes with small areal extent. Random numbers were used as co-ordinates to identify pixels. The number of sample points required to test the accuracy of an image has been questioned by several recent authors (e.g. Van Genderen et al, 1978; Hay, 1979; Curran and Williamson, 1985), although their conclusions differ. Hay (1979) suggests a minimum of 50 per class, while Van Genderen et al state that 30 is sufficient. In this study, it was not possible to achieve large sample sizes for every class, due to the size of the subscene and the small areal coverage of some vegetation types. However, no class has a sample size of less than 24, and most are over 30 (table 6.3).

6.4.2 Error and accuracy

Having compared the field map with the images, and prepared the Pteridium aquilinum class maps, it became apparent that there were

quite major differences between the images and the field map. There are three possible sources of such errors;

a) Data acquisition errors

ATM data are collected from an unstable aircraft platform, subject to unpredictable and sudden small-scale variations in pitch, yaw and roll (Fuller et al, 1988; section 3.6.2 above). Such distortions cannot easily be corrected for by the scanner electronics, but may be considerably reduced by computer warping procedures. A standard geometric correction algorithm was used to correct the data to the National Grid, but the root mean square (RMS) error was 13.22 pixels (section 3.6.5.3). This RMS error is very large, and means there are likely to be large differences between the image and the National Grid base. This was found to be the case, and significant distortions are apparent in the ATM images (section 6.4.5).

b) Misregistration in time

The ATM data were collected in July 1986 and the field mapping of this area was completed in August 1987. Changes between the two years are fairly small on the flat moorland surface, as there is no evidence of a fresh burn within the subscene area, and differences are likely to be a matter of percentage cover, especially in burnt or pioneer Calluna vulgaris. However, there is the possibility of small changes in the location of boundaries between the Pteridium front and the Calluna stands (section 6.4.5). There is also evidence of change in the agricultural fields, especially the bottom, almost triangular, field, half of which appears to be completely bare soil in the ATM data (plate 6.1; figure 6.2).

c) Errors in the absolute accuracy of the reference standard

In the analysis, the field map is taken as "ground truth", being treated as a 100% accurate representation of what is on the ground. However, in most cases there are errors inherent in reference data. Ground observations are subject to instrument malfunction, personnel inaccuracies, ground location errors, misregistration in time (see above), and inadequate sampling design (Justice and Townshend, 1981).

Errors in the ground data used for calibration and accuracy testing have been noted by many authors (e.g. Justice and Townshend, 1981; Curran and Williamson, 1985), and have caused Smedes (1975) to state;

"generally for those classes that can be distinguished from one another by..... remote sensing attributes, the remote sensing map is more accurate than the ground truth map."

Errors in the field map used in this research are quite possible, as there was considerable difficulty in precisely locating the exact position of a diffuse transitional boundary in the field. Thus, although the methodology sought to minimise error, with the use of aerial photographs (section 3.3.3), it is unlikely that the resultant field map is a 100% correct representation of ground conditions (section 6.4.5).

6.4.3 The effect of spatial resolution on class separability and map accuracy

6.4.3.1 Visual interpretation of false colour composite photographic prints

a) 2.5m data (plate 6.1)

The visual separation of vegetation cover types is generally excellent using the 2.5m data. The most striking feature is the clarity and distinctiveness of the burnt category (dark purple). The transition from burnt to pioneer Calluna vulgaris is demonstrated by a lightening of tone and a more mottled appearance representing the patchy recolonisation of Calluna, and the presence of bare soil, grasses and mosses. The bare areas are also clearly identifiable (bright pink), and correspond closely to the field map (figure 6.2).

The Pteridium aquilinum is depicted in light blue/light green, even tones. The general homogeneity is a result of the complete cover of fronds reducing small-scale variations in reflectance.

Mature Calluna
Pioneer Calluna
Burnt Calluna
Degenerate Calluna
Pteridium
Pteridium mix
Grass mix
Wetland
Grassland
Agriculture
Woodland
Bare soil
Road
Footpath
Field boundary
Cliff

0 200
Metres

N

Figure 6.2 Enlarged section of the field map, to show the area covered by the Airborne Thematic Mapper data degradation subscene

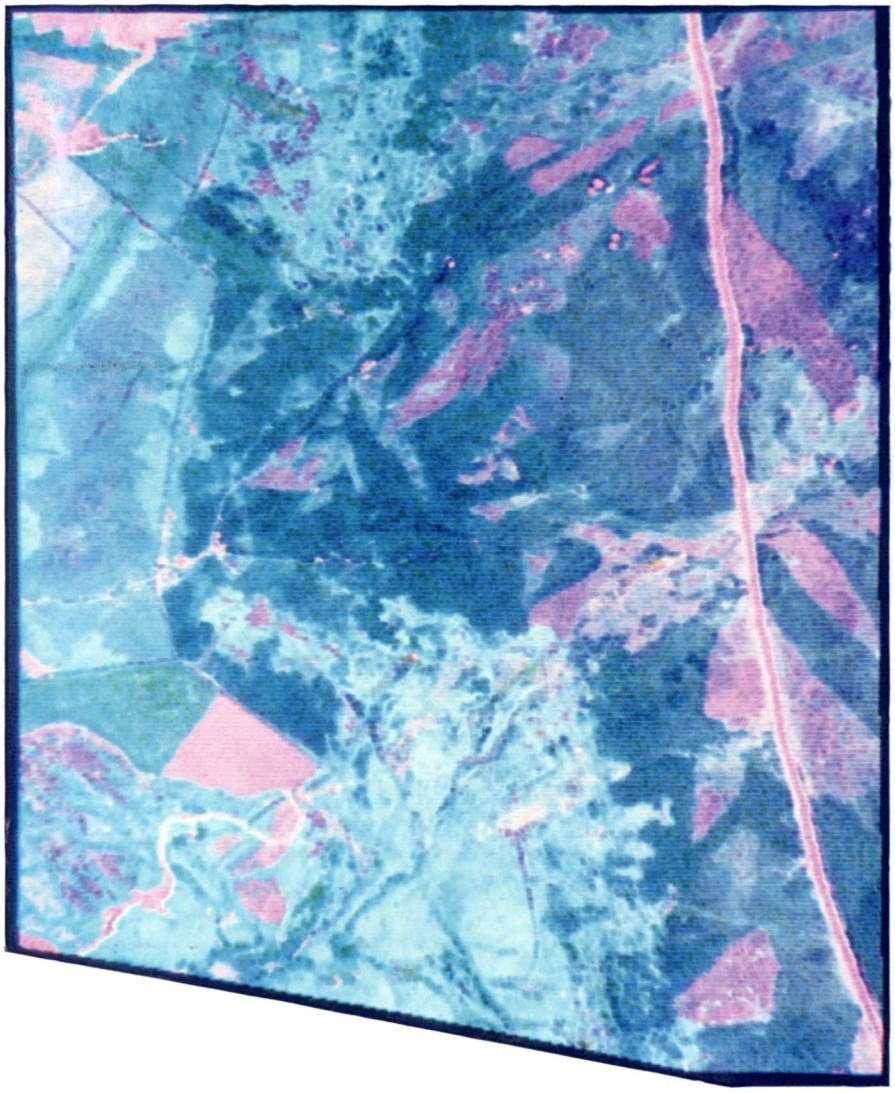

Plate 6.1 False colour composite of ATM subscene showing part of Blakey Ridge, July 1986: channels ATM5, ATM7 and ATM9: 2.5m data

The mixed vegetation classes are shown in predictably mottled tones; green/yellow/pink for grass mix, and light blue/light green/dark blue for the Pteridium mix. This reflects the rapid change from domination by one vegetation type, to domination by another. The mature Calluna is also slightly mottled, being predominantly dark purple/blue, with some dark green pixels. These differences probably represent contrasts within the Calluna canopy; the woody central parts, the green leaves, and the bare ground between bushes.

The degenerate Calluna is hard to separate from the mature, although it has a more pink tinge in some areas, probably due to the higher red reflectance from the greater proportion of bare ground between and within plants.

The grassland class is shown in mottled purple tones, caused by the small-scale variations in the dry, rough grasses. The wetland vegetation appears as two distinct tones on the image. The area in the centre near the road could easily be confused with the grassland, since grasses are the main component of the vegetation in that area. The more sinuous wetland vegetation within the southern Pteridium area is dark green. This area has a higher moisture content (dominated by Sphagnum), causing higher absorption of light resulting in darker tones.

The agriculture also has more than one distinct tone on the image; the bright pink tone, in a triangular field, represents bare soil, the green tone represents the high IR reflectance associated with vigorous crop growth, and the pink/green tone, in the northern fields, represents fairly rough, brown grazing land.

The boundaries are generally sharp, especially the edges of burnt and pioneer Calluna vulgaris areas, and the mature Calluna/Pteridium mix border. The transition between the Pteridium and the Pteridium mix is less clear, as in reality, with a gradual change in domination from one species to another.

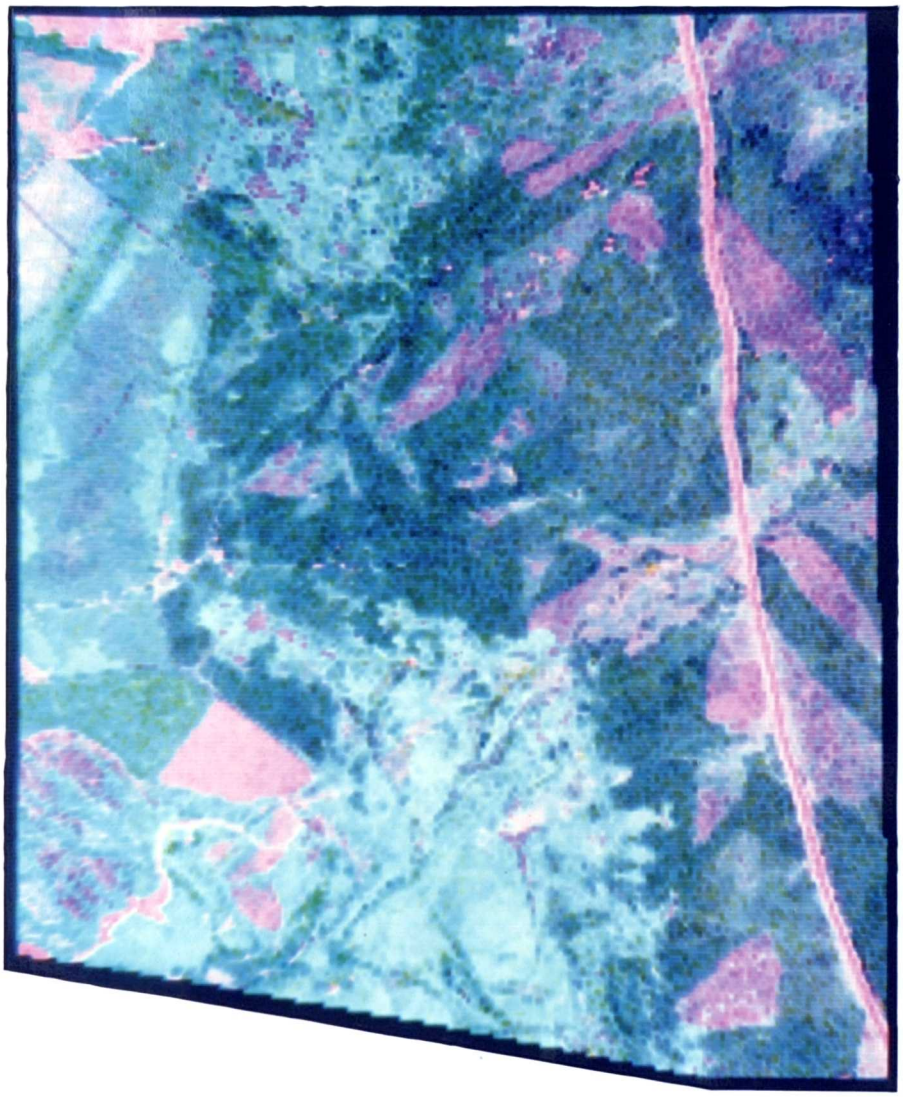

Plate 6.2 False colour composite of ATM subscene showing part of Blakey Ridge, July 1986: channels ATM5, ATM7 and ATM9: 5m data

Linear features are clear and uninterrupted, for example, the field boundaries and footpaths, which show up as dark lines. The road is very sharp and has a dark pink central area representing the bare road surface, and lighter pink strips down both edges, which are the grass banks at the sides of the road, which although only a few metres wide are clearly shown.

b) 5m data (plate 6.2)

The visual separation of vegetation cover types is generally very good, and is similar to that on the 2.5m image, with very little apparent loss of information. The most obvious difference is the slightly stepped nature of diagonal linear features, especially the road, the edges of burnt areas, and the field boundaries. However, this spatial resolution is still capable of showing grass banks at the sides of the road.

Small-scale differences in the mixed classes and Calluna vulgaris are not averaged-out at this resolution, and they are still represented by mottled tones. The boundaries are still clear, although some blurring is evident along the Pteridium mix/Calluna boundary, which suggests the increased influence of boundary pixels on this transitional limit. The shapes and sizes of vegetation blocks are still accurately represented.

c) 10m data (plate 6.3)

This image is more blocky in nature, with individual pixels evident in many areas. Class separation is still good, although linear features are less well represented. The road has become step-like and is only two pixels wide, losing one or both of the road-side grassed strips. Nevertheless, the road is still continuous. The field boundaries have virtually disappeared. The fences, walls and hedges are so narrow that they have been averaged into the neighbouring classes as they represent only a small proportion of the total light from the 10m pixel area.

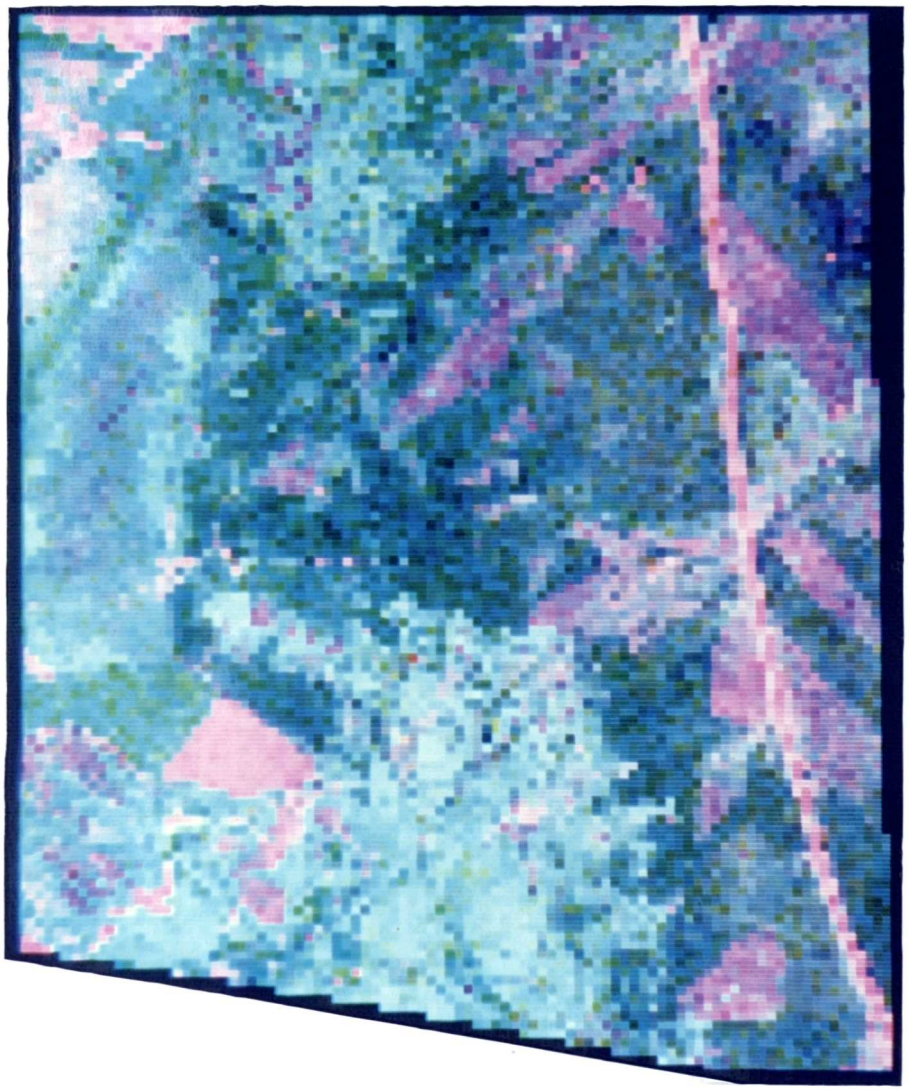

Plate 6.3 False colour composite of ATM subscene showing part of Blakey Ridge, July 1986: channels ATM5, ATM7 and ATM9: 10m data

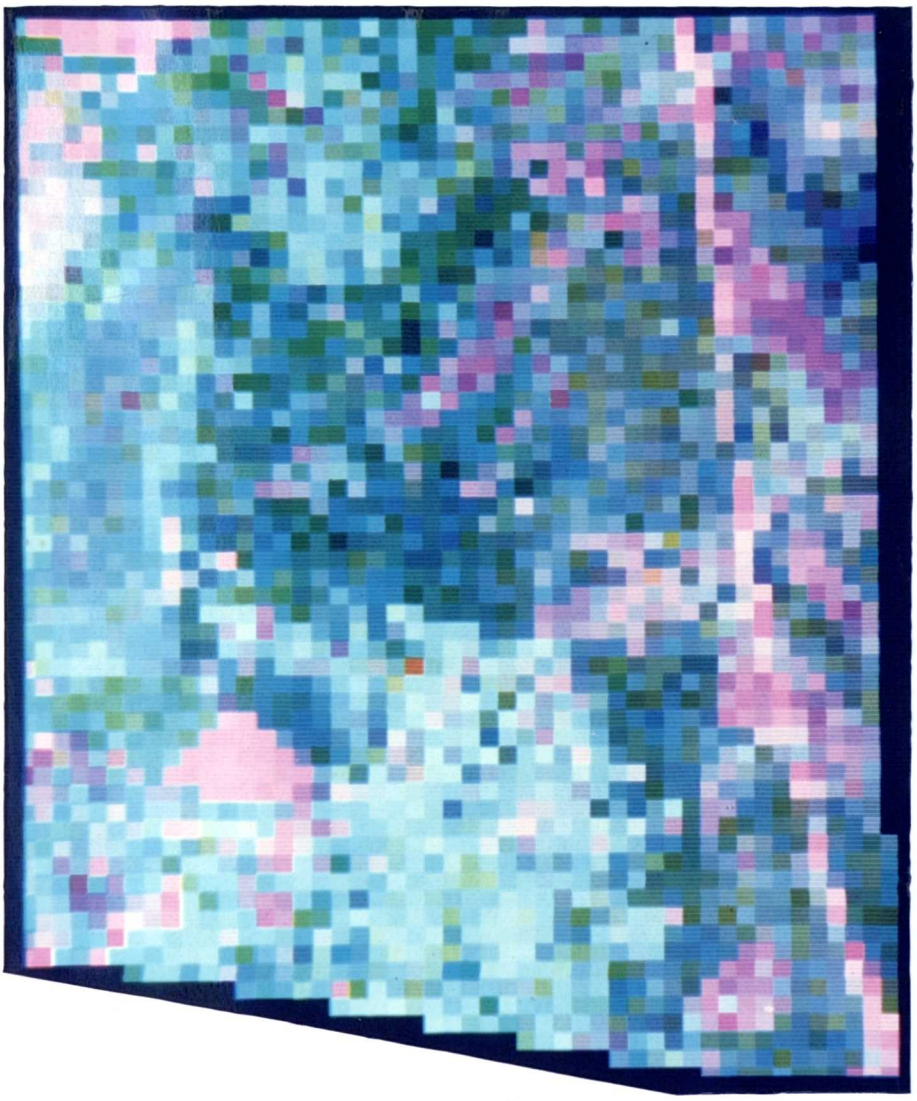

Plate 6.4 False colour composite of ATM subscene showing part of Blakey Ridge, July 1986: channels ATM5, ATM7 and ATM9: 20m data

The sinuous bare feature in the south west of the image has also been partially lost. However, the finger-like extensions of the grassland nearby have remained intact. These are slightly larger than 10m in width and have a great contrast with the background Pteridium. The mixed areas appear to have a fairly homogenous light blue/green background tone, with small areas of contrasting dark tones. The homogeneity is due to the averaging-out of small-scale variations within the larger pixel size, and the darker areas are probably localised damp areas, or dominance by Calluna over a 20m to 30m area.

The shape and size of vegetation blocks are not considerably effected by the degradation, and the general information loss in non-linear features is minimal.

d) 20m data (plate 6.4)

At first sight there is a large degradation in the information apparent on the 20m image. Vegetation classes are still identified by similar distinct tones as on the 10m data, but the shape of blocks have been altered by the step-like nature of the edges. This is especially apparent on the large burnt area in the north east of the image, and the triangular bare field in the south west. The field boundaries have been completely lost, and the fields tend to blend into the moorland vegetation, indicating the strong influence of boundary mixed pixels. The road has been narrowed to one pixel of varying pink/purple tones, but it is still virtually complete. General areas of similar vegetation may be identified, but boundaries are blurred and blocks are misshapen. Some small and narrow features have been lost, for example, the finger-like grassland area in the south west, and the previously clear strips of burnt Calluna in the north east, on both sides of the road.

The large Pteridium area in the south centre of the image is less clear, as mixed boundary pixels on the border between the Pteridium and the wetland, bare and grassland areas, have caused blurring and confusion.

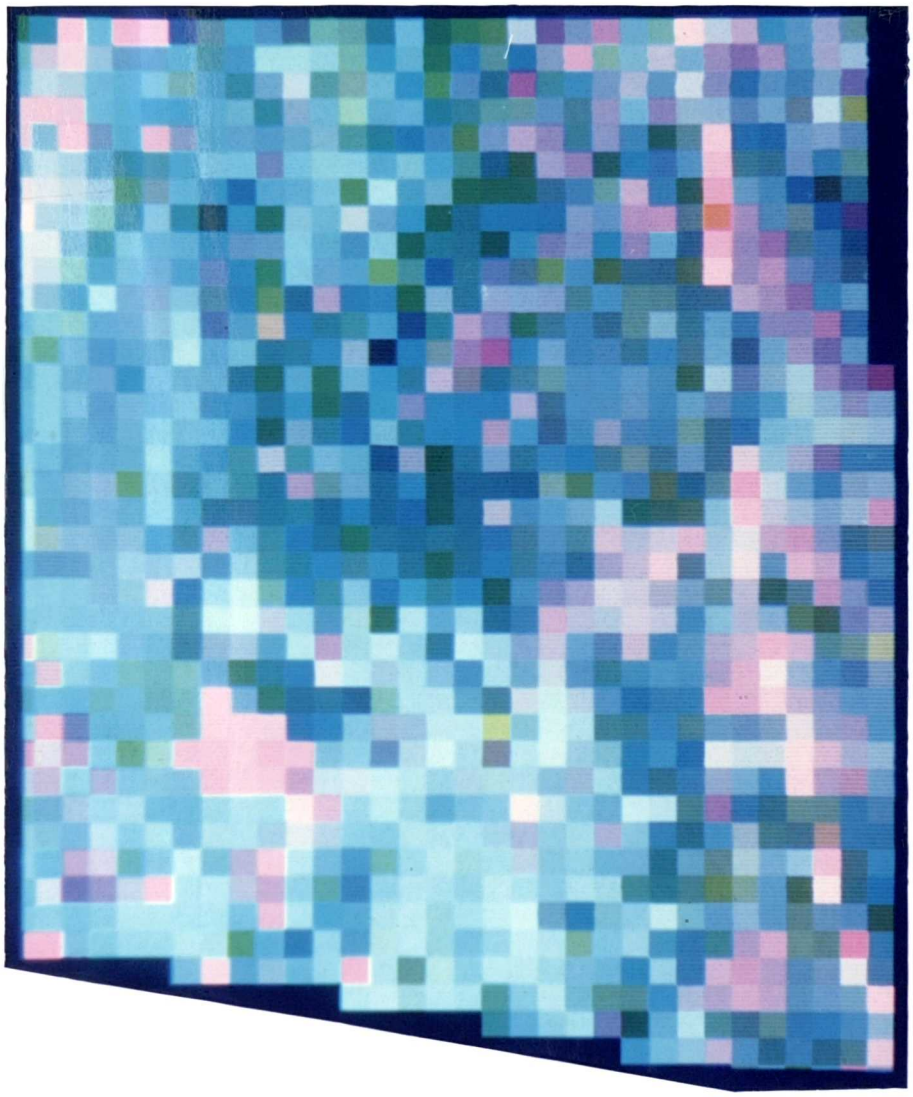

Plate 6.5 False colour composite of ATM subscene showing part of Blakey Ridge, July 1986: channels ATM5, ATM7 and ATM9: 30m data

However, the mixed areas are more homogeneous, as is the Calluna area, as the differences in canopy form and the proportions of bare ground and wooden stems are generally averaged-out at the 20m pixel size.

e) 30m data (plate 6.5)

On the 30m data, within-class heterogeneity has been reduced so that there are large continuous blocks of similar tones. However, the between-class contrast has also been reduced, especially between burnt and bare, burnt and pioneer Calluna, and Pteridium and agriculture. Nevertheless, the vegetation blocks are still quite clear, although the boundaries are very step-like and small areas are highly distorted. Linear features have virtually disappeared, since they are all considerably narrower than 30m. The road is still partially evident, but very discontinuous. The sharp boundaries of the burnt and bare areas remain, but many other parts of the image show considerable confusion as a result of mixed boundary pixels.

6.4.3.2 Quantitative interpretation of false colour composite photographic prints

The accuracy values (relating only to the Pteridium aquilinum areas shown in figures 6.3 to 6.8) closely reflect the results of the visual interpretation (section 6.4.3.1). The overall accuracy is high for the 2.5m, 5m and 10m data, reaching a peak of 76.65% ($\pm$6%) at the 95% confidence level, for the 5m and 10m images (table 6.1; figure 6.9). The difference in accuracy between the three finest resolutions is not significant, considering the size of the error limits. The accuracy then falls quite dramatically, by over 16%, to 60% ($\pm$8%) for the 20m data, and 50% ($\pm$8%) for the 30m data.

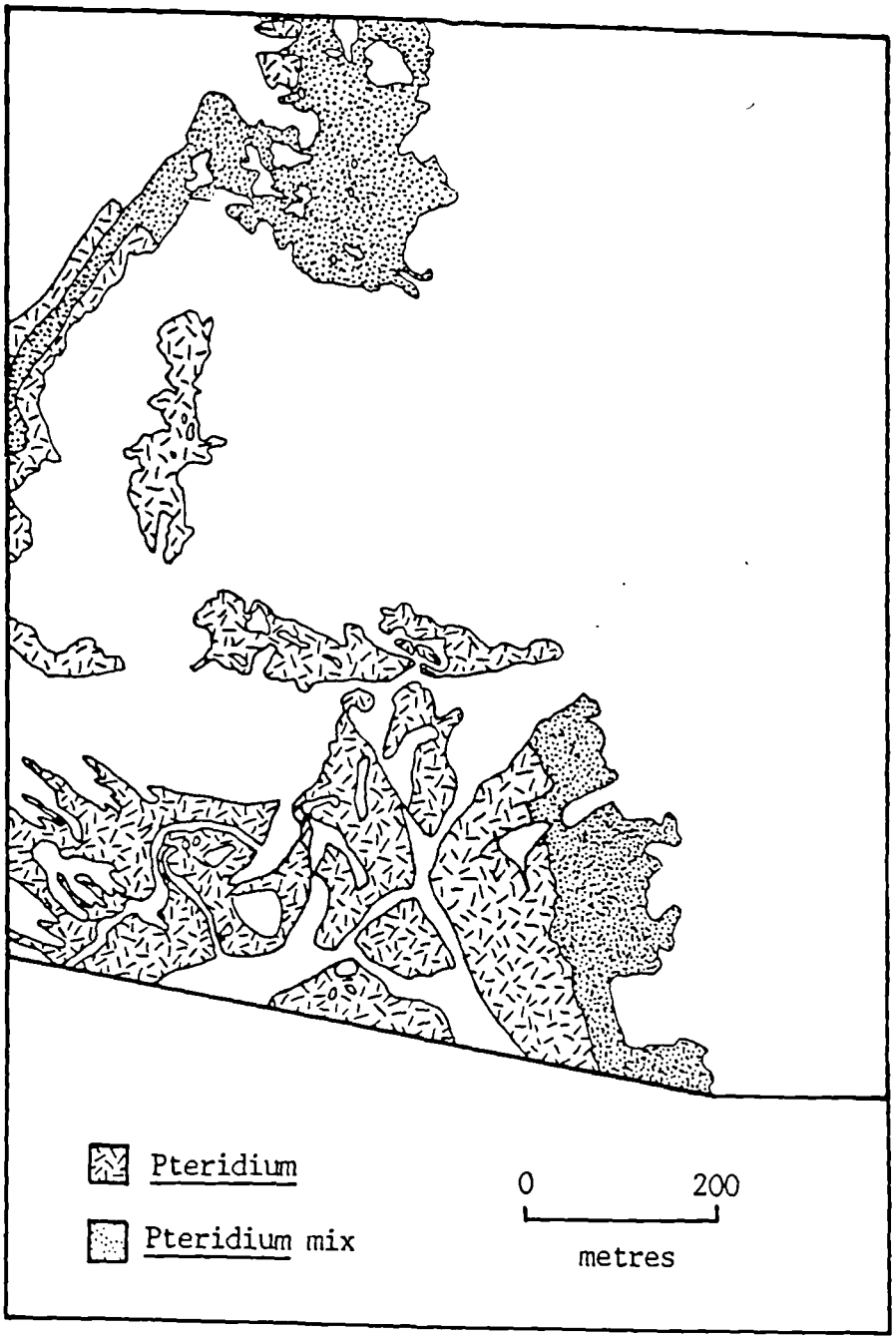

Figure 6.3 Pteridium aquilinum class map: Airborne Thematic Mapper 2.5m data

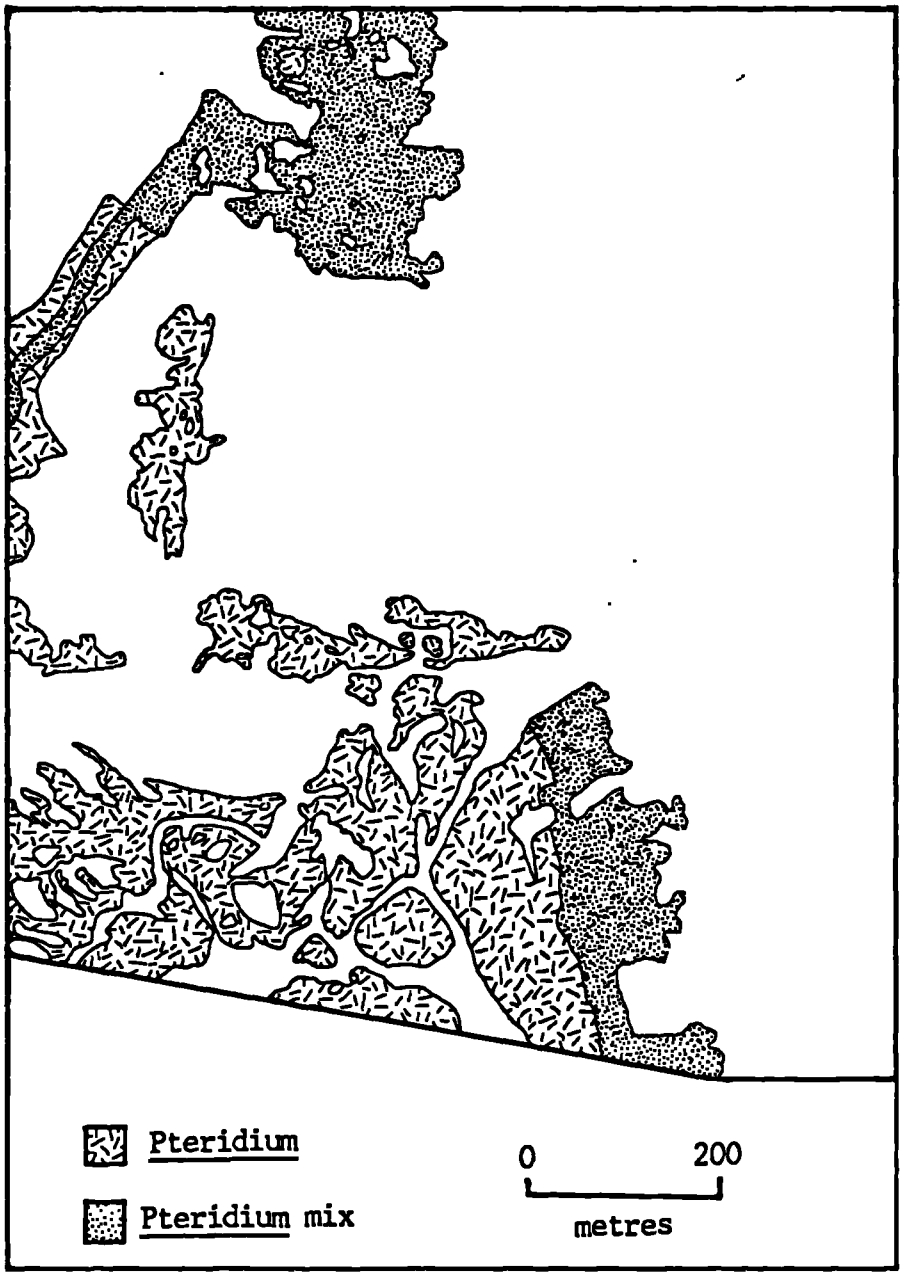

Figure 6.4 Pteridium aquilinum class map: Airborne Thematic Mapper 5m data

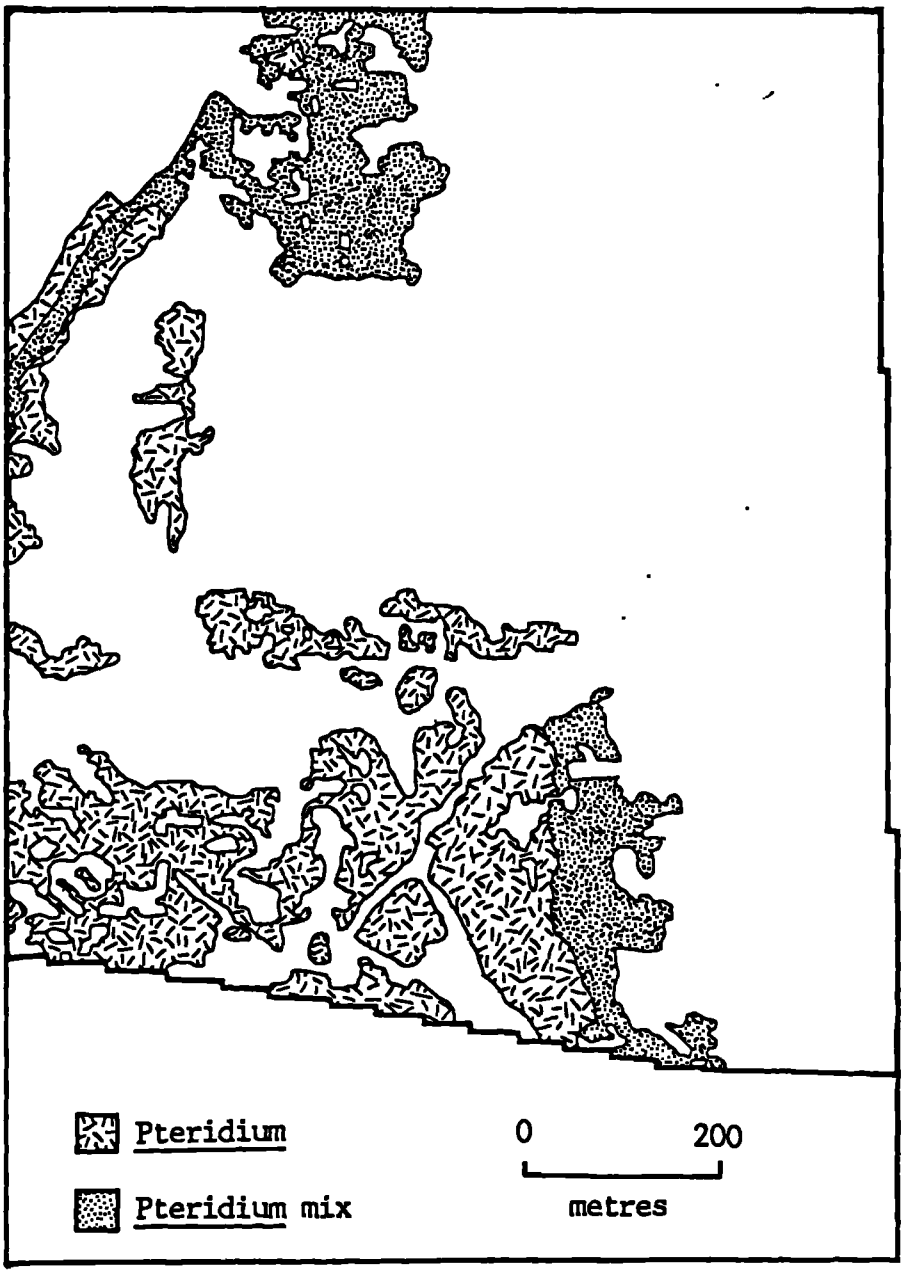

Figure 6.5 Pteridium aquilinum class map: Airborne Thematic Mapper 10m data

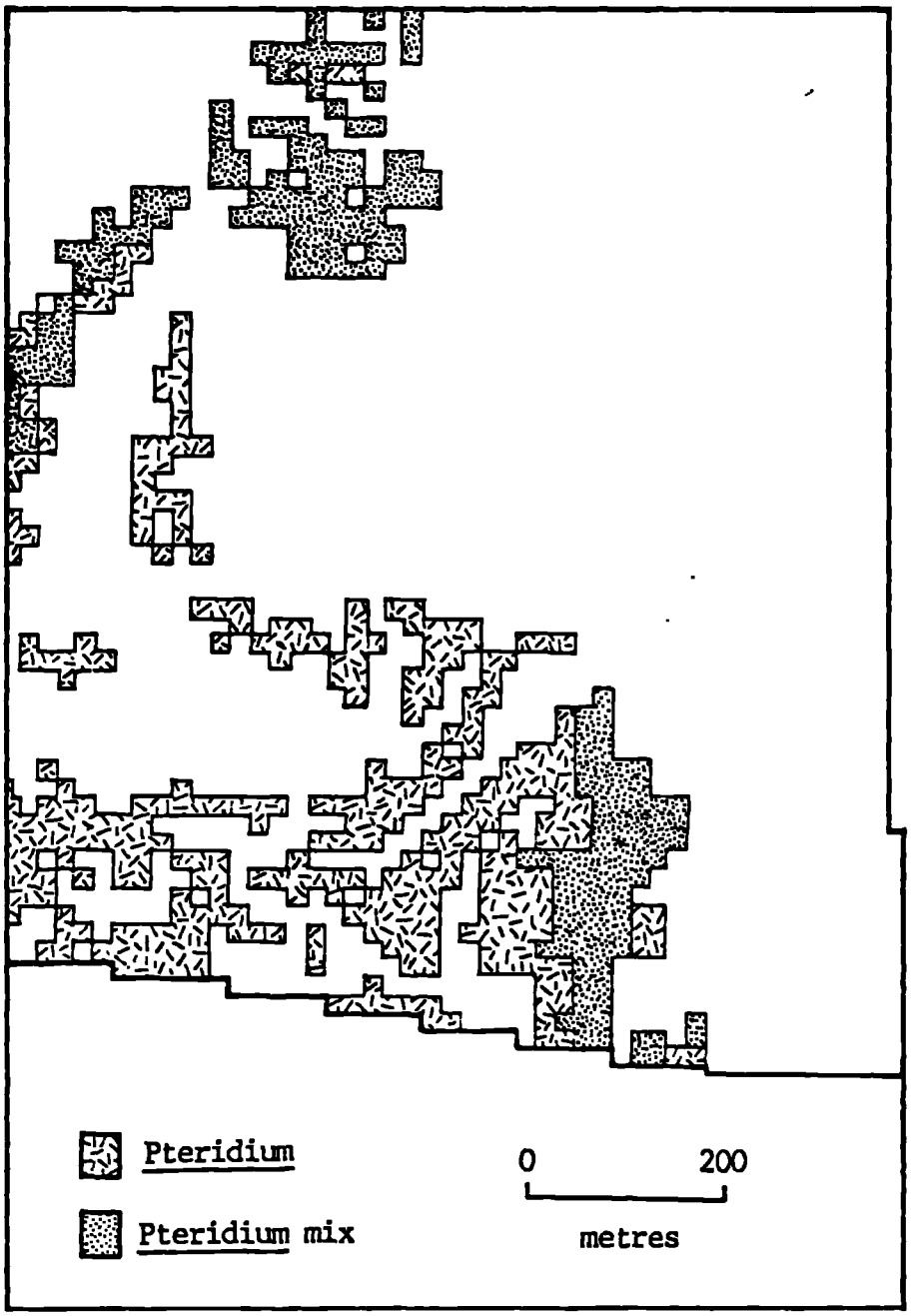

Figure 6.6 Pteridium aquilinum class map: Airborne Thematic Mapper 20m data

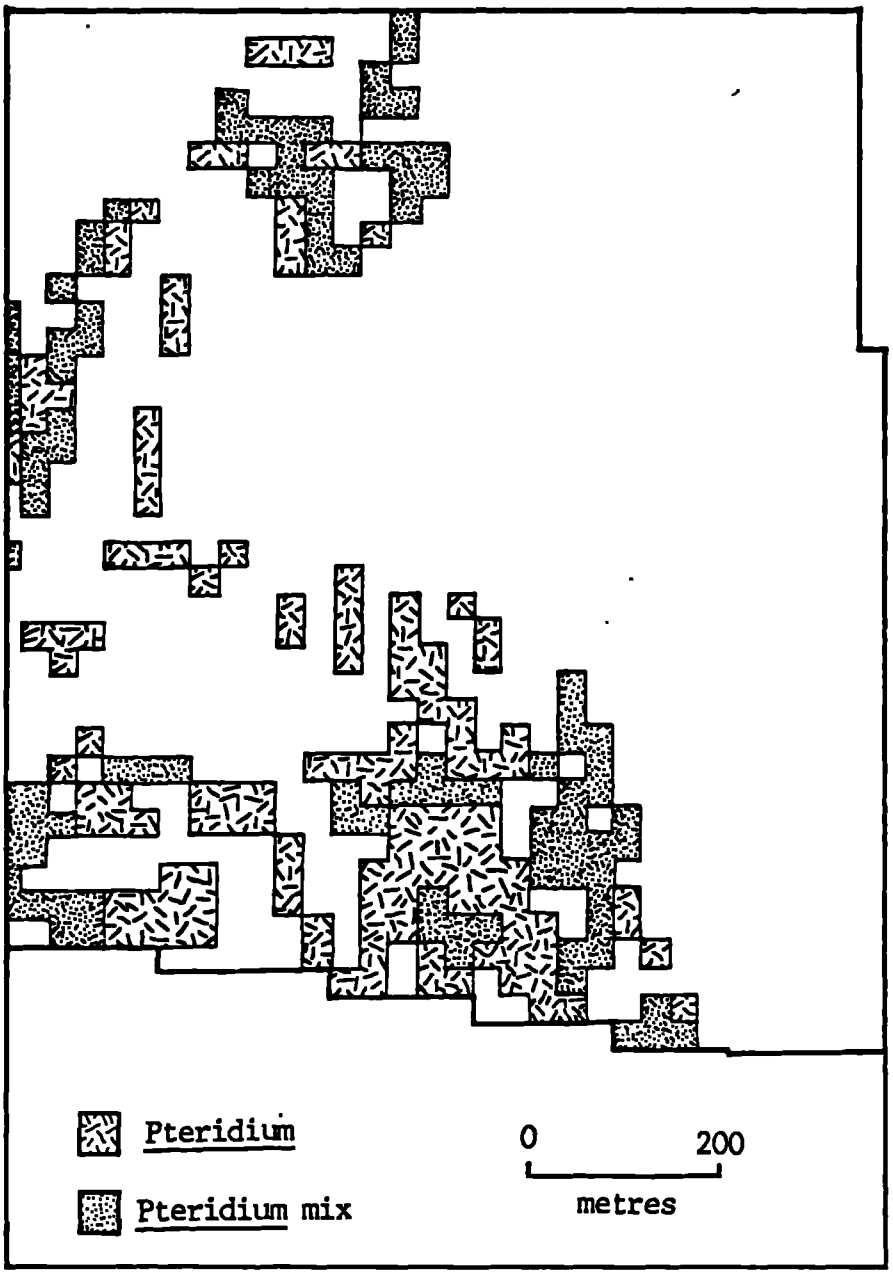

Figure 6.7 Pteridium aquilinum class map: Airborne Thematic Mapper 30m data

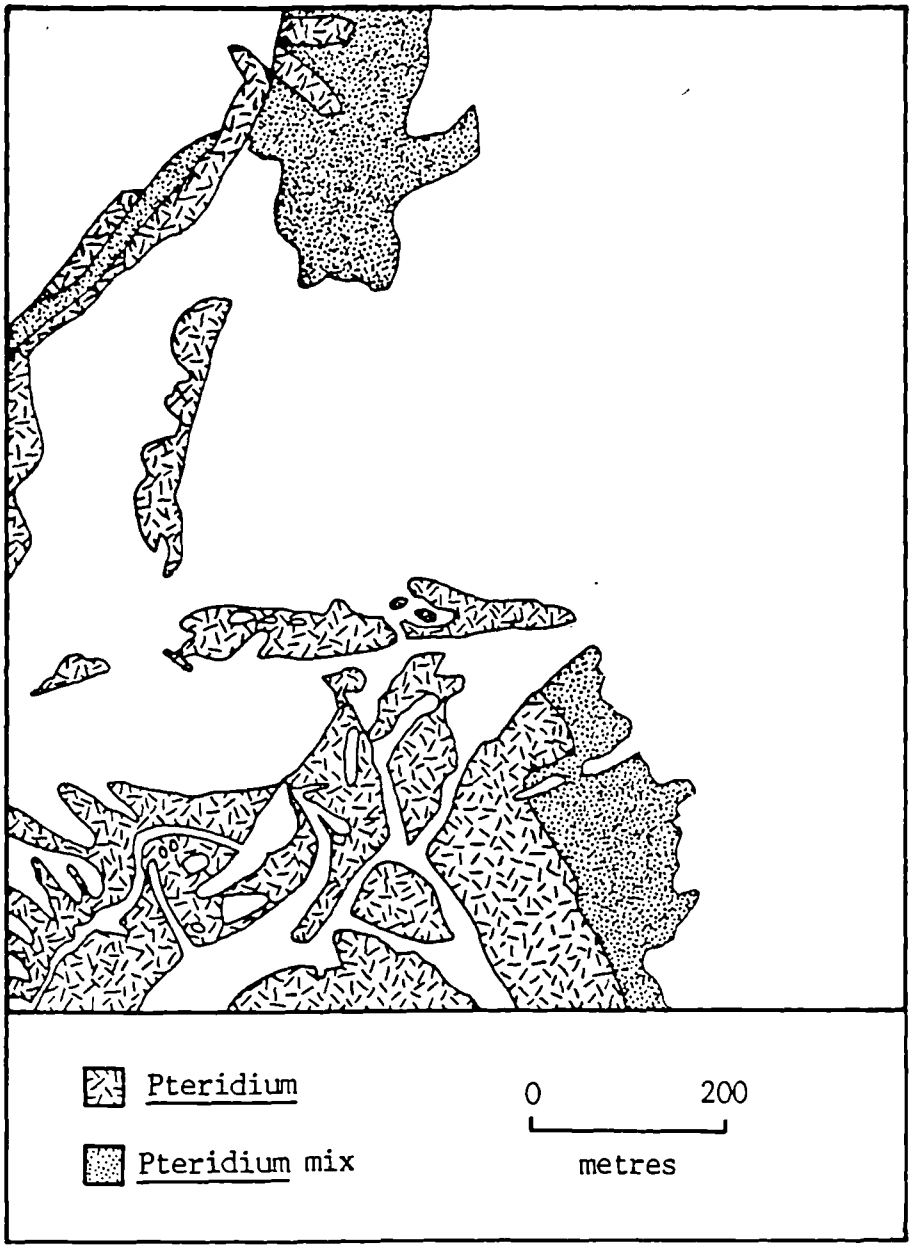

Figure 6.8 Pteridium aquilinum class map: field data

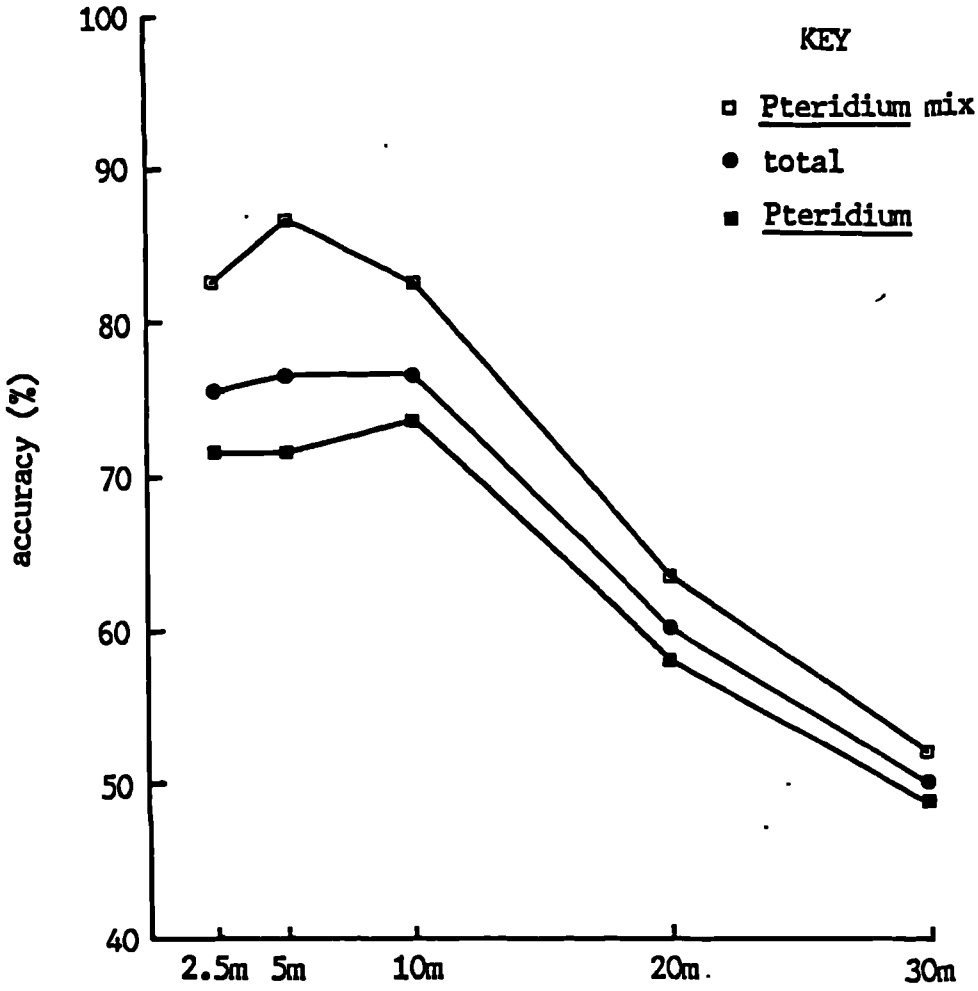

Figure 6.9 Graph to show the change in accuracy associated with a change in spatial resolution

resolution	pure Pteridium	mixed Pteridium	total
2.5m	71.4 (±9)	82.6 (±10)	75.3 (±7)
5m	71.4 (±9)	86.5 (±9)	76.6 (±7)
10m	73.5 (±9)	82.6 (±10)	76.6 (±7)
20m	58.0 (±10)	63.5 (±13)	60.0 (±8)
30m	49.0 (±10)	52.0 (±14)	50.0 (±8)

Table 6.1 Accuracy of Pteridium aquilinum class maps (%)

When the Pteridium and Pteridium mix categories are treated separately, the accuracy patterns are similar, although they are slightly different. In the pure Pteridium class, the 2.5m and 5m images have an accuracy of 71.4% (±9%), while the 10m data stands alone with the highest success rate of 73.5% (±9%). The fall in accuracy on the 20m data is equally dramatic, being over 15%. The 30m data is again the least successful, at 49% (±10%) (table 6.1).

The highest accuracy values are found in the Pteridium mix class, the peak being 86.5% (±9%) on the 5m data. The accuracies of the 2.5m and 10m data are also high (82.6% ±10%), and the same pattern of a large rise in the error rate between the 10m and 20m images is followed (table 6.1).

These results suggest that the 10m data are the optimum spatial resolution for Pteridium aquilinum identification.

6.4.4 The effect of spatial resolution on the accuracy of boundary location

As spectral resolution changes, it may be hypothesised that boundary location and characteristics will also change. A larger pixel size will cause averaging over larger areas, and may lead to expansion, contraction, or blurring of the boundary. If a pixel lies across a boundary, it may be allocated to one or other of the classes, or to a third, totally erroneous, class (section 6.3).

A simplified representation of the hypothesised change in boundary location associated with a change in pixel size is shown in figure 6.10. In example A (fine resolution), the real boundary splits the pixel so that three quarters lie in class 1, and one quarter lies in class 2. Thus the whole pixel will be allocated to class 1 (the dominant class areally), shifting the boundary to the right (diagram C).

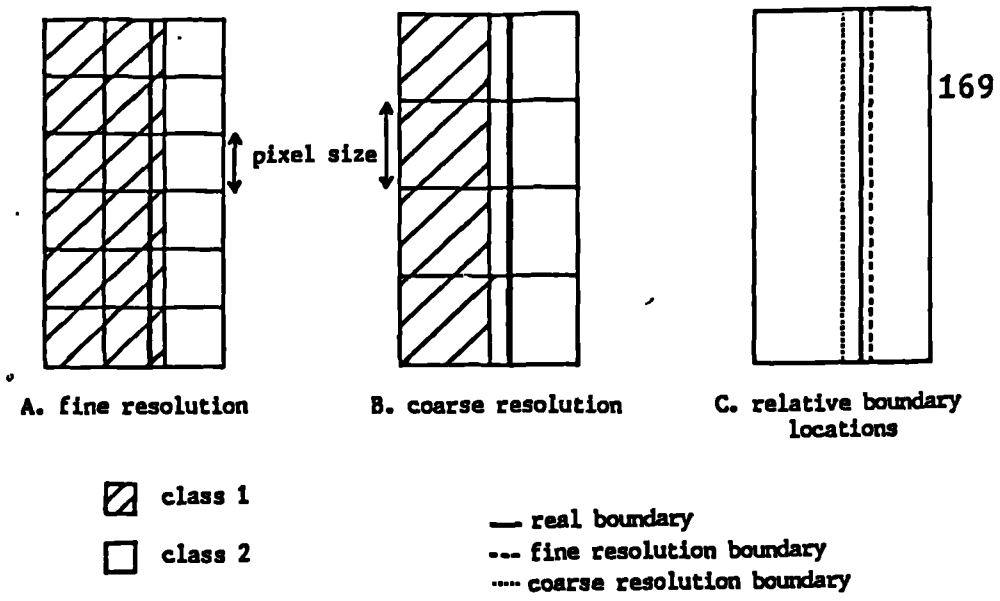

Figure 6.10 The hypothetical change in boundary location and character associated with a change in pixel size: straight boundary

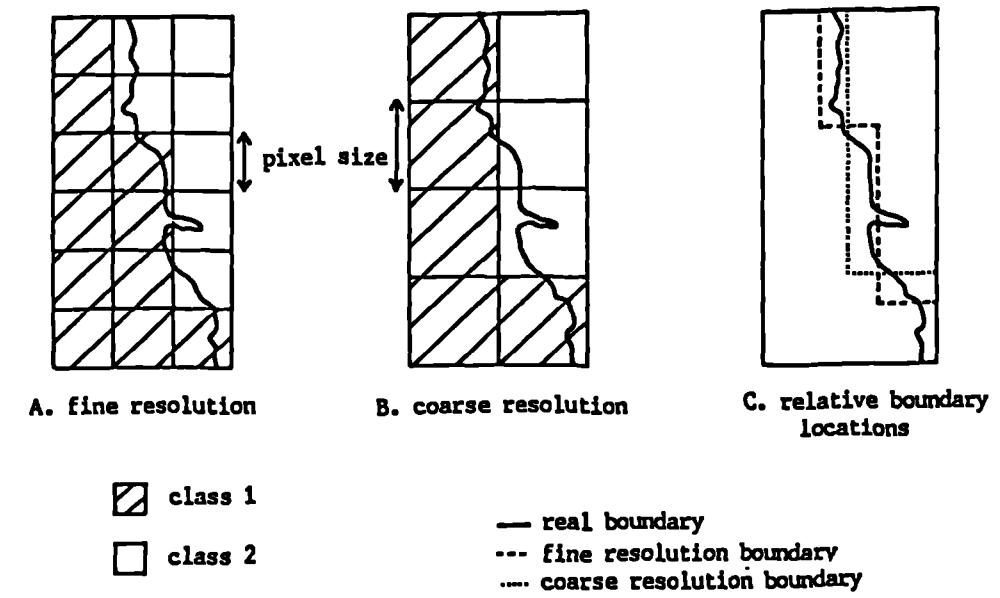

Figure 6.11 The hypothetical change in boundary location and character associated with a change in pixel size: sinuous boundary

In the coarse resolution example (B), the boundary splits the pixel one fifth in class 1, and four fifths in class 2. Thus the pixel will be allocated to class 2, shifting the boundary to the left (diagram C).

However, the above example is simplified so that it takes no account of sinuous boundaries. These will result in a step-like limit, if the resolution is sufficiently coarse (figure 6.11). The steps lag behind changes in the sinuous boundary and small-scale variations and details, such as narrow protuberances, are lost. Thus it may be expected that boundaries will become significantly misaligned and generalised as the spatial resolution becomes more coarse.

However, these hypothetical examples are oversimplified, and do not consider that a third erroneous class may be created, or that sub-pixel areas of great contrast may contribute disproportionately to the reflectance. The exact effect of spatial resolution is also determined by the relative position and orientation of the real boundary and the pixel grid. Nevertheless, it may be expected that a shift in the location, and a change in the characteristics of the boundary, will occur if the pixel size is altered.

The hypothesised change in boundary location and character is apparent on the boundary diagrams (figures 6.12, 6.13 and 6.15 to 6.17). There is very little difference in the boundaries on the 2.5m and 5m images (figures 6.12 and 6.13 respectively). Both show the features present on the field map (shown as a dashed line) in considerable detail, although neither correspond exactly, as they are shifted south west of the field boundary. This is probably a result of geometric errors in the image, misregistration in time, errors in the field map, and errors in the interpretation of the boundary (sections 6.4.2 and 6.5). This shift may also be related to the spatial resolution, and it results in a contraction of the pure Pteridium area to 83.3% of the field map area in the 2.5m data, and to 85.7% in the 5m data (figure 6.14; table 6.2).

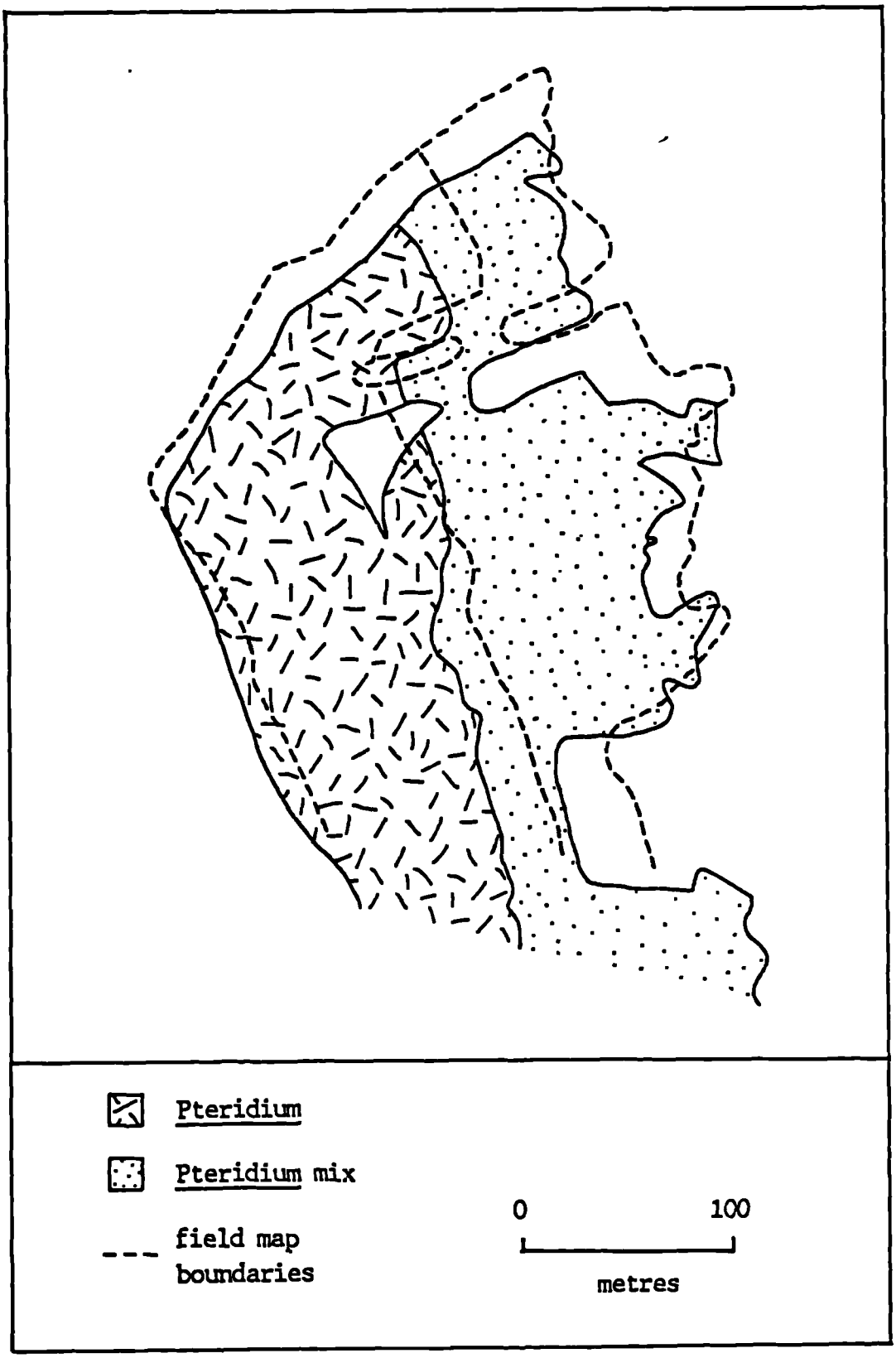

Figure 6.12 Selected Pteridium aquilinum boundary map: Airborne Thematic Mapper 2.5m data (field map boundary shown in dashed line)

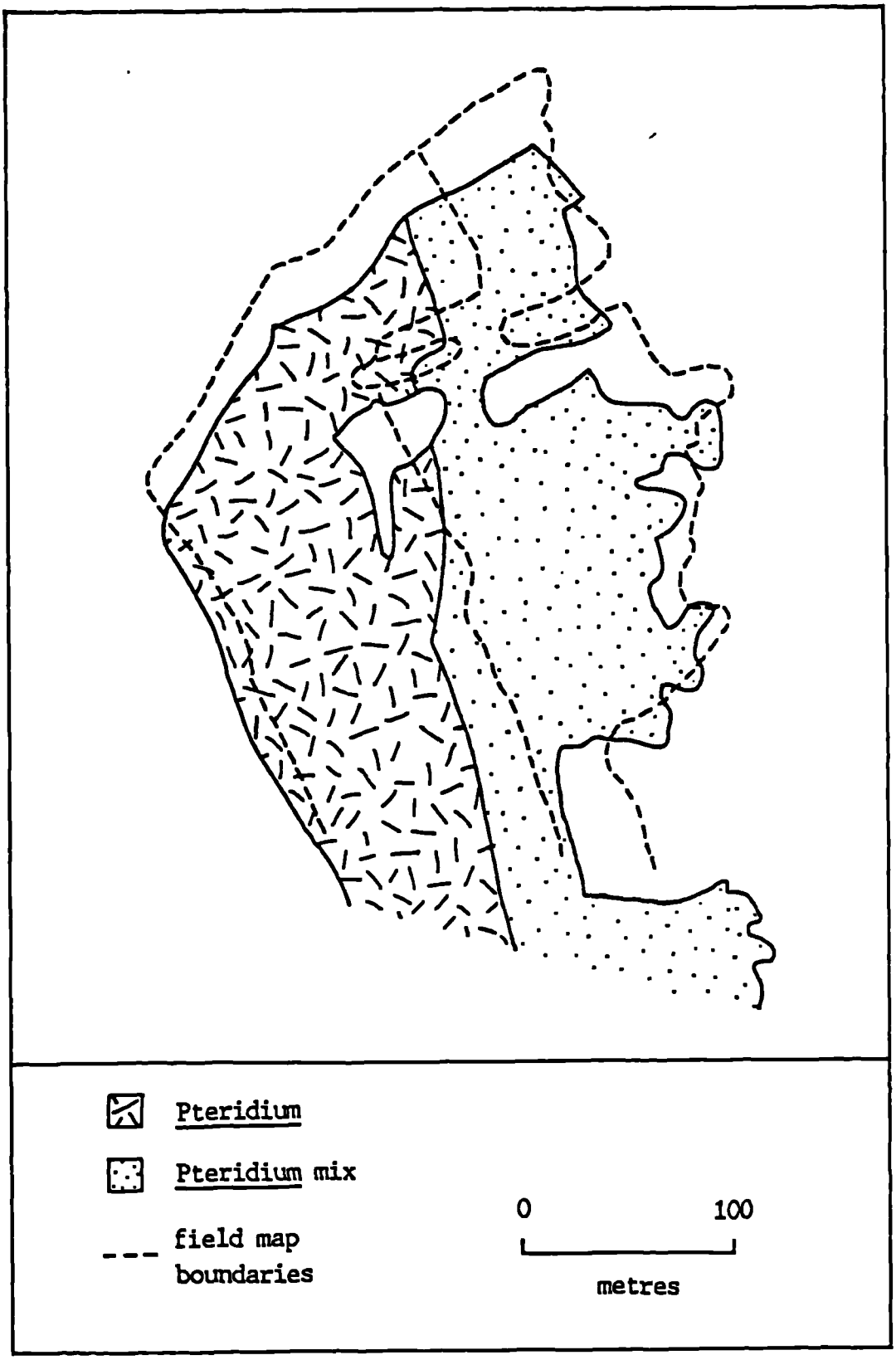

Figure 6.13 Selected Pteridium aquilinum boundary map: Airborne Thematic Mapper 5m data (field map boundary shown in dashed line)

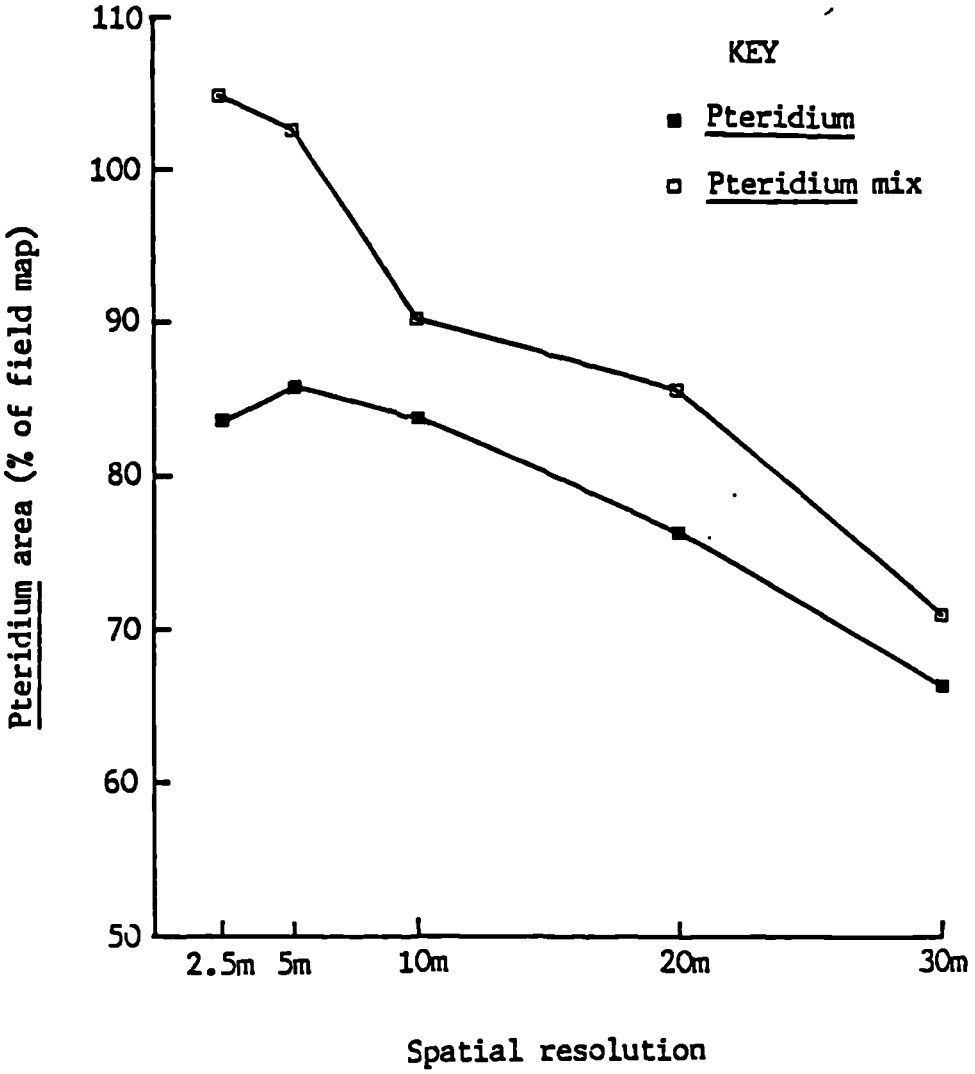

Figure 6.14 Change in Pteridium aquilinum area associated with a change in spatial resolution

However, the mixed category coverage is expanded to 104.9% and 102.4% of the field map area, for the 2.5m and 5m data respectively (figure 6.14; table 6.2). This may be due to a shift into the Calluna vulgaris caused by the position of the pixel grids, or it may be due to the problems of interpreting a definite boundary on a transitional limit, both on the ground and on the image.

resolution	pure Pteridium	mixed Pteridium
2.5m	83.3	104.9
5m	85.7	102.4
10m	83.3	90.2
20m	76.2	85.4
30m	66.6	70.7

Table 6.2 Area of Pteridium aquilinum as a percentage of the field map area

There are, however, subtle differences between the two images; the 5m boundaries are shifted slightly further away from the field map limits, and show slightly less detail (figure 6.13).

There is a more noticeable change when the 10m data are analysed (figure 6.15). The shift away from the field boundary is increased by about one pixel width (10m), causing a contraction in area for both the pure and mixed Pteridium classes (figure 6.14; table 6.2). However, the tongue of bare area indenting the north eastern area of the mixed Pteridium, and the bare area within the pure Pteridium, are both positioned closer to the corresponding areas on the field map, than on the 2.5m and 5m images, although they are larger than they should be.

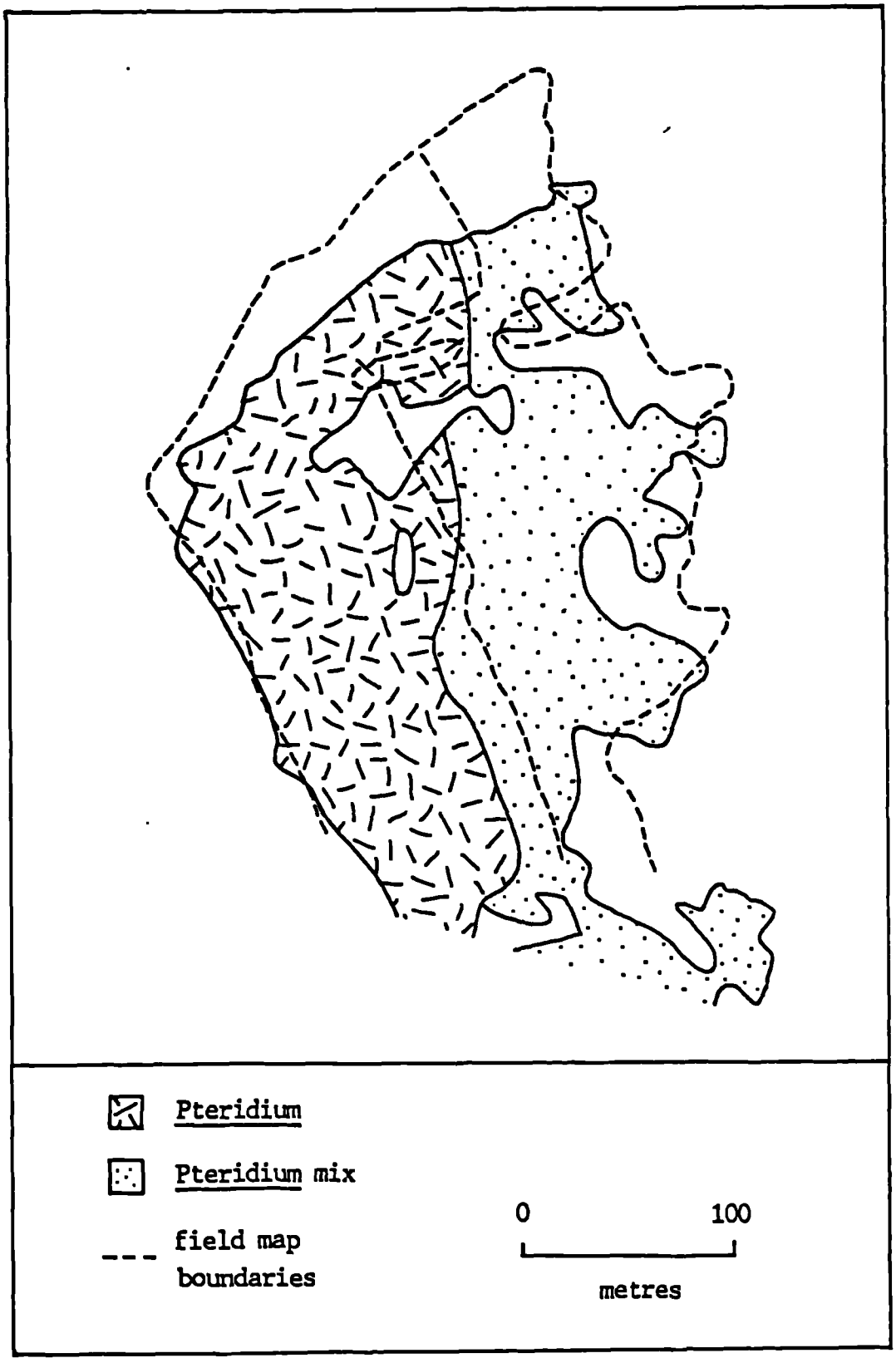

Figure 6.15 Selected Pteridium aquilinum boundary map: Airborne Thematic Mapper 10m data (field map boundary shown in dashed line)

These differences may be due to the position of the indents, relative to the pixel grid, causing a shift northwards in both cases, and widening the indent at the same time, because of the larger pixel size. Such bare areas have a bright reflectance, especially in the red channel, which contrasts strongly with low red reflectance of the Pteridium aquilinum. Therefore, the sub-pixel bare areas may contribute to the reflectance disproportionately to their area, causing a pixel with over 50% Pteridium to be classed as wetland vegetation. In addition, the small undulation in the centre of the mixed/Calluna boundary, has become exaggerated, as has the larger Calluna lobe extending into the mixed area, in the south. This is probably due to the contraction of the Pteridium area, caused by the shift in boundary as a result of the location of the pixel grid.

The changes are more dramatic on the 20m image (figure 6.16). Here the step-like nature of the boundary is clearly exposed, causing a loss of detail and sinuosity. The indented bare area mentioned above has been reduced to one pixel. This is because it is split between pixels due to its narrowness and diagonal position, resulting in the neighbouring pixels being dominated by the surrounding mixed Pteridium. The other bare area, within the pure Pteridium has become enlarged and misshapen. The small Calluna undulation in the centre of the mixed boundary has been greatly exaggerated, and shifted towards the Pteridium area. The larger Calluna lobe has grown, causing the Pteridium in the south east to become detached from the main block. The narrow isthmus joining the two areas has been lost in the averaging process. An additional lobe of Pteridium has become attached to the western side of the main block, because the wetland vegetation separating the two was too narrow to dominate both of the adjacent larger pixels, although one remains classed as wetland.

The 30m image (figure 6.17) shows the greatest contraction of Pteridium coverage, to only 66.6% of the pure area on the field map, and 70.5% of the mixed (figure 6.14; table 6.2). This image, as hypothesised, bares the least resemblance to the field map.

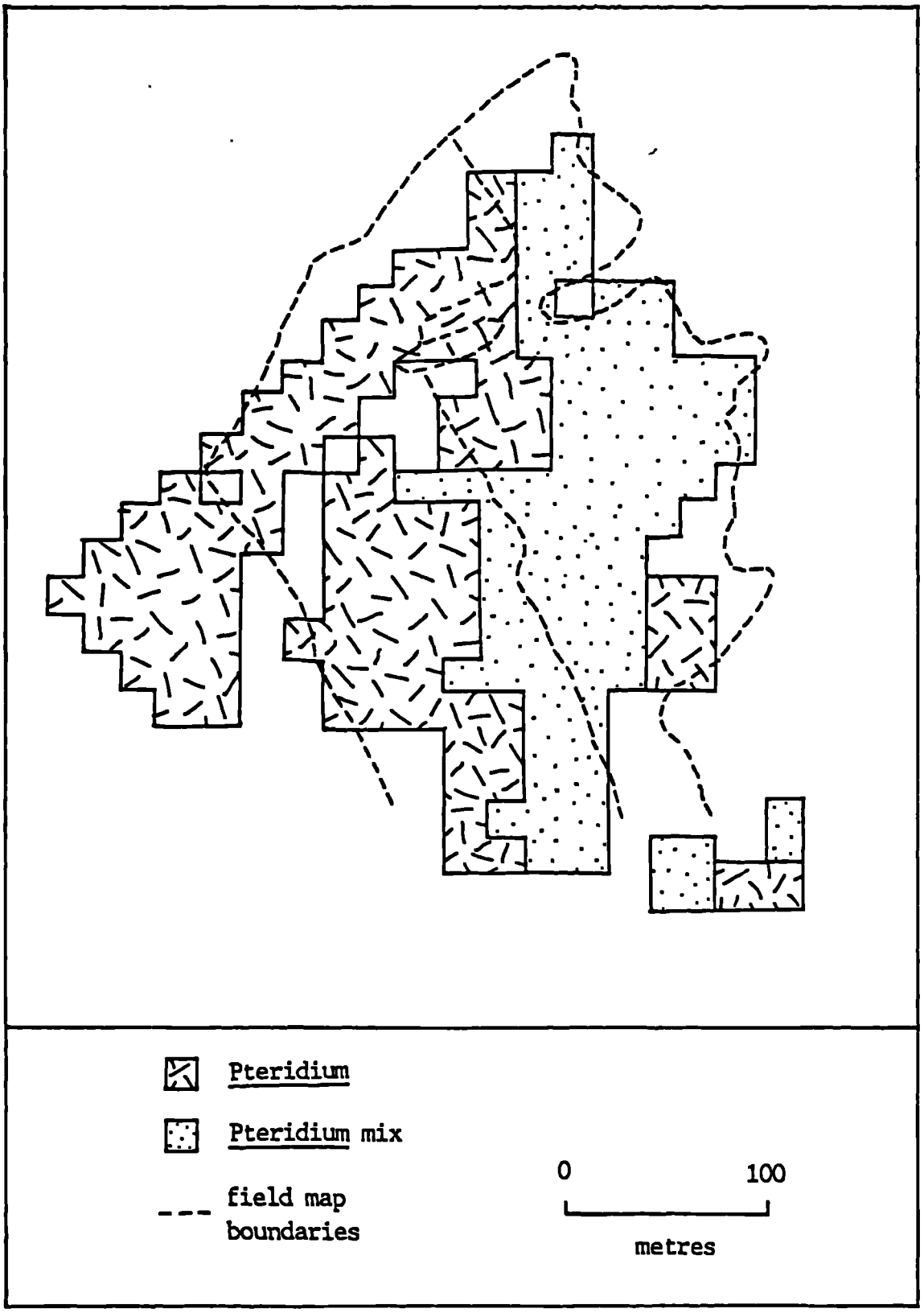

Figure 6.16 Selected Pteridium aquilinum boundary map: Airborne Thematic Mapper 20m data (field map boundary shown in dashed line)

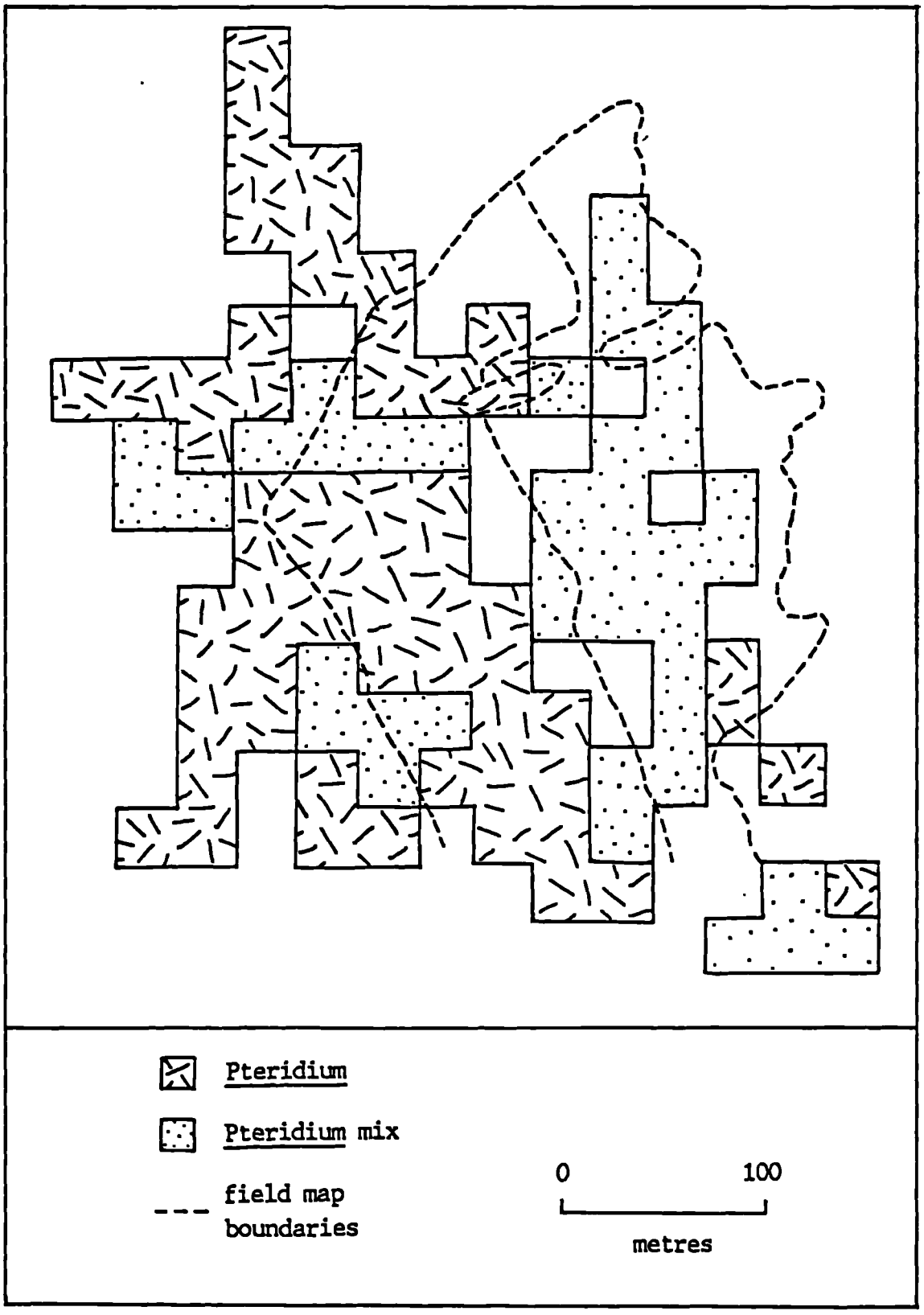

Figure 6.17 Selected Pteridium aquilinum boundary map: Airborne Thematic Mapper 30m data (field map boundary shown in dashed line)

Any small-scale detail and undulations have been lost, and the Pteridium area has become fragmented with overexaggeration of indents and bare areas within the vegetation block. Quite considerable areas within the pure area have been classed as mixed, due to the averaging of the wetland and Pteridium areas, over the 30m pixel. An additional area of Pteridium has become attached to the main block in the north west, again because the narrow wetland vegetation separating them has been lost. However, even at this resolution the area of coverage by the Pteridium, and the pattern of boundaries, are still evident, although they are generalised and tend to lag slightly behind the changes in the field boundary.

6.4.5 Discussion

The majority of errors found when testing the accuracy of the class maps, especially in the 2.5m, 5m and 10m data, are due to the shift of the boundaries on the image slightly to the south west of the field map boundary, causing sample points close to the field boundary to lie outside the image Pteridium limits. This may be caused by five factors (the first three were outlined above, in section 6.4.2).

The first factor is the geometric infidelity of the ATM data so that the distortions were not completely corrected for.

The second factor is misregistration in time, so that the Pteridium aquilinum front had in fact moved towards the Calluna vulgaris in the year between the collection of the two data sets. However, the alleged encroachment would have had to be 35 to 40m in the southernmost area, although the average distance between the two boundaries is approximately 10m. These distances are too great to be attributed solely to advancement of the Pteridium front, and although this factor may be contributory, it is unlikely to account for more than a maximum of 2 to 3m.

The third factor is error in the field map, as the diffuse Pteridium aquilinum boundary could have been positioned wrongly on the map.

The fourth factor is error in the subjective interpretation of the false colour composites, as the tones, especially between the two Pteridium classes, change gradually over the transitional zone.

The final factor is the failure of the spectral data to adequately characterise the Pteridium classes, and to enable successful discrimination.

The inaccuracies are likely to be a result of a combination of all five factors. However, the shape and size of Pteridium blocks are relatively faithful to the field map, and it is the positioning that is in error, suggesting that the dominant errors are locational or geometric, rather than spectral.

This shift of the boundary is partly to blame for the lower accuracy of the 'pure' category. The Pteridium tends to be distributed in narrow bands, which means that if the images are misaligned with the field map there is a greater chance of sample points falling just outside the boundary. The mixed category is generally found in larger blocks.

The errors in the 20m and 30m data are more closely related to the spatial resolution. The step-like nature of boundaries and the loss of narrow or small features, which was predicted above (section 6.4.4), has resulted in far higher inaccuracies.

The pattern of accuracy rates rises gradually upwards from the finest resolution, to a peak at medium resolutions, followed by a reduction in accuracy in the coarsest resolutions, confirming the hypotheses stated above (section 6.3). However, in this case the pattern is very asymmetrical, with relatively high fine resolution accuracies, and relatively low coarse resolution accuracies, with a large and sudden drop from the peak. This pattern does not exactly fit the idealised hypothesis, because of the scene-dependent nature of the balance between scene spatial structure, class homogeneity and the proportion of boundary pixels.

In this case, the spectral characteristics of the Pteridium aquilinum are fairly homogenous, even in the 2.5m data, and so the accuracy changes related to spatial resolution changes are more likely to be influenced the proportion of boundary pixels. An increase in such mixed pixels causes blurring and alteration to the limits between vegetation types. The other important influence on accuracy changes related to resolution changes in this case, is the spatial structure of the Pteridium aquilinum stands. The species tends to occur distributed in narrow bands along the sides of valleys or fields, and to have small-scale finger-like protuberances into the adjacent moorland or agriculture. These small and narrow features are likely to be lost on the coarsest resolutions, and therefore increase errors. Thus, as the heterogeneity of the Pteridium is not of major importance, the balance of the relationship shifts towards the influence of mixed pixels, so that the finer resolutions, which have a lower proportion, are more accurate.

However, the influence of spatial resolution on accuracy is not just scene-dependent, it is also class-dependent. Thus, if Calluna vulgaris had been selected for special attention, the homogeneity of the class would have played a more important role, as the Calluna is quite heterogeneous at the finest resolutions (section 6.4.5).

6.4.6 The effect of spatial resolution on the accuracy of unsupervised cluster analysis

The cluster analysis classification images are shown in plates 6.6 to 6.10. Full classification confusion matrices may be found in Appendix 4 (tables App4.1 to App4.5).

The relative accuracy at each resolution varies quite considerably between vegetation types (table 6.3). The classes may be roughly separated into four groups; those optimally discriminable at fine, medium and coarse resolutions, and those with zero accuracy.

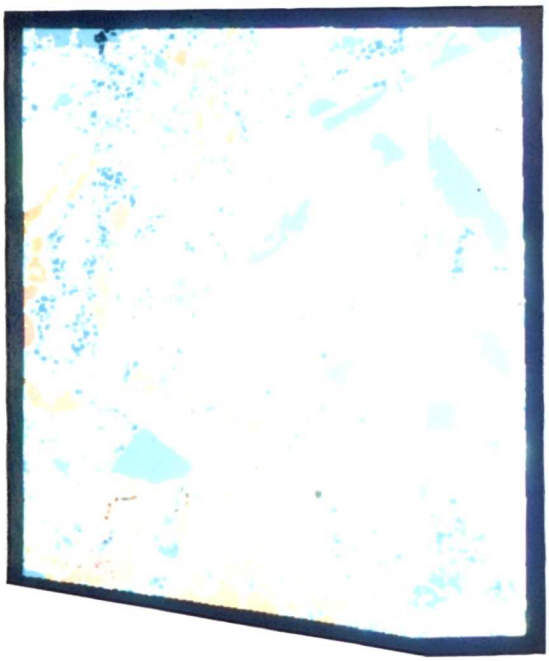

Plate 6.6 Cluster classification of ATM subscene, July 1986: channels ATM5, ATM7 and ATM9: 2.5m data

KEY TO THE CLUSTER CLASSIFICATION IMAGES (plates 6.6 to 6.10)

purple	=	Mature Calluna vulgaris
white	=	Pioneer Calluna vulgaris
light blue	=	Burnt/bare
orange	=	Pteridium aquilinum
yellow	=	Grassland
green	=	Agriculture
dark blue	=	Mixed vegetation

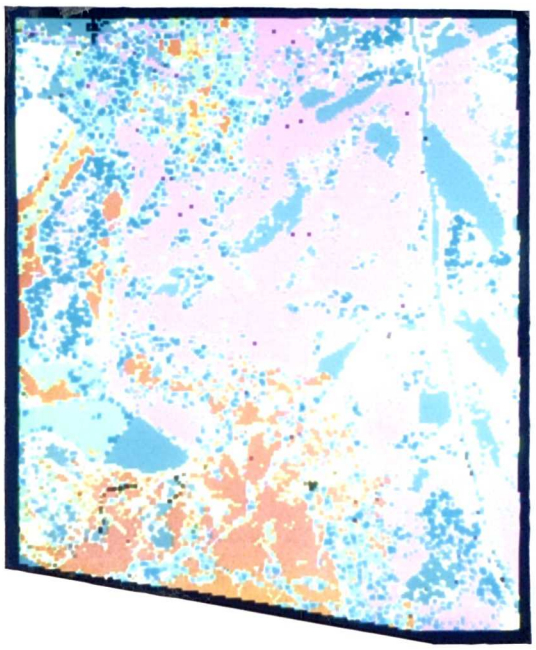

Plate 6.7 Cluster classification of ATM subscene, July 1986: channels ATM5, ATM7 and ATM9: 5m data

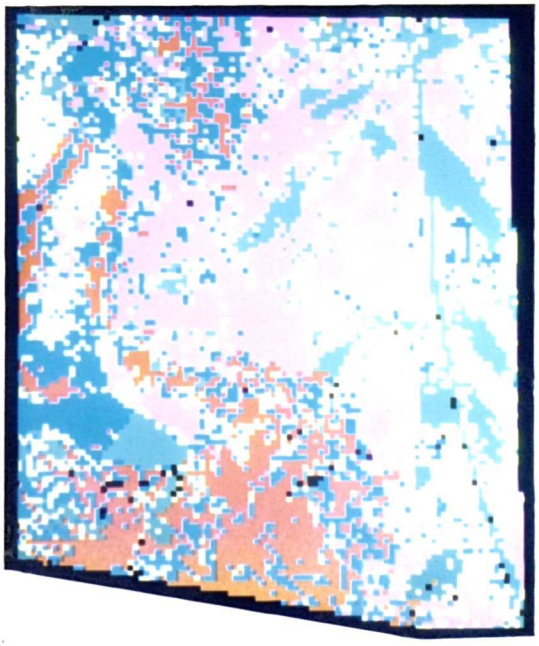

Plate 6.8 Cluster classification of ATM subscene, July 1986: channels ATM5, ATM7 and ATM9: 10m data

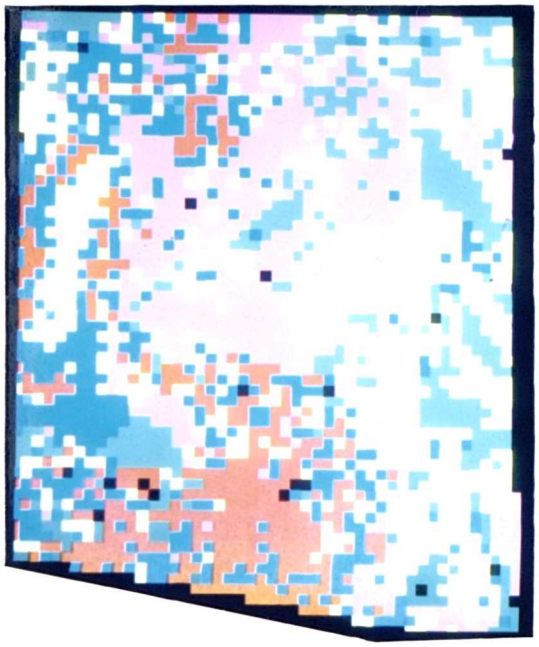

Plate 6.9 Cluster classification of ATM subscene, July 1986: channels ATM5, ATM7 and ATM9: 20m data

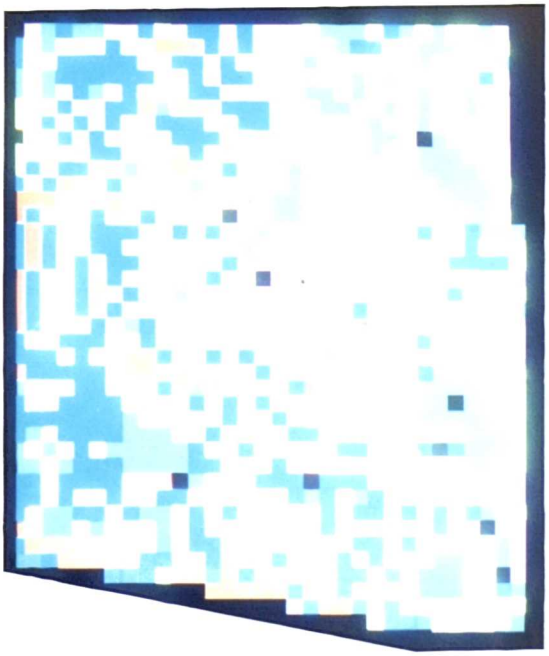

Plate 6.10 Cluster classification of ATM subscene, July 1986: channels ATM5, ATM7 and ATM9: 30m data

class	No.of cases	spatial resolution				
		2.5m	5m	10m	20m	30m
Cv1	60	66.5	83.0	90.5	81.0	74.0
Cv2	26	38.5	46.0	84.5	46.0	61.5
Cv3	50	72.0	72.0	52.0	48.0	64.0
Cv4	34	0	0	0	0	0
Pa	60	46.0	56.0	63.0	60.5	58.0
Gr	34	41.0	53.0	53.0	47.0	35.0
Ag	24	25.0	33.0	0	0	0
Wet	24	0	0	0	0	0
Mix	48	54.0	58.5	58.5	62.5	41.5
Total	360	42.0(±7)	56.0(±7)	56.0(±7)	50.0(±7)	48.0(±7)

Key: Cv=Calluna (1=Mature 2=Pioneer 3=Burnt 4=Degenerate) Pa=Pteridium Gr=Grassland Ag=Agriculture Wet=Wetland vegetation Mix=mixed vegetation Total=overall accuracy at resolution

Table 6.3 Individual class accuracy at each resolution, for cluster analysis (%): Airborne Thematic Mapper data (optimum resolution underlined)

The totally misclassified classes (degenerate Calluna vulgaris and wetland vegetation) are not represented as independent spectral classes. The degenerate Calluna has mainly been allocated to the mature class, while the wetland has been classed as either Pteridium or grassland. These classes are not spectrally distinct using these three spectral channels, at this time of year. However, the possibility exists that they may be separable using other channels, and/or another date.

The optimum spatial resolution of the other three groups is closely related to the homogeneity of the classes.

The burnt/bare class and the agriculture are optimally separable at the finest resolutions (2.5m and 5m), the accuracy being 72% and 33% respectively (tables 6.3, App4.1 and App4.2). These cover types are relatively homogenous, with large areas of fairly constant spectral values. Therefore the proportion of boundary pixels is of greater importance to accuracy than the class heterogeneity. Thus finer resolutions, with lower proportion of mixed pixels will have the highest success rates.

Mature Calluna, pioneer Calluna, Pteridium and grassland are optimally discriminable at a medium resolution (10m); the accuracy values being 90.5%, 84.5%, 63% and 53% respectively (tables 6.3 and App4.3). These vegetation types are reasonably homogenous, but have a certain degree of heterogeneity, especially the two Calluna classes. In this case the relative importance of the proportion of boundary pixels and the class heterogeneity is finely balanced, causing medium resolutions to have the highest success rates.

The mixed category is the only cover type to be optimally discriminable at a coarse resolution (20m); its peak accuracy being 62.5% (tables 6.3 and App4.4). Here the proportion of boundary pixels is of subordinate importance to accuracy values, as the emphasis is on improving class homogeneity, which is very low at fine

resolutions. A coarser image will average out small-scale variations and thus will have the highest success rate.

When the total accuracy of the whole image is considered, the 5m and 10m images have the peak accuracy at 56% (±7%) (tables 6.3, App4.2 and App4.3). The change in accuracy with a change in spatial resolution follows the hypothetical pattern (section 6.3), and is in agreement with the results of the assessment of Pteridium aquilinum accuracy from the false colour composite images (section 6.4.3.2). However, in this case the 2.5m resolution has the highest error rates, confirming that it is a misconception to assume that an increase in spatial resolution will automatically result in an increase in classification accuracy (Townshend, 1980).

The high misclassification at 2.5m is probably a result of the dominance of moorland areas by species with complex and variable canopy forms, on a scale which creates heterogeneity between adjacent 2.5m pixels. The general semi-natural environment also results in higher heterogeneity, because of variations in the vegetation influenced by natural and man-made factors. These include small depressions, which result in localised moist areas, the advancement of Pteridium aquilinum, which results in a mix of species in a transitional zone, old mine workings, which encourage invasion by rough grasses, and the burning regime, which creates patchy regeneration of Calluna vulgaris. Such factors tip the balance of the effect of spatial resolution away from the importance of boundary pixels toward the requirement to increase class homogeneity. Thus, accuracies are low at fine resolutions and remain relatively high even at 30m; 48% (±7%) (tables 6.3 and APP4.5).

6.6 Conclusion

The results of the research reported in this chapter have identified some of the complexities involved in assessing the effect of spatial resolution upon mapping accuracy. The degradation experiment has shown that spatial resolution has a considerable effect upon the

discrimination of vegetation types, the accuracy of maps derived from the imagery, the location and character of class boundaries, and the accuracy of cluster analysis classification maps. In both the visual interpretation and the quantitative assessment of accuracy (of the Pteridium class maps and the cluster analysis), the 10m data were selected as the optimum spatial resolution. These data have the peak Pteridium aquilinum and overall cluster analysis accuracy values, and appear to hold sufficient spectral and spatial information to separate successfully the vegetation types, to retain the shape and size of vegetation blocks, and to represent linear features clearly.

Nevertheless, even the most coarse image (30m) holds valuable information enabling considerable class separation and good representation of the shape of reasonably sized vegetation areas. In addition, it has higher cluster analysis accuracy than the 2.5m image. The usefulness of data at coarse resolutions is highly dependent on the exact aims and requirements of the project. If generalised vegetation mapping, disregarding small-scale features and anomalies, is the purpose of the operation, then a 30m pixel size may be adequate. While for a detailed representation of ground conditions, such as was considered in this experiment, 30m data will be too coarse for the complex moorland environment.

This has important implications for the operational satellite monitoring of semi-natural vegetation in the North York Moors and other upland areas. The 10m optimum spatial resolution identified in this study is only available, from a satellite source, on the single SPOT panchromatic channel (0.51-0.73μm), which may not have the spectral capabilities needed to adequately separate species automatically. The finest commercially available multi-spectral satellite data are SPOT HRV, at 20m pixel size. However, the SPOT satellite has two major drawbacks. The first is that it only has three spectral channels, green (0.50-0.59μm), red (0.61-0.68μm) and near infrared (0.79-0.89μm) (Chevral, et al, 1981). It does not have a short-wave infrared channel, which was selected as the optimum single TM band in this study (table 5.6; section 5.5.3.2). The second

drawback is that because of the increased spatial resolution, the area covered by a single scene is reduced, so that more than one scene is needed to cover large upland areas, such as the North York Moors. This would cause problems of co-registration and radiometric calibration between scenes, and increase the cost of initial purchase and preprocessing.

A sensor with the spatial resolution of SPOT, and the spectral resolution and coverage of Landsat TM, might be ideal for moorland mapping. However, as such data are not available, the balance between the spectral and spatial resolution must be carefully considered in each individual case, before selecting the optimal data source for the task.

CHAPTER 7. MOORLAND MAPPING FROM SATELLITE IMAGERY

7.1 Introduction

The ultimate goal of this research is to develop a routine moorland mapping and monitoring methodology using satellite imagery. An investigation of the temporal, spectral and spatial aspects of the remotely sensed data, together with the identification of the optimum resolution in each case, has formed a firm and scientific base on which to establish such an operational system.

It is the aim of this chapter to produce accurate vegetation maps of the North York Moors National Park, building on the research presented in the previous three chapters. The analysis begins with the visual interpretation of single band and false colour composite TM images. This is followed by a more quantitative assessment of supervised computer classification techniques. Finally, the effect of various smoothing and filtering algorithms on mapping accuracy are evaluated.

7.2 The data

The two Landsat Thematic Mapper scenes (26.4.84 and 31.5.85) were selected for the task of large-scale moorland mapping, as they were the only data available to this research that cover the whole of the National Park (section 3.7). Unfortunately, neither of these data sets have optimal temporal or spatial resolution for moorland remote sensing. It has been concluded that a late summer image would be most promising (section 4.5.6), and that a pixel size of 10m would offer most information (section 6.6). However, at the onset of the research there were no cloud-free late summer TM scenes available for the North York Moors, although subsequently one has become available (20.8.87). In addition, at the beginning of the project, satellite images at a spatial resolution finer than the 30m TM data, were not commercially available, although SPOT data may now be purchased at

10m (panchromatic) and 20m (multispectral) (Chevrel et al, 1981). However, there are several drawbacks, both spectral and coverage, which limit the operational potential of SPOT data for moorland mapping (section 6.6).

Thus, the following analysis is completed with temporally sub-optimal data, and it may reasonably be expected that results would improve if a late summer scene was used.

7.3 Methodology

The first step in the analysis was the visual interpretation of the data using the I^2S image processor. All TM bands were separately displayed and assessed. The best individual band was chosen for each date; TM5 (SWIR) for the April 1984 data, and TM4 (near IR) for the May 1985 data. Their selection was based on visual and statistical criteria; the two bands appeared to give more visual detail than any other band, and they were also the two bands selected as the optimum single bands using discriminant analysis (section 5.5.3.2; table 5.6).

The best three spectral channels were displayed as scaled false colour composites. The bands were TM2, TM4 and TM5 for the April 1984 data, and TM7, TM4 and TM5 for the May 1985 data. Again, these offered the most visual information and were chosen as the optimum three band combinations by discriminant analysis.

The second step was the analysis of photographic prints of single bands and false colour composites, taken from the screen of the I^2S. The images were photographed in entirety (plates 7.2 to 7.5), and each one was then divided into eight subscenes, which were enlarged to fill the whole screen. An example subscene is shown in plate 7.1, together with a location map (figure 7.1). Photographs of the subscenes were used during all further analysis to allow a more detailed interpretation.

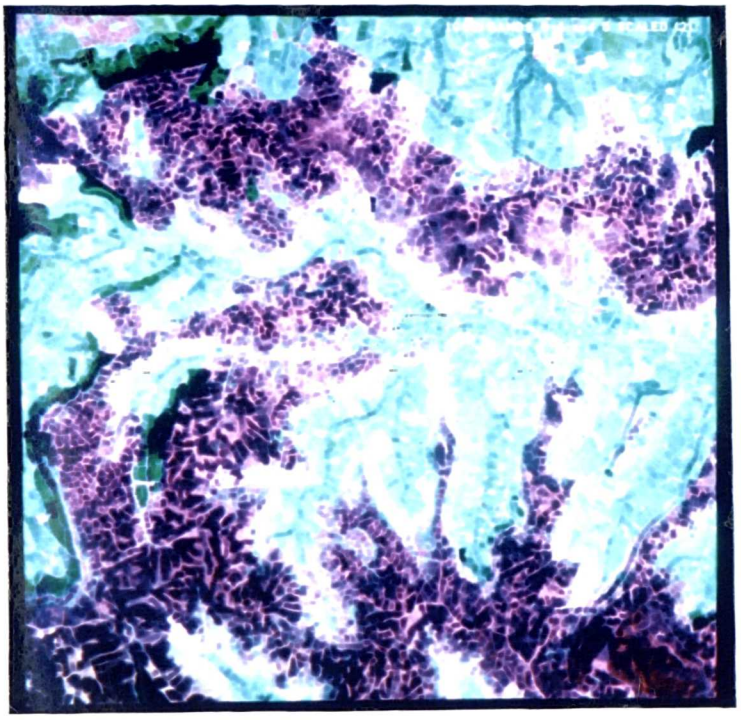

Plate 7.1 Landsat Thematic Mapper example subscene: false colour composite of bands TM7, TM4, TM5, May 1985

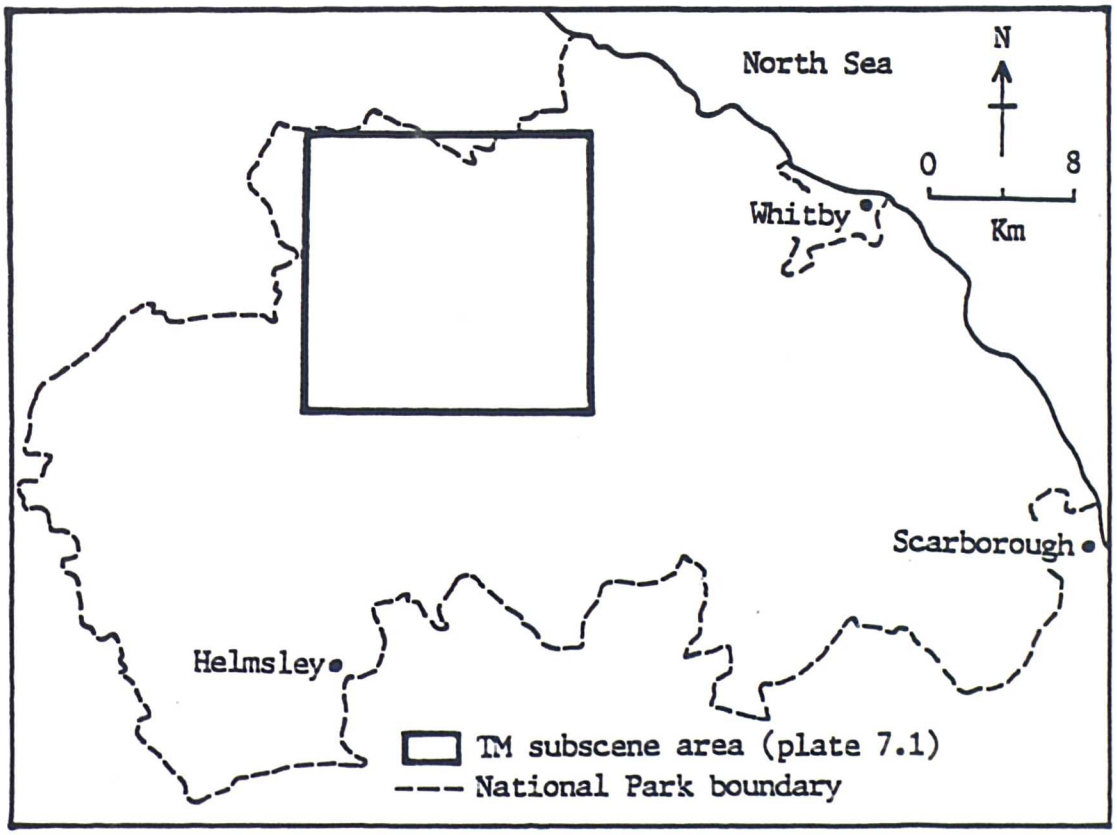

Figure 7.1 The location of the Landsat Thematic Mapper example subscene

Pteridium aquilinum and moorland class maps were drawn from the false colour composite subscenes (figures 7.7 to 7.10). As with the ATM experiment reported in chapter 6 (section 6.4.1), there is bound to be some subjectivity in the visual interpretation of images. Nevertheless, great care was taken to avoid mistakes, and the North York Moors National Park published maps were used as a guideline (North York Moors National Park Committee, 1984b; figures 7.5 and 7.6). However, some areas which were on the National Park maps were not apparent on the images, and vice versa.

The maps drawn from the images were overlaid on the National Park maps and the accuracy was calculated using the method described above (section 6.4.1). The sample check points were located using random numbers. Any points falling within the boundaries of either the Pteridium aquilinum or the moorland on the National Park published maps were selected. There were 100 Pteridium and 100 moorland sample points.

The third part of the analysis was the supervised classification of the two TM images. Unlike the cluster analysis reported in the previous chapter (section 6.4.1), supervised classification is based on external knowledge of the areas shown in the image (Mather, 1987). Training areas must first be defined, and this was done using the tracker-ball unit of the I^2S image processor. The scaled three-band false colour composites were used to delimit the training regions on the screen, with reference to the field maps (Appendix 1).

It is crucial that the training data are reliable, for if they are not representative the accuracy of the resultant classification will be lower (Schowengerdt, 1983; Lillesand and Kiefer, 1979). Mather suggests a training sample size of 30 times the number of bands for each class, although more are needed if if contiguous blocks are used, to avoid autocorrelation between neighbouring pixels (Mather, 1987). In order to reduce autocorrelation large numbers of pixels in more than one training area per class must be used. However, the I^2S training algorithm would not accept too many separate areas for each

class, so in all cases only one, two or three were possible for each cover type. The number of pixels in each sample are shown in table 7.1. Three agriculture classes were used, in order to represent three separate spectral classes; improved pasture, rough grazing and arable. These three were later coloured the same to form one agriculture class. It had been intended to include separate mature, pioneer and degenerate Calluna vulgaris classes, but attempts to achieve this with the data and time available, proved unsuccessful. Therefore, the three growth stages were combined into one Calluna vulgaris class. This "moorland" class, together with the burnt areas, was taken as equivalent to the National Park moorland category (excluding Pteridium aquilinum areas) (North York Moors National Park Committee, 1984b).

class	number of training pixels
Calluna vulgaris	108
Burnt	92
Pteridium aquilinum	122
Water	137
Forest	129
Cloud	127
Grassland	98
Agriculture (1)	115
Agriculture (2)	104
Agriculture (3)	99

Table 7.1 The number of training pixels in each class, used in the supervised classification of Landsat Thematic Mapper data

The pixel values within the training regions for each class in each band were extracted, and summary statistics were calculated; means, minimums, maximums, standard deviations, eigenvalues, and covariance and eigenvector matrices (I^2S, 1987).

Another reason for taking training data from more than one contiguous area is to avoid singular covariance matrices. When the pixel values in two bands, for one class, are identical, or those in one band are a multiple of those in another, a singular covariance matrix will result (I^2S, 1987). Classification cannot proceed with classes which have singular covariance matrices. Thus training areas which are too homogenous must be avoided. This causes difficulties in trying to delimit training regions which are representative, but which are also not too 'pure'. If the values in each band remain constant, a singular covariance matrix will result, or there may be misclassification of pixels, which, although belonging to the class, have a mixed element (figure 7.2a). If the training sample for a class is too heterogeneous (e.g. class 1 in figure 7.2b), either mistakenly, or deliberately in order to avoid a singular covariance matrix, pixels belonging to other classes, may be misclassified into that class (e.g. classes 2 or 3 in figure 7.2b).

The theoretical ideal is to define a training sample which is truly representative of the whole population (Justice and Townshend, 1981; figure 7.2c). However, in practice it is difficult to achieve this, especially in a complex environment with mixing of vegetation types. For example, in this study, the Pteridium aquilinum is fairly homogenous over large areas, but there may be subtle differences in reflectance on slopes facing different directions, or on different slope angles. In addition, some Pteridium-dominated areas may be mixed with other vegetation types (Calluna vulgaris, Vaccinium myrtillus and grasses).

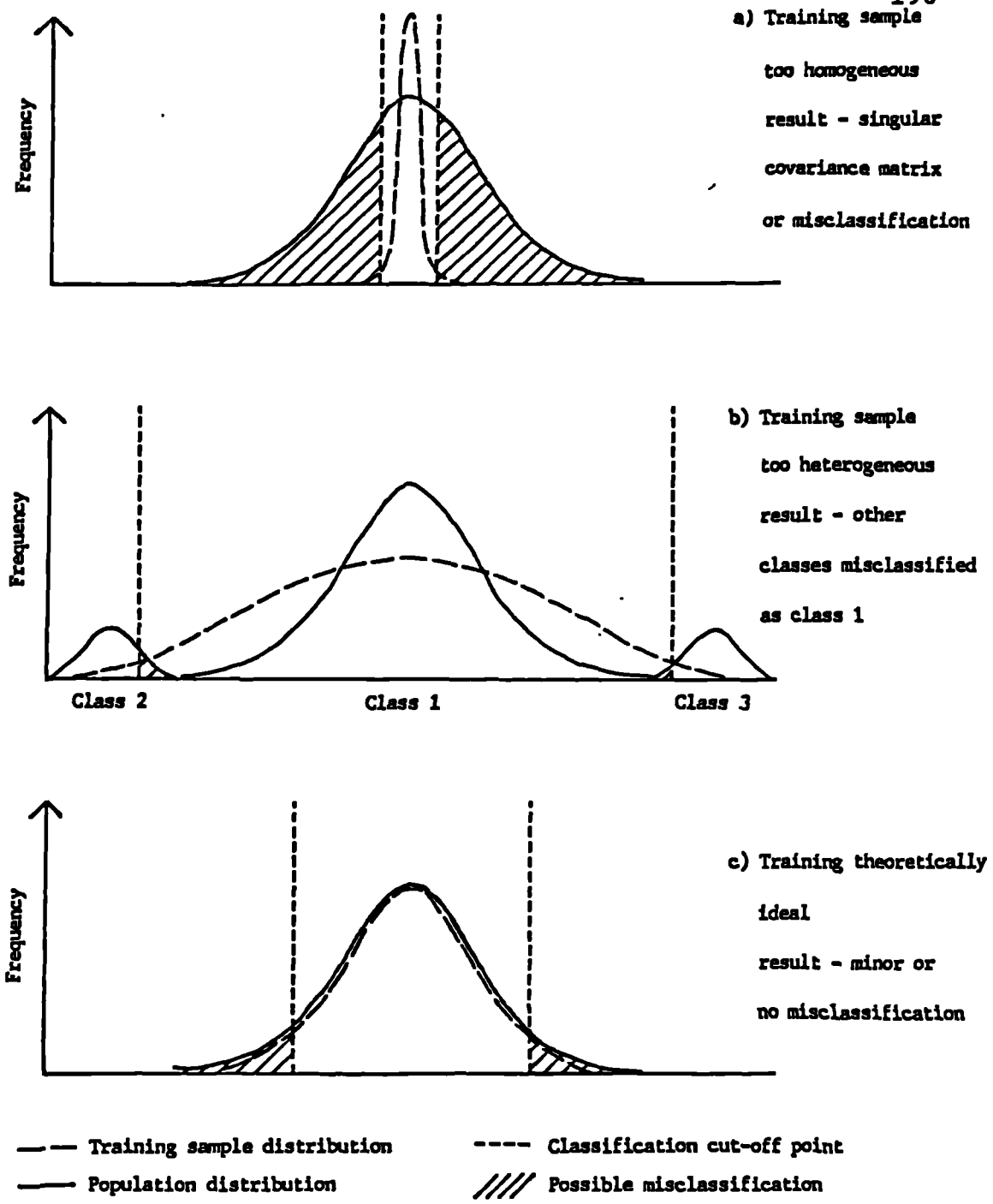

Figure 7.2 The effect of different hypothetical training sample distributions on classification accuracy

If a 'pure' area is selected for training, it may result in either a singular covariance matrix, or large misclassification of Pteridium and Pteridium-dominated areas. If a more mixed training sample is used, it allows the calculation of the covariance matrix, but some non-Pteridium areas may be included in the class.

Thus, a careful balance must be reached. In this case it was done iteratively, expanding or contracting training areas and re-running the classification, in conjunction with the close examination of the statistics and a comparison with the field map, at each editing stage.

The statistics calculated from the training data within the field mapping area (figure 3.1; Appendix 1), were used to extrapolate out to the whole of the North York Moors TM subscene area. Supervised classification techniques often calculate the centroid (mean centre) of each class, and allocate pixels into the class with the nearest centroid. A maximum likelihood algorithm was used in this study, and using this method, distance from the centroid is not the only criterion for classification decision-making, as elliptical probability contours are calculated, based on the covariance matrices (Mather, 1987; Lillesand and Kiefer, 1979). Thus a pixel may have a higher probability of belonging to one class, even though it is closer to another class centroid (figure 7.3).

Various combinations of bands were classified in order to identify most accurate class map image. The optimum TM spectral resolution, identified by discriminant analysis, was entered first; TM4 and TM5 (section 5.5.3.2; table 5.7). Subsequently the optimum three band combination (TM2, TM4 and TM5 in April, and TM4, TM5 and TM7 in May), was tried. The accuracy of each class map image was calculated using the method described above (section 6.4.1). The North York Moors National Park map was divided into sub-sections in order to give an even and complete coverage. Accuracy check points were then randomly selected within 300m of key roads and footpaths in each sub-section.

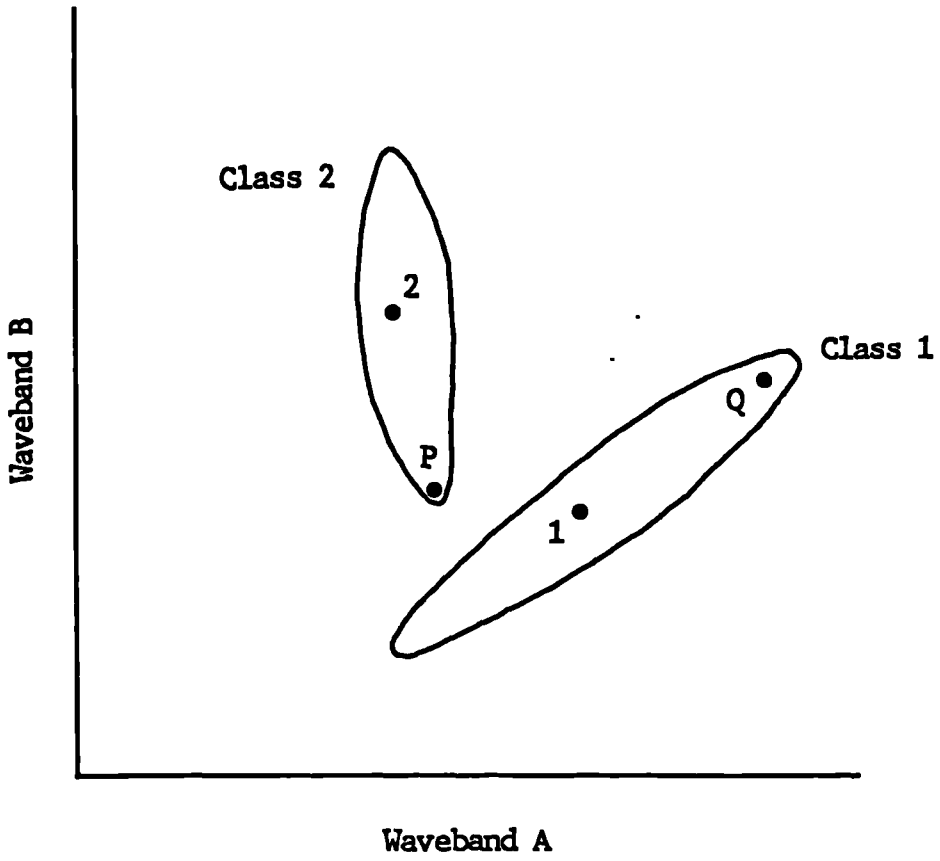

Figure 7.3 Graph showing the bivariate-normal probability ellipses for two classes, similar to those calculated during maximum likelihood classification. Point P is more likely to belong to class 2 than class 1, on the basis of class membership probability, even though P is closer to the centroid of class 1 (after Mather, 1987)

Two hundred and twenty points were selected (table 7.2; figure 7.4), and each one, except for the sea check points, was visited in the field. An area of 120m x 120m (the equivalent of 16 TM pixels) was measured out, centred on each point, using a tape measure and compass. The distribution of vegetation within each area was sketched, and the proportions of species were estimated. Each accuracy check area was classified as the dominant vegetation type. The fact that the sample points were within 300m of roads and footpaths may have slightly biased the representiveness of the sample, as these areas are more likely to be disturbed, and more isolated areas were not sampled. However, footpaths crossing isolated areas were included, giving a fairly even distribution of check points (figure 7.4). It was not possible to collect full-scale non-stratified random sample, because of logistical and time constraints. It was also impossible to visit restricted military danger areas, and this caused the exclusion of a fairly large area in the north east of the moorland (on Fylingdales Moor).

class	number of accuracy check points
Calluna vulgaris	58
Burnt/bare	19
Pteridium aquilinum	29
Water	30
Forest	33
Grassland	12
Agriculture	39
Total	220

Table 7.2 The number of field check points in each class, used to calculate the accuracy of the supervised classification of Landsat Thematic Mapper data

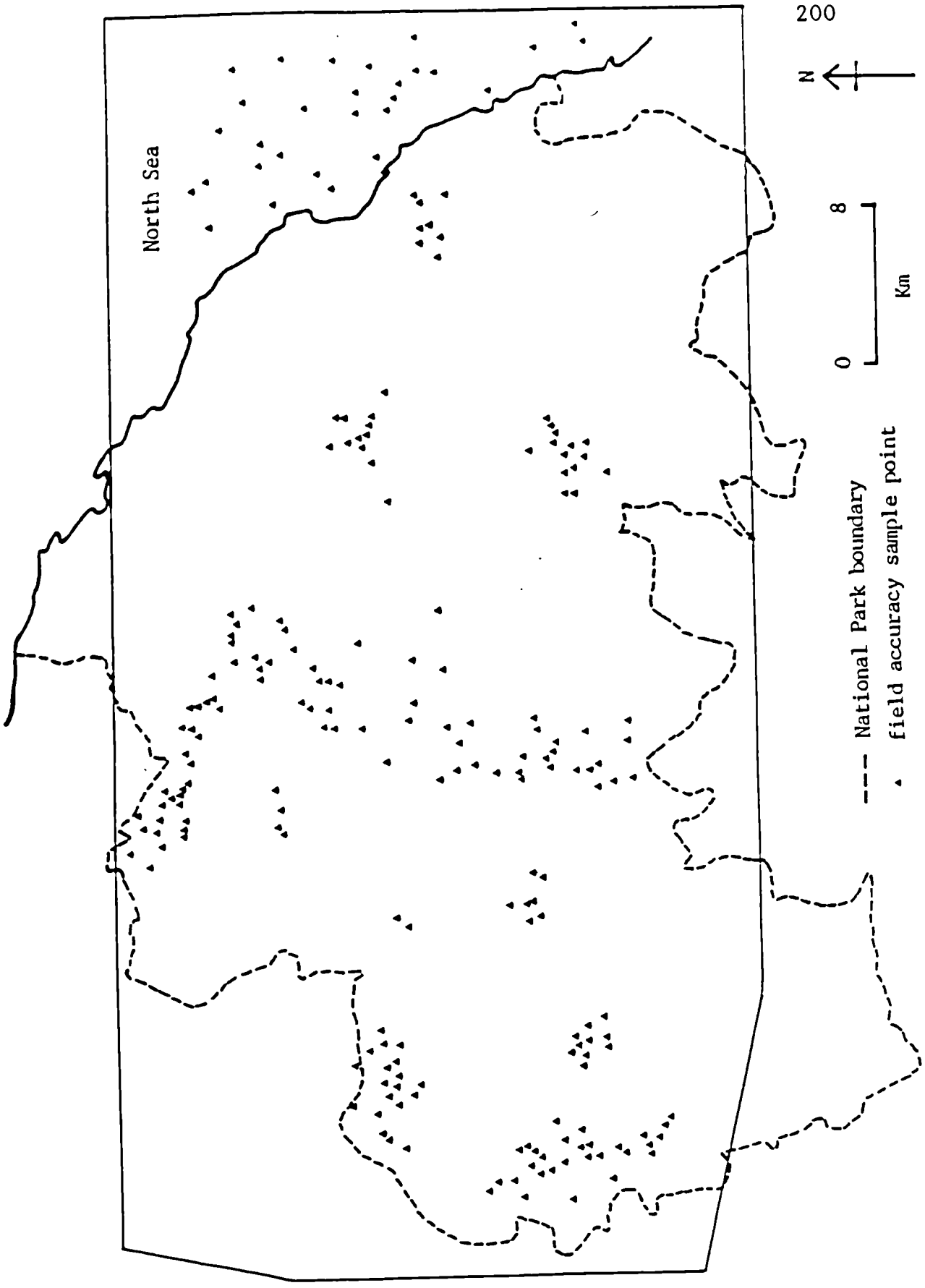

Figure 7.4 The location of the field accuracy check points

The final step in the analysis was an assessment of the effect of various smoothing and filtering algorithms on mapping accuracy. These were performed on the optimum three band combinations, prior to classification, to reduce small-scale fluctuations or anomalies, and to remove local variability, in order to enable the identification of general trends in the vegetation distribution, and to attempt improvement in accuracy.

Low-pass spatial-domain filters were used on the two TM images. Such methods use a moving kernel (or window), which passes over the entire image causing a general smoothing. This is achieved by the removal of unwanted high frequency detail, or scene noise, to reveal the background pattern (Mather, 1987).

A mean filter was tried, using 3x3 and 5x5 pixel kernels. As the kernel moves over the image it averages the values within the window and replaces the central pixel value with the mean (Cushnie and Atkinson, 1985). This reduces the overall variation of the image, but tends to lead to the blurring of boundaries (Showengerdt, 1983).

A two-dimensional Tukey median filter with a 3x3 square kernel was subsequently used (I^2S, 1987). This is an alternative, non-linear technique, which attempts to avoid blurring. In this case the median of the kernel replaces the central pixel value (Cushnie and Atkinson, 1985). The median method smooths the image in a similar way to the mean filter, cutting out unwanted noise, but has the advantage of preserving sharp edges (Mather, 1987; Atkinson et al, 1985).

The accuracy of each filtered classification image map was calculated using the method described above (section 6.4.1) and the 220 field visited accuracy check points (table 7.2; figure 7.4).

In addition, the Pteridium aquilinum and moorland areas were drawn from the most accurate classifications for each TM date (figures 7.13 to 7.16). The accuracy of these class maps, compared to the North York Moors National Park Published maps (North York Moors National

Park Committee, 1984b; figures 7.5 and 7.6), were calculated using the same method and 200 check points described above for the false colour composite class maps.

7.4 Visual interpretation of photographic prints of individual wavebands

The optimum individual bands (TM5 in April 1984, and TM4 in May 1985) are shown in plates 7.2 and 7.3. On these black and white images, spectral DN values are represented by grey-tones; the darker the tone the lower the reflectance. Although it may be possible to separate pairs of cover types successfully using only one band (section 5.5.3.2; table 5.5), it is difficult to separate all moorland surfaces adequately without using at least two wavebands (section 5.5.3.3; table 5.6). Thus it may be expected that the use of single band black and white images will be problematic.

Nevertheless, considerable information is held within these images. The general outline of the upland Calluna vulgaris moorland (figure 7.5), is quite evident, especially on the 1985 TM scene (plate 7.3). The moorland is shown in dark tones. However, on this image there is little distinction between moorland, forest (mainly in a large block in the south east of the image) and water (mainly the North Sea), all of which have similar dark grey or black tones.

On the 1984 image (plate 7.2), there is greater contrast between the forest and the moorland, as the moorland has a lighter appearance. However, on this scene, the lighter tones of the moorland are similar to the agricultural areas, which are represented as light grey or white on both TM images.

Pteridium aquilinum areas (figure 7.6) are evident, particularly on the 1985 data, as a mid-grey tone, mainly in narrow bands surrounding the moorland. However, such Pteridium areas do not contrast greatly with either the moorland or the agriculture, and they are almost indistinguishable from grassland.

Plate 7.2 Landsat Thematic Mapper band TM5, April 1984

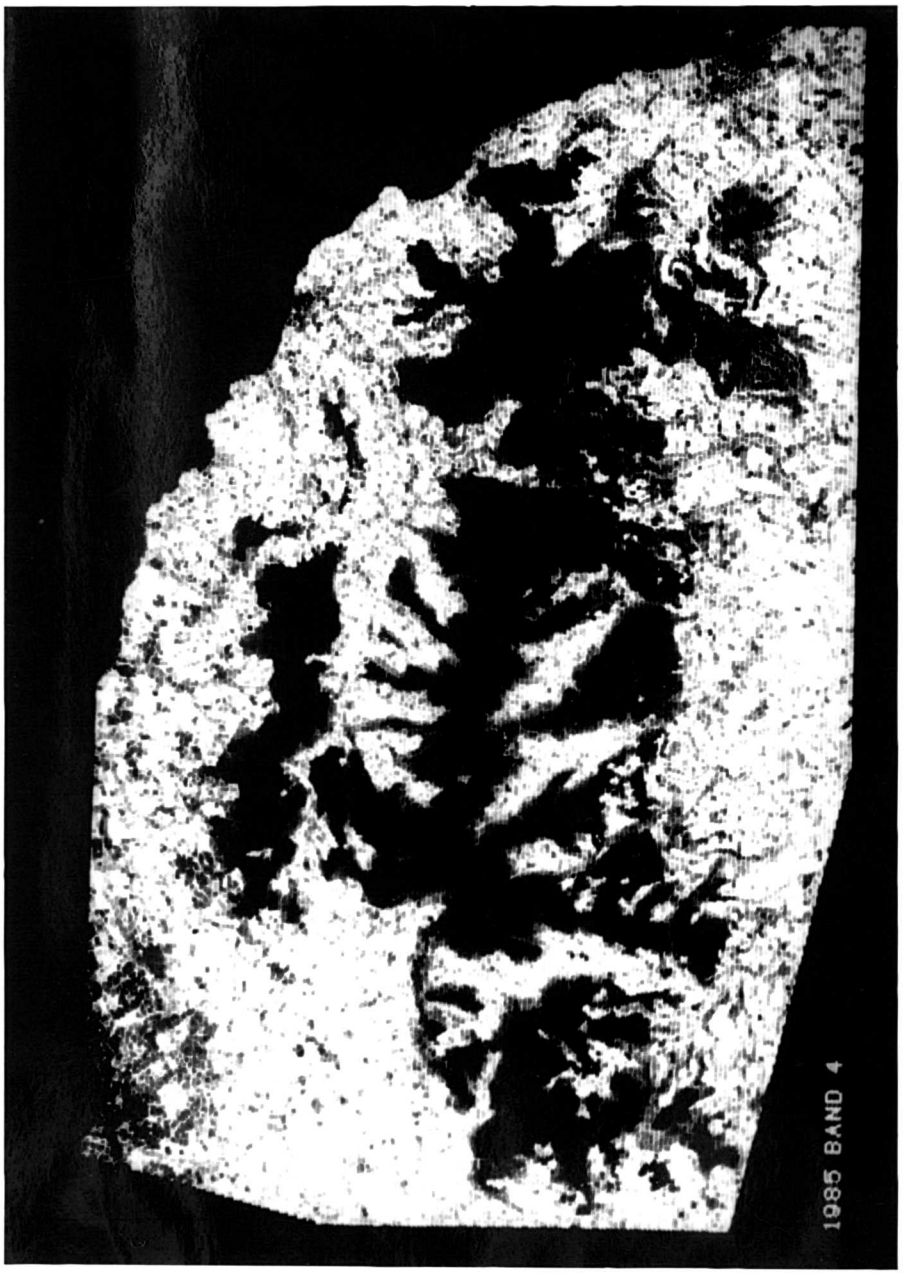

Plate 7.3 Landsat Thematic Mapper band TM4, May 1985

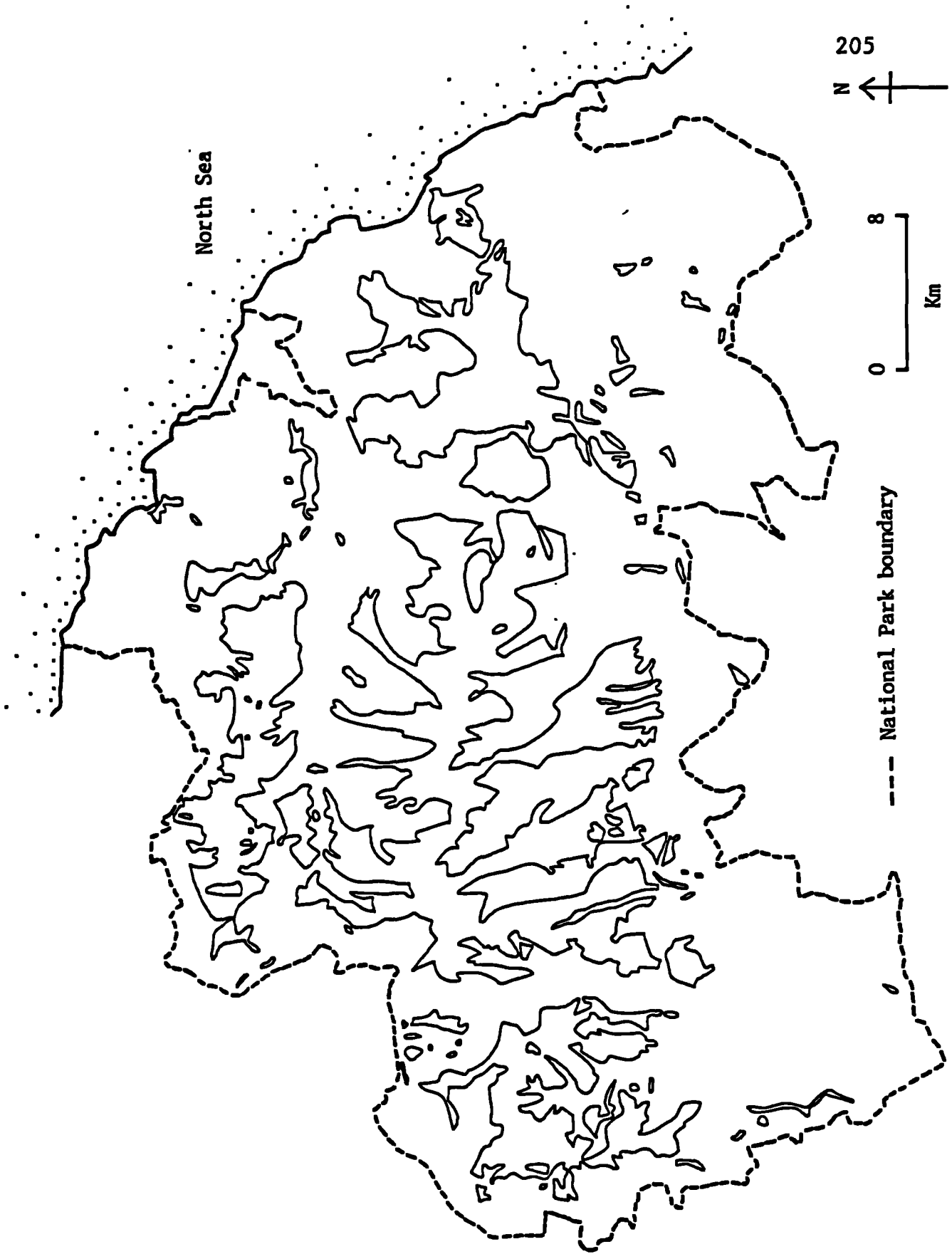

Figure 7.5 Moorland class map: North York Moors National Park Map
(after North York Moors National Park Committee, 1984b)

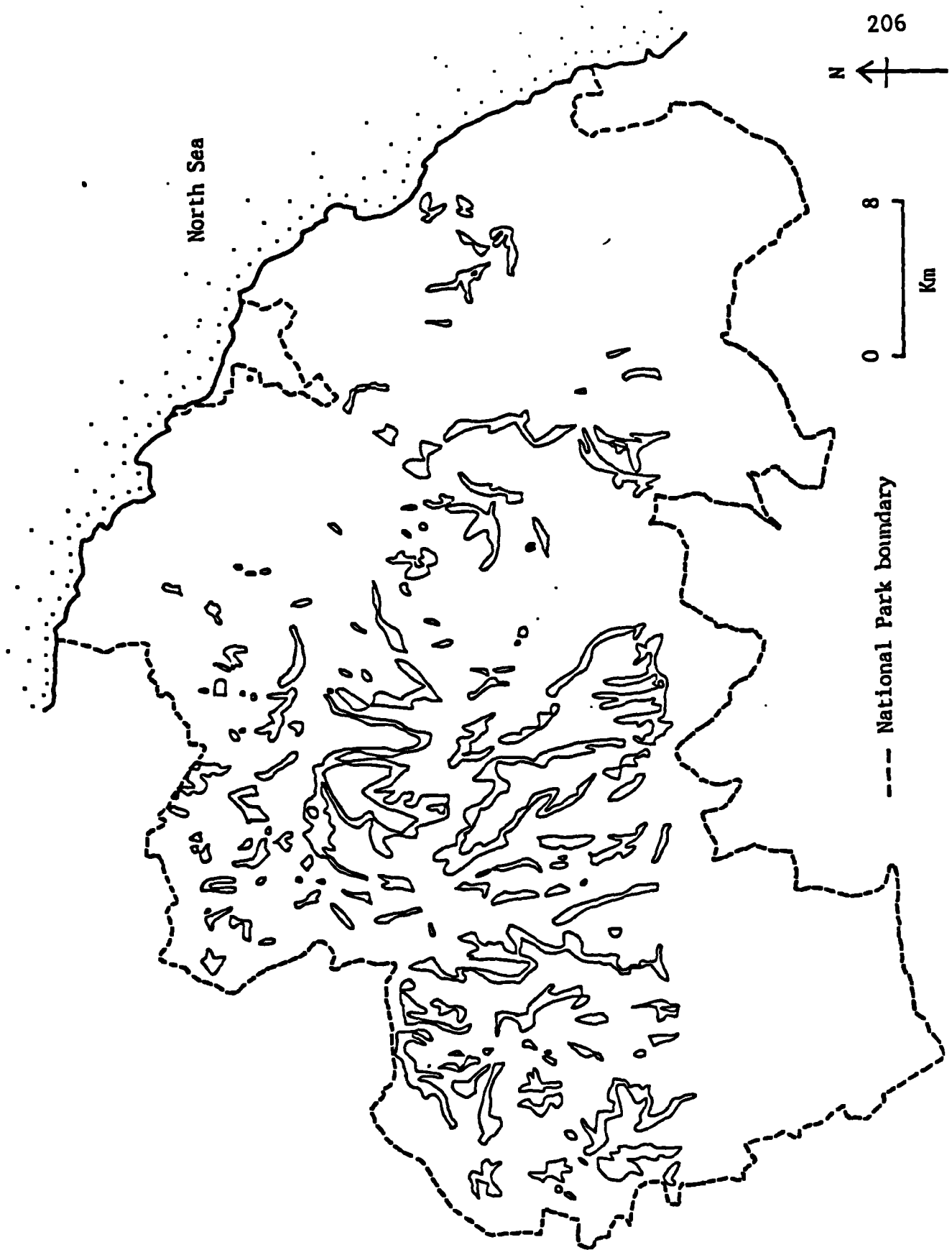

Figure 7.6 Pteridium aquilinum class map: North York Moors National Park Map (after North York Moors National Park Committee, 1984b)

Thus, as was suggested above, selected single bands may allow for successful pair-wise separation of classes, but discrimination between many classes is virtually impossible. Information about the spectral characteristics of surfaces is restricted to one portion of the electro-magnetic spectrum, and differences in reflectance in that one spectral region, are represented by subtle variations in grey-tone, which are, in many cases, imperceptible to the human eye.

7.5 False colour composites

Multispectral data give a further dimension to aid interpretation. The use of three bands in a false colour composite allows classes to appear more visually separable, on the basis of colours and shades, rather than just grey-tones, which are more easily detected by the human eye. This creates the potential for a greater contrast between surface types.

7.5.1 Visual interpretation of false colour composite photographic prints

The greater contrast between basic cover types, compared to the black and white images, is evident on both false colour composite images (plates 7.4 and 7.5). On the April 1984 image (green, near IR and SWIR; plate 7.4) the upland moor area (figure 7.5) is clearly shown as a patchwork of purple and dark blue tones. On closer examination of the eight subscenes, blocks of various shades become apparent, and these represent contiguous areas of similar aged Calluna vulgaris, brought about as a result of the burning management regime. Lighter blue areas correspond to pioneer or recently burnt Calluna, and the lightest tones, with a pink tinge, represent disturbed areas where Calluna is mixed with grasses.

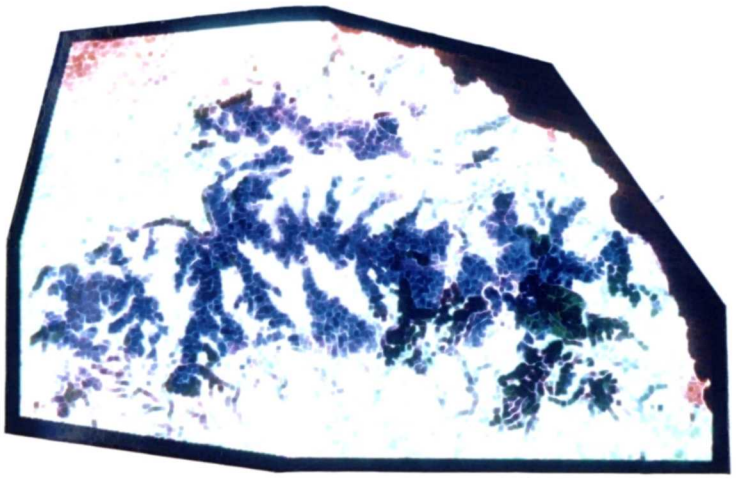

Plate 7.4 Landsat Thematic Mapper false colour composite: April 1984, bands TM2, TM4 and TM5

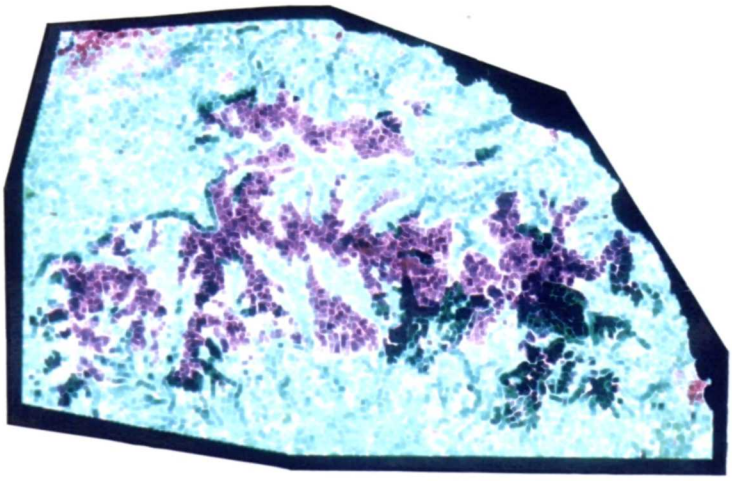

Plate 7.5 Landsat Thematic Mapper false colour composite: May 1985, bands TM7, TM4 and TM5

The narrow Pteridium aquilinum areas surrounding the moorland (figure 7.6) are shown in pink, with a blue/grey tinge. The limits between moorland and Pteridium are sharp in some cases, but in others the change in colour is transitional, recording the mixing of species in the boundary zone. There appears to considerable similarity between tones associated with Pteridium, grassland and some agricultural fields, reflecting the lack of green vegetation present at the surface in all three cases.

The water (mainly the sea) is represented by very dark, almost black, tones, due to the high absorption of light in all wavebands. The forested areas are also quite distinct, especially the evergreen conifer plantations, which are mainly in the south east of the scene. These areas are shown in dark green. However, closer examination reveals brown or purple/brown areas, both within plantations, and in independent small blocks. Such colours denote areas of deciduous woodland, including deciduous conifers, such as Larix kaempferi (Japanese larch), within plantations.

The agricultural areas are in marked contrast to the moorland, being primarily characterised by light tones; mid to light green, light pink and white. Individual fields are clearly apparent, especially in regions outside the moorland valleys, to the south and north west of the scene. The different tones represent different landuse; improved pasture, ploughed fields and rough grazing.

Urban areas are depicted in dark pink or red; the major built-up areas being Middlesbrough in the north west, and Whitby and Scarborough on the coast. The darkest red areas represent the central, most intensively built-up areas, and these are quite distinctive. However, areas close to to the edge of urban areas are shown by a lighter pink, together with light green and white tones. These probably represent gardens, open spaces, allotments or parks in the more spacious suburbs.

Most major roads are visible only where they cross the moorland, as the contrast with the background is great (this is more apparent on the enlarged subscenes). In the agricultural areas the roads become lost among the pale shades of the fields.

On the May 1985 image (TM7, TM4 and TM5; plate 7.5) cover types are represented by similar colours to the 1984 scene, the main differences being in the tones associated with moorland and agriculture. The moorland area is more purple than blue and the pioneer and recently burnt areas are pink. The agricultural areas are dominated by pale blue/green and white tones, and there are few pink fields, probably reflecting the fewer number of bare fields at this more advanced stage of the crop cycle.

The Pteridium aquilinum areas are denoted by light pink/white tones and they are more sharply contrasted with the moorland and agriculture than on the 1984 scene.

There is less variation within the conifer plantations than in 1984, with the brown deciduous areas now being coloured mid-green, again probably due to the later date of the scene.

Overall, the replacement of the green band (TM2) by a SWIR band (TM7) and the slightly later date of the image in the growing season, have resulted in stronger colours and a greater contrast between surface types, especially Pteridium, on the 1985 image.

7.5.2 Quantitative interpretation of false colour composite photographic prints

7.5.2.1 error

At first glance the maps extracted from the TM images (figures 7.7 to 7.10) appear to resemble closely the National Park class maps (figures 7.5 and 7.6). The general shape, relative location and size of vegetation blocks seem very similar in all cases.

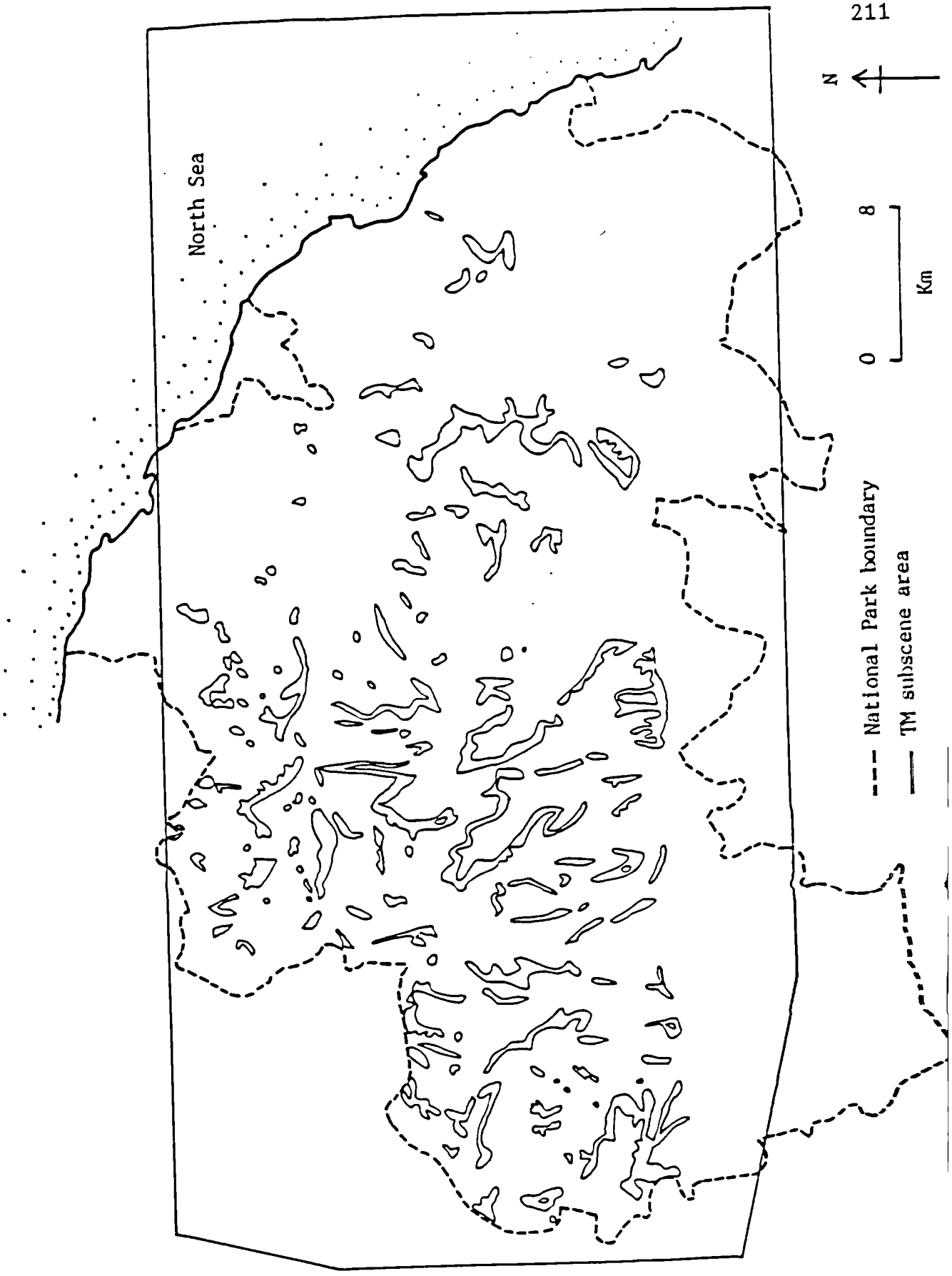

Figure 7.7 Pteridium aquilinum class map: 1984 Landsat Thematic Mapper false colour composite (TM2, TM4 and TM5)

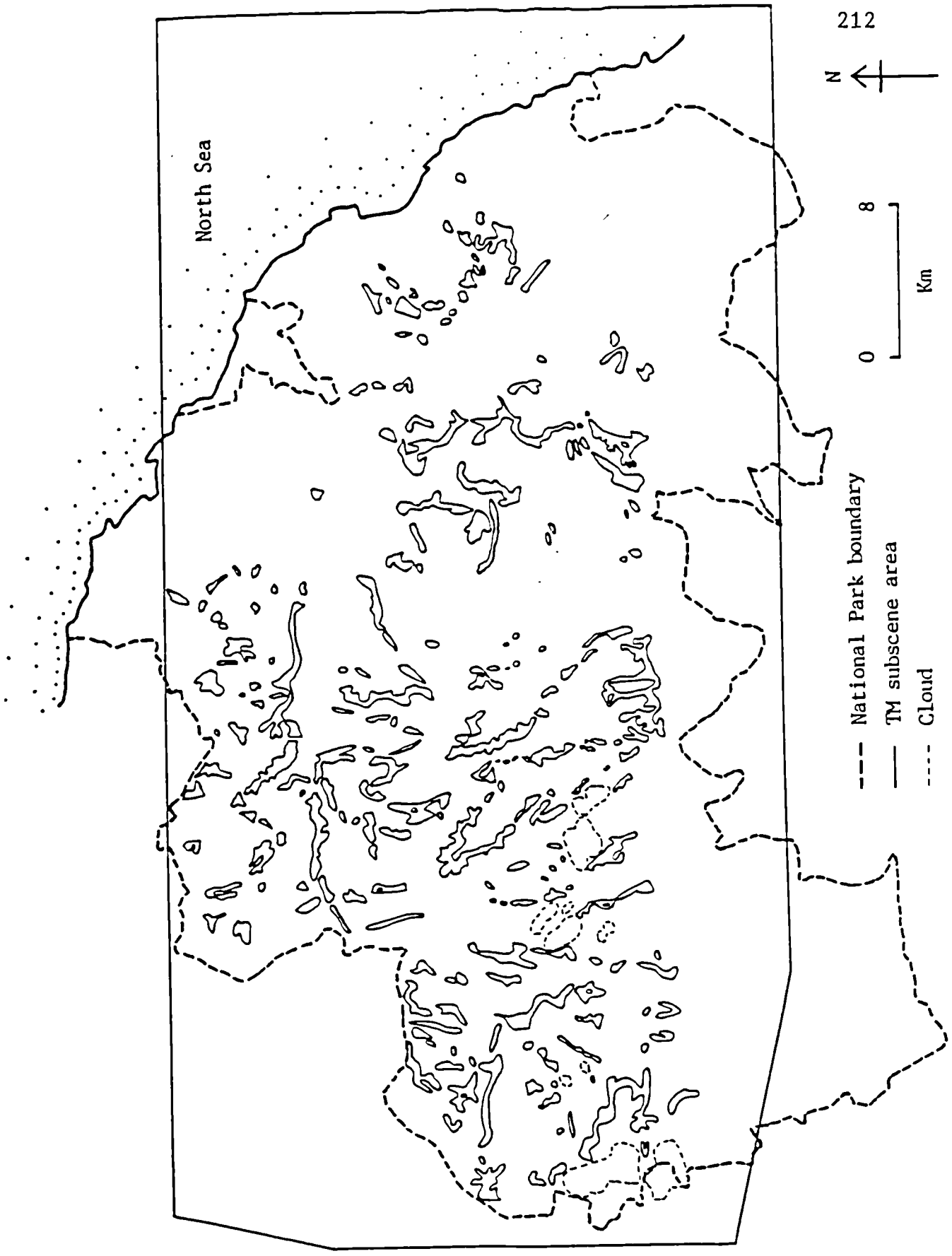

Figure 7.8 Pteridium aquilinum class map: 1985 Landsat Thematic Mapper false colour composite (TM4, TM5 and TM7)

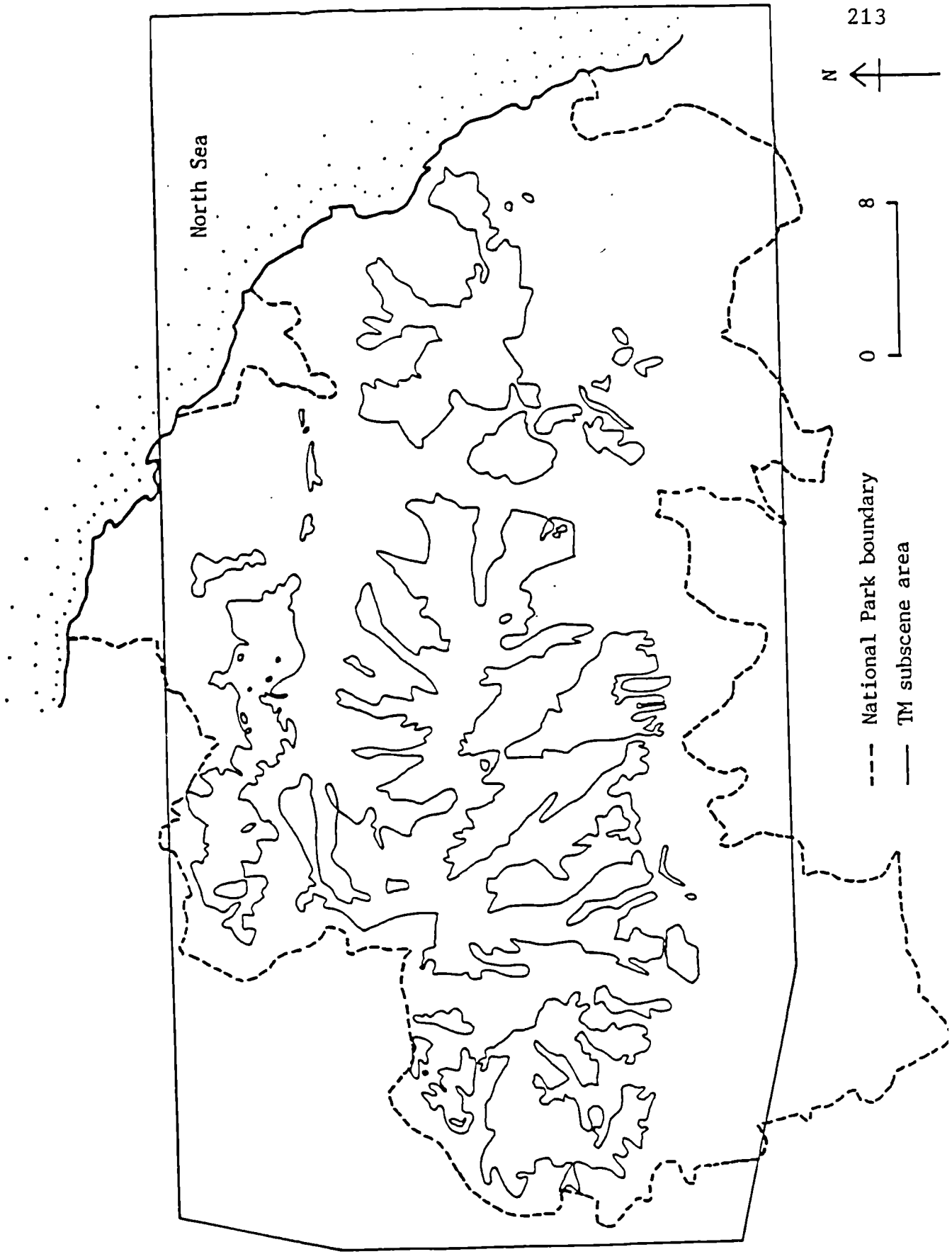

Figure 7.9 Moorland class map: 1984 Landsat Thematic Mapper false colour composite (TM2, TM4 and TM5)

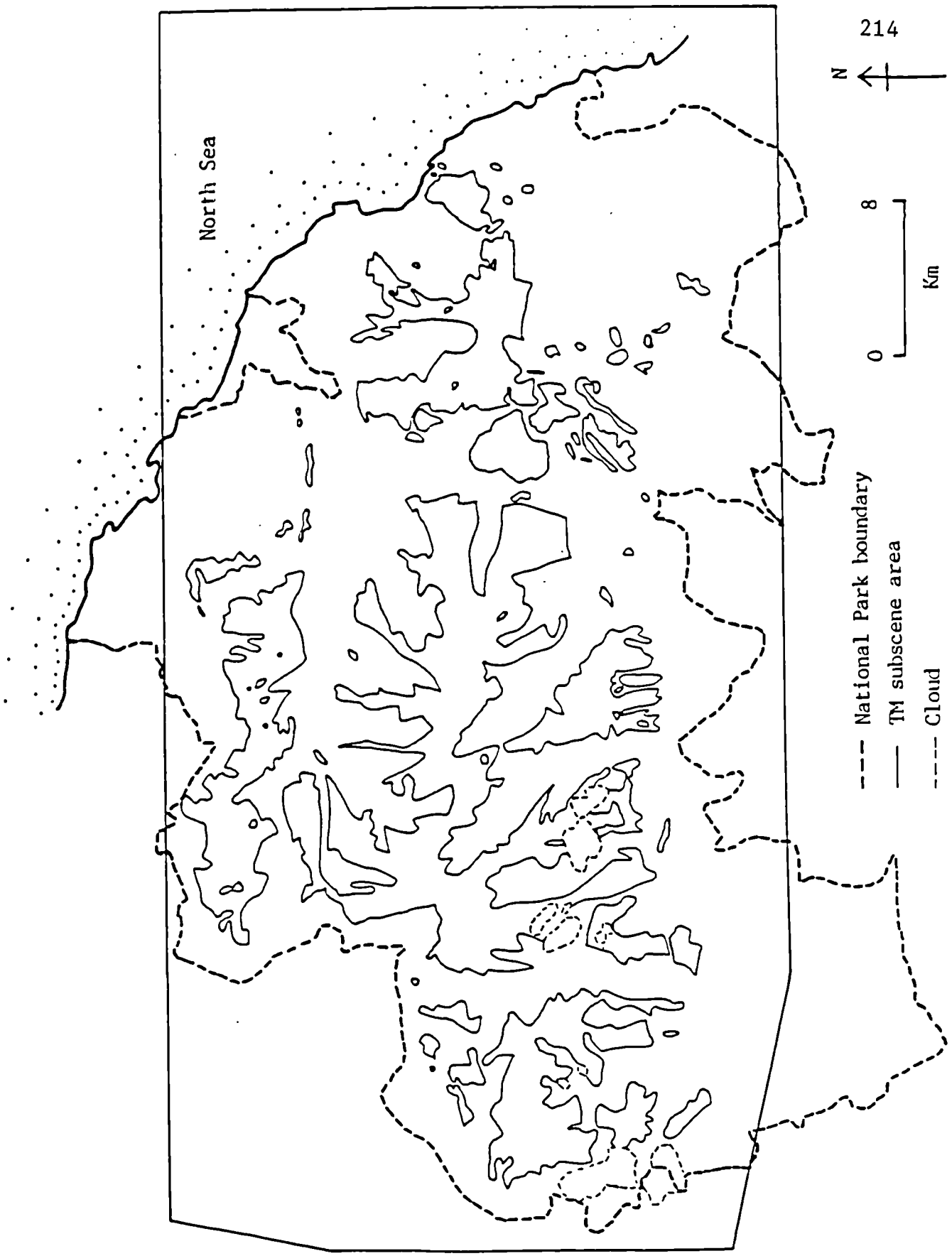

Figure 7.10 Moorland class map: 1985 Landsat Thematic Mapper false colour composite (TM4, TM5 and TM7)

Nevertheless, a quantitative assessment of the success of the false colour composites in mapping these two vegetation types, results in relatively low accuracy values, especially the Pteridium (table 7.3). These results were surprisingly low, considering the general visual similarity between the two sets of maps. However, closer examination and map overlay identified key sources of potential error.

	accuracy (%)	
year	Moorland	Pteridium
1984	79(±8)	43(±10)
1985	82(±7)	45(±10)

Table 7.3 Accuracy values for extracted class maps (figures 7.7 to 7.10); Landsat Thematic Mapper false colour composite images

The primary cause of inaccuracies appears to be the geometric infidelity of the images. Geometric correction and co-registration was completed on the two TM scenes (section 3.7.5.2), but the root mean square (RMS) error was 3.4 pixels, which is around 100m. As with the ATM data (section 6.4.5), such distortions will lead to error. For example, the Pteridium aquilinum areas within the Blakey Ridge study area, are 350m at the widest point, and most blocks are are less than 200m wide (figure App1.2). A shift of 100m in the

boundaries will obviously cause large inaccuracies, with up to 50% of some Pteridium areas on the images, lying outside the map limits. The degree of inaccuracy is clearly dependent on the shape and size of vegetation areas, and is especially bad in the cases of Pteridium aquilinum, which is distributed in narrow strips, and cover types with small areal extent, for example burnt areas and deciduous woodland. An overlay of the National Park map and the image class maps indicates that areas on the images are just to the west of corresponding areas on the National Park base map in the west of the scene, and just east of the base map in the east of the scene. The geometric problems are illustrated by the maximum likelihood classification subscenes (plates 7.9 to 7.14). When the moorland and Pteridium areas taken from the National Park maps are overlaid on the images, the distortions in the subscenes are quite evident, especially on the western side of the images.

Another important likely source of error is the failure of the spectral data to characterise adequately the classes, especially the Pteridium aquilinum, resulting in unsatisfactory discrimination. This error is quite possible, especially on the 1984 image, as expert knowledge was required to exclude areas with similar tones to the Pteridium, which were within the fields of the areas well away from the moorland, and therefore unlikely to be Pteridium. It is a real possibility that areas close to or adjacent to the Pteridium blocks, which were in fact ploughed fields, were included as Pteridium, and that some areas that were assumed to be fields, were in fact infested by Pteridium. The similarity in spectral characteristics, represented by tones, made it impossible to be certain in discriminating between these classes in all cases.

A third source of error is the nature and classification techniques of the National Park maps (figures 7.5 and 7.6). Boundaries appear to be smoothed, and in some cases areas which, on the images appear to be discrete patches of Pteridium along a valley side, have been drawn as contiguous blocks on the National Park map. These generalisations have been confirmed by field work within the Blakey Ridge study area,

and may be seen by a comparison of the National Park map (figure 7.6) with the field map (figure App1.2). Such smoothing is probably due to the classification criteria and methodology used in map preparation, which relate to the requirements of the National Park. Thus, more detail is apparent on the TM images (especially on the 1985 scene; plate 7.5; figure 7.8), than on the National Park map. This suggests that a 30m pixel size would meet the present requirements of the National Park, and is adequate for such large scale vegetation mapping.

Other inaccuracies may have occurred as a result of misregistration in time. Although the National Park map was published in 1984, the same date as the first TM image, they were prepared earlier. Thus differences may have occurred in the vegetation distribution between the time of the map and of the images. However, these changes are likely to be sub-pixel with a 30m pixel size, and would not result in the large errors which are apparent.

A final factor increasing inaccuracy, is error in the subjective interpretation of the false colour composites, especially where the tones change gradually over the transitional zone between vegetation types.

Thus the errors in the image class maps, resulting in low accuracy rates (table 7.3), are caused by a combination of all the above factors, although the geometric distortions and deficiencies in the data are the primary causes. The situation may be improved by more careful geometric correction, using a greater number of ground control points, attempting to get the RMS errors as low as possible, in conjunction with the use of data collected at an optimum temporal resolution (section 4.5.6), to improve the quality of spectral discrimination between surface cover types.

7.5.2.2 Pteridium aquilinum

The geometric distortions have had a large effect on the accuracy values of Pteridium, which tends to occur in narrow bands surrounding the moorland. A shift in the boundary will cause many of the Pteridium accuracy check points to fall just outside the limits of the species on the images, even though the shape of blocks are correctly represented. Discounting the obvious geometrical errors, the shapes and sizes of the Pteridium areas visually extracted from the false colour composite satellite images are very similar to those represented on the National Park map, even with these temporally sub-optimal data. The 1985 data were slightly more accurate than the 1984 data, being 45%($\pm$10%) compared with 43%($\pm$10%) for the 1984 data (table 7.3) (although with error limits of $\pm$10% they are not significantly different). But visually, the 1984 class map resembles the National Park map more closely than the more detailed 1985 map. This is due to the necessary generalisation during interpretation of the 1984 scene, because of the lack of contrast between Pteridium areas and both moorland and agriculture (section 7.5.1). Small-scale boundary undulations and protuberances visible on the more sharply defined Pteridium on the 1985 image, were not distinguishable on the 1984 scene.

7.5.2.3 Moorland

Exactly the same errors which caused inaccuracies in the Pteridium aquilinum class maps, cause similar inaccuracies in the moorland image class maps (figures 7.9 and 7.10). The moorland areas on the images are shifted, because of geometric distortions, compared with the corresponding areas on the National Park map (figure 7.5). However, in this case, the accuracy values are considerably higher; 79%($\pm$8%) for the 1984 image, and 82%($\pm$7%) for the 1985 image (table 7.3). The main reason for this is the larger size of contiguous blocks of moorland, compared to the narrow strips of Pteridium, which means that even if the moorland is shifted, the accuracy points are

still likely to be within the boundaries. Only those points close to the limits will be affected by the geometric problems.

7.5.2.4 Discussion

A skilled interpreter, trained on an area where ground conditions are known (in this case the field study area; appendix 1), and with a general field knowledge of the environment, may successfully and quickly produce reasonably accurate representations of Pteridium aquilinum and moorland areas, from false colour composite image photographic prints, equal to or exceeding the detail required by the National Park for their published maps. The National Park maps were prepared using expensive and time-consuming field work, with the support of aerial photographs, with all the geometric problems inherently associated with an unstable aircraft base. The mapping project was completed over a two year period, with a budget of £80,000 (Dr. R. Brown, personal communication). The National Park procedure took considerably longer, and cost more, than the interpretation of false colour composite TM images described above. If the geometric quality of the scene can be improved, and an optimal date selected, it would appear possible to produce class maps comparable to the present National Park maps, accurately, quickly and relatively inexpensively, using Landsat TM images.

7.6 Maximum likelihood classification of Landsat TM images

The maximum likelihood classification of different TM bands and filter combinations, resulted in a fairly large range of accuracy values, from a low of 52.7%($\pm$7%) for a 5x5 mean filter of TM4, TM5 and TM7 in 1985, to a high of 65.5%($\pm$6%) for bands TM3 and TM4 in 1984 (plate 7.6), a 3x3 mean filter of bands TM2, TM4 and TM5 in 1984 (plate 7.7), and the unfiltered TM4, TM5 and TM7 in 1985 (plate 7.8) (figure 7.11; table 7.4). The effect of spatial filtering on classification accuracy is considered below (section 7.7).

KEY TO THE MAXIMUM LIKELIHOOD CLASSIFICATION IMAGES (plates 7.6 to 7.14)

purple	=	Calluna vulgaris
dark grey/green	=	Burnt/bare
red	=	Pteridium aquilinum
dark blue	=	Water
brown	=	forest
yellow	=	Grassland
green	=	Agriculture

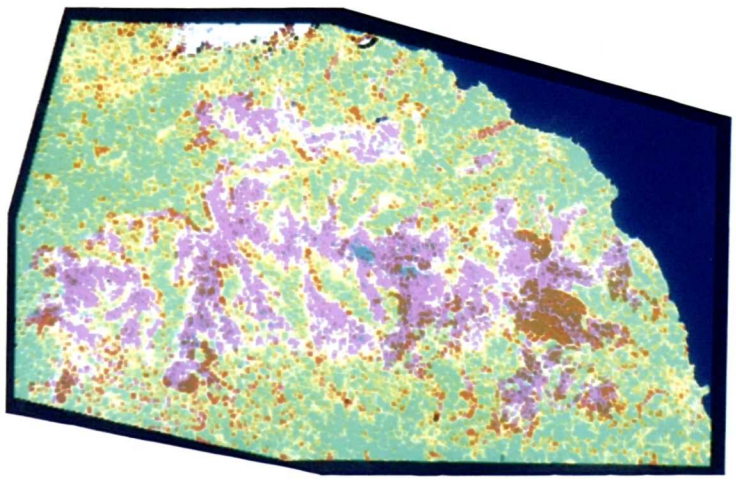

Plate 7.6 Maximum likelihood classification image: Landsat Thematic Mapper bands TM3 and TM4, April 1984

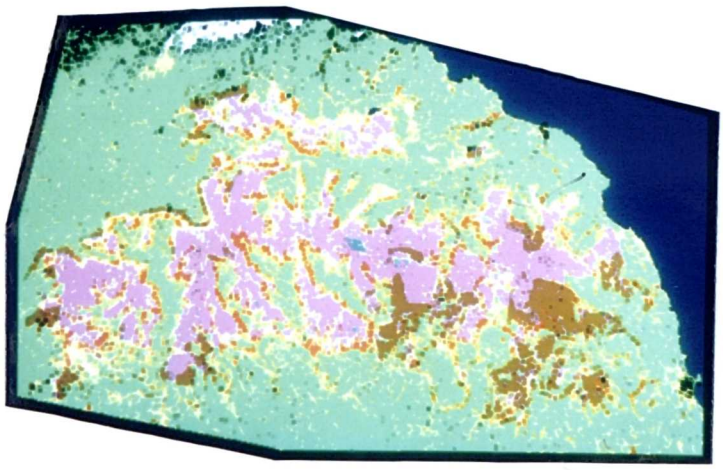

Plate 7.7 Maximum likelihood classification image: Landsat Thematic Mapper, 3x3 mean filter of bands TM2, TM4 and TM5, April 1984

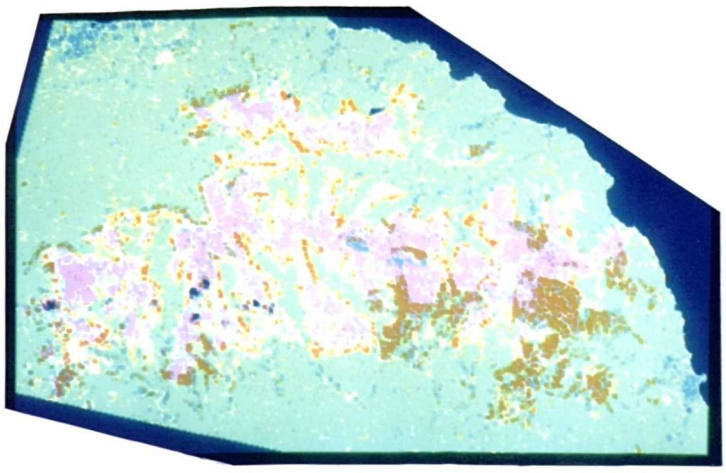

Plate 7.8 Maximum likelihood classification image: Landsat Thematic Mapper, bands TM4, TM5 and TM7, May 1985

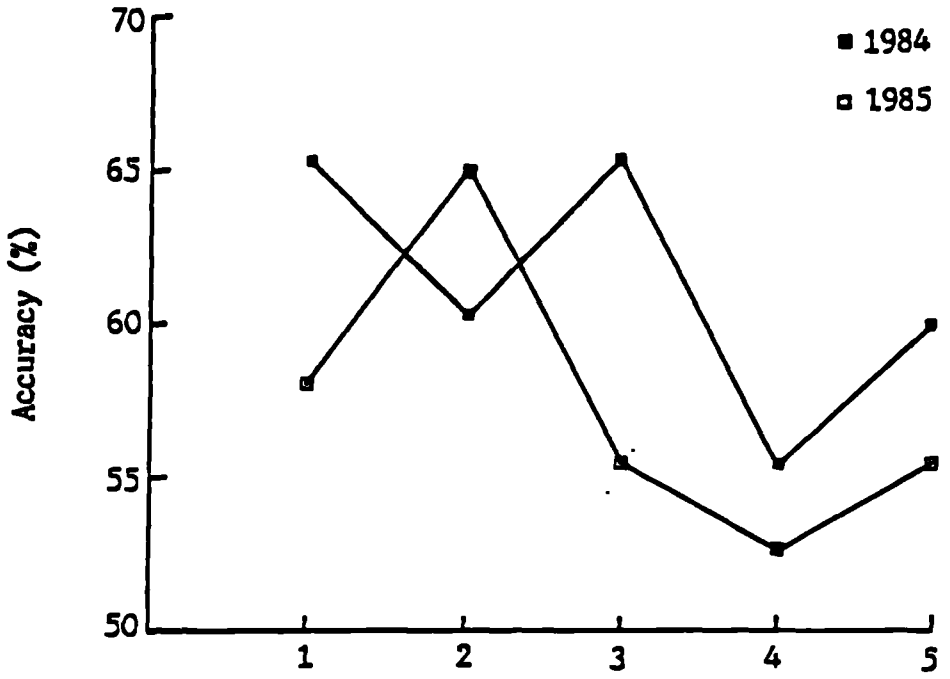

KEY

1=TM3 and TM4

2=TM2,TM4 and TM5 (1984) and TM4,TM5 and TM7 (1985)

3=3x3 (mean) TM2,TM4 and TM5 (1984) and TM4,TM5 and TM7 (1985)

4=5x5 (mean) TM2,TM4 and TM5 (1984) and TM4,TM5 and TM7 (1985)

5=3x3 (median) TM2,TM4 and TM5 (1984) and TM4,TM5 and TM7 (1985)

Figure 7.11 The accuracy of maximum likelihood classifications of various Landsat Thematic Mapper band and filter combinations

year	accuracy (%)				
bands*	1	2	3	4	5
1984	65.5 (±6)	60.5 (±6)	65.5 (±6)	55.9 (±7)	60.0 (±6)
1985	58.2 (±7)	65.0 (±6)	55.9 (±7)	52.7 (±7)	55.5 (±7)

*KEY
1=TM3 and TM4
2=TM2,TM4 and TM5 (1984) and TM4,TM5 and TM7 (1985)
3=3x3 (mean) TM2,TM4 and TM5 (1984) and TM4,TM5 and TM7 (1985)
4=5x5 (mean) TM2,TM4 and TM5 (1984) and TM4,TM5 and TM7 (1985)
5=3x3 (median) TM2,TM4 and TM5 (1984) and TM4,TM5 and TM7 (1985)

Table 7.4 Comparison of Maximum Likelihood classification accuracy values, for different combinations of Landsat Thematic Mapper bands and filter techniques

The accuracy values calculated with the 220 field check points may not completely reflect the overall accuracy of the image as a whole. This may be illustrated by the three best classification images. All have the same accuracy value, but there are striking differences between them. The most obvious of these is the large error in agricultural areas being misclassified as grassland and Pteridium aquilinum, particularly in the 1984 TM3 and TM4 image (plate 7.6), and to a slightly lesser extent in the other 1984 image (plate 7.7). The 1985 image shows a large number of fields classified as grassland, but few as Pteridium (plate 7.8). However, few of these errors were picked-up in the accuracy assessment, as the field

accuracy check points were mainly on the actual moorland area, or in agricultural fields close to the moorland. Thus, although it is apparently visually obvious that there is greater misclassification in the 1984 data (particularly the two-band image), all three classification images have an identical accuracy value.

Having stated that there is probably a greater degree of misclassification than is reflected in the accuracy values (figure 7.11; table 7.4), it must also be mentioned that of the misclassification recorded at the field accuracy check points, a fairly large proportion were inaccurate merely because of a shift in vegetation areas caused by geometric distortions. In many cases the size and shape of vegetation blocks were correctly represented, but they were in slightly wrong locations (section 7.5.2.1). Thus the generally low values (none above 65%) may be a true reflection of the overall level of inaccuracy present in the classification images (including the large agriculture misclassification), but may be an underestimate of the potential of the data to map accurately the vegetation of the central moorland area. The areas of moorland (figure 7.5), Pteridium aquilinum (figure 7.6), sea and forest, are generally fairly accurately represented in all three images. Therefore, it may be concluded that if the geometric errors were reduced, accuracy values would rise quite considerably.

It is difficult to appreciate details on a photograph of the whole moorland area, and the types of cover which are correctly classified, and the classes where errors are more common, may be more easily described with reference to a more detailed subscene. Therefore, one of the eight subscenes was chosen as a representative example to illustrate the discussion (plates 7.9 to 7.11; the location of the subscene is shown in figure 7.1). The areas of Pteridium aquilinum and moorland for the part of the National Park covered by the subscene has been enlarged to the same scale for comparison (figure 7.12), and is shown as an overlay on each subscene.

Moorland Pteridium

KEY

purple	=	Calluna vulgaris
dark grey/green	=	Burnt/bare
red	=	Pteridium aquilinum
dark blue	=	Water
brown	=	forest
yellow	=	Grassland
green	=	Agriculture

Plate 7.9 Subscene of maximum likelihood classification image: Landsat Thematic Mapper bands TM3 and TM4, April 1984 (the overlay shows an extract from the National park maps; figure 7.12)

Moorland Pteridium

KEY

purple	=	Calluna vulgaris
dark grey/green	=	Burnt/bare
red	=	Pteridium aquilinum
dark blue	=	Water
brown	=	*forest*
yellow	=	Grassland
green	=	Agriculture

Plate 7.10 Subscene of maximum likelihood classification image: Landsat Thematic Mapper, 3x3 mean filter of bands TM2, TM4 and TM5, April 1984 (the overlay shows an extract from the National park maps; figure 7.12)

Moorland Pteridium

KEY

purple	=	Calluna vulgaris
dark grey/green	=	Burnt/bare
red	=	Pteridium aquilinum
dark blue	=	Water
brown	=	forest
yellow	=	Grassland
green	=	Agriculture

Plate 7.11 Subscene of maximum likelihood classification image: Landsat Thematic Mapper, bands TM4, TM5 and TM7, May 1985 (the overlay shows an extract from the National park maps; figure 7.12)

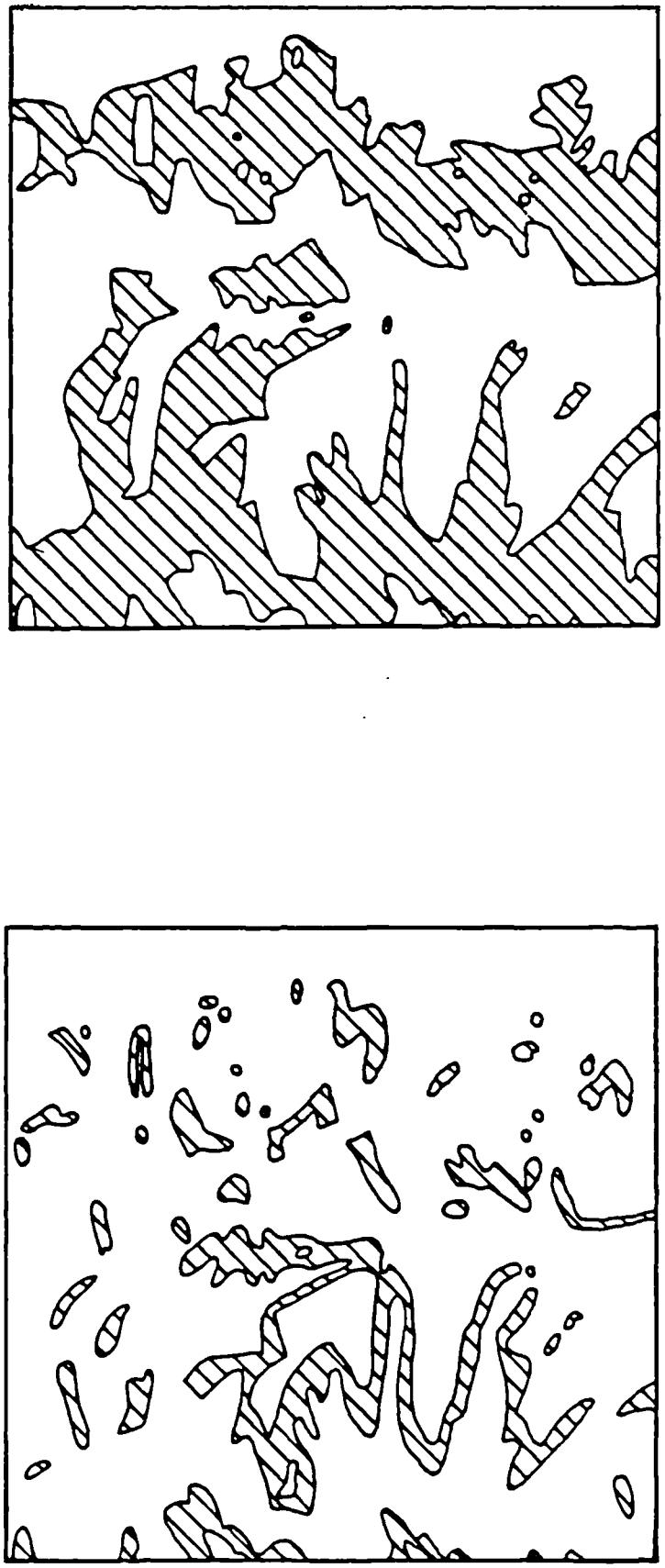

Figure 7.12 An enlarged section of the National Park map, covering the area of the example Landsat Thematic Mapper subscene

The most accurate category in all three cases is the water at 93% (tables 7.5 to 7.7). This class is practically absent from the subscene area, the main area being the North Sea, but there are two small triangular-shaped lakes towards the top of the subscene image (shown in dark blue/black). These are shown accurately in all three of the images. The two water accuracy check points that were misclassified, were in error due to the geometric inaccuracies; they were close to the coast on the National Park map, and due to the differences, were over the land on the images.

The agricultural class (shown in green), has the second highest accuracy in two of the images (plates 7.10 and 7.11); being 72% on the 1984 three band filtered image (table 7.6) and 82% on the 1985 image (table 7.7). The accuracy was slightly lower on the two band 1984 image, being only 62% (table 7.5). The lower accuracy of the agriculture class on this image is illustrated on the subscene, where a large number of fields and field boundaries have been mistakenly allocated to other classes (plate 7.9). The majority of the misclassification of agriculture in all cases was into the grass (yellow) and Pteridium (red) categories due to spectral similarities between these three surface types in the early part of the growing season.

The burnt/bare category (shown in dark grey/green) has relatively high accuracy rates for the two band 1984 image (73%; table 7.5), and the 1985 image (78%; table 7.7). The three band filtered 1984 image has a lower burnt accuracy of 57% (table 7.6). In all cases the misclassification is into four other classes, Calluna vulgaris, Pteridium aquilinum, grassland and agriculture. The main reason for the misclassification is because of the relatively small size of the burnt areas, which results in errors when the images are geometrically distorted. The small size of such areas is also responsible for the lower accuracy of the three band 1984 image for this class; this image was filtered (3x3) prior to classification, and this resulted in the loss through averaging of many small-scale features.

real class	No. of cases	image class						
		Cv	Bu	Pa	Wa	For	Gr	Ag
Cv	58	65.5	2.0	8.5	0	0	20.5	3.5
Bu	19	5.5	73.0	5.5	0	0	10.5	5.5
Pa	29	17.0	0	59.0	0	0	17.0	7.0
Wa	30	0	0	3.5	93.0	0	0	3.5
For	33	20.5	0	14.5	0	27.0	20.5	17.5
Gr	12	0	0	0	0	0	83.5	16.5
Ag	39	2.5	0	5.0	0	0	30.5	62.0

Overall accuracy = 65.5% (±6%)

Class Key: Cv=Calluna Bu=Burnt/bare Pa=Pteridium Wa=Water
Gr=Grassland Ag=Agriculture

Table 7.5 Maximum Likelihood classification accuracy confusion matrix; 1984 Landsat Thematic Mapper data, bands TM3 and TM4

real class	No. of cases	image class						
		Cv	Bu	Pa	Wa	For	Gr	Ag
Cv	58	63.5	2.0	8.5	0	0	14.0	12.0
Bu	19	5.5	57.0	10.5	0	0	16.0	5.5
Pa	29	17.0	0	69.0	0	0	10.5	3.5
Wa	30	0	0	0	93.0	0	3.5	3.5
For	33	21.0	6.0	21.0	0	34.0	9.0	9.0
Gr	12	8.5	0	0	0	0	66.5	25.0
Ag	39	0	0	7.5	0	2.5	18.0	72.0

Overall accuracy = 65.5% ($\pm$6%)

Class Key: Cv=Calluna Bu=Burnt/bare Pa=Pteridium Wa=Water Gr=Grassland
Ag=Agriculture

Table 7.6 Maximum Likelihood classification accuracy confusion matrix; 1984 Landsat Thematic Mapper data, bands TM2, TM4 and TM5 (3x3 mean filter)

real class	No. of cases	image class						
		Cv	Bu	Pa	Wa	For	Gr	Ag
Cv	58	62.0	1.7	5.0	0	0	27.5	3.5
Bu	19	5.5	78.0	5.5	0	0	5.5	5.5
Pa	29	20.5	0	52.0	0	3.5	13.5	10.5
Wa	30	0	0	0	93.0	0	0	7.0
For	33	18.0	3.0	0	0	39.5	24.0	15.5
Gr	12	8.5	0	0	0	0	66.5	25.0
Ag	39	2.5	0	2.5	0	0	13.0	82.0

Overall accuracy = 65.5% (±6%)

Class Key: Cv=Calluna Bu=Burnt/bare Pa=Pteridium Wa=Water
Gr=Grassland Ag=Agriculture

Table 7.7 Maximum Likelihood classification accuracy confusion matrix; 1985 Landsat Thematic Mapper data, bands TM4, TM5 and TM7

This may be seen on the example subscenes, where there are far fewer small areas of burnt (shown in dark grey/green) within the moorland region (plate 7.10). The extensive bare area on Glaisdale Moor (in the extreme south east of the subscene), which resulted from a severe fire in 1976, is clearly evident on all three images.

The grassland class (shown in yellow) has identical success rates on the 1984 three band and the 1985 images; 66.5% (tables 7.6 and 7.7). However, the accuracy value of the two band 1984 data is considerably higher at 87.5% (table 7.5). The main reason for this seemingly greater accuracy is probably due to an overestimation of grassland areas on this image (plate 7.9). This results in a greater proportion of accuracy check points falling within the image grassland areas, when the geometric shift is taken into account, than on the other two images (plates 7.10 and 7.11), which more accurately represent the percentage cover and shape of grassland blocks. The primary misclassification of this class is into the agriculture category, which is to be expected, as they both contain areas of grass species.

The Calluna vulgaris class (shown in purple) has accuracy values in the mid to low 60's in all cases, being highest on the two band 1984 image at 65.5% (table 7.5). The predominant misclassification is into the neighbouring grassland class, but there is also mistaken allocation to the burnt/bare, Pteridium aquilinum and agriculture classes. The majority of these errors appear to be due to geometric distortions. The Calluna class was extracted from both the three band images (figures 7.13 and 7.14), for comparison with the National Park map (figure 7.5) and the false colour composite image class maps (figures 7.9 and 7.10). The most obvious differences between the class maps is the less extensive coverage of moorland in the classification image maps (figures 7.13 and 7.14), resulting in lower accuracy values for the classification extracted class maps than for the false colour composite maps; 61%($\pm$9%) for the 1984 class map, and 67%($\pm$9%) for the 1985 map (table 7.8).

year	accuracy (%)	
	Moorland	Pteridium
1984*	61(±9)	47(±10)
1985*	67(±9)	55(±9)

*KEY
1984 = TM2,TM4 and TM5
1985 = TM4,TM5 and TM7

Table 7.8 Accuracy values for extracted class maps (figures 7.7 to 7.10); Landsat Thematic Mapper false colour composite images

This is directly a result of differences in classification criteria between the National Park and the present research. The National Park include grassland, such as Molinia caerulea (purple grass moor) and Nardus stricta (mat grass), as part of the moorland category (North York Moors National Park Committee, 1984a). Grassland was treated as a separate and individual class during classification in this research. This is a problem since the 'moorland' extracted from the images is not completely compatible with the National Park moorland maps, as to be so, the grassland and Calluna vulgaris classes should be combined. However, there were problems of large over-representation of grassland (especially into agricultural areas), which meant that it was felt more meaningful to separate the two classes and to use only the Calluna category for this purpose.

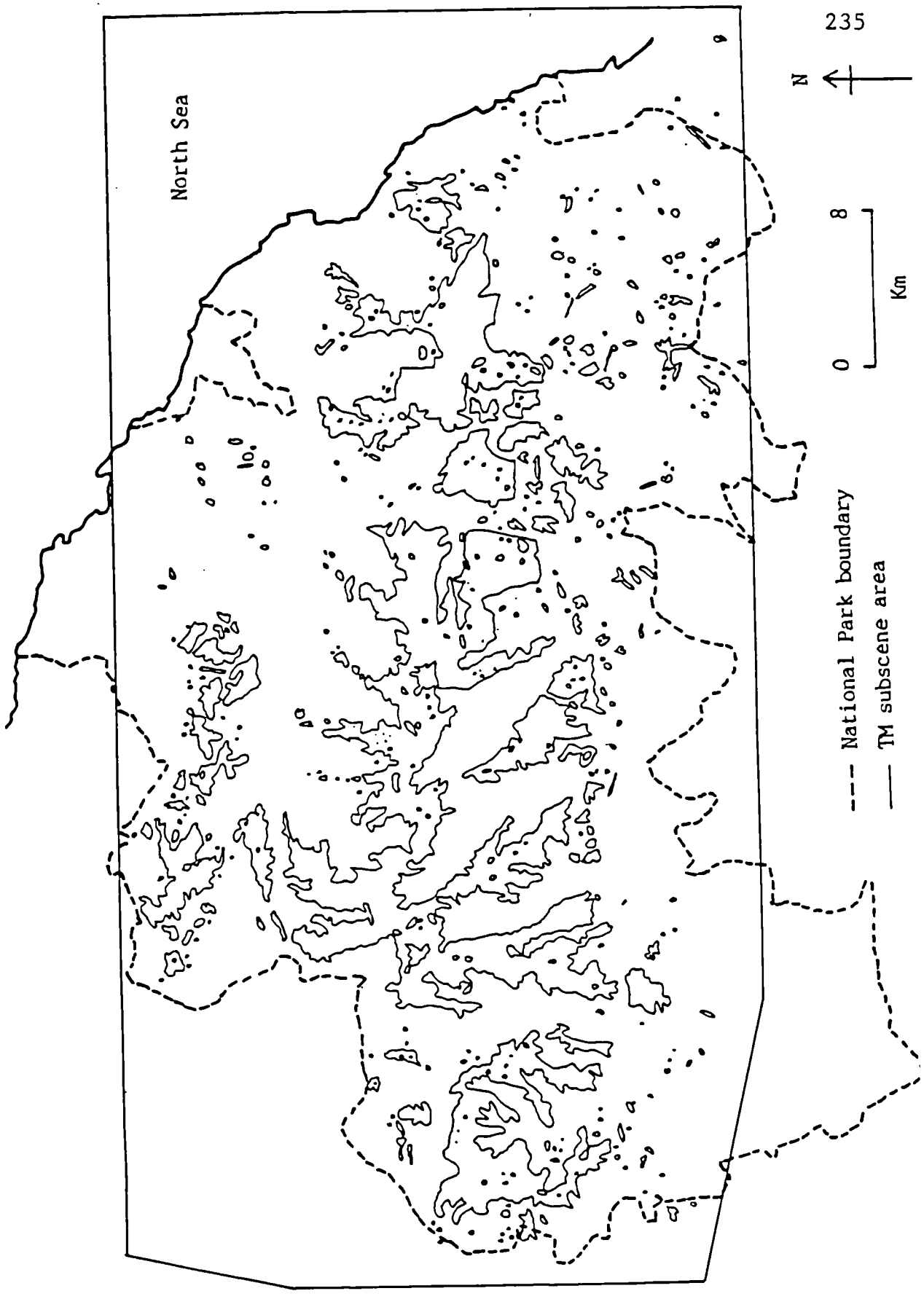

Figure 7.13 Moorland class map: 1984 Landsat Thematic Mapper maximum likelihood classification (3x3 mean filter of TM2, TM4 and TM5)

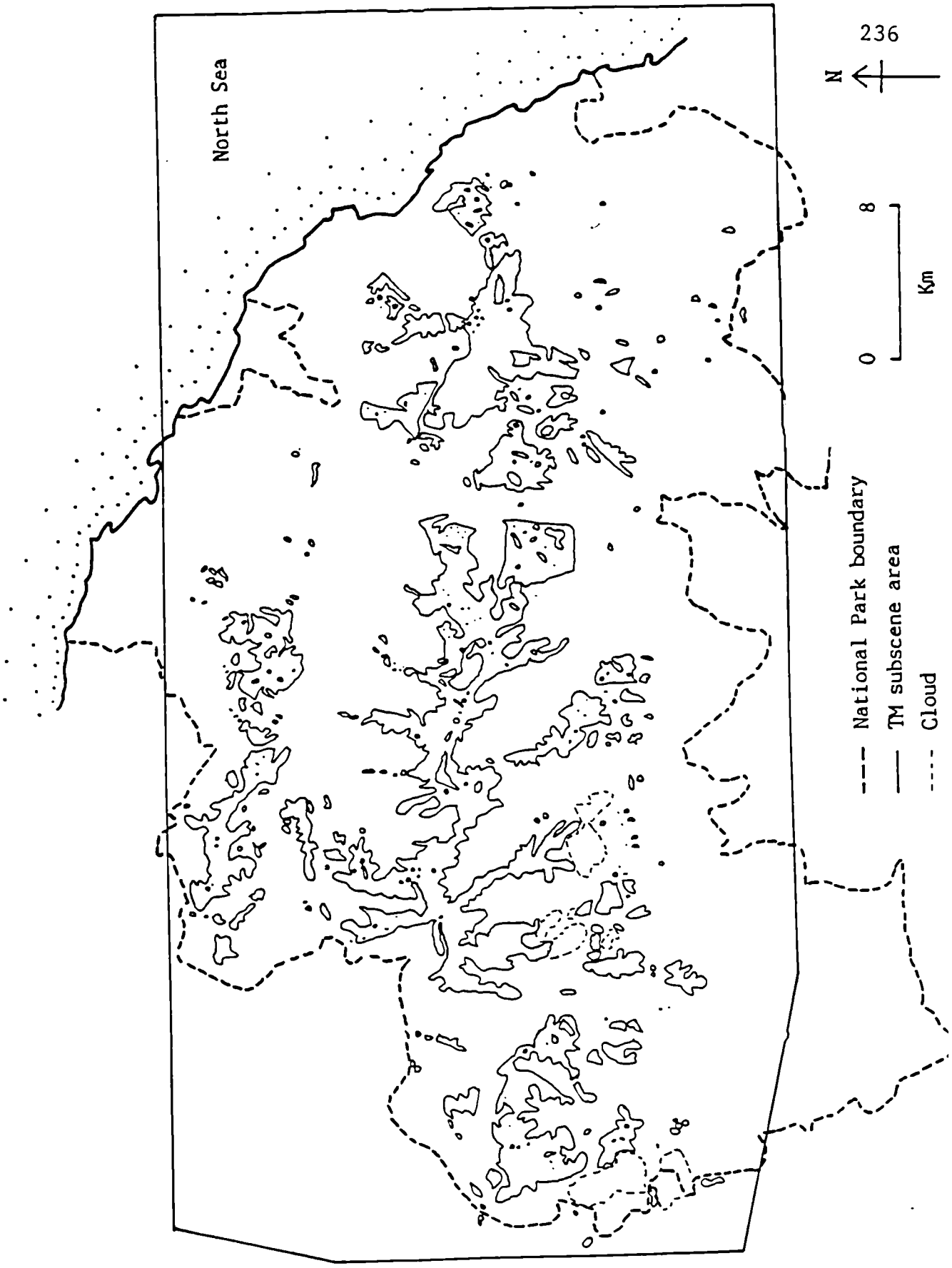

Figure 7.14 Moorland class map: 1985 Landsat Thematic Mapper maximum likelihood classification (TM4, TM5 and TM7)

The Pteridium aquilinum class (shown in red) has accuracy values that are relatively low, ranging from 52% on the 1985 image (table 7.7) to 59% on the two band 1984 image (table 7.5). In all cases there is substantial misclassification into the Calluna, grassland and agriculture classes, and this is predominantly due to the geometric shift adversely affecting the narrowly distributed Pteridium stands. The Pteridium areas appear reasonably well reproduced on the two three band images (plates 7.10 and 7.11), but there are considerable problems on the other image (plate 7.9). In this case the Pteridium is under-represented in its true locations, especially on the edges of the finger-like lobes of the central watershed in the centre of the subscene, and is overestimated in agriculture and forest areas. This illustrates the inadequacy of a two band combination to successful separate all cover types. Without the extra dimension of an additional band, large-scale errors result.

There are similar, but less considerable, errors in the Pteridium class in the other two classification images. The maps extracted from the images (figures 7.15 and 7.16) indicate the large misclassification of agricultural fields as Pteridium. This is especially the case on the 1984 image map (figure 7.15), where the whole of the map is dotted with small areas mistakenly allocated to the Pteridium class, and the accuracy is 47%($\pm$9%) (table 7.8). The 1985 map (figure 7.16) has fewer areas of misclassification, and this reflects the later date of the image, increasing the contrast between Pteridium and bare agricultural fields. However, there are still considerable errors in this map (55%($\pm$9%) accuracy; table 7.8). Both maps show considerable detail, as in the 1985 false colour composite image map, suggesting that if the geometric distortions were decreased, they would offer more than enough information than is required by the National Park for their vegetation maps.

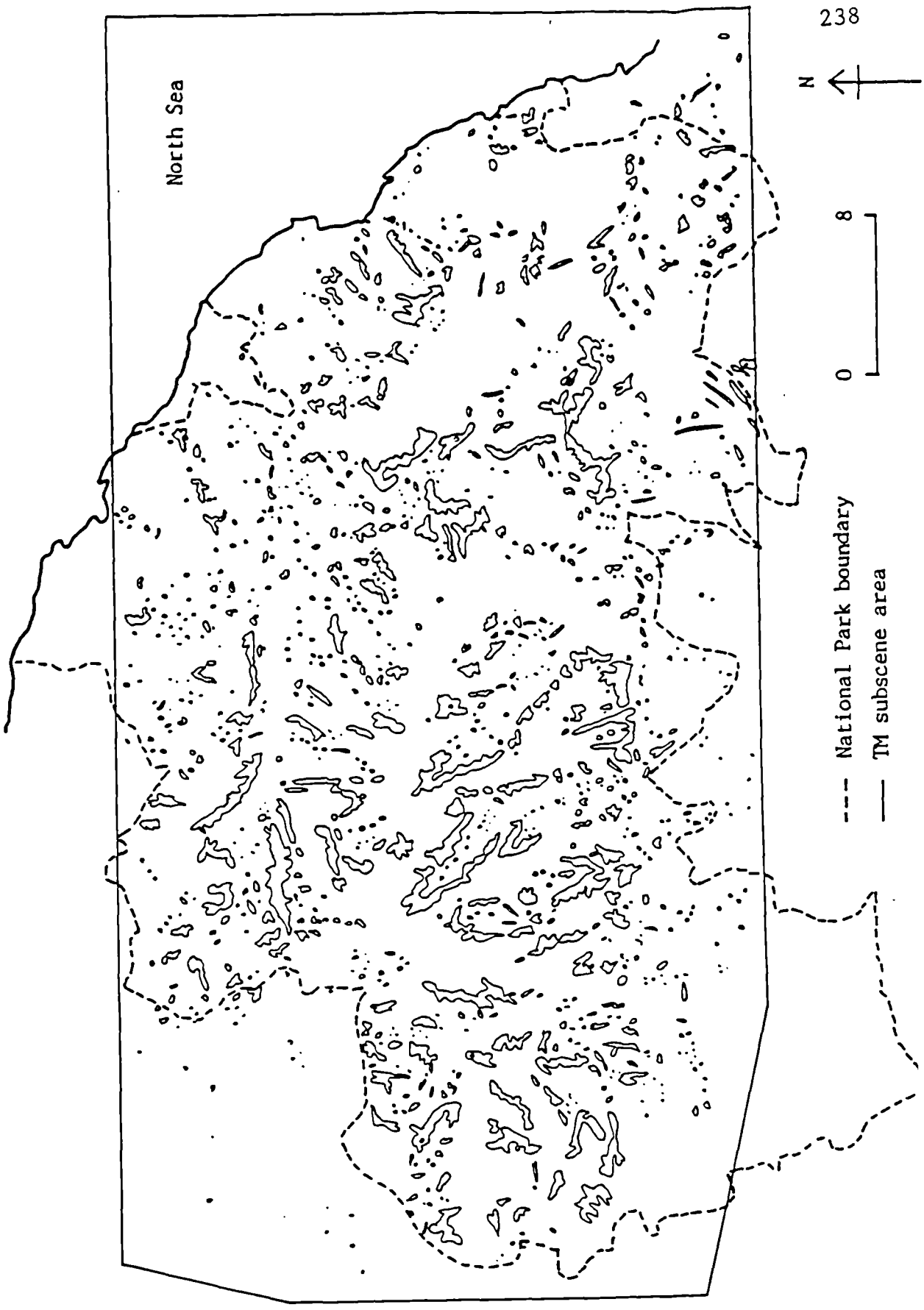

Figure 7.15 Pteridium aquilinum class map: 1984 Landsat Thematic Mapper maximum likelihood classification (3x3 mean filter of TM2, TM4 and TM5)

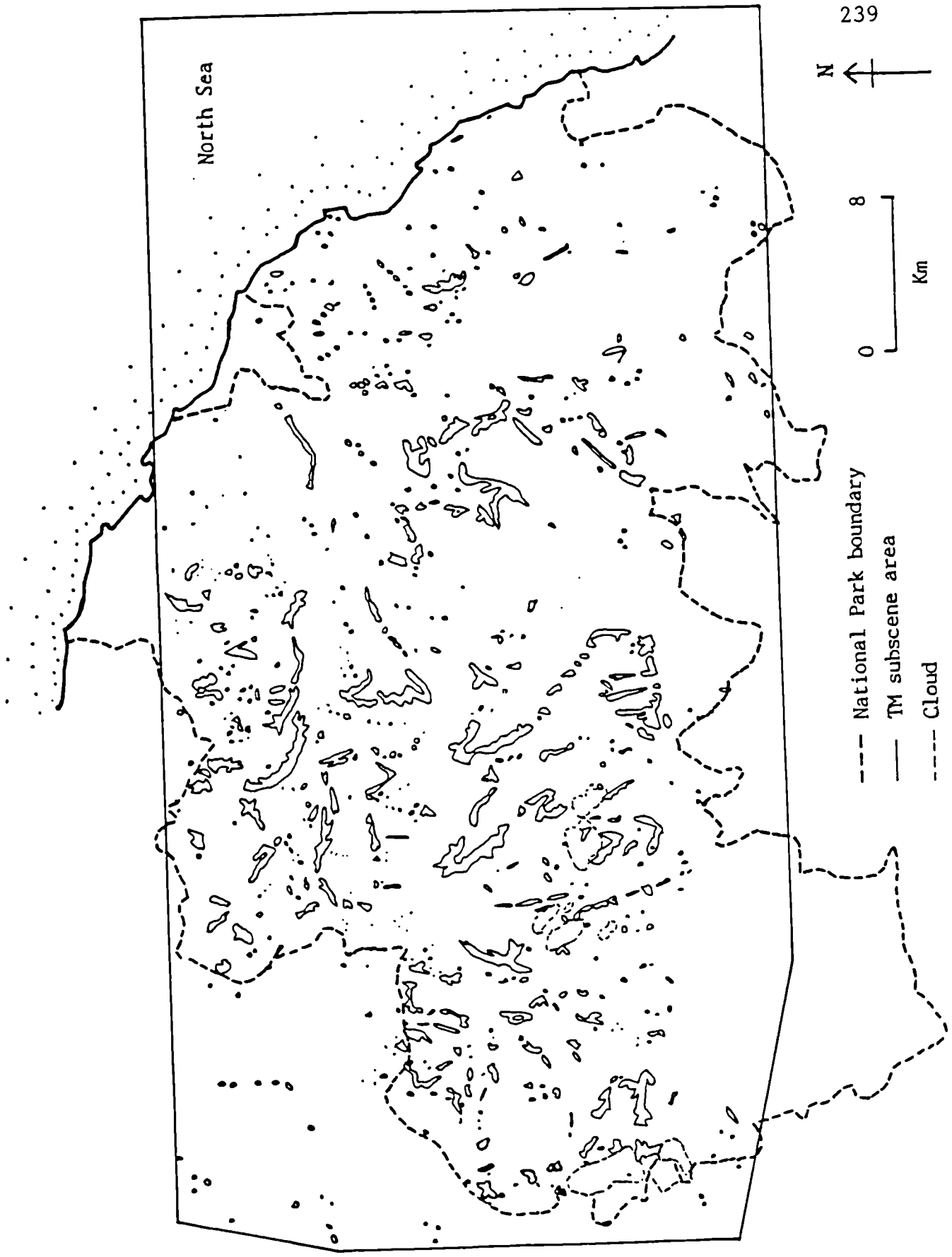

Figure 7.16 Pteridium aquilinum class map: 1985 Landsat Thematic Mapper maximum likelihood classification (TM4, TM5 and TM7)

The lowest class accuracies in all three images were found in the forest category (shown in brown); ranging from 27% on the two band 1984 image (table 7.5), to 39.5% on the 1985 image (table 7.7). These differences are clearly illustrated on the subscenes for these two images. The 1985 image (plate 7.11) has representative areas of forest, especially in the eastern edge of the subscene, in strips along the edge of the moorland fringe, and a larger rectangular block in the extreme north west. On the two band 1984 image (plate 7.9). these areas have virtually disappeared, being classed as Pteridium and Calluna. The woodland in the subscene area is predominantly in coniferous plantations which have been converted from moorland since 1951 (North York moors National Park Committee, 1984b), and the 1984 two band image holds insufficient spectral information to separate it from the other surfaces at this time of year. The main misclassification in all three images is the allocation of deciduous woodland into the Calluna vulgaris, grassland and Pteridium aquilinum classes. At this time of year deciduous trees have exposed woody branches, similar in nature to the Calluna branches, or grassland and Pteridium understoreys, which are revealed due to the lack of foliage.

7.7 The effect of spatial filtering on classification accuracy

The basic pattern appears to be a general reduction in classification accuracy associated with an enlargement of the size of the filter kernel. The lowest accuracies at both dates are for the 5x5 mean filters, although the 3x3 median filtered images also appear to have relatively low success rates (figure 7.11; table 7.4).

However the above section has suggested inadequacies in the calculation of accuracy values for the classification images, as illustrated by the three images with the best accuracy values. The assumption that accuracy values would rise dramatically if geometric errors were reduced (section 7.6), may also be applied in the case of the filtered images, so that they may be less inaccurate than the

accuracy values suggest (table 7.4). The 1984 scene was selected for close examination because the image initially had a greater amount of noise than the 1985 data, and therefore the effect of the filters could be more easily assessed.

Again, subscenes have been used to allow the illustration of greater detail (plates 7.10 and 7.12 to 7.14).

There are three major features of an image which change when it is filtered; vegetation blocks become more internally homogenous, boundaries become smoothed, and small-scale or linear features are lost through averaging. Change in these three factors may be observed in the series of mean filtered images, each with a progressively larger kernel size (plates 7.10, 7.12 and 7.13).

The original unfiltered image (plate 7.12) shows evidence of large-scale heterogeneity within vegetation blocks. For instance, the agricultural area (green) is dotted with pixels erroneously classified as grassland (yellow) and Pteridium (red). In addition, the Calluna (purple), Pteridium and forest (brown) blocks are scattered with many small areas of other classes. Some of these areas, especially burnt areas within the Calluna, are accurate representations of ground conditions, but many are inaccuracies, and may be considered as unwanted noise. The boundaries are intricate and detailed, clearly representing small-scale undulations and protuberances in the vegetation limits. This is most clearly illustrated by the Pteridium boundaries. Many small and linear features, such as burnt areas and some roads across the main moorland, are evident.

The underlying pattern of vegetation is more clearly revealed using a 3x3 mean filter on the image (plate 7.10). In this case the main vegetation blocks have become far more internally homogenous. Much of the unwanted noise has vanished, being averaged-out in the filtering procedure.

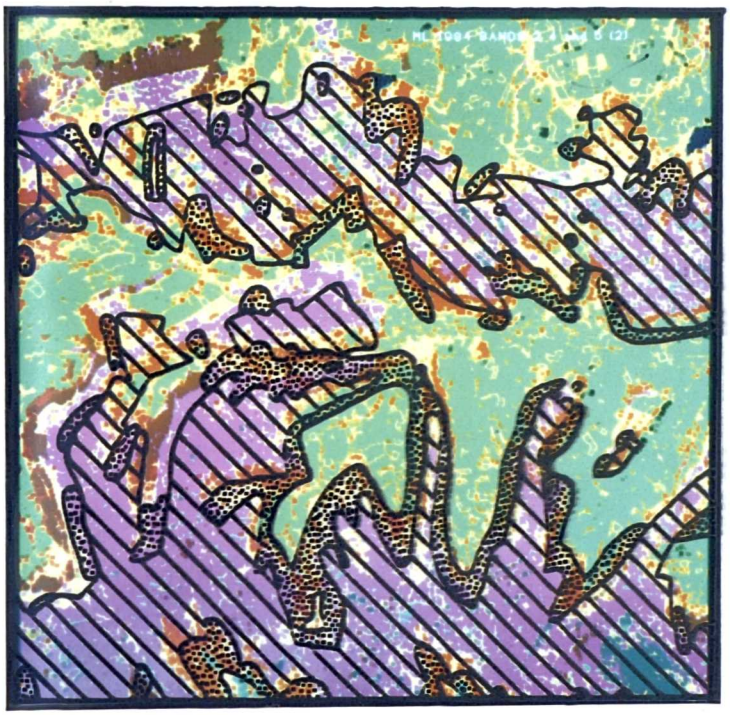

Moorland Pteridium

KEY

purple	=	Calluna vulgaris
dark grey/green	=	Burnt/bare
red	=	Pteridium aquilinum
dark blue	=	Water
brown	=	forest
yellow	=	Grassland
green	=	Agriculture

Plate 7.12 Subscene of maximum likelihood classification image: Landsat Thematic Mapper, bands TM2, TM4 and TM5, April 1984 (unfiltered) (the overlay shows an extract from the National park maps; figure 7.12)

Moorland Pteridium

KEY

purple	=	Calluna vulgaris
dark grey/green	=	Burnt/bare
red	=	Pteridium aquilinum
dark blue	=	Water
brown	=	forest
yellow	=	Grassland
green	=	Agriculture

Plate 7.13 Subscene of maximum likelihood classification image: Landsat Thematic Mapper, 5x5 mean filter of bands TM2, TM4 and TM5, April 1984 (the overlay shows an extract from the National park maps; figure 7.12)

Moorland Pteridium

KEY

purple	=	Calluna vulgaris
dark grey/green	=	Burnt/bare
red	=	Pteridium aquilinum
dark blue	=	Water
brown	=	forest
yellow	=	Grassland
green	=	Agriculture

Plate 7.14 Subscene of maximum likelihood classification image: Landsat Thematic Mapper, 3x3 median filter of bands TM2, TM4 and TM5, April 1984 (the overlay shows an extract from the National park maps; figure 7.12)

This is evident in both the agriculture and Calluna classes, which show far larger contiguous regions where the local variations have been removed. In addition, the boundaries have been considerably smoothed. Small-scale fluctuations and anomalies have disappeared, and limits between vegetation types have been generalised. However, despite the cleaner appearance of the image, many of the small-scale and linear features apparent on the unfiltered image have been lost. This is especially the case with burnt patches and roads.

The 5x5 mean filtered image shows the greatest degree of smoothing (plate 7.13). In this case almost all of the local variation has been removed, revealing the background pattern of vegetation distribution. Boundaries have been further generalised and small features have virtually disappeared. However, the moorland and Pteridium areas on this image resemble the National Park maps (figure 7.12) more closely than the less smoothed data, reflecting the generalised nature of the boundaries on the National Park maps (section 7.5.2.1).

The 3x3 median filtered image combines some of the qualities of both the filtered and unfiltered images (plate 7.14). Vegetation blocks are more homogenous, while boundary details and some small-scale features are retained. However, there is still considerable noise within the main moorland and agriculture areas, confusing the general trends of vegetation distribution, and resulting in a 'bitty' appearance, similar to the unfiltered image.

Thus a balance must be achieved between the computationally simple unfiltered image, which has a wealth of detail, some of which may be considered as noise, and the computationally more complex 5x5 filtered image, which emphasises the underlying patterns, but may be oversimplifying the variation on the ground. Nevertheless, the similarity between the moorland and Pteridium distribution on the 5x5 filtered image and the National Park maps, perhaps suggests that a filtered image may be a more suitable base for the production of

vegetation maps meeting the requirements of the National Park, in this complex semi-natural environment, than would an unfiltered image.

7.8 Conclusion

The research reported in this chapter has demonstrated the ability of Landsat TM data to map successfully the vegetation of the North York Moors National Park. Moorland and Pteridium aquilinum class maps, visually extracted from false colour composite images show detail exceeding that apparent on the present National Park category maps, and appear to represent faithfully the shape and size of vegetation blocks. This is possible using temporally sub-optimal data, and the success of results may be expected to improve further if a late summer scene was used. However, the false colour composite images suffer from fairly large geometric errors, which lower the absolute accuracy of the extracted class maps, and create difficulties in the selection of the best maximum likelihood classification image. A 3x3 mean filtered 1984 image (TM2, TM4 and TM5) and an unfiltered 1985 image (TM4, TM5 and TM7) have the highest accuracy values, but closer examination of the subscenes and an assessment of the effects of spatial filtering, has suggested that a filtered image may be the most suitable data to classify. The choice of data is strongly influenced by the exact aims of the project. Thus, if small-scale vegetation detail is required, an unfiltered or 3x3 filtered image is optimum; but if the aim is to produce generalised maps, similar to the present National Park moorland maps, then an image filtered with a larger kernel size is more suitable.

CHAPTER 8. CONCLUSION

8.1 Introduction

Open moorland occupies 35% of the total area of the North York Moors National Park, and one of the statutory objectives of the National Park Committee is the "preserving and enhancing of the natural beauty of the park" (North York Moors National Park Committee, 1985). This has been interpreted to include the conservation of visually critical features and wildlife habitats, and management is primarily defined as the positive implementation of conservation techniques (North York Moors National Park Committee, 1984b). Four of the principal concerns of the Committee at present, are the encroachment of Pteridium aquilinum into Calluna vulgaris moorland and agricultural fields, the overaging of Calluna, the conversion of moorland to agriculture and forestry, and moorland erosion and degradation (North York Moors National Park Committee, 1984b).

Before the true extent of these problems can be assessed, it is critical to have a complete and accurate view of present vegetation and land use status and distribution. Only when such information is available may conservation management be successfully implemented. In addition, it is a statutory requirement of all National Park Committees to prepare, print and put on sale, a map showing areas of moor and heath which it is considered particularly important to conserve (Wildlife and Countryside Act, 1981).

Thus it is both vital for management, and legally necessary, to produce accurate vegetation and landuse maps of the National Park. It was the intention of this research to produce such maps, particularly of moorland and Pteridium aquilinum, using remote sensing techniques. The research reported in this thesis has been based on an investigation of the nature of the three main interconnected facets of remote sensing; the temporal, spectral, and spatial resolutions. Only when details of all three aspects have been examined and

understood, may the optimum data source and methodology be adopted in order to produce authentic moorland maps.

This final chapter falls into two sections. In the first section a summary of the major findings of the research is presented, and in the second section, ideas for the direction of future research are outlined.

8.2 Principal findings of the research

8.2.1 Temporal resolution

Temporal factors have a considerable influence over the spectral character of surfaces. Such factors include: seasonal changes in vegetation canopy structure, geometry, size and colour; moisture and soil conditions; illumination angles; atmospheric and weather patterns; and man-induced changes, principally concerned with the agricultural regime.

The identification of an optimum temporal resolution is not a simple task, as the complex mix of temporally-varying cover types in the study area necessitates a compromise decision. No single time period is optimal for all moorland surfaces, since the contrast between cover types, and the homogeneity and distinctiveness within classes, varies with each pairwise relationship between surfaces.

Nevertheless, late summer appears to be the most practical time period, because although it is not optimum in all cases, it offers the best overall opportunity for segregating between most classes. The winter and spring periods are affected by considerable problems; firstly because of adverse weather conditions, especially snow and cloud; and secondly, since confusion between moorland surfaces is maximised during these seasons. This is due to a lack of green vegetation at the surface in the cases of deciduous plants, such as Pteridium and grasses, and arable fields, and to the subdued nature

of growth in evergreen species, such as Calluna and other types of heather.

The early summer and autumn are possible alternative temporal resolutions to late summer. However, the unpredictability of the exact time of the onset of plant growth and the end of the growing season provides problems for moorland mapping. The occurrence of frost is one of the main controls on plant growth, and this fluctuates considerably from year to year.

During late summer, in late August and September, Pteridium aquilinum is at its peak growth, allowing a greater chance of discrimination between growth stages, and separation from bare surfaces and deciduous grasses. At this time many moorland species, such as Calluna and Vaccinium, are flowering or fruiting, which increases the likelihood of their differentiation from Pteridium, and enhances subtle distinctions between heather species. This period also allows maximum discrimination between Calluna vulgaris growth and management stages, and offers clear separation between Calluna and deciduous woodland.

8.2.2 Spectral resolution

The underlying assumption of multispectral remote sensing is that surfaces are spectrally distinct. This is valid in many cases, but in others, cover types are not separable. Spectral response is dependent on a number of factors including: the reflective and emissive properties of the surface; the illumination and site environmental conditions; the atmosphere and weather; and the sensor parameters.

Spectral data sets extracted from the field spectral, Airborne Thematic Mapper and Landsat Thematic Mapper data, were examined in detail. It was found that although pairwise discrimination of moorland surfaces can be achieved in many cases using only one spectral channel, when more than two cover types are included in the analysis, more spectral information is usually required, in order to

separate all the classes adequately. The highest accuracy for discriminant analysis using only one channel was 81.96% for the April 1984 TM data (band TM5), but accuracy values for the other data sets were much lower, being only 53.85% for channel 3 in the June field spectral data, and 59.2% for ATM7 in the May ATM data.

No single waveband is optimum in all cases, although the near infrared is generally the most useful. No combination of bands is consistently successful, although two channels are reasonably successful for both the field spectral data (channels 1 (green) and 3 (near infrared)), and the Thematic Mapper data (bands TM4 (near infrared) and TM5 (short wave infrared)). The Airborne Thematic Mapper data requires the use of three channels to separate the selected classes; ATM2 (blue), ATM5 (red) and ATM7 (near infrared) in May, and ATM5 (red), ATM7 (near infrared) and ATM9 (short wave infrared) in July.

It is impossible to discriminate between the Pteridium aquilinum growth and management stages using the field spectral data alone; discriminant analysis accuracy values being as low as 49.3% using all four channels (August data). Therefore it is considered extremely unlikely that it would be possible using spatially coarse satellite data. There is also significant confusion between mature and degenerate Calluna vulgaris, even in the best data sets. For example, 13.1% of the degenerate class were misclassified as mature, and 15.1% of the mature class were misclassified as degenerate, in the optimum ATM combination (ATM2, ATM5 and ATM7 in May).

In most cases the accuracy values from discriminant analysis are extremely high; reaching a peak of 100% for the August field spectral data (channels 1 and 3), and being as high as 99.48% for the optimum two-band 1984 TM combination (TM4 and TM5). This suggests that it is possible to achieve successful classification of air or satellite imagery. However, if a whole scene is considered, confusion is increased by the greater variety of classes and transitional mixed

zones, and this is likely to result in a reduction of the accuracy of any classification.

8.2.3 Spatial resolution

There is much controversy over the exact effect of spatial resolution on classification accuracy. It is a common misconception that an increase in spatial resolution automatically brings an increase in accuracy. The relationship between pixel size and accuracy is complex, and is closely connected with the balance between the heterogeneity of a class and the proportion of mixed or boundary pixels in that class. Thus it may be hypothesised that mapping accuracy will rise from a low point at fine resolutions, caused by the great heterogeneity within classes, to a peak at medium resolutions, where there is homogeneity within classes and a relatively low number of boundary pixels. Beyond this, accuracy will decrease once more, as a result of the large number of boundary pixels, and lower between class contrast, due to overaveraging within pixels.

The degradation experiment reported in chapter 6, demonstrates that spatial resolution has a considerable effect on the discrimination of vegetation types, the accuracy of maps derived from the imagery, the location and character of class boundaries, and the accuracy of cluster analysis classification maps. In both the qualitative and quantitative analysis, 10m data provides the optimum spatial resolution, having the peak cluster analysis accuracy value of 56%($\pm$7%), and successfully representing the shape and size of vegetation blocks in detail. The boundaries between classes and linear features are clearly and realistically represented. Accuracy values are lower for both finer (e.g. 42%($\pm$7%) for the 2.5m data) and coarser resolutions (e.g. 48%($\pm$7%) for the 30m data), confirming the hypothetical rise and fall in accuracy with a gradual coarsening of the resolution. In addition, the boundaries are step-like and misplaced in the images with a larger pixel size, especially the 20m and 30m images.

However, even the 30m data hold considerable information showing a generalised view of the vegetation distribution, although boundaries are step-like at this coarse resolution. The North York Moors National Park published maps (presented in chapter 7; figures 7.5 and 7.6) are more generalised than those extracted from the ATM data. Boundaries are smoothed and small discrete areas have been drawn as contiguous blocks, representing the overall pattern of distribution at the expense of small-scale variations. For such generalised mapping, 30m data are adequate; but for a more detailed representation of ground conditions, a finer resolution is required, and 10m data are optimum.

This has important implications for large scale mapping of moorland areas using satellite data. A 10m spatial resolution is only available on the SPOT panchromatic channel. This channel has limited spectral resolution making it impractical for use in the operational satellite monitoring of complex semi-natural vegetation. The 20m multispectral SPOT channels offer more spectral information, although there is no SWIR channel, which was found to be very useful in the analysis of TM data. In addition, SPOT data have scenes which cover a limited area, so that it would be necessary to mosaic several scenes together to cover an area the size of the North York Moors, causing problems of geometric coregistration and radiometric calibration. Landsat Thematic Mapper, at 30m spatial resolution, with a scene size large enough to cover the whole National Park, is the most promising data source for the more generalised large-scale vegetation mapping which is required in the North York Moors.

8.2.4 Moorland mapping from satellite imagery

The research in this thesis demonstrates that a skilled interpreter trained on a small area where ground conditions are known, may successfully, quickly and inexpensively, produce vegetation class maps, comparable to the National Park maps, from false colour composite Thematic Mapper images. Similar maps may also be produced from maximum likelihood classification images. These closely resemble

the National Park maps, accurately illustrating the shape and size of vegetation blocks. However, due to the geometric distortion of the data, resulting in a shift in the relative location of areas, accuracy values are unrepresentatively low; in no cases exceeding 66%. Without considerable improvement in the geometric quality of the data, it is difficult to reliably quantify any change in the vegetation distribution between the two scenes. Filtering techniques used prior to classification to remove unwanted noise, indicate that for generalised vegetation mapping, a mean filter will improve results. Such data may cause the oversimplification of the variation on the ground, but are capable of producing maps similar to those used at present by the National Park Authority.

8.3 Recommendations for further study

The following ideas are suggestions for future research into areas which may result in accuracy improvements, and lead to the development of an operational system for the monitoring of moorland environments using remote sensing techniques.

8.3.1 Optimum temporal resolution

Although the research reported in this thesis has been successful in mapping generalised land cover classes, there was some confusion between several basic cover types. Confusion on spring and early summer images is particularly between areas with no green vegetation at the surface, such as Pteridium aquilinum, grassland and agricultural fields; between Calluna vulgaris growth stages, especially mature and degenerate; and between Calluna and deciduous woodland. The analysis of data collected in late August or September, holds greater potential for the spectral separation of these surfaces, which is likely to result in a more realistic representation of ground conditions, and more accurate automatic classification maps.

8.3.2 Improvements in the geometric quality of the data

The results of the analysis of both the Airborne Thematic Mapper and the Landsat Thematic Mapper, show that the shapes and sizes of vegetation blocks have been faithfully reproduced, but that geometric distortions have shifted their locations slightly, causing a dramatic reduction in the accuracy of images. Before an operational system can be developed, the geometric quality of the data must be considerably improved. The root mean square error of 3.4 pixels, achieved during the geometric correction in this research, is not low enough, and effort must be directed at reducing this to a more acceptable level.

8.3.3 Geographical Information Systems (GIS)

In many cases during the automatic classification in the present research, areas of "known" cover type, such as forestry plantations, water bodies, and agricultural and urban areas, were misclassified into other classes, due to similarities in spectral 'colour'. During visual interpretation, such areas were automatically discounted due to the context of their location, shape and general appearance. The development of a simple GIS, containing information about the location of these areas, could be used to mask known areas, prior to classification, so that they are excluded from the analysis, thus helping to reduce confusion and increase mapping accuracy (Healey, et al, 1988). In addition, a more complex GIS could incorporate details of slope angles, the occurrence of frost, drainage conditions etc. This could be used to discount areas where certain species, in particular Pteridium, would be unlikely to survive, thus masking additional areas prior to classification (Quarmby, et al, 1988).

8.3.4 Accounting for relief and topography

The North York Moors, like many other National Parks, contains significant areas of high relief and sloping topography. Relief can cause large changes in spectral response, resulting from partial shadowing, which causes confusion between and within cover types.

This may be overcome to some extent by the use of band ratios, which should be investigated in any future research. In addition, the development of a digital elevation model (DEM), could aid mapping from satellite imagery, and could be used in association with a GIS, to compensate for slope and aspect changes using a mathematical model (Jones et al, 1988).

8.3.5 Filtering techniques

Although filtering techniques were partially examined in the present research, resource and time constraints did not allow a thorough investigation of their full potential. The use of textural filters is a possible avenue for accuracy improvement. Such filters divide the image up into small areas (windows) and quantitatively measure the texture within each sub-array of pixels. Values for such textural measures are derived in a number of ways; a common method is to use the local standard deviation. Once calculated, the texture values may be incorporated into spectral classifications as the equivalent of an extra waveband (Weaver and Wright, 1986; Harris, 1987). Pre-classification filters were used in this research, but the implementation of post-classification modal filters may result in an improvement in accuracy (Cushnie, 1984).

8.3.6 Hard-copy products

A high standard of hard-copy output is an essential, and often overlooked, requirement for any operational remote sensing system. Therefore, the development of an substitute product to replace photographic prints taken of the screen, is a key area of future investigations. Alternative output is accessible to the remote sensing community at present, but was not available for this thesis. An additional problem is the conversion of the hard-copy satellite images to a traditional map format, for everyday use and integration with other mapped information. This problem may be reduced by the implementation of a GIS, which would directly link the satellite image with a map base (section 8.3.3).

8.3.7 Mixture models

Such models estimate the proportion of different elements or objects within each pixel (e.g. Marsh, et al, 1980; Drake, et al, 1988). These models concentrate on sub-pixel detail and may be especially useful in areas with high local variance and a high proportion of boundary pixels. Such an approach is complementary to a normal spectral classifier and may increase accuracy in the complex moorland environment.

8.4 Conclusion

The thorough investigation of the temporal, spectral and spatial aspects of the remote sensing of a moorland environment, presented in this thesis, has laid a firm foundation for the development of an operational moorland monitoring and mapping system using satellite data. This research has shown that, in conjunction with traditional field-mapping, Landsat Thematic Mapper data may be used successfully in the mapping of generalised moorland vegetation distribution. If the recommendations for further research are implemented, the potential exists for satellite remote sensing techniques to be routinely incorporated as a useful management tool in the efficient running of not only the North York Moors National Park, but of all upland areas.

APPENDIX 1. FIELD MAPS

KEY TO THE BASE MAP USED FOR THE FIELD VEGETATION MAPS

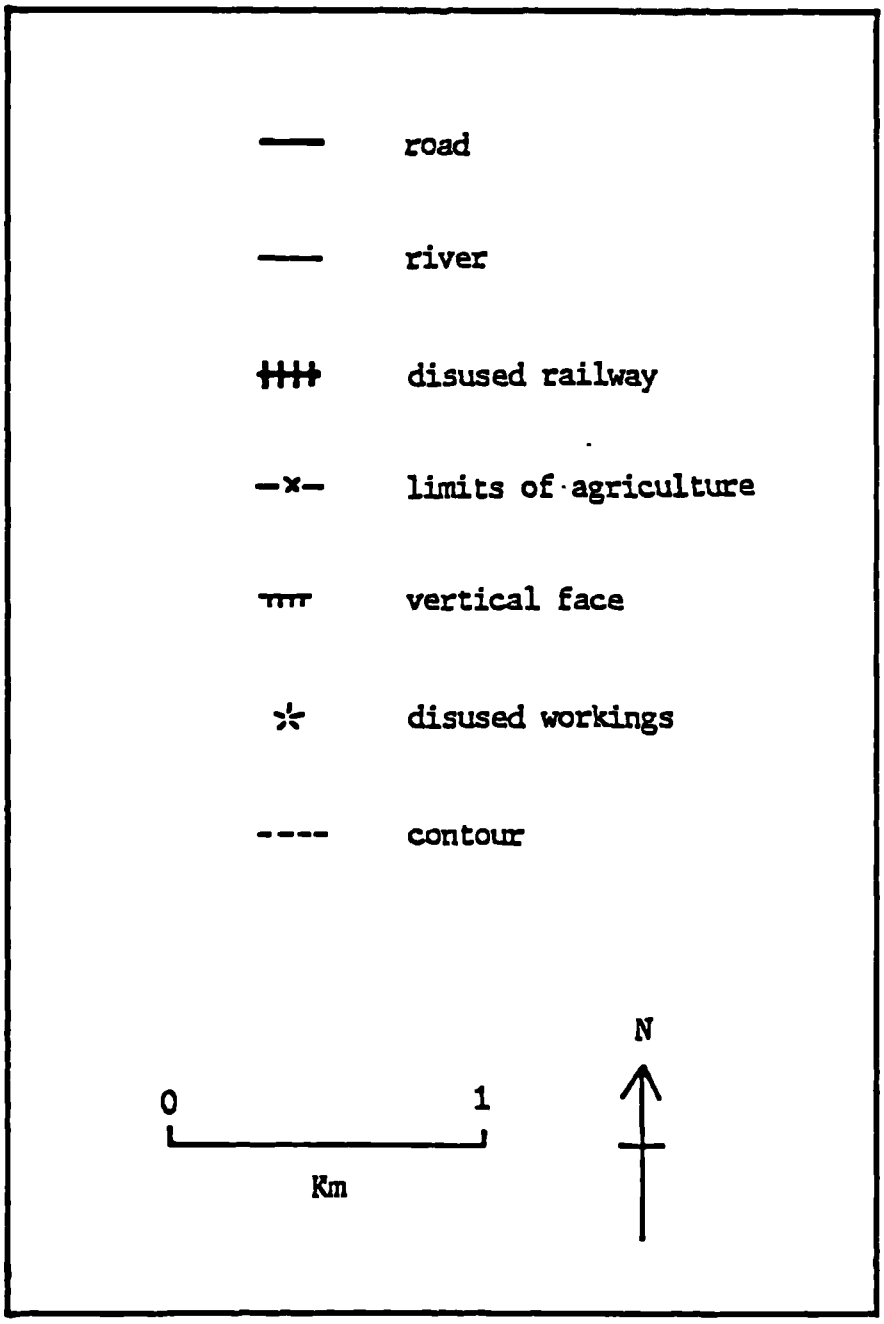

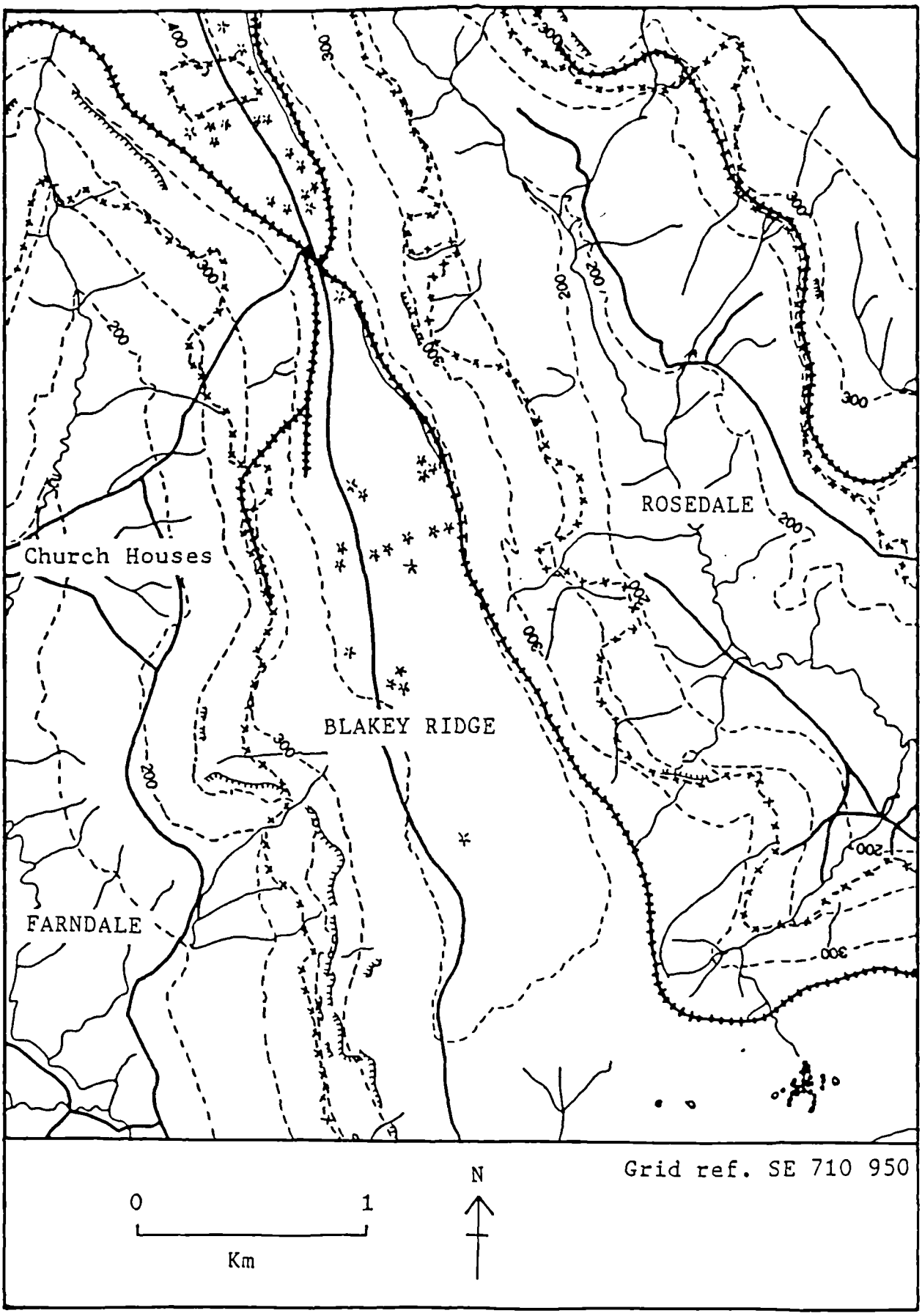

Figure App1.1a Base for the field maps of the northern half of Blakey Ridge

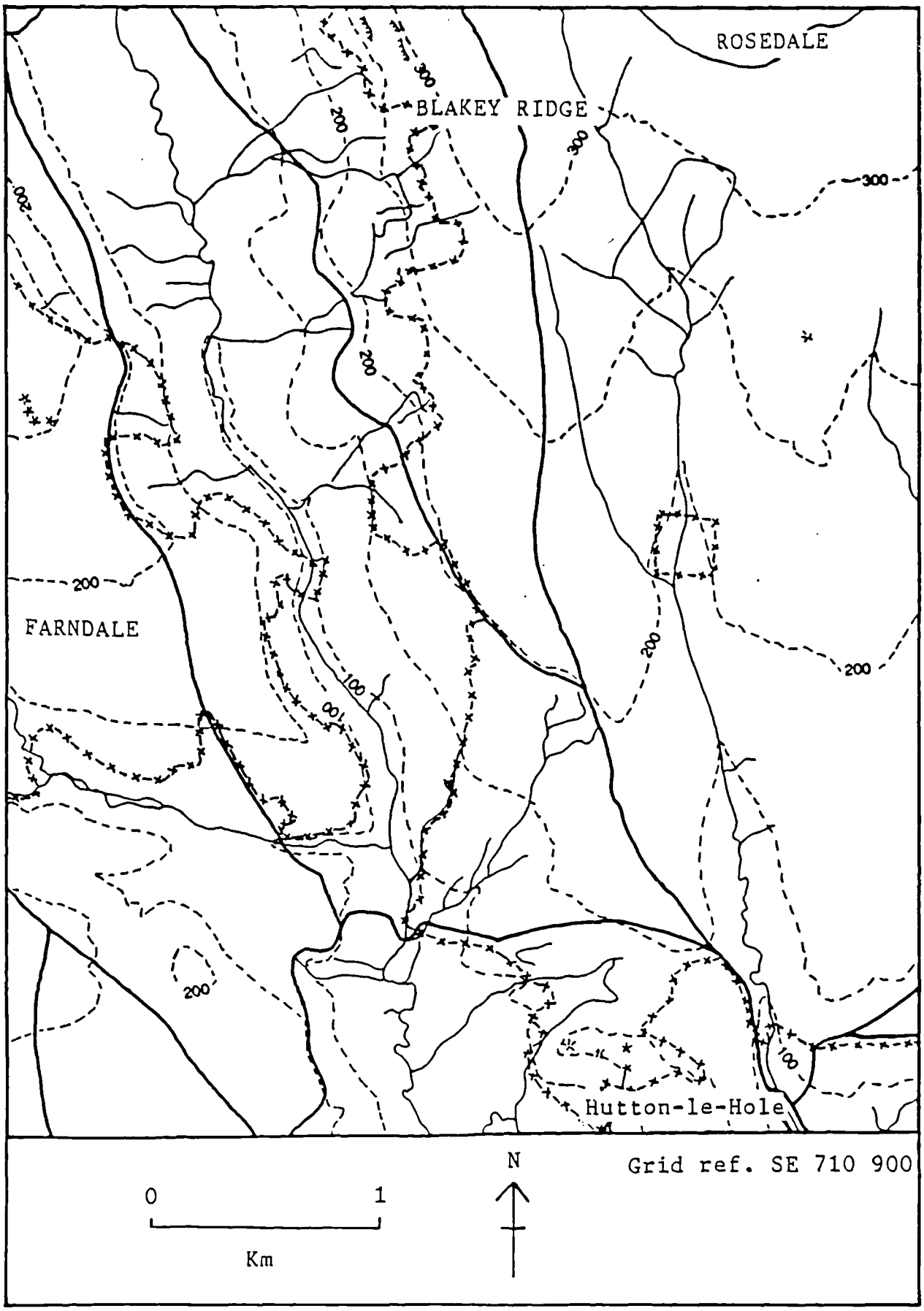

Figure App1.1b Base for the field maps of the southern half of Blakey Ridge

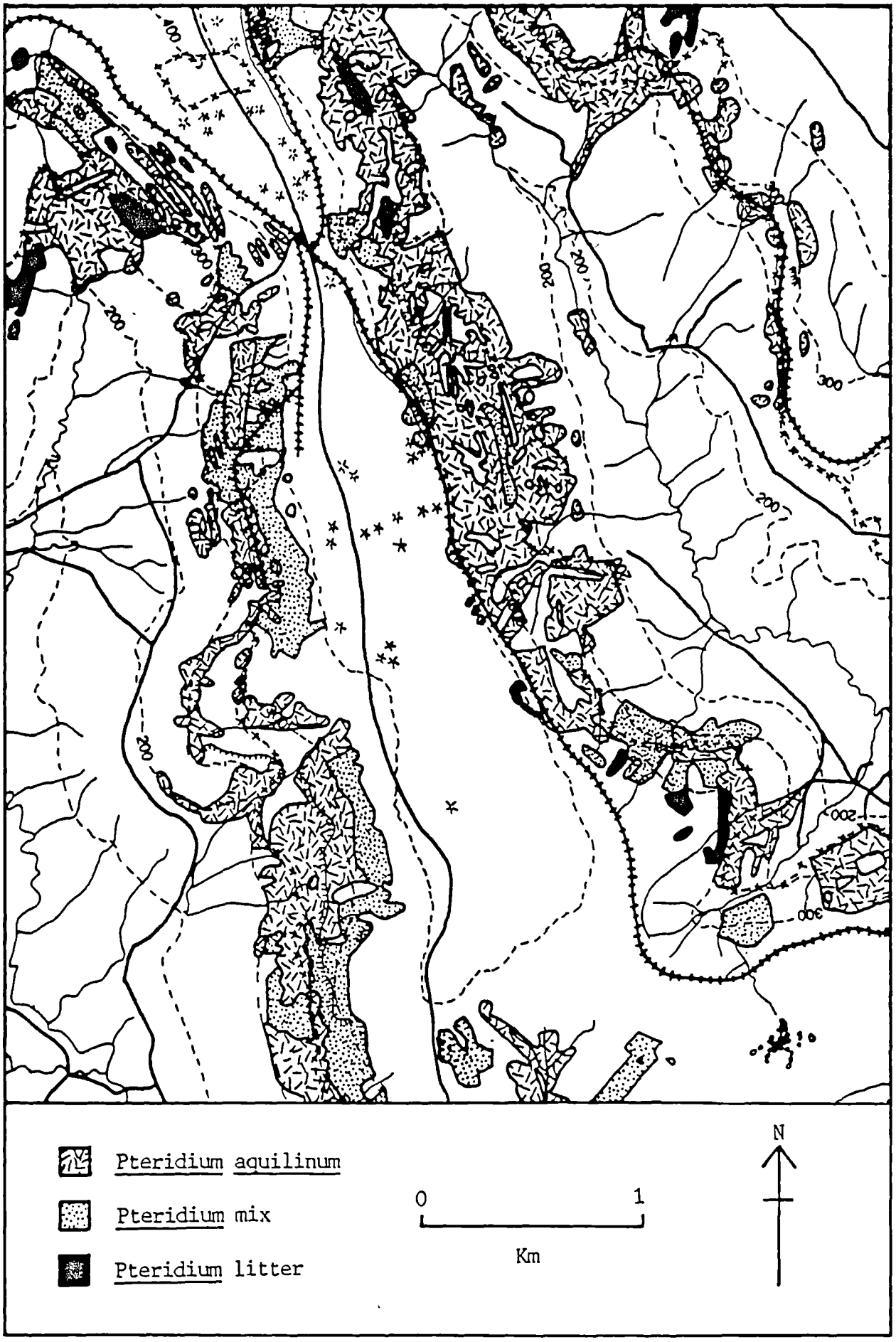

Figure App1.2a Field map of the northern half of Blakey Ridge: Pteridium aquilinum

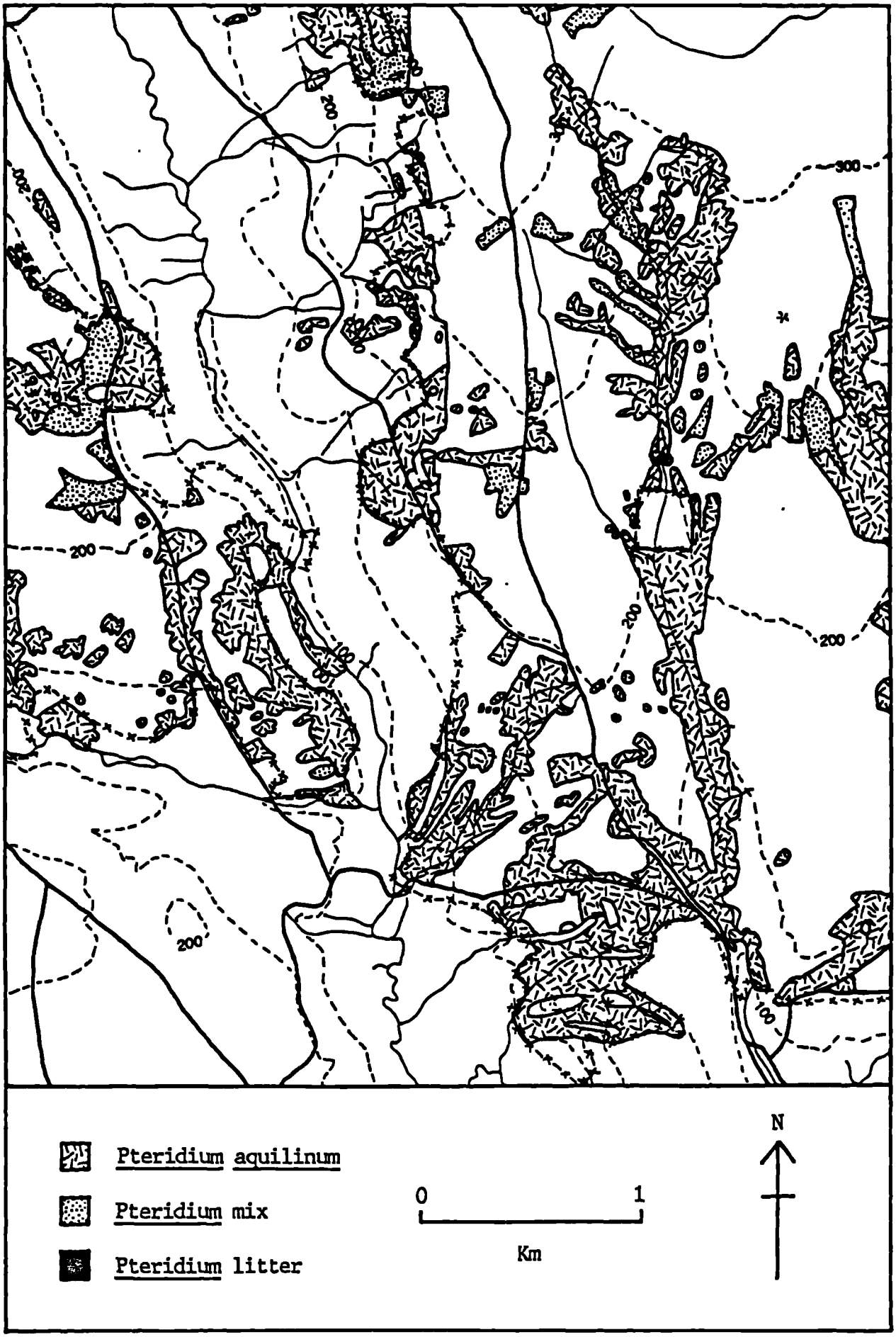

Figure App1.2b Field map of the southern half of Blakey Ridge:
Pteridium aquilinum

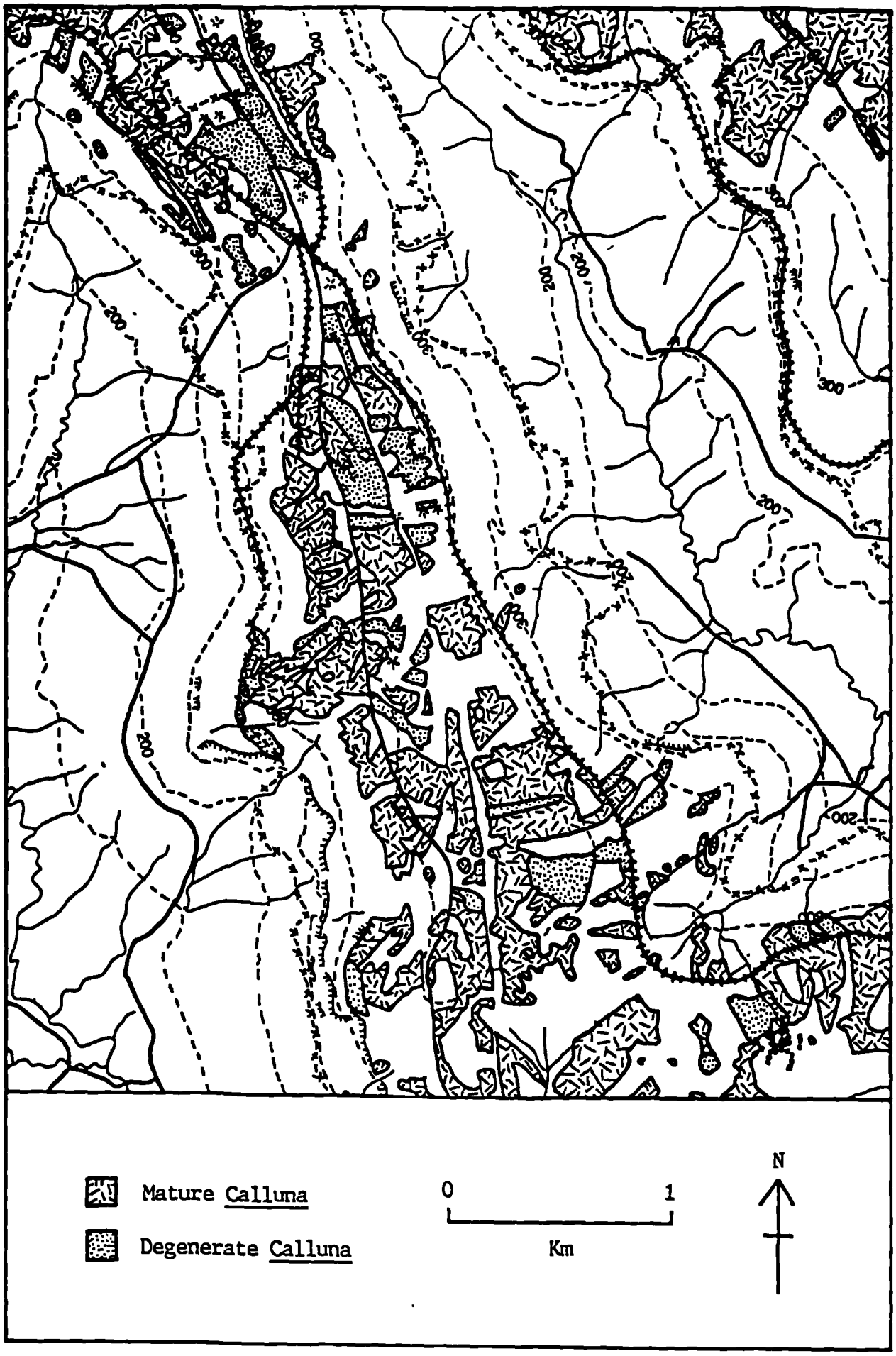

Figure App1.3a Field map of the northern half of Blakey Ridge: mature and degenerate Calluna vulgaris

Figure App1.3b Field map of the southern half of Blakey Ridge: mature and degenerate Calluna vulgaris

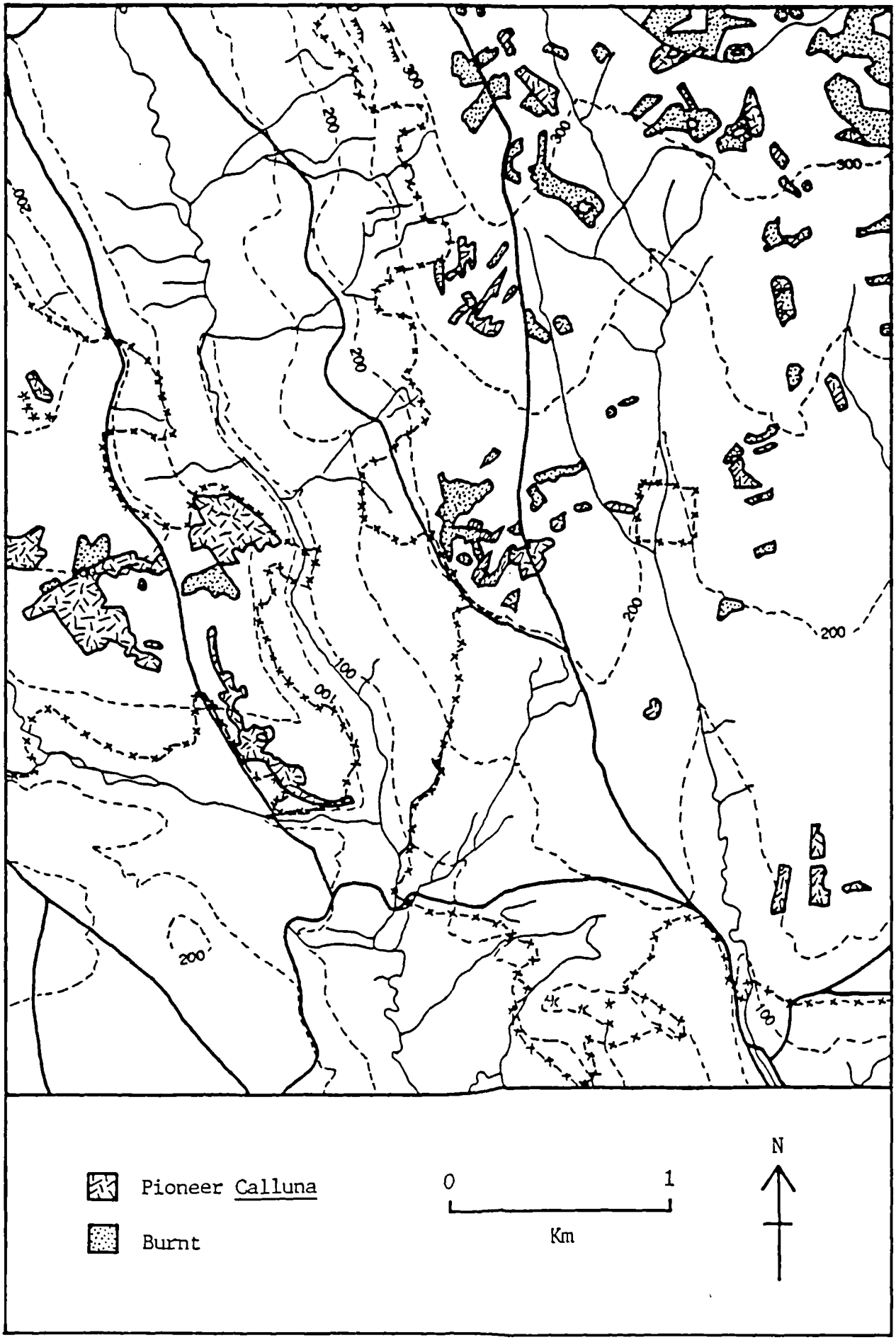

Figure App1.4a Field map of the southern half of Blakey Ridge: pioneer and burnt Calluna vulgaris

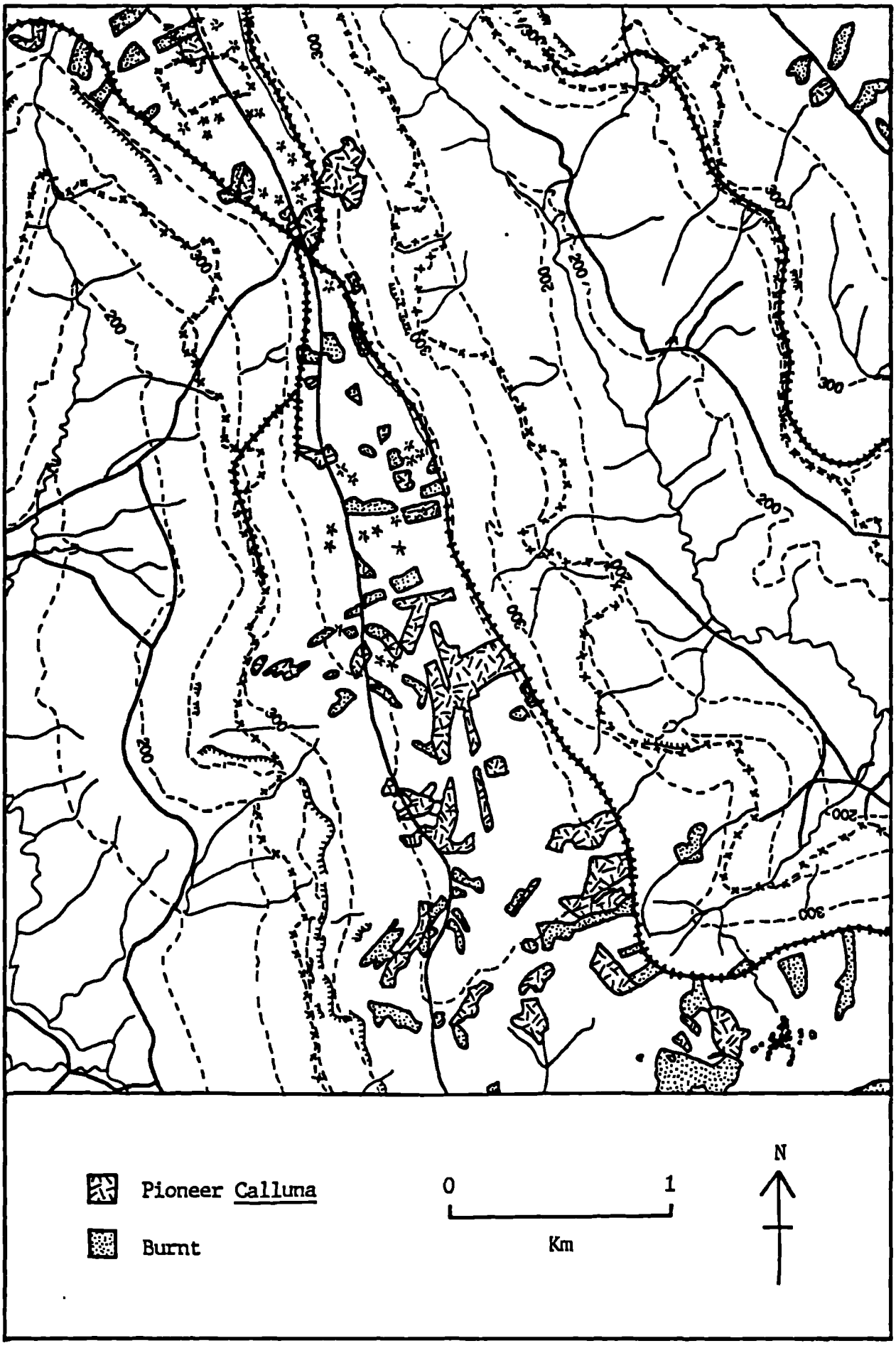

Figure App1.4b Field map of the northern half of Blakey Ridge: pioneer and burnt Calluna vulgaris

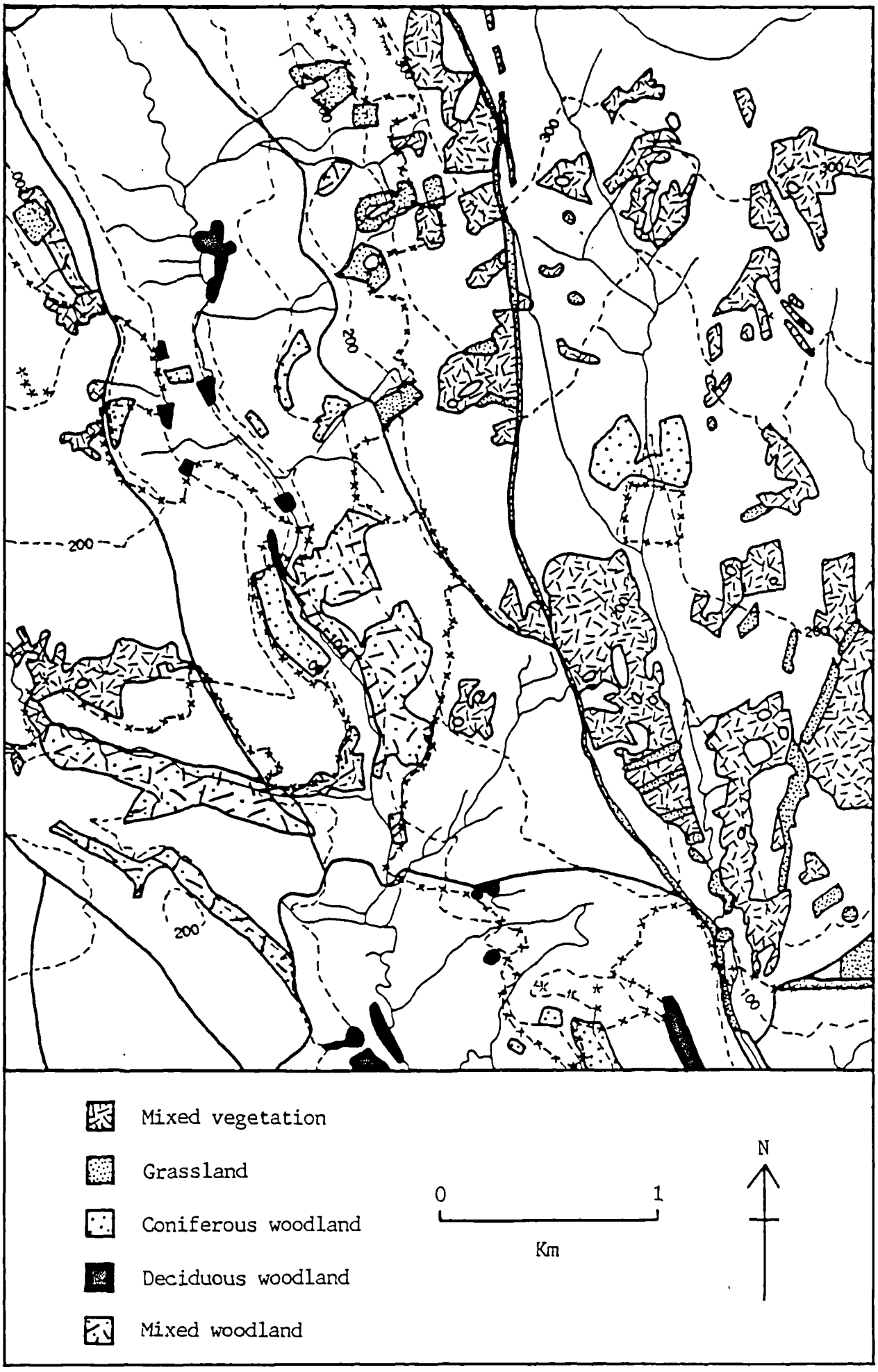

Figure App1.5a Field map of the northern half of Blakey Ridge: Mixed vegetation, grassland and woodland

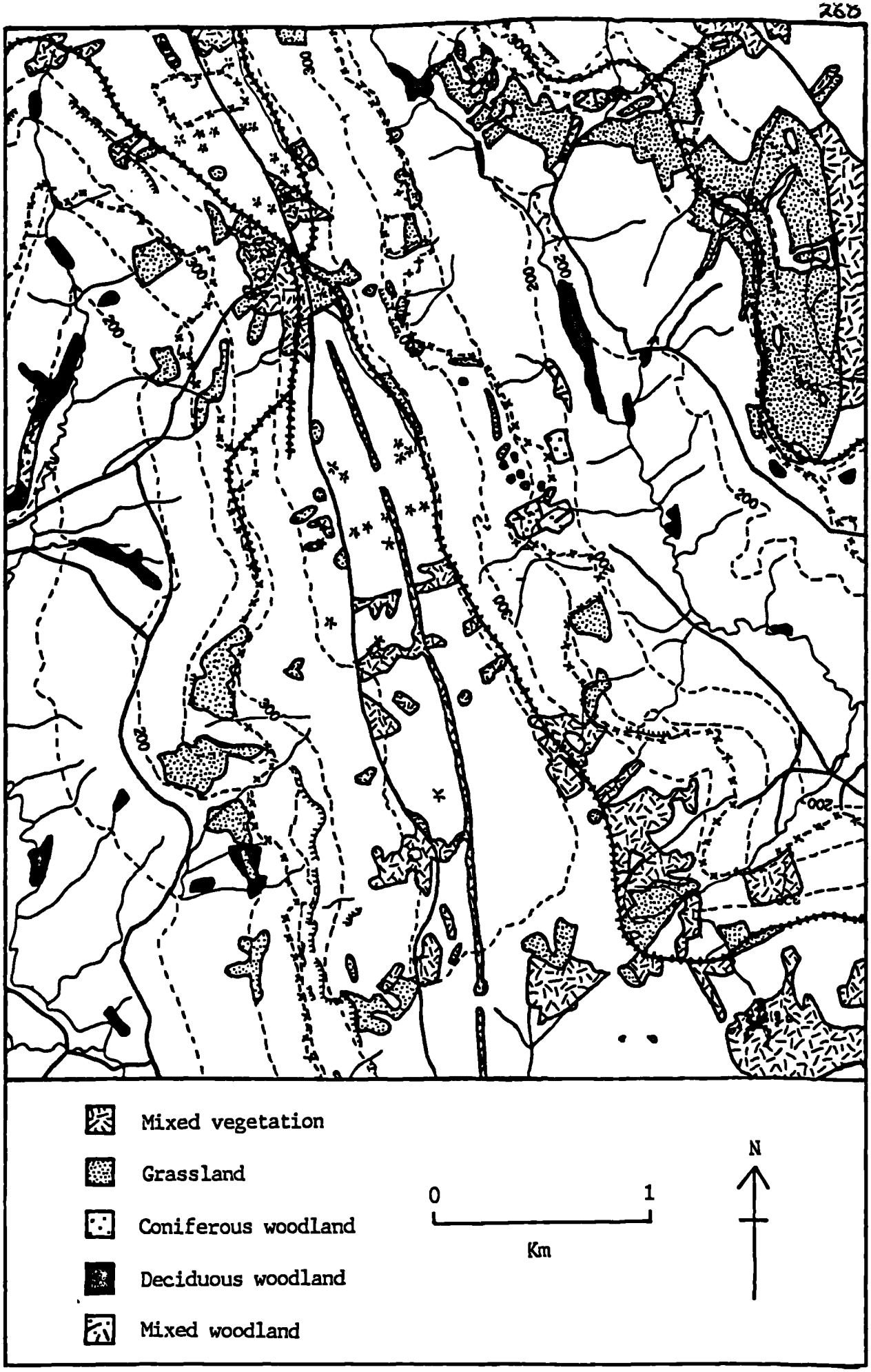

Figure App1.5b Field map of the southern half of Blakey Ridge:
Mixed vegetation, grassland and woodland

APPENDIX 2. SUMMARY STATISTICS FOR SPECTRAL DATA SETS

class	channels							
	mean				standard deviation			
	FS1	FS2	FS3	FS4	FS1	FS2	FS3	FS4
Pa1	8.4	6.4	37.0	27.4	1.2	0.7	3.9	2.1
Pa2	8.5	6.6	36.5	29.8	1.2	1.9	6.3	2.6
Pa3	8.5	8.8	32.9	28.4	1.2	0.9	3.9	1.9
Pa4	7.9	6.7	31.2	25.0	1.1	0.9	9.1	2.2
Pa5	7.4	6.6	28.9	23.9	1.1	1.1	2.7	1.5
Pa6	8.7	10.9	23.9	30.2	1.0	1.2	2.4	2.8
Pa7	7.5	9.1	27.9	29.3	0.7	0.5	3.6	1.8
Cv	6.6	5.5	40.8	25.4	0.4	0.8	2.4	1.3
Et	2.9	3.2	24.0	16.0	0.4	0.4	2.6	1.8
Vm	6.5	6.8	30.2	22.5	0.7	1.0	4.5	2.9

Class Key: Pa=Pteridium (1=Mature (litter) 2=Mature (Vm) 3=Pioneer (Cv) 4=Pioneer (Et) 5=Treated (litter) 6=Treated (Vm) 7=Degenerate) Cv=Calluna Et=Erica Vm=Vaccinium

Table App2.1 Summary statistics for field spectral data: June 1986

class	channels							
	mean				standard deviation			
	FS1	FS2	FS3	FS4	FS1	FS2	FS3	FS4
Pa1	5.3	4.5	60.8	37.2	0.8	0.5	4.9	5.8
Pa2	6.4	4.0	60.0	37.7	0.5	0.3	3.8	2.3
Pa3	7.3	4.0	53.9	32.1	0.9	0.4	5.9	4.6
Pa4	6.3	4.7	51.5	36.6	0.8	0.4	6.4	4.6
Pa5	5.4	3.8	58.3	38.2	0.6	0.3	3.6	3.4
Pa6	6.5	7.8	25.2	28.7	0.7	1.1	2.0	1.7
Pa7	7.2	7.2	32.5	28.8	0.6	0.8	3.8	1.9
Cv	6.0	5.0	40.0	27.9	0.7	0.3	5.0	2.4
Et	3.4	7.4	33.2	20.4	0.4	0.7	1.7	1.6
Vm	4.4	4.8	27.9	23.4	0.3	0.3	1.6	2.0

Class Key: Pa=Pteridium (1=Mature (litter) 2=Mature (Vm) 3=Pioneer (Cv) 4=Pioneer (Et) 5=Treated (litter) 6=Treated (Vm) 7=Degenerate) Cv=Calluna Et=Erica Vm=Vaccinium

Table App2.2 Summary statistics for field spectral data: August 1986

class	channels									
	mean					standard deviation				
	ATM1	ATM2	ATM3	ATM4	ATM5	ATM1	ATM2	ATM3	ATM4	ATM5
Cv1	18.1	19.7	24.7	56.6	5.8	1.2	0.8	1.2	3.0	1.1
Cv2	26.6	28.2	32.2	58.1	8.7	2.3	2.3	2.3	5.1	1.0
Cv3	29.3	30.6	35.4	43.6	8.5	1.8	2.1	2.2	3.3	1.2
Cv4	20.9	22.5	26.9	54.7	6.3	1.7	1.9	1.6	5.0	1.0
Pa	40.7	49.9	59.3	77.1	11.3	1.0	1.2	1.4	3.5	1.0
Gr	38.9	46.8	50.6	84.4	9.4	2.5	3.3	2.7	8.3	0.9
Ag	32.9	44.2	43.6	105.3	8.4	2.7	2.8	2.8	7.2	1.1

Class Key: Cv=Calluna (1=Mature 2=Pioneer 3=Burnt 4=Degenerate)
Pa=Pteridium Gr=Grassland Ag=Agriculture

Table App2.3 Summary statistics for Airborne Thematic Mapper data: May 1986

class	channels									
	mean					standard deviation				
	ATM1	ATM2	ATM3	ATM4	ATM5	ATM1	ATM2	ATM3	ATM4	ATM5
Cv1	14.5	19.8	23.5	100.8	3.8	1.0	1.1	1.0	5.7	0.9
Cv2	25.0	28.1	33.5	81.9	5.6	2.2	1.8	1.9	7.6	0.9
Cv3	33.3	34.7	37.3	43.8	6.5	1.9	1.9	1.9	2.4	0.8
Cv4	16.3	19.7	26.3	87.2	3.5	1.0	0.5	0.9	3.4	0.8
Pa	17.6	29.9	27.7	191.0	4.6	1.1	1.5	1.0	11.5	0.8
Gr	23.3	29.0	33.8	74.6	6.2	2.7	3.6	3.4	27.6	1.1
Ag	17.8	26.0	25.7	134.8	3.6	1.1	1.0	0.9	5.1	0.9

Class Key: Cv=Calluna (1=Mature 2=Pioneer 3=Burnt 4=Degenerate)
Pa=Pteridium Gr=Grassland Ag=Agriculture

Table App2.4 Summary statistics for Airborne Thematic Mapper data: July 1986

class	bands											
	mean						standard deviation					
	TM1	TM2	TM3	TM4	TM5	TM7	TM1	TM2	TM3	TM4	TM5	TM7
Cv1	66.8	22.5	20.9	34.6	39.6	16.0	0.9	0.7	0.7	1.1	2.1	1.9
Cv2	76.6	29.5	31.7	38.7	79.5	42.3	1.5	0.5	0.6	0.5	2.0	1.3
Cv3	69.0	24.1	24.4	26.8	44.3	23.9	1.2	0.6	0.6	0.7	1.2	1.0
Cv4	70.3	25.2	24.8	41.0	52.1	20.8	1.0	0.8	0.8	1.4	5.9	2.0
Pa	82.2	35.2	44.6	58.7	102.7	45.3	1.3	0.7	1.9	2.0	4.9	3.0
Gr	76.6	31.8	29.3	81.9	74.8	26.7	1.1	1.1	0.9	3.8	2.6	1.3
Ag	85.2	37.4	43.1	50.1	80.6	48.4	1.7	0.9	1.4	1.6	3.8	2.6
Con	67.2	23.7	20.3	40.0	29.9	10.5	0.9	0.9	0.9	2.2	2.7	1.6

Class Key: Cv=Calluna (1=Mature 2=Pioneer 3=Burnt 4=Degenerate)
Pa=Pteridium Gr=Grassland Ag=Agriculture Con=Conifers

Table App2.5 Summary statistics for Landsat Thematic Mapper data: April 1984

class	bands											
	mean						standard deviation					
	TM1	TM2	TM3	TM4	TM5	TM7	TM1	TM2	TM3	TM4	TM5	TM7
Cv1	58.7	19.6	17.7	35.0	46.9	19.4	1.2	0.8	1.0	1.3	3.7	3.2
Cv2	69.5	27.3	28.5	46.9	87.0	43.8	0.9	0.7	1.2	1.1	3.6	1.9
Cv3	59.2	20.5	18.9	24.0	39.9	20.1	0.9	0.5	0.8	1.9	5.0	3.7
Cv4	62.3	22.5	20.4	46.3	59.3	23.4	1.8	0.8	0.9	1.9	3.5	2.3
Pa	79.2	34.9	43.8	64.2	116.4	49.2	1.5	1.2	2.4	2.4	4.2	2.2
Gr	64.4	26.9	19.8	118.6	64.1	17.9	1.7	0.9	1.3	4.7	7.3	2.5
Ag	70.9	42.0	38.9	133.6	64.9	19.6	5.4	13.8	16.7	6.9	2.5	1.9
Con	59.9	21.6	17.1	48.7	32.1	10.2	0.9	0.8	0.6	7.5	2.4	1.6

Class Key: Cv=Calluna (1=Mature 2=Pioneer 3=Burnt 4=Degenerate)
Pa=Pteridium Gr=Grassland Ag=Agriculture Con=Conifers

Table App2.6 Summary statistics for Landsat Thematic Mapper data: May 1985

APPENDIX 3. SPECTRAL RESPONSE PATTERN DIAGRAMS

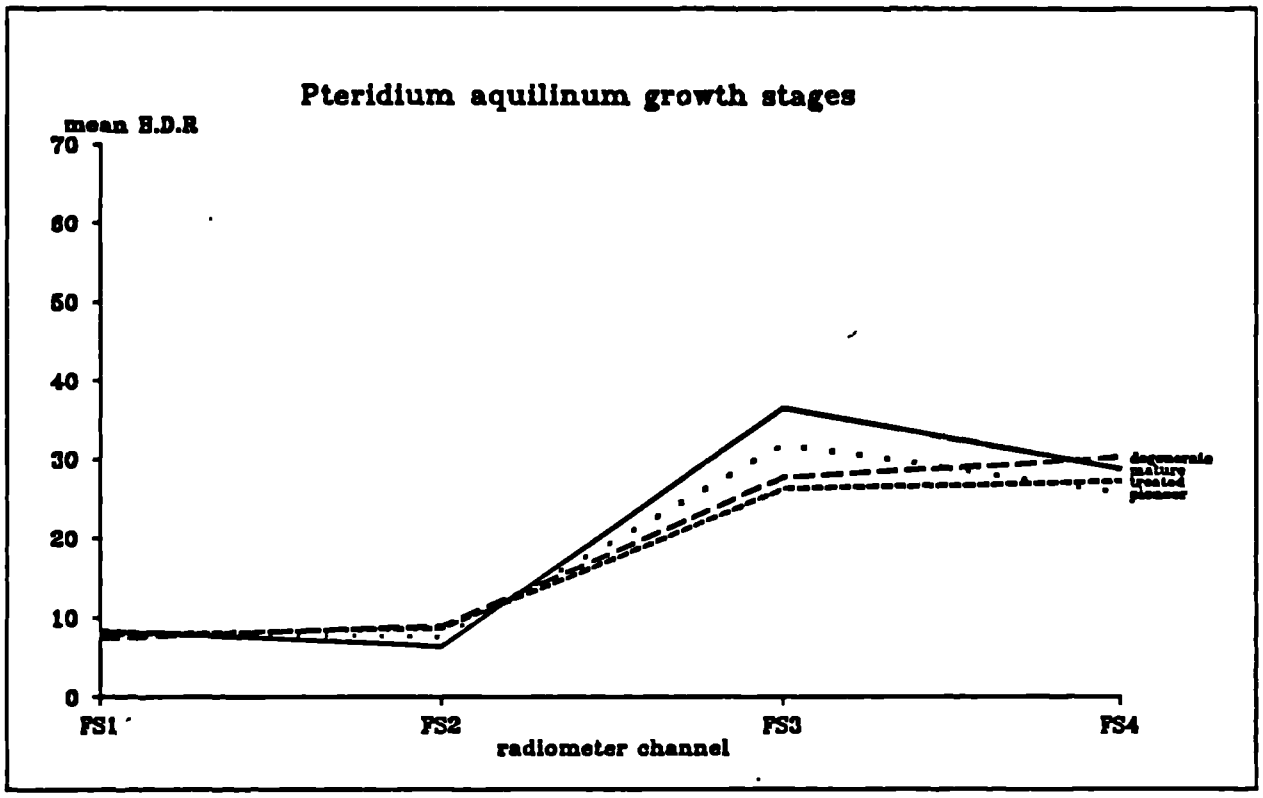

a) June 1986

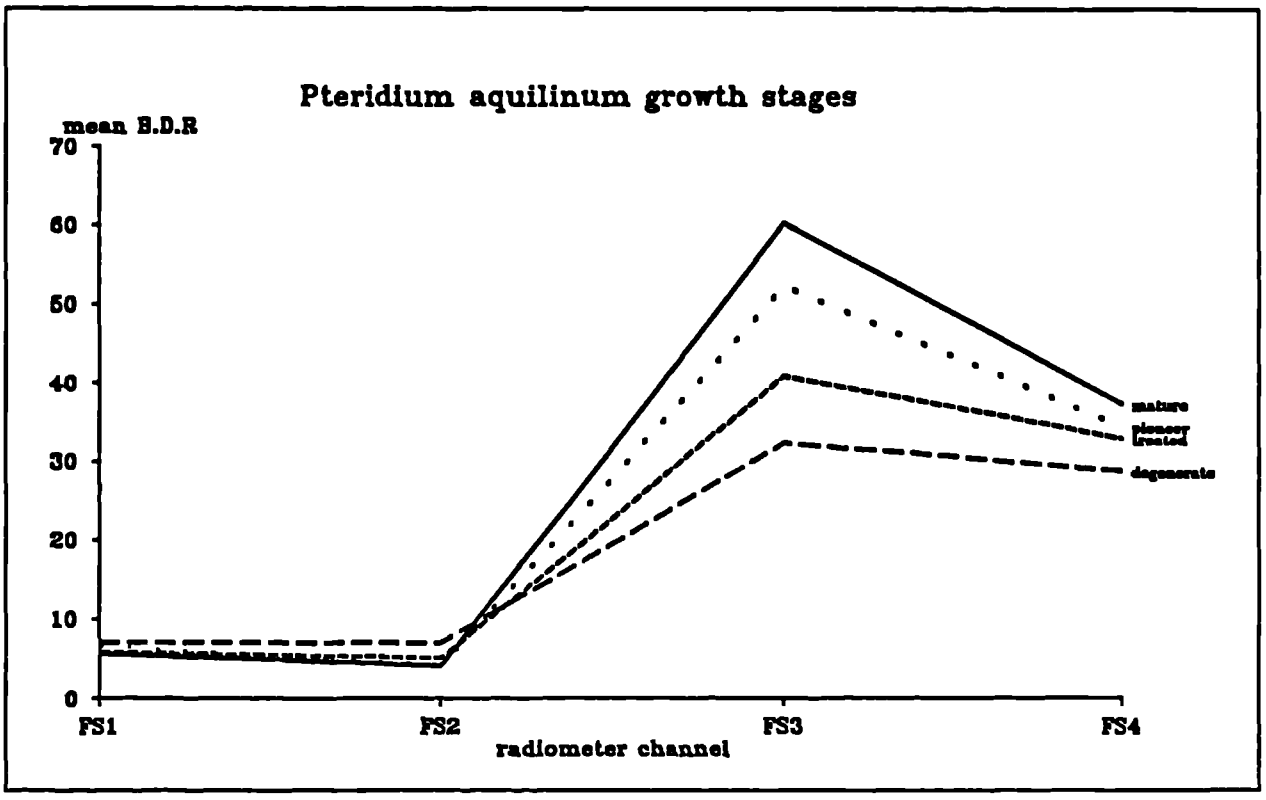

b) August 1986

Figure App3.1 Spectral response patterns for Pteridium aquilinum growth stages: field spectral data

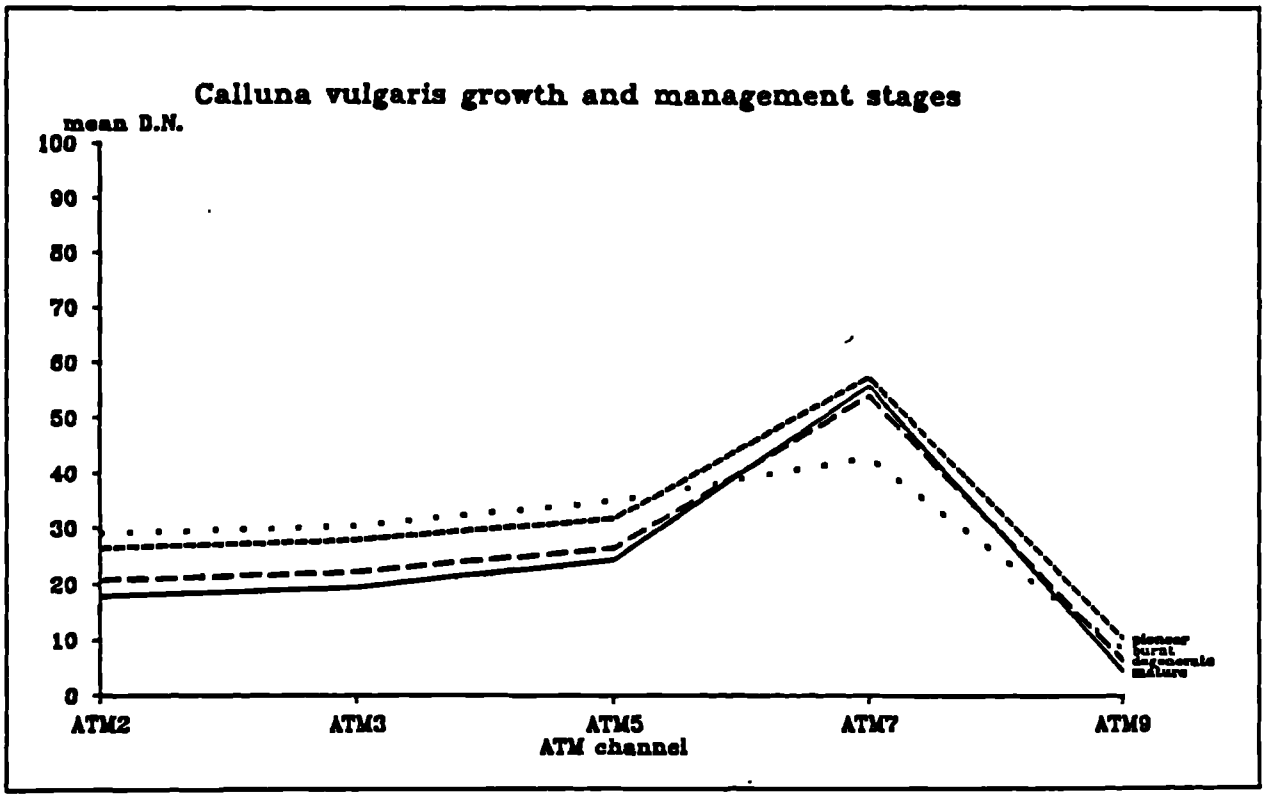

a) May 1986

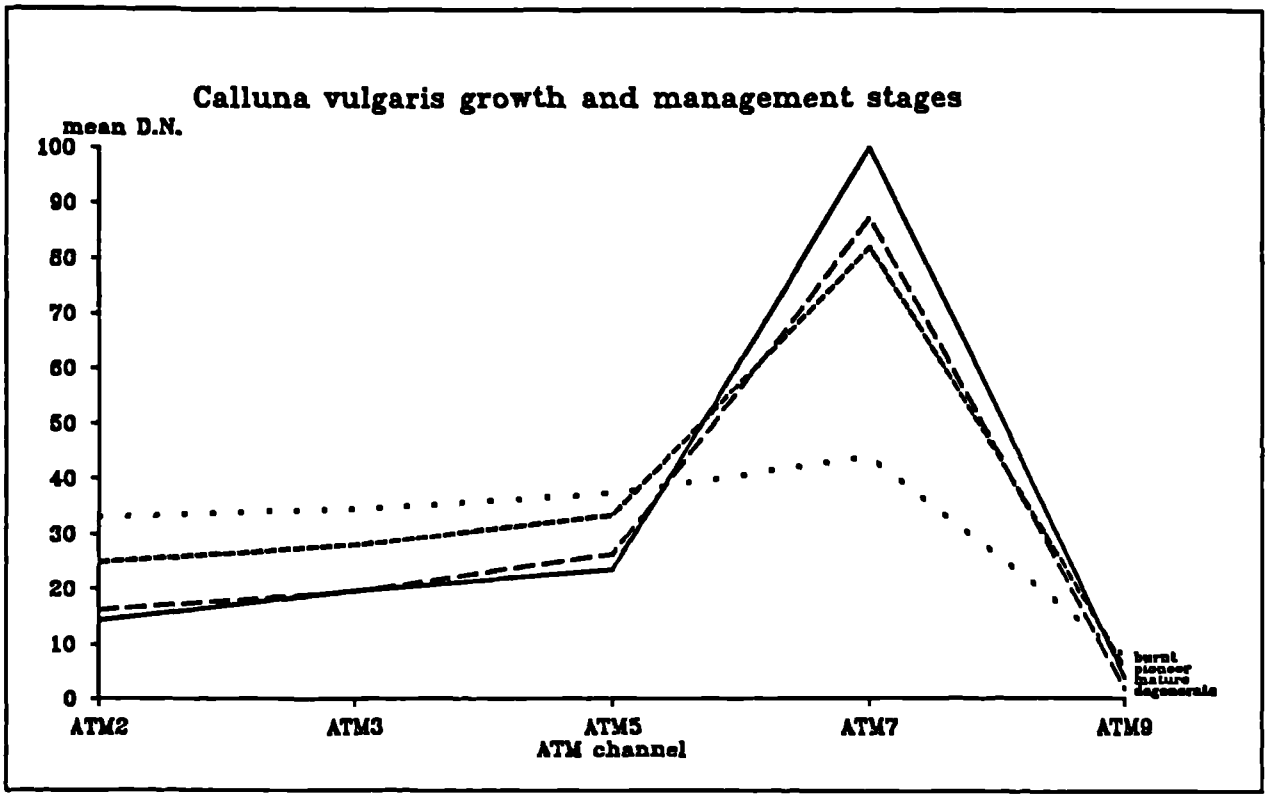

b) July 1986

Figure App3.2 Spectral response patterns for Calluna vulgaris growth and management stages: Airborne Thematic Mapper data

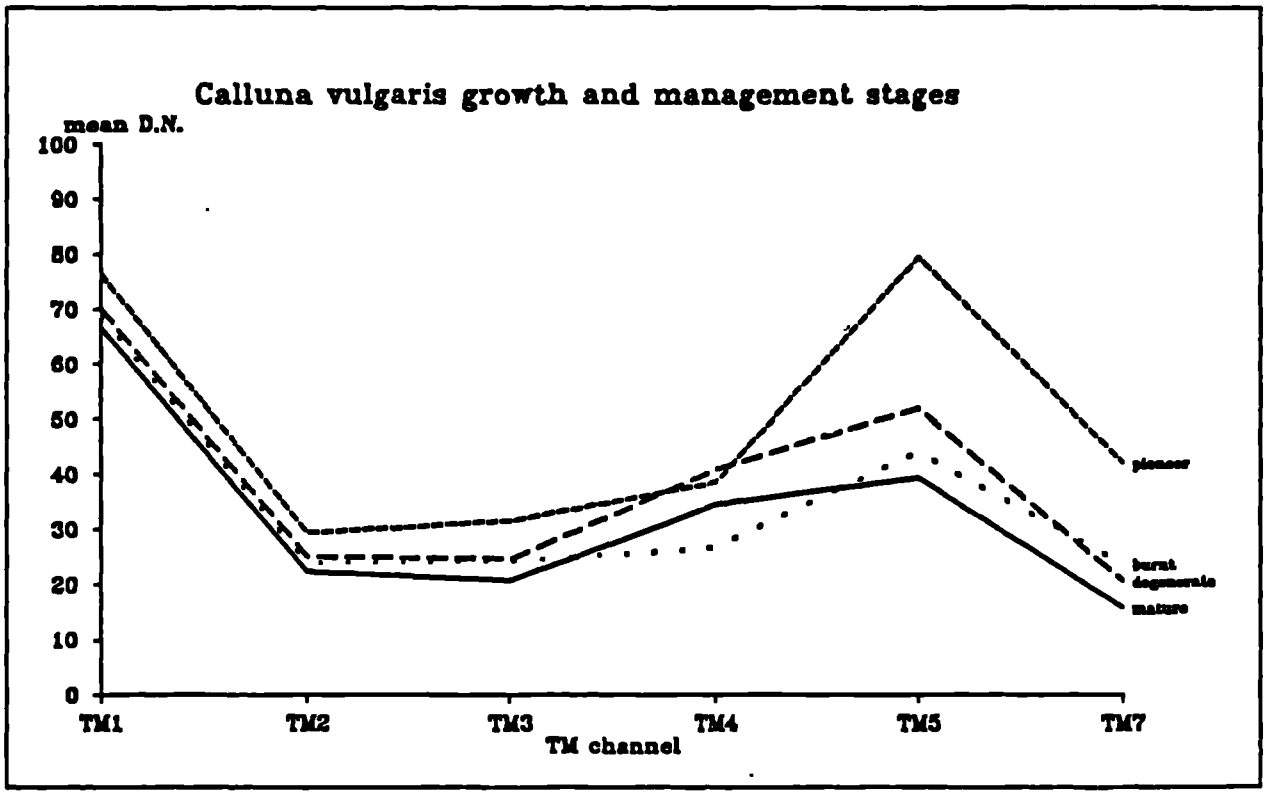

a) April 1984

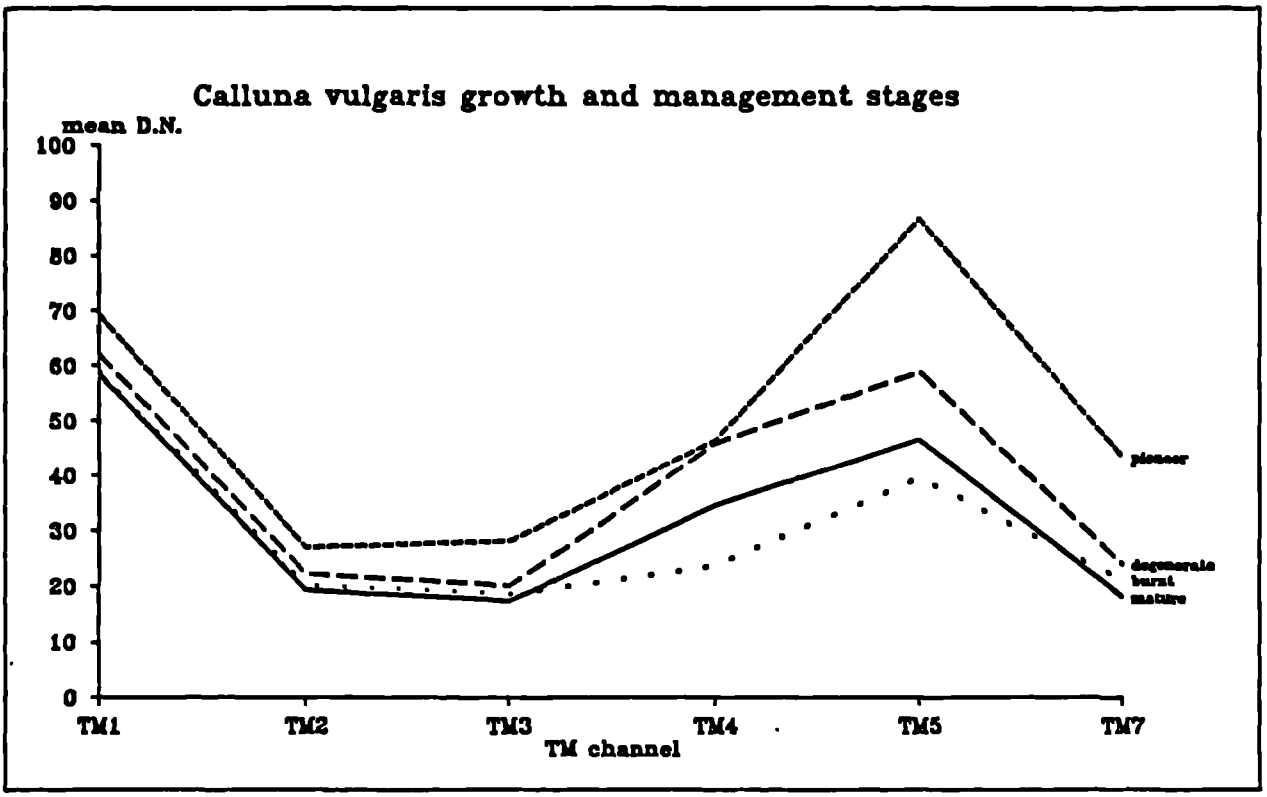

b) May 1985

Figure App3.3 Spectral response patterns for Calluna vulgaris growth and management stages: Landsat Thematic Mapper data

APPENDIX 4. CLUSTER ANALYSIS CONFUSION MATRICES

real class	No. of cases	image class								
		Cv1	Cv2	Cv3	Cv4	Pa	Gr	Ag	Wet	Mix
Cv1	60	66.5	31.0	0	0	0	2.5	0	0	0
Cv2	26	15.5	38.5	38.5	0	0	7.5	0	0	0
Cv3	50	16.0	0	72.0	0	0	12.0	0	0	0
Cv4	34	70.5	6.0	6.0	0	0	11.5	0	0	6.0
Pa	60	7.0	0	4.5	0	46.0	23.5	2.5	0	16.0
Gr	34	18.0	0	0	0	6.0	41.0	11.5	0	23.5
Ag	24	0	0	16.5	0	0	42.0	25.0	0	16.5
Wet	24	0	0	0	0	44.5	33.5	0	0	22.0
Mix	48	21.0	0	0	0	4.0	21.0	0	0	54.0

Overall accuracy = 42% (±7%)

Key: Cv=Calluna (1=Mature 2=Pioneer 3=Burnt 4=Degenerate)
Pa=Pteridium Gr=Grassland Ag=Agriculture Wet=Wetland vegetation Mix=mixed vegetation

Table App4.1 Cluster analysis accuracy confusion matrix: Airborne Thematic Mapper, 2.5m data

real class	No. of cases	image class								
		Cv1	Cv2	Cv3	Cv4	Pa	Gr	Ag	Wet	Mix
Cv1	60	83.0	5.0	9.5	0	0	2.5	0	0	0
Cv2	26	31.0	46.0	23.0	0	0	0	0	0	0
Cv3	50	12.0	4.0	72.0	0	0	8.0	0	0	4.0
Cv4	34	65.0	0	11.5	0	6.0	11.5	0	0	6.0
Pa	60	7.0	0	4.5	0	56.0	9.5	7.0	0	16.0
Gr	34	23.5	0	0	0	6.0	53.0	17.5	0	0
Ag	24	0	0	16.5	0	0	50.0	33.5	0	0
Wet	24	0	0	0	0	44.5	33.5	0	0	22.0
Mix	48	25.0	0	0	0	0	16.5	0	0	58.5

Overall accuracy = 56% (±7%)

Key: Cv=Calluna (1=Mature 2=Pioneer 3=Burnt 4=Degenerate)
Pa=Pteridium Gr=Grassland Ag=Agriculture Wet=Wetland
vegetation Mix=mixed vegetation

Table App4.2 Cluster analysis accuracy confusion matrix: Airborne Thematic Mapper, 5m data

real class	No. of cases	image class								
		Cv1	Cv2	Cv3	Cv4	Pa	Gr	Ag	Wet	Mix
Cv1	60	90.5	0	0	0	0	7.0	0	0	2.5
Cv2	26	15.5	84.5	0	0	0	0	0	0	0
Cv3	50	12.0	24.0	52.0	0	0	12.0	0	0	0
Cv4	34	70.5	6.0	11.5	0	6.0	6.0	0	0	0
Pa	60	7.0	0	4.5	0	63.0	9.5	0	0	16.0
Gr	34	6.0	0	0	0	0	53.0	0	0	41.0
Ag	24	0	0	25.0	0	0	41.5	0	0	33.5
Wet	24	0	0	0	0	66.5	22.5	0	0	11.0
Mix	48	25.0	0	0	0	0	16.5	0	0	58.5

Overall accuracy = 56% (±7%)

Key: Cv=Calluna (1=Mature 2=Pioneer 3=Burnt 4=Degenerate) Pa=Pteridium Gr=Grassland Ag=Agriculture Wet=Wetland vegetation Mix=mixed vegetation

Table App4.3 Cluster analysis accuracy confusion matrix: Airborne Thematic Mapper, 10m data

real class	No. of cases	image class								
		Cv1	Cv2	Cv3	Cv4	Pa	Gr	Ag	Wet	Mix
Cv1	60	81.0	12.0	2.5	0	0	4.5	0	0	0
Cv2	26	15.5	46.0	38.5	0	0	0	0	0	0
Cv3	50	8.0	20.0	48.0	0	8.0	16.0	0	0	0
Cv4	34	47.0	17.5	12.0	0	0	23.5	0	0	0
Pa	60	9.5	0	4.5	0	60.5	9.5	0	0	16.0
Gr	34	6.0	0	6.0	0	6.0	47.0	0	0	35.0
Ag	24	0	0	17.0	0	0	41.5	0	0	41.5
Wet	24	0	0	0	0	78.0	11.0	0	0	11.0
Mix	48	16.5	0	0	0	0	21.0	0	0	62.5

Overall accuracy = 50% (±7%)

Key: Cv=Calluna (1=Mature 2=Pioneer 3=Burnt 4=Degenerate)
Pa=Pteridium Gr=Grassland Ag=Agriculture Wet=Wetland vegetation Mix=mixed vegetation

Table App4.4 Cluster analysis accuracy confusion matrix: Airborne Thematic Mapper, 20m data

real class	No. of cases	image class								
		Cv1	Cv2	Cv3	Cv4	Pa	Gr	Ag	Wet	Mix
Cv1	60	74.0	0	2.5	0	0	19.0	0	0	4.5
Cv2	26	15.5	61.5	23.0	0	0	0	0	0	0
Cv3	50	4.0	0	64.0	0	0	16.0	0	0	16.0
Cv4	34	0	17.5	6.0	0	70.5	6.0	0	0	0
Pa	60	11.5	0	2.5	0	58.0	0	0	0	28.0
Gr	34	12.0	0	0	0	0	35.0	0	0	53.0
Ag	24	8.5	0	16.5	0	16.5	33.5	0	0	25.0
Wet	24	22.5	0	0	0	55.5	11.0	0	0	11.0
Mix	48	21.0	0	0	0	16.5	21.0	0	0	41.5

Overall accuracy = 48% ($\pm$7%)

Key: Cv=Calluna (1=Mature 2=Pioneer 3=Burnt 4=Degenerate) Pa=Pteridium Gr=Grassland Ag=Agriculture Wet=Wetland vegetation Mix=mixed vegetation

Table App4.5 Cluster analysis accuracy confusion matrix: Airborne Thematic Mapper, 30m data

REFERENCES

Adomeit, E.M., Jupp, D.L.B., Margules, C.R. and Mayo, K.K. (1981) The separation of traditionally mapped land cover classes by Landsat data. In Gillison, A.N. and Anderson, R.J., (eds.) Vegetation classification in Australia, 150-166. Canberra, Australia.

Alam M.S. (1987) The application of remote sensing in open moorland soil erosion studies: a case study of Glaisdale Moor, Northern England. Unpublished PhD thesis, Department of Geography, University of Durham.

Alam, M.S. and Harris, R. (1987) Moorland soil erosion and spectral reflectance. International Journal of Remote Sensing, Volume 8, 593-608.

Anderson, G.D. (1958) A preliminary investigation of the soils of the north-east Yorkshire moors. Unpublished PhD thesis, Kings College, Newcastle-upon-Tyne.

Asrar, G., Weiser, R.C., Johnson, D.E., Kanemasu, E.T. and Killeen, J.M. (1986) Distinguishing among tall-grass prairie cover types from measurement of multi-spectral reflectance. Remote Sensing of Environment, Volume 19, 159-169.

Atherden M.A. (1972) A contribution to the vegetation and landuse history of the eastern central North York Moors. Unpublished PhD Thesis, University of Durham.

Atkinson, P., Cushnie, J.L., Townshend, J.R.G. and Wilson, A. (1985) Improving Thematic Mapper land cover classification using filtered data. International Journal of Remote Sensing, Volume 6, 955-961.

Barrett, E.C. and Curtis, L.F. (1976) Introduction to environmental remote sensing. Chapman and Hall; London.

Bauer, M.E. (1985) Spectral inputs to crop identification and condition assessment. Proceedings of the IEEE, Volume 73, 1071-1085.

Birnie, R.V. (1983) Mapping bracken (Pteridium aquilinum) infestation in Scotland: an assessment of remote sensing based mapping techniques. Proceedings of IPS Commission 1, 115-126. Aberdeen.

Birnie, R.V. (1985) An assessment of the bracken problem in relation to hill farming in Scotland. Soil Use and Management, Volume 1, 57-60.

Boodle, L.A. (1904) The structure of the leaves of bracken (Pteris aquilina Linn.) in relation to environment. Botanical Journal of the Linnean Society, Volume 35, 659-669.

Bryant, J. (1979) On the clustering of multi-dimensional pictorial data. Pattern recognition, Volume 11, 115-125.

Budd, and Milton, E.J. (1982) Remote sensing of salt marsh vegetation in the first four proposed Thematic Mapper bands. International Journal of Remote Sensing, Volume 3, 147-161.

Carlson, R.E., Yarger, D.N. and Shaw, R.H. (1971) Factors affecting the spectral properties of leaves with special emphasis on leaf water status. Agronomy Journal, Volume 63, 486-489.

Carrol, D.M. and Bendelow, V.C. (1981) Soils of the North York Moors. Soil Survey, Special Survey, No.13; Hapenden, Hertfordshire.

Chahine, M.T. (1983) Interaction mechanisms within the atmosphere. In Colwell, R.N. (ed.), Manual of remote sensing (second edition), Volume 1, 165-230. American Society of Photogrammetry; Falls Church, Virginia, U.S.A.

Chevrel, M., Courtois, M. and Weill, G. (1981) The Spot satellite remote sensing mission. Photogrammetrical Engineering and Remote Sensing, Volume 47, 1163-1171.

Clark, A.M. (1983) The bracken problem - a study of management attempts on the North Yorkshire Moors. Unpublished M.A. thesis, School of Geography, University of Leeds.

Clark, J. and Bryant, N.A. (1976) Landsat-D Thematic Mapper simulation using aircraft multi-spectral scanner data. Proceedings of 11th International Symposium on the Remote Sensing of the Environment, 483-491. Environment Research Institute of Michigan; Ann Arbor, U.S.A.

Colvocoresses, A.P. (1979) Effective resolution element (ERE) of remote sensors. Memorandum for the record, February 8th 1979. Geological Survey, Department of the Interior. Virginia, U.S.A.

Congalton, R.G., Oderwald, R.G. and Mead, R.A. (1983) Assessing Landsat classification accuracy using discrete multivariate analysis statistical techniques. Photogrammetrical Engineering and Remote Sensing, Volume 49, 1671-1678.

Conway, D. and Holz, R.K. (1973) The use of near infrared photography in the analysis of surface morphology of an Argentine alluvial floodplain. Remote Sensing of Environment, Volume 2, 235-242.

Cormack, E. and Gimmingham, C.H. (1964) Litter production by Calluna vulgaris. Journal of Ecology, Volume 52, 285-297.

Cundill, P.R. (1971) Ecological history and development of peat on the Central Watershed of the North York Moors. Unpublished PhD thesis, University of Durham.

Curran, P.J. (1981) The estimation of the surface moisture of a vegetated soil using aerial infrared photography. International Journal of Remote Sensing, Volume 2, 369-370.

Curran, P.J. (1983) Multispectral remote sensing for the estimation of green leaf area index. Philosophical Transactions of the Royal Society, Volume 309, 257-270.

Curran, P.J. (1985a) Aerial Photography for the Assessment of Crop Condition: A Review. Applied Geography, Volume 5, 347-360.

Curran, P.J. (1985b) Principles of Remote Sensing. Longman; London.

Curran, P.J. and Williamson, H.D. (1985) The accuracy of ground data used in remote sensing investigations. International Journal of Remote Sensing, Volume 6, 1637-1651.

Cushnie, J.L. (1984) The effect of resampling on image accuracy. Satellite remote sensing - review and preview. Proceedings of the 10th International Conference of the Remote Sensing Society, Reading, 329-339.

Cushnie, J.L. (1987) The interactive effect of spatial resolution and degree of internal variability within land-cover types in classification accuracies. International Journal of Remote Sensing, Volume 8, 15-29.

Cushnie, J.L. and Atkinson, P. (1985) Effect of spatial filtering on scene noise and boundary detail in Thematic Mapper imagery. Photogrammetrical Engineering and Remote Sensing, Volume 51, 1483-1493.

Daedalus Enterprises Inc. (1986) Daedalus Scanner Applications, Worldwide. Ann Arbor, Michigan, U.S.A.

Darlington, A. (1978) Mountains and moorlands. Book Club Associates; London.

Dimbleby, G.W. (1952) Soil regeneration on the North-East Yorkshire Moors. Journal of Ecology, Volume 40, 331-341.

Dimbleby, G.W. (1962) The development of British heathlands and their soils. Oxford Forestry Memoir, 23.

Dixon, W.J. (ed.) (1975) Boimedical computer programs. University of California Press; Berkley, California, U.S.A.

Drake, N., Mackin, S., Munday, T.J., Settle, J. and Al-Sari, A., (1988) Mapping the distribution and abundance of lithological units and surface mineralogies at Jabal Sa'id, Saudi Arabia: an application of spectral mixture modelling. In Remote sensing: moving towards the 21st century, Proceedings of the IGARSS'88 conference, Volume 1, 367-368.

Duggin, M.J. (1980) The field measurement of reflectance factors. Photogrammetrical Engineering and Remote Sensing, Volume 46, 643-647.

Duggin, M.J. and Phillipson, W.R. (1985) Relating ground, aircraft and satellite radiance measurements: spectral and spatial considerations. International Journal of Remote Sensing, Volume 6, 1665-1670.

Elgee. F. (1912) The moorland of north-east Yorkshire. London.

Elgee. F. (1914) The vegetation of the eastern moorlands of Yorkshire. Journal of Ecology, Volume 2, 1-18.

Elgee, F. (1930) Early man in north-east Yorkshire. John Bellows; Gloucester.

Estes, J.E. (1974) Imaging with photographic and non-photographic sensor systems. In Estes, J.E. and Senger, L.W. (eds.), Remote sensing techniques for environmental analysis, 15-50. Hamilton; Santa Barbara, California, U.S.A.

Estes, J.E., Hajic, E.J. and Tinney, L.R. (1983) Fundamentals of image analysis: analysis of visual and thermal infrared data. In Colwell, R.N. (ed.), Manual of remote sensing (second edition), Volume 1, 987-1124. American Society of Photogrammetry; Falls Church, Virginia, U.S.A.

Everett, J. and Simonett, D.S. (1976) Principles, concepts and philosophical problems in remote sensing. In Lintz, J. and Simonett, D.S. (eds.) Remote sensing of environment, 85-133. Addison-Wesley; Reading, Massachusetts, U.S.A.

Forshaw, M.R.B., Haskell, A., Miller, P.F., Stanley, D.J. and Townshend, J.R.G. (1980) A review paper: spatial resolution of remotely sensed imagery. Paper submitted to the U.S. Committee for peaceful uses of outer space.

Fox-Strangeways, L., Reid, C. and Barrow, G. (1885) The geology of Eskdale, Rosedale and county. Memoirs of the Geological Survey; London (Sheet 43).

Fraser, R.S. and Curran, R.J. (1976) Effects of the atmosphere on remote sensing. In Lintz, J. and Simonett, D.S. (eds.), Remote sensing of environment, 34-84. Addison-Wesley; Reading, Massachusetts, U.S.A.

Freden, S.C. and Gordon, F. (1983) Landsat satellites. In Colwell, R.N. (ed.), Manual of remote sensing (second edition), Volume 1, 517-570. American Society of Photogrammetry; Falls Church, Virginia, U.S.A.

Fuller, R.M., Devereux, B.J., Carter, L. and Parsell, R.J., (1988) The Airborne Thematic Mapper for applied ecology surveys of lowland Britain. In Proceedings of the N.E.R.C. 1985 Airborne Campaign Workshop, 13-26. N.E.R.C.; Wallingford.

Gausman, H.W. (1977) Reflectivity of leaf components. Remote sensing of environment, Volume 6, 1-9.

Gimmingham, C.H. (1960) Calluna vulgaris. Journal of Ecology, Volume 48, 455-489.

Gladwell, D.R., Lett, R.E. and Lawrence, P. (1983) Applications of reflectance spectrometry to mineral exploration using a portable radiometer. Economic Geology, Volume 78, 699-710.

Haffey, D. (1978) A recreational and ecological assessment of the moorlands of the North York Moors National Park. Unpublished M.Phil. thesis, University of York.

Hammond, R. and McCullagh, P.S. (1978) Quantitative techniques in Geography: an introduction. (second edition) Clarendon Press; Oxford.

Hardy, J.R. (1981) Data collection by remote sensing for land resources survey. In Townshend, J.R.G., Terrain analysis and remote sensing. George, Allen and Unwin; London.

Harris, R. (1987) Satellite remote sensing: an introduction. Routledge and Kegan Paul; London.

Hay, A.M. (1979) Sampling designs to test land-use map accuracy. Photogrammetrical Engineering and Remote Sensing, Volume 45, 529-533.

Healey, R., Dowie, P., Mowle, A. and Holbrook, J. (1988) Integrating remote sensing data into a geographical information system: a foundation for rural land use strategies - Nature Conserancy Council project. In Remote sensing: moving towards the 21st century, Proceedings of the IGARSS'88 conference, Volume 1, 111-112.

Hoffer, R.M. (1978) Biological and physical considerations in applying computer-aided analysis techniques to remote sensing data. In Swain, P.H. and Davis, S.M. (eds.), Remote sensing: the quantitative approach, 227-289. McGraw Hill; New York, U.S.A.

Hook, S.J. and Donoghue, D.N.M. (1988) Calibration and correction of view angle effects in visible, near infrared and thermal data. In Proceedings of the N.E.R.C. 1985 Airborne Campaign Workshop, 187-202. N.E.R.C.; Wallingford.

Hord, R.M. and Brooner, W. (1976) Land-use map accuracy criteria. Photogrammetrical Engineering and Remote Sensing, Volume 42, 671-677.

Howard, A.D. (1965) Photogeologic interpretation of structure in the Amazon Basin: a test study. Geological Society of America Bulletin, No. 76, 395-406.

Hunting Geology and Geophysics Ltd. (1986) Daedalus 1268: The Airborne Thematic Mapper. Boreham Wood, Hertfordshire.

Innes, J.B. (1981) Environmental alteration by Mesolithic communities in the North York Moors. Unpublished M.Phil thesis, University of Durham.

I^2S Inc. (1987) I^2S System 600 command reference manual. Two volumes. I^2S publication.

Jackson, R.D., Pinter, P.J., Reginato, R.J., and Idso, S.B. (1980) Hand-held radiometry. Set of notes developed for use at the workshop on hand-held radiometry, Phoenix Arizona.

James, M. (1985) Classification algorithms. Collins; London.

Jeffreys, H. (1917) On the vegetation of four Durham coal-measure fells. Journal of Ecology, Volume 5, 129-154.

Jones, A.R., Settle, J.J. and Wyatt, B.K. (1988) Use of digital terrain data in the interpretation of SPOT-1 HRV multispectral imagery. International Journal of Remote Sensing, Volume 9, 669-682.

Justice, C.O. and Townshend, J.R.G. (1981) Integrating ground data with remote sensing. In Townshend, J.R.G. (ed.), Terrain analysis and remote sensing. George, Allen and Unwin; London.

Kent, P. (1980) Eastern England from the Tees to the Wash. British regional geology (2nd edition); London.

King, C.A.M. (1965) The Scarborough District. British landscapes through maps, No. 7; Sheffield.

Klecka, W.R. (1980) Discriminant analysis. Quantitative applications in the Social Sciences. Sage Publications; Beverly Hills, California, U.S.A.

Landgrebe, D.A. (1978) The quantitative approach: concept and rationale. In Swain, P.H. and Davis, S.M. (eds.), Remote sensing: the quantitative approach, 1-20. McGraw Hill; New York, U.S.A.

Landgrebe, D.A. (1980) The development of a spectral-spatial classifier for earth observation data. Pattern Recognition, Volume 12, 165-175.

Lillesand, T.M. and Kiefer, R.W. (1979) Remote sensing and image interpretation. John Wiley and Sons; New York, U.S.A.

Lo, C.P. (1981) Land use mapping of Hong Kong from Landsat images: An evaluation. International Journal of Remote Sensing, Volume 2, 231-252.

Lo, C.P. (1986) Applied remote sensing. Longman; New York, U.S.A.

Longshaw, T.G. (1974) Field spectroscopy for multispectral remote sensing: an analytical approach. Applied Optics, Volume 13, 1487-1493.

Lowe, D.S. (1976) Non-photographic optical sensors. In Lintz, J. and Simonett, D.S. (eds.) Remote sensing of environment, 155-193. Addison-Wesley; Reading Massachusetts, U.S.A.

Maltby, E. (1980) The impact of severe fire on Calluna moorland in the North York Moors. Bulletin D'Ecologie, Volume 11, 683-708.

Markham, B.L. and Townshend, J.R.G. (1981) Land cover classification accuracy as a function of sensor spatial resolution. 15th International Symposium on Remote sensing of Environment, 1075-1085. Environment Research Institute of Michigan; Ann Arbor, U.S.A.

Marsh, S.E. and Lyon, R.J. (1980) Quantitative relationships of near surface spectra to Landsat radiometric data. Remote Sensing of Environment, Volume 10, 241-261.

Marsh, S.E., Switzer, P., Kowalick, W.S. and Lyon, R.J. (1980) Resolving the percentage of component terrains within single resolution elements. Photogrammetrical Engineering and Remote Sensing, Volume 46, 1079-1086.

Mather, P.M. (1987) Computer processing of remotely sensed images: an introduction. John Wiley and Sons; Chichester.

Mather, P.M. (1976) Computational methods of multivariate analysis in physical geography. John Wiley and Sons; London.

Milton, E.J. (1986) Series 100 Milton Multiband Radiometers: notes for Users. Geodata Unit, University of Southampton.

Milton, E.J. (1987) Principles of field spectroscopy. International Journal of Remote Sensing, Volume 8, 1807-1827.

Milton, E.J. and Rollin, E.M. (1987) Field spectroscopy of lowland heath. Discussion Paper No. 32, Department of Geography, University of Southampton.

Milton, E.J. and Wardley, N.W. (1987) Vegetation canopy reflectance models: a review. Discussion Paper No. 31, Department of Geography, University of Southampton.

Milton, E.J., Styles, P.J. and Schott, M.H. (1986) Remote sensing of complex vegetation canopies. Proceedings of N.E.R.C. 1985 Airborne Campaign Workshop; N.E.R.C.; I.T.E. Monks Wood.

Morain, S. (1974) Interpretation and mapping of natural vegetation. In Estes, J.E. and Senger, L.W. (eds.), Remote sensing techniques for environmental analysis, 127-166. Hamilton; Santa Barbara, California, U.S.A.

Myers, V.I. (1983) Remote sensing applications in agriculture. In Colwell, R.N. (ed.), Manual of remote sensing (second edition), Volume 2, 2111-2228. American Society of Photogrammetry; Falls Church, Virginia, U.S.A.

Nicholson I.A. and Paterson, I.S. (1976) The ecological implications of bracken control to plant/animal systems. Botanical Journal of the Linnean Society, Volume 73, 269-283.

North York Moors National Park Committee (1979a) Geology of the North York Moors. Helmsley.

North York Moors National Park Committee (1979b) Moorland research 1977-1979. Helmsley.

North York Moors National Park Committee (1982) The future of the moorlands : National Park consultation paper. Helmsley.

North York Moors National Park Committee (1984a) Moor and heath conservation in the North York Moors. Helmsley.

North York Moors National Park Committee (1984b) North York Moors National Park plan: first review. Helmsley.

North York Moors National Park Committee (1985) Moorland management project 1983-1985: final report. Helmsley.

Norton, A. (1982) Bracken management on the North York Moors. Unpublished M.Sc. thesis, Wye College, London.

Norwood, V.T. and Lansing, J.C. (1983) Electro-optical imaging sensors. In Colwell, R.N. (ed.) Manual of remote sensing (second edition), Volume 1, 335-368. American Society of Photogrammetry; Falls Church, Virginia, U.S.A.

Palmer, J. (1973) Geology and relief. In Eyre, S.E. and Palmer, J. (eds), The face of North-east Yorkshire. Clapham, Yorkshire.

Parihar, N.S. (1962) An introduction to embryophyta: volume 2. Pteridophytes. (4th edition) Central Book Depot; Allahabad.

Pearson, R.C., Tucker, C.J., and Miller, L.D. (1976) Spectral mapping of short-grass prairie biomass. Photogrammetrical Engineering and Remote Sensing, Volume 42, 317-323.

Philipson, W.R., and Liang, T. (1975) Airphoto analysis of the tropics: crop identification. Proceedings of 10th International Symposium on the Remote Sensing of the Environment, 1079-92. Environment Research Institute of Michigan; Ann Arbor, U.S.A.

Polunin, O. (1976) Trees and bushes of Europe. Oxford University Press; London.

Quarmby, N.A., Cushnie, J.L. and Smith, J. (1988) The use of remote sensing in conjunction with geographic information systems for local planning. In Remote sensing: moving towards the 21st century, Proceedings of the IGARSS'88 conference, Volume 1, 89-92.

Raines, G.L. and Canney, F.C. (1980) Vegetation and geology. In Siegal, B.S. and Gillespie, A.R. (eds.), Remote sensing in geology, 365-380. John Wiley and Sons; New York, U.S.A.

Rothery, D.A., and Lefebvre, R.H. (1985) The cause of age dependent changes in the spectral response of lavas, Craters of the Moon, Idaho, U.S.A. International Journal of Remote Sensing, Volume 6, 1484-1489.

Ryan, T.A., Joiner, B.L. and Ryan, B.F. (1982) MINITAB reference manual. Duxbury press; Boston, Massachusetts, U.S.A.

Rymer, L. (1976) The history and ethnobotany of bracken. Botanical Journal of the Linnean Society, Volume 73, 151-176.

Sabins, F.F. (1987) Remote sensing principles and interpretation. (2nd edition) W.H. Freeman; New York, U.S.A.

Sadowski, F.G., Malila, W.A., Sarno, J.E. and Nalepka, R.F. (1976) The influence of multispectral scanner spatial resolution on forest feature classification. Proceedings of 15th International Symposium on the Remote Sensing of the Environment, 1279-1285. Environment Research Institute of Michigan; Ann Arbor, U.S.A.

Schanda, E. (1986) Physical fundamentals of remote sensing. Springer-Verlag; Berlin.

Schowengerdt, R.A. (1983) Techniques for image processing and classification in remote sensing. Academic Press; London.

Senger, J.E. (1971) Quantitative investigations of leaf pigments from inception in buds through autumn coloration to decomposition in falling leaves. Ecology, Volume 52, 1075-1089.

Short, N.M. (1982) The Landsat tutorial workbook: basics of satellite remote sensing. N.A.S.A. Publication; Washington, U.S.A.

Silva, L.R. (1978) Radiation and instrumentation in remote sensing. In Swain, P.H. and Davis, S.M. (eds.), Remote sensing: the quantitative approach, 21-135. McGraw Hill; New York, U.S.A.

Silva, L.R., Hoffer, R.M. and Cipra, J. (1971) Extended wavelength field spectroradiometry. Tropics: crop identification. Proceedings of 7th International Symposium on the Remote Sensing of the Environment, 1509-1518. Environment Research Institute of Michigan; Ann Arbor, U.S.A.

Simmons, I.G. (1969) Pollen diagrams from the North York Moors. New Phytologist, Volume 68, 807-827.

Simmons, I.G. (1975) Rural recreation in the industrial world. Edward Arnold; London.

Simmons, I.G. (1981a) The ecology of natural resources (second edition). Edward Arnold; London.

Simmons, I.G. (1981b) Culture and environment. In Simmons, I.G. and Tooley, M.J. (eds.), The environment in British pre-history, 282-291. Duckworth; London.

Simmons, I.G., and Innes, J.B. (1987) Mid-Holocene adaptations and later Mesolithic forest disturbance in northern England. Journal of Archaeological Science, Volume 14, 385-403.

Simonett, D.S. (1983) The development and principles of remote sensing. In Colwell, R.N. (ed.) Manual of remote sensing (second edition), Volume 1, 1-36. American Society of Photogrammetry; Falls Church, Virginia, U.S.A.

Sinclair, T.R., Hoffer, R.M. and Schreiber, M.M. (1971) Reflectance and internal structure of leaves from several crops during a growing season. Agronomy Journal, Volume 63, 864-867.

Slater, P.N. (1975) Photographic systems for remote sensing. In Reeves, R.G. (ed.), Manual of remote sensing (first edition), 235-321. American Society of Photogrammetry; Falls Church, Virginia, U.S.A.

Slater, P.N. (1980) Remote sensing: optics and optical systems. Addison-Wesley; Reading, Massachusetts, U.S.A.

Slater, P.N. (1983) Photographic systems for remote sensing. In Colwell, R.N. (ed.) Manual of remote sensing (second edition), Volume 1, 231-292. American Society of Photogrammetry; Falls Church, Virginia, U.S.A.

Smedes, H.W. (1975) The truth about ground truth. Proceedings of 10th International Symposium on the Remote Sensing of the Environment, 821-825. Environment Research Institute of Michigan; Ann Arbor, U.S.A.

Smith , J.A. (1983) Matter-energy interaction in the optical region. In Colwell, R.N. (ed.) Manual of remote sensing (second edition), Volume 1, 62-114. American Society of Photogrammetry; Falls Church, Virginia, U.S.A.

Smith, R.T. (1977) Bracken in Britain : I. Background to the problem of bracken infestation. Working paper 189, School of Geography, University of Leeds.

SPSS Inc. (1983) SPSSX users guide. McGraw-Hill; New York, U.S.A.

Steiner, D. and Salerno, A.E. (1975) Remote sensing data systems processing and management. In Reeves, R.G. (ed.) Manual of remote sensing (first edition), 611-803. American Society of Photogrammetry; Falls Church, Virginia, U.S.A.

Steven, M.D. (1987) Ground truth: an underview. International Journal of Remote Sensing, Volume 8, 1033-1518.

Stoner, E.R., Baumgardner, M.F., Weismiller, R.A., Biehl, L.L. and Robinson, B.F. (1980) Extension of laboratory measured soil spectra to field conditions. Journal of the Soil Science Society of America, Volume 44, 572-574.

Suits, G.H. (1972) The calculation of the directional reflectance of a vegetation canopy. Remote Sensing of Environment, Volume 2, 117-125.

Tansley, A.G. (1939) The British Islands and their vegetation. Cambridge University Press; Cambridge.

Thomas, I.L., Ching, N.P., Benning, V.M. and D'Aguanno, J.A. (1987) A review of multi-channel indices of class separability. International Journal of Remote Sensing, Volume 8, 331-350.

Thompson, M.M. (ed.) (1966) Manual of photogrammetry. 2 volumes. American Society of Photogrammetry; Virginia, U.S.A.

Tinsley, H.M. (1981) The Bronze Age. In Simmons, I.G. and Tooley, M.J. (eds.), The environment in British pre-history, 210-249. Duckworth; London.

Townshend, J.R.G. (1980) The spatial resolving power of earth resources satellites: a review. NASA technical memorandum no. 82020, Godard Space Flight Centre, Greenbelt, U.S.A.

Townshend, J.R.G. (1981a) An Introduction to the study of terrain. In Townshend, J.R.G. (ed.), Terrain analysis and remote sensing. George, Allen and Unwin; London.

Townshend, J.R.G. (1981b) Appendix: some basic measures in remote sensing. In Townshend, J.R.G. (ed.), Terrain analysis and remote sensing. George, Allen and Unwin; London.

Townshend, J.R.G. (1984) Agricultural land cover discrimination using Thematic Mapper spectral bands. International Journal of Remote Sensing, Volume 5, 681-698.

Townshend, J.R.G. and Justice, C.O. (1980) Unsupervised classification of MSS Landsat data for mapping spatially complex vegetation. International Journal of Remote Sensing, Volume 1, 105-120.

Townshend, J.R.G. and Justice, C.O. (1988) Selecting the spatial resolution of sensors required for global monitoring of land transformations. International Journal of Remote Sensing, Volume 9, 187-236.

Tucker, C.J (1979) Red and photographic infrared linear combinations for mapping vegetation. Remote Sensing of Environment, Volume 8, 127-150.

Van Genderen, J.L., Lock, B.F. and Vass, P.A. (1978) Remote sensing: statistical testing of thematic map accuracy. Remote Sensing of Environment, Volume 7, 3-14.

Wardley, N.W., Milton, E.J. and Hill, C.T. (1987) Remote sensing of structurally complex semi-natural vegetation - an example from heathland. International Journal of Remote Sensing, Volume 8, 31-42.

Watt, A.S. (1955) Bracken versus heather; a study in plant sociology. Journal of Ecology, Volume 43, 490-506.

Watt, A.S. (1947) Contribution to the ecology bracken (Pteridium aquilinum): IV. The structure of the community. New Phytologist, Volume 46, 97-121.

Waugh, T.C. and McCalden, J. (1983) GIMMS reference manual. Edinburgh.

Weaver, R.E. (1984) Integration of remote sensing data for moorland mapping. Satellite remote sensing: review and preview. Proceedings of the 10th Anniversary International Conference of the Remote Sensing Society, Reading, 191-201.

Weaver, R.E. (1986) Use of remote sensing to monitor bracken encroachment in the North York Moors. In Smith, R.T. and Taylor, J.A. (eds), Bracken: ecology, landuse and control technology. Proceedings of International Conference; Bracken '85, Leeds University.

Weaver, R.E. (1987) Spectral separation of moorland vegetation in Airborne Thematic Mapper data. International Journal of Remote Sensing, Volume 8, 43-55.

Weaver, R.E. and Wright, R. (1986) The use of multi-spectral airborne scanner data for mapping upland vegetation. In Proceedings of the N.E.R.C. 1985 Airborne Campaign Workshop, A27-A40. N.E.R.C.; I.T.E., Monks Wood.

White, L.P. (1977) Current systems and services for remote sensing in relation to common user requirements. In Barrett, E.C. and Curtis, L.F. (eds), Environmental remote sensing 2: practices and problems. Proceedings of 2nd Bristol Symposium on Remote Sensing, University of Bristol.

Wildlife and Countryside Act (1981) Map of moor and heath. Section 43.

Williams, J.H. (1987) Improving the mapping of upland vegetation from TM data using pre- and post-classification image filtration. Paper presented at a workshop on: Remote sensing of grasslands, University College of North Wales, Bangor.

Williams, J.H., Brown, N.J. and Norris, D.A. (1987) An experimental GIS for upland managment information in Snowdonia. Postgraduate workshop on applications of remote sensing. Remote Sensing Society Monograph, Number 2.

Williams, G.H. and Foley, A. (1976) Seasonal variations in the carbohydrate content of bracken. Botanical Journal of the Linnean Society, Volume 73, 87-93.

Wilson, A. (1986) Calibration of ATM data. In, Proceedings of the N.E.R.C. 1985 Airborne Campaign Workshop, E25-E40. N.E.R.C.; I.T.E., Monks Wood.

Wolf, P.R., (1974) Elements of photogrammetry. McGraw-Hill; New York.

Woodcock, C.F. and Strahler, A.H. (1987) The factor of scale in remote sensing. Remote Sensing of Environment, Volume 21, 311-332.

Wooley, J.T. (1971) Reflectance and transmittance of light by leaves. Plant Physiology, Volume 47, 656-662.